BULLETIN 162

PNG 10

Geochronology of Igneous and Metamorphic Rocks in the New Guinea Highlands

R. W. PAGE

ABSTRACT

The Phanerozoic tectonic history of New Guinea has been influenced by the island's situation between the relatively stable Australian continent to the south, and an active volcanic-geosynclinal belt marginal to the Pacific Ocean in the north. In these two environments in the Central Highlands of mainland Papua New Guinea, ages of most of the major plutonic bodies and volcanic units, and of some metamorphic terrains, have been determined by the K-Ar and Rb-Sr methods.

The earliest-known granitic intrusions are late Palaeozoic (about 240 m.y.), and, together with other small Mesozoic intrusives dated as 190 m.y., 172 m.y., and 90 m.y., form a major component of the southern half of the island, onto which later Mesozoic and Tertiary belts were accreted.

Late Oligocene to early Miocene ages of 20 to 26 m.y. for granodiorites, diorites, and greenschist metamorphic rocks reflect the beginnings of Tertiary tectonic activity in the New Guinea Mobile Belt. K-Ar results, confirmed by Rb-Sr mineral and whole-rock isochron data, show that this activity reached a climax, with huge outpourings of andesitic volcanic rocks and the intrusion of associated diorites and granodiorites (some associated with porphyry copper), between 12 and 15 m.y. ago in the mid-Miocene. Dating of volcanic rocks interbedded with foraminiferal sediments has defined more precisely the East Indies letter stage time scale. Uniform initial Sr^{87}/Sr^{86} ratios (0.7041 ± 0.0002) for all the igneous rocks suggest that the magma was derived from the mantle, with little or no crustal contamination. This short-lived but dramatic mid-Miocene upsurge of igneous activity is associated with major faulting and folding in a curvilinear mountain belt over 600 km long, and plate tectonic considerations suggest that interaction and collision between the Australian and Pacific Plates were likely triggering mechanisms of this important tectonic regime.

CONTENTS

TABLES

PLATE (at back of volume)

FIGURES

SUMMARY

The island of New Guinea lies in an area of complex tectonic interaction between the relatively stable Australian continental landmass and the geologically active circum-Pacific Belt. Thus the Palaeozoic-Mesozoic history of the southern half of the island is closely related to the Palaeozoic-Mesozoic development of northeastern Australia, whereas in the northern half of the island there are Cainozoic geosynclinal and volcanic belts which cross-cut the Palaeozoic-Mesozoic basement and are parallel to the circum-Pacific margin in this region.

In mainland Papua New Guinea, intrusive igneous activity before Tertiary time was restricted to the southern part of the Central Highlands and, from the data available, appears to have been rather sporadic. The Upper Permian Kubor Granodiorite, dated at about 240 m.y., represents the largest and oldest-known igneous massif in New Guinea. A number of small Mesozoic granitic bodies were emplaced in the Early Jurassic (190 m.y.), Early to Mid-Jurassic (172 m.y.), and mid-Cretaceous (90 m.y.).

Increased tectonism in the mid-Tertiary is evidenced by several late Oligocene and early Miocene results (26 to 20 m.y. range) in four metamorphic terrains and in granitic intrusives in the south Sepik area. Volcanic and plutonic igneous activity reached a climax in the mid-Miocene, between 12 and 15 m.y. ago. K-Ar dating on some of these volcanic rocks in close stratigraphic relationship with palaeontologically controlled sedimentary rocks provided the basis for constructing a physical time scale for the East Indies letter stages.

The 12-15 m.y. (mid-Miocene) pulse of plutonic activity continued to a lesser degree in the late Miocene and Pliocene. These Miocene-Pliocene bodies lie in an arcuate northwest-trending belt (New Guinea Mobile Belt) over 700 km long. Porphyry copper and gold mineralization events are temporally and spatially associated with the middle Miocene and Pliocene high-level intrusives in this belt.

All the volcanic and plutonic rocks have low initial Sr^{87}/Sr^{86} ratios, suggesting that they were derived from mantle sources with little or no contamination by crustal material.

A close relation between the major tectonic processes of faulting, volcanism, and plutonism in the New Guinea Mobile Belt, over a relatively short time span of a few million years in the mid-Miocene, corresponds to the waning stages of the Papuan Geosyncline sedimentary history and the beginning of the main mountain-building processes in the New Guinea highlands. It is hypothesized that this climactic upsurge in the tectonic history of New Guinea was triggered in the early to mid-Miocene by interaction and collision between the Pacific Plate and the northward-moving Australian Plate, which has New Guinea at its leading edge.

1. INTRODUCTION

New Guinea lies in the equatorial southwest Pacific immediately north of Australia and east of the Indonesian Archipelago (Fig. 1). New geological data presented in this Bulletin are restricted to part of Papua New Guinea, which comprises the eastern half of the main island (east of longitude 141°E), New Britain, Bougainville, and New Ireland, and smaller islands offshore from all four.

The most conspicious physiographic province in mainland New Guinea is the central mountain chain, or Main Cordillera (Carey, 1938), part of which forms the area of the detailed geochronological study. This chain (Fig. 2), which is the backbone of New Guinea, runs continuously for over 2500 km from the Vogelkop (the 'bird's head' of Irian Jaya) through the Snow Mountains, the Star Mountains, and the southeast-trending highland ranges to the Owen Stanley Range as far as eastern Papua. The southeast-trending ranges between longitude 142°E and 146°40'E, which are referred to in the text as the Central Highlands, constitute the study area. Another distinct province, the North Coast Range (north New Guinea coastal mountain range), is separated from the Main Cordillera by the Meervlakte Depression in Irian Jaya and the Sepik-Ramu-Markham Depression in eastern and north-central New Guinea. South of the Main Cordillera, and marginal to the Australian continent, is the Coastal Plains province. These three provinces, which are closely related to gross structural elements, came into existence at quite a late stage in geological history; they occupy an area that was mostly open sea from at least Jurassic to Miocene times, and their comparative youth is evident from Upper Tertiary marine limestone cappings which occur in many places over 3000 m above sea level. Parts of both the New Britain Arc and the Solomon Islands, which are separated from the mainland by the deep New Britain Trench in the Solomon Sea, are active volcanic regions.

The first geological reports of areas of mineral potential in the New Guinea highlands were made in the 1930s, shortly after the first white man had crossed the rather unwelcome terrain. Most of the geological information in western Papua has been provided by oil exploration results since about 1911. In 1950, a general account of the geology of 'Australian New Guinea' was published as Chapter XIV of Sir Edgeworth David's 'Geology of the Commonwealth of Australia', edited by W. R. Browne. Later, Visser & Hermes (1962) summarized the geology of what was then known as 'Netherlands New Guinea', and they attempted a tectonic synthesis of the whole region.

Systematic mapping of the mountain ranges of mainland Papua New Guinea was begun in the 1950s by the Bureau of Mineral Resources and the Territory of Papua and New Guinea Department of Lands, Surveys, and Mines. Since 1960, with improved communications, transport facilities, and aerial-photograph coverage, the momentum of this task has considerably increased. The author participated in the mapping program during 1967 and 1968, and also collected suitable material for the New Guinea geochronological study. The interesting tectonic position of the island as part stable continent, part active orogenic belt, and part volcanic island arc, together with our increased knowledge of the regional geology, clearly warranted such a study.

Aims

This geochronological study is directed at the following objectives:

(i) To relate the physical time scale with the Tertiary biostratigraphic time scale used in New Guinea and throughout the East Indies. The establishment of a convincing link between the relative and physical time scales would provide a more precise subdivision of the East Indies Tertiary stages, and would enable better correlations with Tertiary stages dated elsewhere in the world.

O/9/31

Fig. 1. New Guinea region with gross bathymetric features.

(ii) To determine the chronology of igneous activity and metamorphism throughout the Central Highlands of New Guinea.

(iii) To investigate time factors for such processes as the cooling of igneous intrusions, metamorphism, and the rates of uplift in the relatively juvenile terrain.

(iv) To investigate the strontium-isotope geochemistry of the Central Highlands igneous rocks.

(v) To investigate models for the geological evolution of New Guinea in terms of the geochronological, geological, and geophysical data put forward.

Fieldwork

Sampling was carried out intermittently for six months betwen July 1967 and February 1970. A preliminary study, early in 1967, of 36 samples collected from a number of localities throughout the New Guinea Highlands by D. B. Dow and R. R. Harding helped in planning the main sampling program from July to November 1967 in the Central Highlands and Sepik regions (Fig. 2, Plate 1). Two other field trips were made, in mid-1968 and early 1970, during which more areas of the Central Highlands were sampled. A few of the samples came from other sources, including BMR regional mapping parties in New Guinea and BP Petroleum Development Australia Pty Ltd.

Sampling was carried out mainly with a view to K-Ar dating; it was necessary to collect massive fresh samples of holocrystalline volcanic rock (for whole-rock studies) and fresh samples of biotite-bearing or hornblende-bearing plutonic rock. From the larger intrusions a spectrum of several acid and basic igneous rocks was sampled for possible Rb-Sr whole-rock work. Over 350 samples were collected, covering the majority of the igneous rocks so far mapped in the Central Highlands (Fig. 2, Plate 1).

The logistics in each area and hence the methods of collection varied considerably.
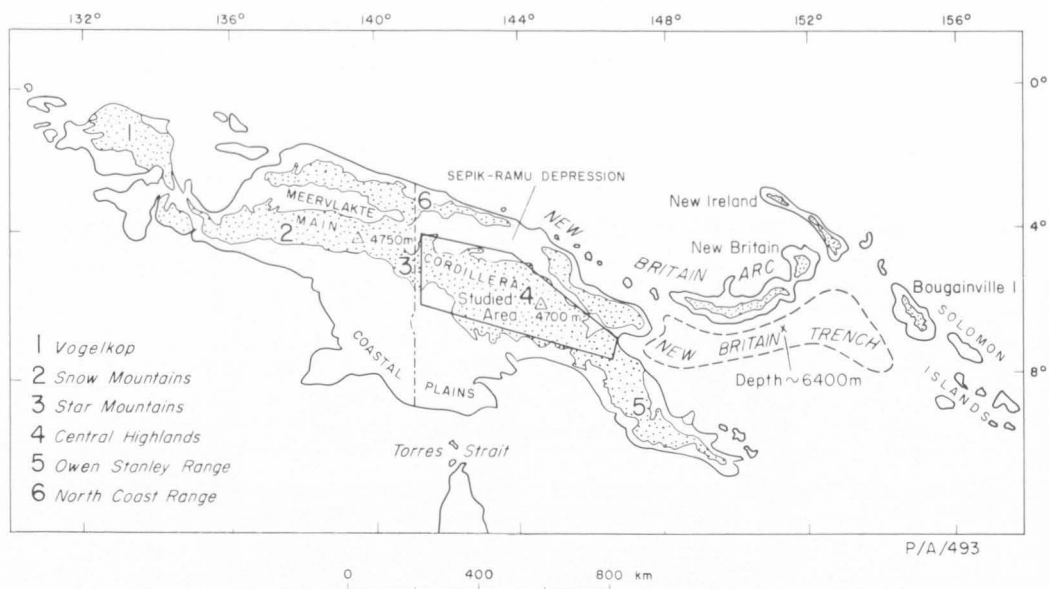
Fig. 2. Gross morphology of the New Guinea region.

Over much of the Central Highlands, conventional methods could be employed: selected outcrops were reached by road, and either drilled and blasted or shattered with a sledge-hammer to obtain fresh samples. However, many samples from the south Sepik region and some collected in the Western Highlands were not in situ. Much of the south Sepik region is rugged jungle and is virtually uninhabited, and there are no roads or walking tracks; jet-boats and helicopters provided the means to collect adequate samples. In most of New Guinea, much of the geological information is obtained in stream and river sections, which present a few somewhat weathered outcrops in the mountainous areas. Hence in many places the only samples available were boulders in creek beds. Streams with a restricted watershed provided the most representative samples, and enabled the limits of the area sampled to be defined by the stream boulders. The locality of each sample is shown in the various text-figures, and the samples themselves are listed in Appendix 2.

Acknowledgements

4

2. AN OUTLINE OF NEW GUINEA GEOLOGY

2.1 TECTONIC SETTING

The island of New Guinea occupies a complex structural position between two continents (Australia and Asia) and two oceans (the Pacific and Indian). This complexity is particularly evident in the western part of the island, where structure is influenced by the structural trends of the East Indies. Papua New Guinea, however, occupies a structural position between the continent of Australia in the south and the geologically active circum-Pacific Belt in the north: its southern part has close affinities to the Palaeozoic-Mesozoic development of eastern Australia, whereas in its northern part there are Cainozoic geosynclinal and volcanic belts which cross-cut the Palaeozoic-Mesozoic basement and are parallel to the circum-Pacific margin in this region. The close relation between physiography and geology in New Guinea reflects the youthfulness of the area, and frequent earthquakes and numerous active volcanoes testify to continuing instability. These juvenile, so-called mobile belts are the most prominent features of circum-Pacific geology, and since they have been historically the most

active major features of the Earth's crust their manner of development might hold the key to the origin, growth, and real nature of continents.

As previously stated, New Guinea contains elements of a relatively stable platform, as well as a Tertiary to present-day active tectonic belt in the north. Such history recorded on the one landmass assumes some importance in terms of the now widely accepted plate tectonic model (Isacks, Oliver, & Sykes, 1968; Heirtzler, Dickson, Herron, Pitman, & Le Pichon, 1968; Le Pichon, 1968), incorporating the ideas of continental drift and seafloor spreading. The plate tectonic model postulates that the outer 50 to 100 km of the Earth consists of a number of rigid plates in relative motion. Where plates interact, earthquakes occur, and the foci of the shallow earthquakes represent boundaries between two (or more) plates. Most earthquakes in oceanic regions occur in narrow belts associated with deep trenches, ridges, and fracture zones, which are the surface features of the plate boundaries. The world seismicity map (Fig. 3) reveals that the New Guinea region is associ-
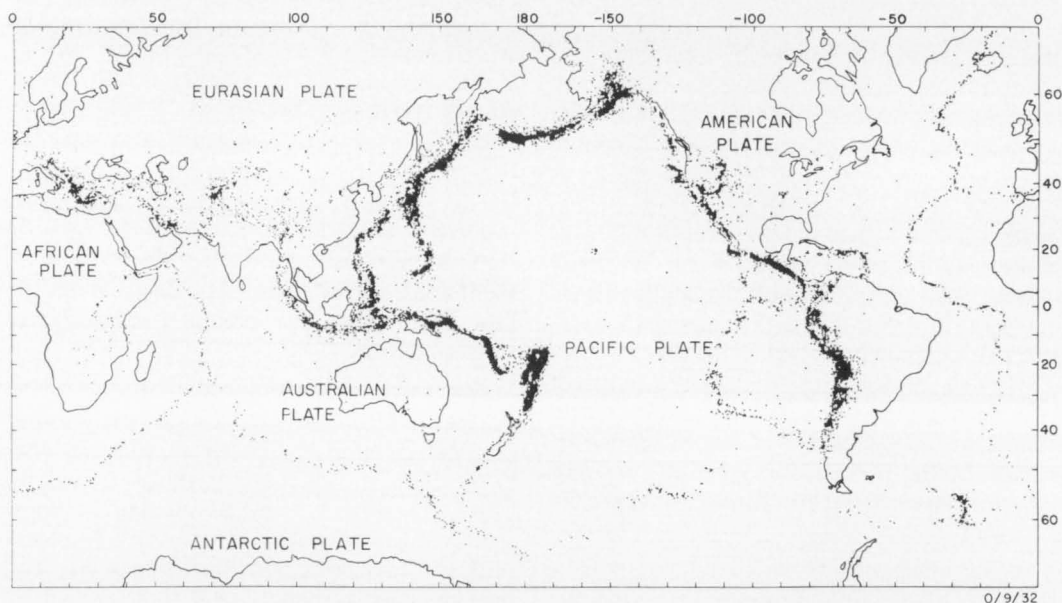
Fig. 3. Seismicity of the Earth, 1961-1967, depths 0-700 km.

ated with a plate boundary, which, for Papua New Guinea at least, can be considered as the juncture between the Australian and the Pacific Plates

In many areas of the circum-Pacific, the plate margins are marked by present-day volcanism (e.g. New Hebrides arc, New Britain arc, Phillipines arc), but this does not apply on the north coast of New Guinea (west of 144°E, Fig. 1), although seismically it is a plate margin. Hess (1948) suggested that this apparently anomalous circum-Pacific segment may represent an advanced stage in the tectonic development of the circum-Pacific. By examining the distribution and chronology of igneous activity and metamorphism in New Guinea, it may be possible to recognize past or fossilized plate margins.

2.2 CRUSTAL STUDIES

2.21 *Seismology*

Since 1965 much geophysical information has been obtained in the New Guinea/Solomon Islands region about crustal and upper mantle structures. Early seismicity studies by Gutenberg & Richter (1954) provided a general description of the area, as did the Rayleigh-wave studies by Santo (1963), who assigned the whole of the New Guinea/ Bismarck Sea area to the same 'Continental' subdivision as Australia. The seismicity patterns now recognized (Fig. 4) result from the detailed analyses by Denham (1969), and have since been substantiated by Johnson (1970) and Santo (1970). In the New Britain/Bougainville area, a well defined zone of earthquakes (Benioff zone) dips steeply to the north or northeast under these islands. Although the earthquake pattern under mainland New Guinea is diffuse most workers have suggested that the Benioff zone probably dips to the south (Denham, 1969; Johnson & Molnar, 1971; Isacks & Molnar, 1971; see also Curtis, 1973a, b; Finlayson & Cull, 1973; Connelly, 1974).

Two other seismic belts in Figure 4 are worth noting. One is an east-west line of shallow earthquakes stretching across the Bismarck Sea from the Gazelle Peninsula of New Britain to the Torricelli Mountains of New Guinea. Denham (1969) referred to this as the Bismark Sea seimic lineation and suggested that it is either an embryo mid-oceanic ridge, an embryo trench, or a simple fault zone; it does not, however, correlate
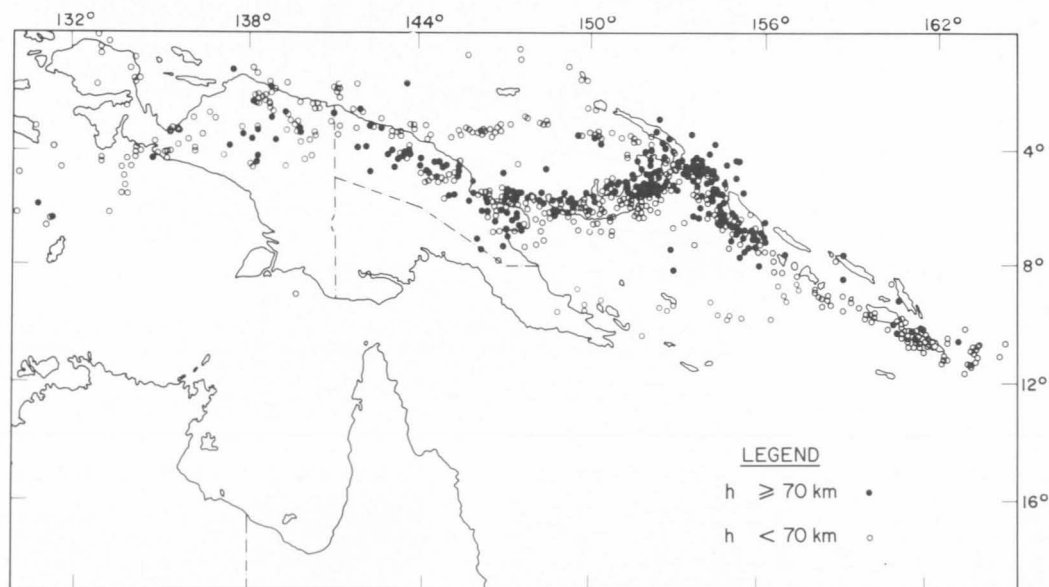
0/9/32

Fig. 4. Earthquakes with magnitudes ⩾ 5 in New Guinea, 1958-1966.

with any known bathymetric features. The other seismic belt is an arc of shallow earthquakes cutting across the Solomon Sea between New Georgia and eastern Papua. This lineation is not continuous, but its east-west trend corresponds fairly well to that of the topographic high between 8°S to 9°S and 150°E to 156°E near Woodlark and Trobriand Islands (cf. Figs 1 and 4). Denham's (1969) suggestion of an embryonic ridge in the Bismarck Sea may equally well apply to the Solomon Sea feature. Further implacations of the distribution of earthquakes in the New Guinea/Solomon Islands region are discussed later in relation to the geological and geochronological evidence.

2.22 Crustal thickness determinations

There are now several independent estimates of depth to the M-discontinuity in the New Guinea region. Brooks & Ripper (1966), in a study of group velocities of Rayleigh waves recorded at Port Moresby, found that the crust is 'normal continental' ($\sim$35 km) under most of the Arafura Sea and western Papua, and generally thicker under the central mountain chain of New Guinea and Irian Jaya. Brooks (1969b) estimated an 'average' crustal thickness, also based on Rayleigh-wave group velocities, of 33 km beneath the Main Cordillera of New Guinea. Denham (1968) deduced a crustal thickness of about 31 km at Port Moresby from spectral studies of deep earthquake P waves, and Doyle & Webb (1963) reached a similar conclusion from a study of arrivals from Bikini and Eniwetok nuclear explosions. The shear velocity Rayleigh-wave profiles of Brooks (1969a) covered much of western Papua and southern Irian Jaya, and from them he inferred an average crustal thickness of 33 $\pm$ 1 km, without any pronounced crustal discontinuities. All these studies are therefore concordant and suggest a crustal thickness of 30 to 33 km for the southern and central New Guinea region. In the Gulf of Papua a crustal thickness of 'greater than 24 km' was determined from the gravity measurements of Solomon & Biehler (1969).

Below the North Coast Range, Brooks (1969b) reported a tentative continental crustal thickness based on the shear velocity Rayleigh-wave profiles of about 37 km. This is consistent with St John's (1967) gravity data interpretations (using a density contrast of 0.5 g/cm^3 at the M-discontinuity), which also suggested continental crust characteristics in this region.

Immediately north of New Guinea, in the Bismarck Sea, the independent gravity data obtained by St John (1967) indicate a fairly rapid crustal thinning to about 20 km. Thus the Bismarck Sea is not a typical continental area as suggested by Visser & Hermes (1962) and Santo (1963), but the inferred crustal thickness of about 20 km suggests that it is intermediate between oceanic and continental crust.

St John's (1967) regional gravity survey over much of Papua New Guinea showed that the Southern Stable Platform (see 2.31) and Main Cordillera are broadly compensated, whereas the north New Guinea area is still isostatically unstable. In a qualitative manner, St John (1967) also concluded that the gravimetric crust (usually assumed as equal to continental 'seismic' crust) is much thicker in some areas (e.g. the Bismarck, Kubor, and Owen Stanley Ranges) than elsewhere on the island. A similar crustal thickening under the central ranges of Irian Jaya was also found from reconnaissance gravity profiling in that area (Visser & Hermes, 1962).

Crustal studies are currently being made in the Solomon Sea/New Britain region by BMR and the Hawaiian Institute of Geophysics. Earlier magnetic and gravity measurements reported by Rose, Woollard, & Malahoff (1968) enabled them to make provisional estimates for depths to the M-discontinuity of 12 to 15 km beneath the Solomon Sea southwest of Bougainville Island. Furumoto, Hussong, Campbell, Sutton, Mallahoff, Rose, & Woollard (1970) have recently confirmed the results by seismic refraction studies. Recent work farther south in the Solomon Sea (Furumoto et al., 1970) reveals a far more complicated picture in which the crust thickens to the south before thinning again to an oceanic type
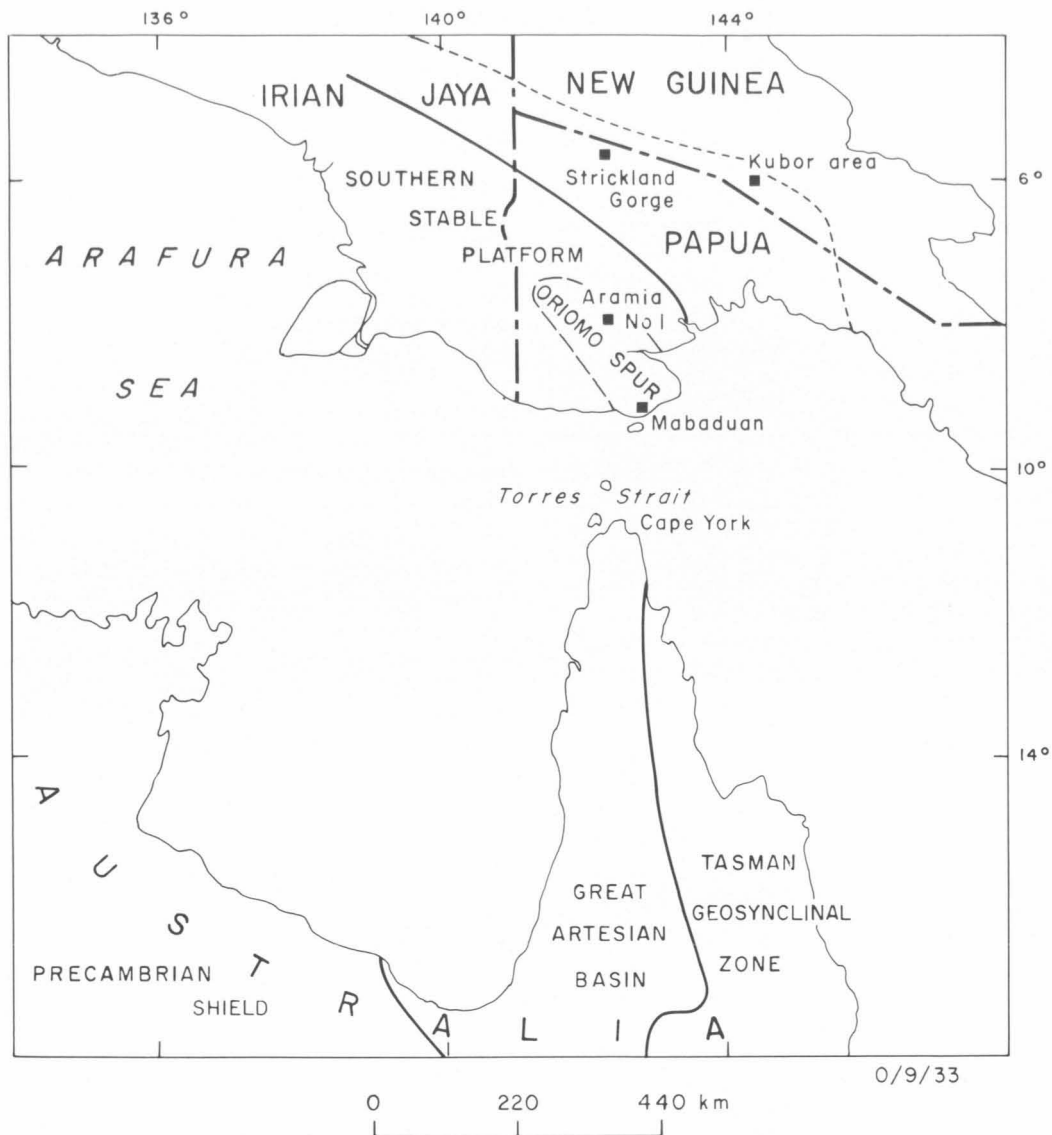
Fig. 5. Major geological subdivisions in Australia and southern New Guinea.

beneath 'The Slot' (New Georgia Sound), which separates the Solomon Islands.

Results from seismic crustal studies in the east Bismarck Sea/New Britain and New Ireland areas show a number of sharp breaks in crustal thickness between these two areas (Furmoto et al., 1970; Wiebenga, 1973). The crust of the Bismarck Sea north of New Britain is typically oceanic (12 to 15 km thick), whereas the crust under part

of New Ireland and the Ontong-Java Plateau (Fig. 1) is unexpectedly thick, exceeding 35 km.

2.3 REGIONAL GEOLOGICAL FRAMEWORK

Analyses of the regional geology of all or parts of New Guinea have been made by David & Browne (1950), Glaessner (1950), APC (1961), Visser & Hermes (1962), Thompson & Fisher (1965), Osborne

(1966), Thompson (1967), St John (1967), Rickwood (1968), Harrison (1969), Marchant (1969), and Bain (1973). In this section relevant parts of these papers are collated, together with some recent regional mapping by BMR.

During much of the Mesozoic and Tertiary, up to the Pliocene, the area occupied by New Guinea was, in general, open sea, beneath which the crust was gradually subsiding northward and northeastward from the edge of the Australian continent. Thus the southern part of New Guinea has acted as a relatively stable platform, north and northeast of which a complex en echelon geosynclinal system began to form in the early Mesozoic. This geological framework is now briefly summarized. The Southern Stable Platform and Papuan Basin relate directly to the areas of this geochronological study. The other main structural units of Papua New Guinea have only minor relevance to the study, and the reader is referred to a recent summary by Bain (1973).

2.31 Southern Stable Platform

The Southern Stable Platform (Fig. 5) is the area under which 'crystalline basement' lies at a shallow depth, and the overlying strata are unfolded or perhaps affected only by gentle warping and faulting (APC, 1961; Glaessner, 1950). Because of the sparseness of exposure, information about the basement has been derived mainly from geophysical surveys and the logs of scattered drill holes, which indicate that the granitic basement continues north and northwest in western Papua as a basement swell termed the Oriomo Spur (Fig. 5). The basement crops out at Mabaduan, the southernmost point of western Papua, and forms the northerly exposure of a spur of granitic rock extending across Torres Strait from Cape York. Richards & Willmott (1970) obtained K-Ar ages of 286 to 302 m.y. for granite samples from this area, which suggest a Late Carboniferous age. A biotite K-Ar age of 236 m.y. was determined on granite cored in Aramia No. 1 well, 170 km northwest of Mabaduan (J. R. Richards, *in* Harding, 1969). The Southern Stable Platform, whose northern boundary has not been accurately determined, is thus interpreted as an upper Palaeozoic granitic landmass which underlies much of the southern part of New Guinea and is probably coextensive with the granitic rocks of Cape York.

The limit of the Australian continent, including the active marginal areas, extends much farther north than the Southern Stable Platform. Thompson (1967) believes that the Australian continental basement underlies all New Guinea except the North Coast Range. Earlier, southern New Guinea was shown to have a crustal thickness of continental proportions ($\sim$32 km), and initial estimates indicated the presence of a thick crust north of here too. The dotted line in Figure 5 is close to that which Thompson (1967) interpreted as representing the northern limit of the continental part of New Guinea. The area south of this line is somewhat arbitrarily taken to include all the known pre-Mesozoic to lower Mesozoic rocks in New Guinea. In Irian Jaya it would include the few lower to upper Palaeozoic rocks which straddle the southern side of the Central Ranges (Visser & Hermes, 1962). In Papua New Guinea the line is extrapolated from the known basement outcrops in the Strickland Gorge and 250 km to the east in the Kubor Range (see 4.2 and 4.3). Some authors (McMillan & Malone, 1960; Smith, 1965; Pitt, 1966; Brooks, 1969a) have inferred that the Bismarck massif is also part of the pre-Mesozoic basement platform, but, as stressed by APC (1961), its age cannot be determined with reference to fossiliferous rocks. Results presented later (5.3) show that this mass is indeed quite young (Late Tertiary).

The possible relations between southern New Guinea and the principal geological units of northern Australia (the Precambrian Shield, the Great Artesian Basin, and the Tasman Geosyncline) have been discussed by Glaessner (1950) and Visser & Hermes (1962), who suggested that the southwesternmost part of New Guinea may be an extension of the Precambrian Shield (cf. Fig. 5). They also suggested that the east Australian Tasman Geosyncline may have extended north and be partly represented in the Irian
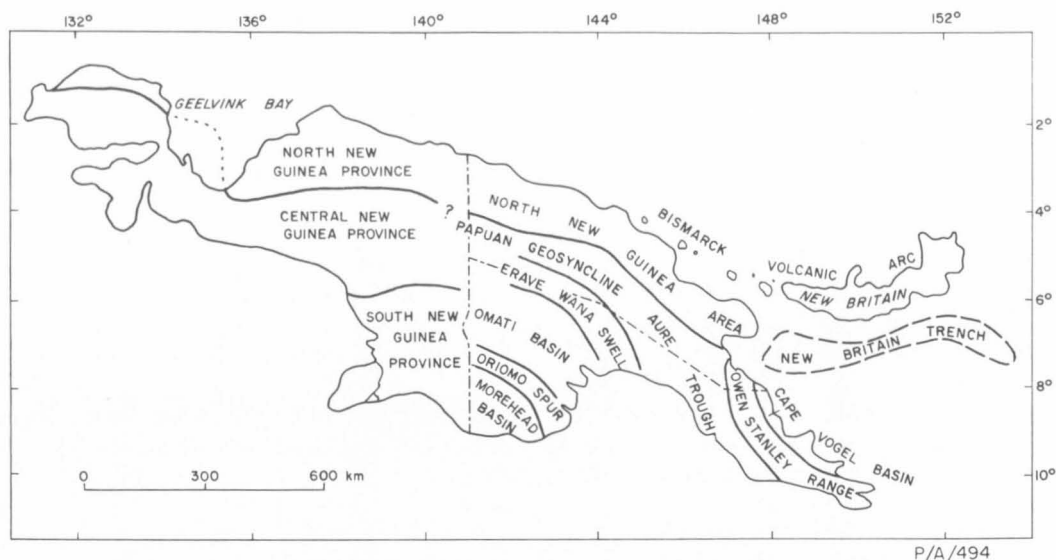
Fig. 6. Major geological subdivisions in New Guinea.

Jaya ranges. Osborne (1966) and Glaessner (1950) also drew attention to the possibility that Mesozoic sediments of the Great Artesian Basin extended to New Guinea. The limited geochronological data on the granites of Torres Strait (Richards & Willmott, 1970) and southwest Papua (Richards, *in* Harding, 1969) indicate periods of emplacement from at least the Late Carboniferous to Late Permian, and this may be regarded as support for the idea that the Tasman Geosyncline extended into southern New Guinea.

2.32 *Papuan Basin*

The Papuan Basin postdates, and to a large extent is developed on top of, the Southern Stable Platform. Like the major physiographic features in New Guinea, the marine basins which form this geosynclinal system are arranged in arcuate fashion round north Australia. The fundamental subdivisions of the Papuan Basin (after Osborne, 1966) are the Papuan Geosyncline-Aure Trough, the Omati Basin, and the Morehead Basin; these are schematically shown in Figure 6.

Sedimentation in Papua New Guinea had a sporadic beginning in Permian and Triassic times (Rickwood, 1955; Dow & Dekker, 1964), but the continuously dated record does not begin until the Jurassic. Visser & Hermes (1962) divided the Irian Jaya sector into three stratigraphic provinces (Fig. 6) in which the continuous sedimentary record began in the Permo-Carboniferous. Geographically, the northern part of Visser & Hermes's (1962) Central New Guinea Province and the southern part of their North New Guinea Province more or less correspond to the Papuan Geosyncline. The following generalized history of the Papuan Basin draws mainly from examples in Papua New Guinea.

Permian to Cretaceous. During the late Palaeozoic to early Mesozoic the Southern Stable Platform was an area of shallow sedimentation. By the Cretaceous, both the central area of New Guinea and the Southern Stable Platform had been completely invaded by a marine transgression from the north with sediment being derived mainly from the uplifted Australian shield. The sedimentary environment remained much the same throughout the Mesozoic: north from the shore of the Australian landmass a shallow sea opened into a subsiding deep-water trough. Thick marine basic volcanics and volcanic-derived greywackes were deposited in a flanked trough during the Jurassic (Mongum Volcanics of Dow &

Dekker, 1964; Dow, Smit, Bain, & Ryburn, 1972) and Cretaceous (Kondaku Tuff and Kumbruf Volcanics of Dow & Dekker, 1964), in marked contrast to the quartz-rich clastics of the shallower-water, miogeosynclinal environment to the south (APC, 1961).

Thus, by the latter part of the Mesozoic an arcuate geosynclinal complex was initiated; in its northern part, there was a deep eugeosynclinal trough known as the Papuan Geosyncline (Osborne, 1966). An active basement high known as the Erave-Wana Swell separated the eugeosyncline from the miogeosynclinal facies of the Omati Basin. Farther south, and separated by another basement high (the Oriomo Spur), was the third basin (Morehead Basin), which formed on the stable shelf bordering the north Australian continent. Rickwood (1968) estimated that, by the end of the Late Cretaceous, between 6000 and 9000 m of sediment had been deposited in the Papuan Geosyncline.

Eocene. At the end of the Mesozoic, much of southwest Papua emerged and underwent a period of erosion which continued into Early Tertiary time. To the north, however, deep geosynclinal sedimentation continued during the Eocene, and the area now occupied by the Western Highlands of New Guinea received thick terrigenous sediment and intercalated volcanic debris (e.g. Lagaip Beds, Salumei Formation of Dekker & Faulks, 1964; Dow et al., 1972) from Late Cretaceous to Eocene time. There appears to have been no break in sedimentation to the southeast too, near Port Moresby, where about 1500 m of Lower Tertiary sediments are developed (Glaessner, 1952; Osborne, 1966).

Oligocene. The Oligocene in the Central Highlands region was probably a period of general emergence, as the only known deposits of this age are small isolated outcrops of *Nummulites* limestone (McMillan & Malone, 1960).

Miocene. At the end of the Oligocene and in the early Miocene, active geosynclinal development recommenced, and a pattern similar to that of the late Mesozoic was established. From this time on, however, the sediment supply came not from the Australian continent, but from the rising landmasses (e.g. the Owen Stanley and Central Ranges) within the New Guinea region itself. A deepening eugeosyncline called the Aure Trough (Fig. 6) received more than 9000 m of greywacke and shale throughout the Miocene and Pliocene (Osborne, 1966). In the early to middle Miocene, sedimentation was accompanied by the most widespread volcanic activity found in the New Guinea geological record (Dow, 1969; Dow et al., 1972). This volcanism was an important feature in the tectonically unstable belt named by Dow et al. (1972) the New Guinea Mobile Belt. The time and space relations between this Miocene volcanism and an arcuate front of deep magmatic activity which extended over the whole length of what are now the highlands of Papua New Guinea are discussed later.

Throughout the Miocene, the miogeosynclinal facies of the Omati and Morehead Basins continued to develop as a limestone shelf upon the northern extension of the Australian continental mass. Deposition of the Miocene sediments may be summarized by a traverse northwards from the Central Range of present-day New Guinea: on the southern slopes of the Central Range, middle Miocene reef limestone forms peaks over 3000 m above sea level; farther north in the Western Highlands, the lower to middle Miocene sediments are pelagic limestone, sandstone, and foraminiferal claystone (Dekker & Faulks, 1964); and still farther north, on the Sepik fall, the Miocene sediments are tuffaceous clastics and, in places, conglomerate. Most of the Central Range became emergent during the late middle Miocene, and the resultant landmasses along the centre of New Guinea and Papua were the dominant features by the end of the Miocene and throughout the Pliocene. This uplift was associated with many west-north-west-trending faults in the New Guinea Mobile Belt, and was accompanied by large-scale intrusive activity, folding of the sediments, and very rapid erosion (cf. Plate 1).

Pliocene. In the Pliocene, thick sediments and tuffaceous material accumulated in restricted, partly terrestrial basins: the isolated Strickland Basin in northwestern Papua, and the Delta and Lakekamu Embayments in southern Papua (APC, 1961). Uplift, faulting, and intrusive activity continued.

Quaternary. Restricted Pleistocene to Recent sediments and volcanic accumulations are evident in many areas of New Guinea. In the Papuan Basin area, by far the most striking products of the present time are the great volcanic cones which dominate the landscape of extensive areas of western Papua and adjacent parts of New Guinea. APC (1961) has summarized the geomorphological features of these thirteen volcanoes, all of which rest on folded Pliocene and older strata and are now evidently extinct. Jakes & White (1969) and Mackenzie & Chappell (1972) gave petrological and chemical data for some of these volcanoes and concluded that the lavas are of the shoshonitic (i.e. high-potassium) rock association.

General. Many of the sediments in the Papuan Basin geosynclinal complex exhibit diagenetic metamorphic effects as a result of deep burial and subsequent tectonic processes. Higher-grade rocks of the glaucophane-schist, greenschist, and amphibolite facies (McMillan & Malone, 1960; Dow et al., 1972) characterize some isolated pockets in the Eastern Highlands (Goroka Formation) and the Sepik Districts (Ambunti and Salumei Metamorphics). The geological setting, and the history of metamorphism and its relation to the emplacement of many granitic batholiths and ultramafic bodies throughout the Central Range, are further discussed in sections 4 to 6.

2.33 *Owen Stanley Range/Cape Vogel Basin area*

The region considered here is the southeastern peninsula of mainland Papua New Guinea (Fig. 6). Although this area is of only minor relevance to the present New Guinea geochronological study, it is important in the later discussion of the complete geological development of the island. From west to east, the Owen Stanley Metamorphics, the Papuan Ultramafic Belt, and the Cape Vogel Basin are the major geological units. The structural trends are dominated by the Owen Stanley Fault, which separates the Owen Stanley Metamorphics from the Papuan Ultramafic Belt (cf. Plate 1). This fault can be traced along two-thirds of the length (450 km) of the peninsula, and crosses the coast south of Lae.

The Owen Stanley Metamorphics comprise the Cretaceous or pre-Cretaceous Kaindi Metamorphics as well as definite Cretaceous metasediments, and are the oldest rocks in the area (Dow & Davies, 1964). As post-Cretaceous sediments do not occur in the metamorphic belt it is considered that the greater part of the unit was an emergent landmass, probably an island, throughout the Tertiary (Thompson & Fisher, 1965; Thompson, 1967). This raises an important distinction between the development of the Papuan Basin of central New Guinea and that of the Owen Stanley area. On the one hand, throughout most of the Tertiary, particularly the latter half, central New Guinea was linked to northern Australia by a broad platform which was the site of mainly miogeosynclinal limestone deposition. On the other hand, the Owen Stanley area was apparently separated from northeastern Australia throughout the Tertiary by the deep sea which occupied the Aure Trough/Coral Sea depression.

The Papuan Ultramafic Belt is an elongated complex (more than 400 km long and up to 40 km wide) of ultrabasic, basic, and intermediate intrusive and extrusive rocks extending from the New Guinea coast south of Lae to beyond the Musa River in eastern Papua (Plate 1). Thompson (1957) was the first to describe the complex; subsequent detailed mapping by Davies (1968), and gravity work by St John (1967) and Milsom (*in* Davies, 1971) gave support to the hypothesis that the Ultramafic Belt is a segment of oceanic upper mantle and crust which has been thrust westward over the sialic core of eastern Papua, the Owen Stanley metamorphic block, since the Cretaceous.

The Ultramafic Belt has a regional easterly dip and consists mainly of ultramafics (dunite, peridotite, pyroxenite, and serpentinite) grading upwards into gabbroic and noritic rocks, which are overlain by a basaltic layer.

Palaeontological control on sediments intercalated with the basalts in the Ultramafic Belt tentatively suggests a Cretaceous age (Davies, 1971). Two tentative K-Ar age determinations on very low-potassium gabbroic rocks (H. L. Davies & R. W. Kistler, pers. comm., 1970) from the Ultramafic Belt give ages of about 150 m.y., indicating crystallization and cooling in the Late Jurassic. Tonalites which intrude the gabbros and basalts of the Ultramafic Belt have also been dated, by myself and A. W. Webb, again using the K-Ar method; age determinations of one hornblende and three plagioclase samples of the tonalites are in the range 50 to 55 m.y. (early Eocene), and provide an upper limit for the time of cooling of the Papuan Ultramafic Belt.

Implicit in the discussion is the possibility that the metamorphism of the Owen Stanley rocks was related to the emplacement of the Papuan Ultramafic Belt. If the Belt does represent a slice of the upper mantle and oceanic crust thrust up over the metamorphics, as interpreted by Davies (1968), then the intervening region of the Owen Stanley Fault and adjacent metamorphics can be regarded as the boundary of two lithospheric plates which converged and overlapped one on the other. This relation is consistent with the sedimentary record, which clearly indicates that the Owen Stanley area began to emerge after the Cretaceous.

The Cape Vogel Basin was discussed by Carey (1938), Paterson & Kicinski (1956), Thompson & Fisher (1965), and Davies & Smith (1971). It is a structurally and topographically depressed coastal zone to the northeast of the Papuan Ultramafic Belt. Coastal sections reveal a 4000-m-thick sequence of Miocene to Pliocene clastic sediments. These sediments were probably derived from erosion of the emergent Owen Stanley metamorphic block, and occupy an analogous position to the Upper Tertiary clastics of north New Guinea. The Cape Vogel Basin probably extends offshore to the east, where present-day sedimentation is occurring in the region of the Trobriand and D'Entrecasteaux Islands.

2.34 North New Guinea area

The North New Guinea area (Fig. 6) consists of a predominantly volcanic basement on which has developed an elongate series of geosynclinal basins of Neogene age. As pointed out by Bain (1973), little is known about the ages of and relations between the 'basement' igneous and metamorphic rocks and the overlying Neogene sediments. Recent reconnaissance K-Ar data (Page, unpubl.) show that a complex plutonic history is present; ages range from Mid-Jurassic, through Cretaceous, to Miocene. Additional K-Ar measurements (AMDEL Report AN3101/73) and mapping now in progress (Hutchison & Norvick, pers. comm.) indicate that a good deal of the plutonic activity in the Torricelli and Bewani Mountains area is early Oligocene (35-40 m.y.).

3. THE EAST INDIES TERTIARY TIME SCALE

3.1 INTRODUCTION

Because the Tertiary in different parts of the world has been subdivided into units based on a variety of criteria, correlations between regions still remain the subject of much discussion. Isotopic dating in conjunction with stratigraphic methods can assist in clarifying the numerous difficulties of worldwide biostratigraphic correlations which are

especially recognizable in the Tertiary. The subdivisions of the New Guinea Tertiary are based on the East Indies letter stages. The literature contains few or no physical dates associated with the East Indies letter stages, and, in the past, physical age boundaries have had to be extrapolated from dated stratigraphic equivalents elsewhere. Such extrapolations depend upon accurate strati-
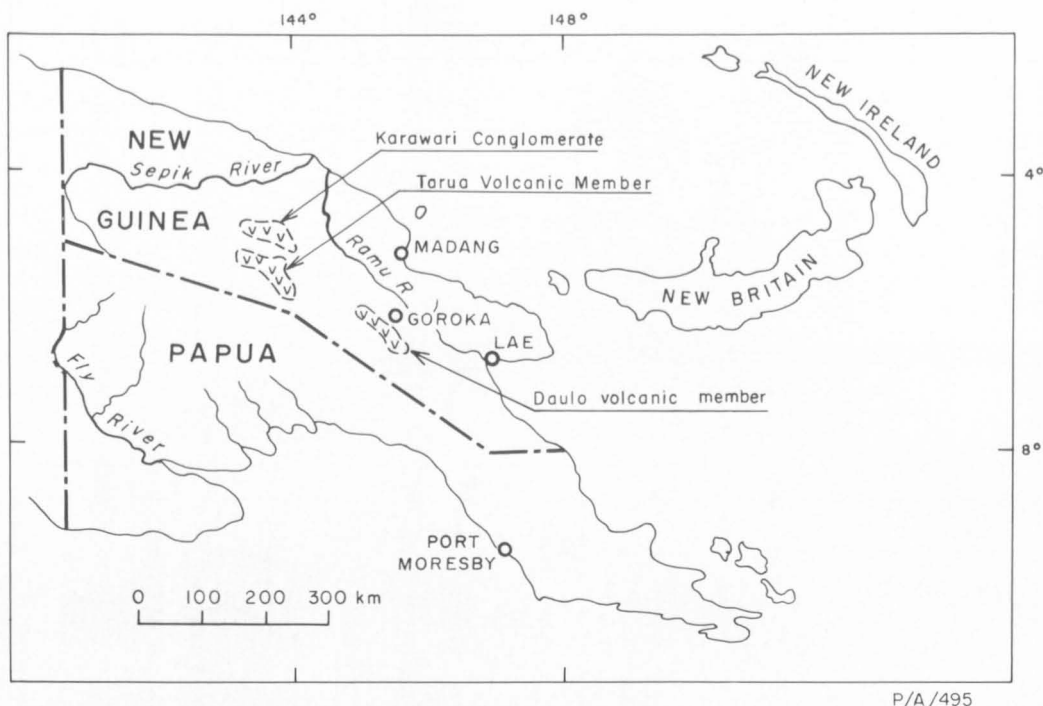
Fig. 7. Location map of Tertiary lower f-stage volcanics studied.

graphic correlations between the East Indies stages and the stages physically dated in other areas of the world.

In an attempt to (i) provide further control for the physical time scale of the East Indies letter stages, (ii) enable worldwide correlations to be made with greater precision, and (iii) determine the relative stratigraphic position of other physically dated rocks upon which there may be no, or little, stratigraphic control, K-Ar ages were measured for several lavas from the Central Highlands. Sedimentary rocks interbedded with the lavas contain foraminifera which give excellent stratigraphic control and limit the period of volcanism to the Tertiary lower f stage.

3.2 GEOLOGY OF THE NEW GUINEA LOWER f-STAGE VOLCANICS

The rocks studied were basalts, andesites, and trachytes from both the Burgers Formation (Tarua Volcanic Member) and the Karawari Conglomerate in the Western Highlands, and the Yaveufa Formation (Daulo volcanic member) in the Eastern

Highlands of New Guinea (Fig. 7). These rocks are part of the most widespread volcanic activity found in the New Guinea geological record (Dow, 1969; Dow et al., 1972). They are interpreted as part of the large belt of volcanism and tectonism (the New Guinea Mobile Belt) which extends for several hundred kilometres along the highlands of New Guinea and into central Papua.

The Tarua Volcanic Member (Figs. 8 and 9) is mapped at the base of the Burgers Formation and crops out on the northern limb of the Lai Syncline in a northwest-trending belt about 70 km long (Dow et al., 1972). The member consists of intermediate to basic volcanic rocks in a marine sequence (conglomerate, sandstone, and siltstone), which is mainly reworked volcanic material. The maximum thickness developed is about 2750 m. It is underlain by the Pundugum Formation, which contains a Tertiary e-stage fauna (Dow et al., 1972). Foraminifera from impure coralline limestones near the base of the Tarua Volcanic Member include the following: *Lepidocyclina (Nephrolepi-*
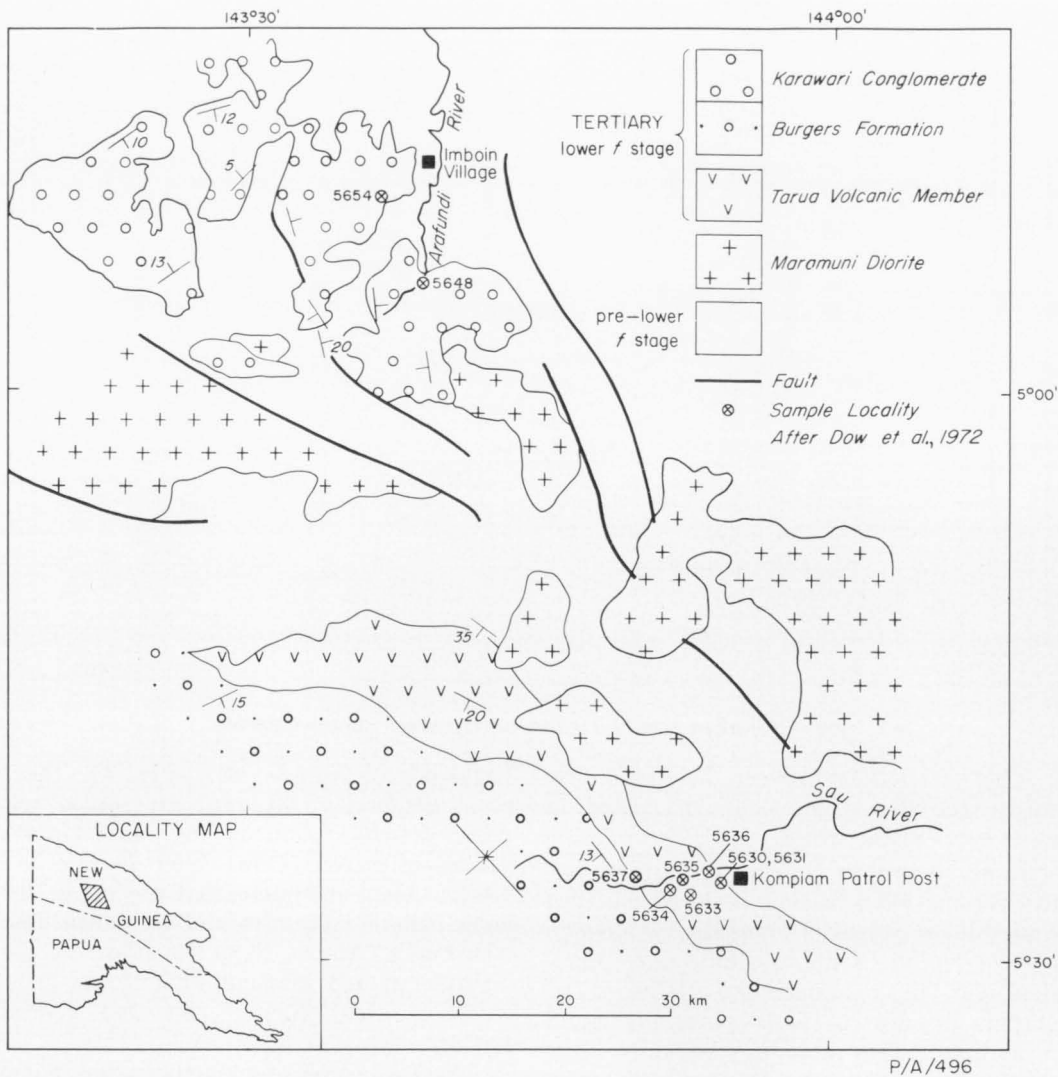
Fig. 8. Simplified geological map of the Tarua Volcanic Member and Karawari Conglomerate.

dina) ferreroi, Lepidocyclina (N.) sp., Mio-gypsina sp., Elphidium sp. Belford (in Dow et al., 1972) places this assemblage in the Tertiary lower f stage, and, as the base of the overlying part of the Burgers Formation is of the same age, the Tarua Volcanic Member must lie wholly within this stage.

The basic to intermediate volcanics which constitute the base of the Karawari Con-glomerate (Figs. 8 and 9) also overlie Ter-tiary e-stage sediments, and are generally similar to the Tarua Volcanic Member 19

km south (Dow et al., 1972). There are no fossils in the Karawari Conglomerate, but the basal volcanics are regarded as the same age (Tertiary lower f stage) as the Tarua Volcanic Member.

The Daulo volcanic member (Figs. 9 and 10) of the Yaveufa Formation lies 190 km southeast of the Tarua-Karawari sequence. It consists of basic and intermediate lavas and agglomerates, many of which are amygdaloidal and deuterically altered. Bain, Mackenzie, & Ryburn (in press) mapped the
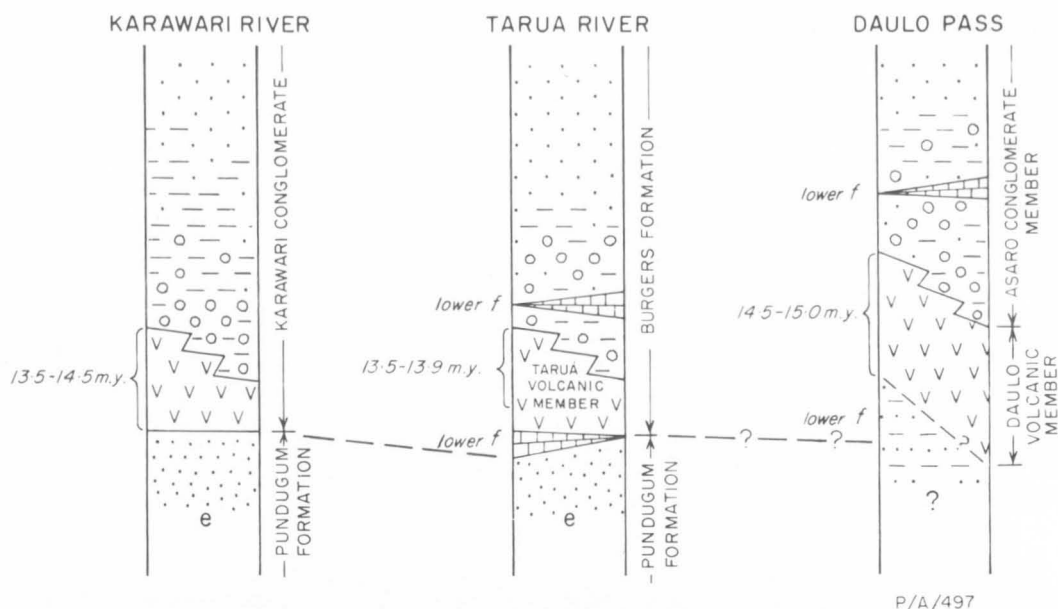
Fig. 9. Generalized stratigraphic relations and K-Ar ages of Tertiary lower f-stage volcanics.

Yaveufa Formation in a broad syncline 65 km long. The Daulo volcanic member overlies a thick sequence of foraminiferal shale, mudstone, and limestone, which, in the Watabung area, contain the following assemblage reported as Tertiary lower f stage by Crespin & Belford (1957): *Lepido-cyclina (Nephrolepidina) angulosa, L. (N.) sumatrensis, L. (N.) parva, L. (Trybliolepi-dina) verrucosa, Miogypsina kotoi, M. polymorpha, M. mammillata,* and *Katacyclo-clypeus annulatus.* Also in the sediments underlying the volcanics, Belford (pers. comm.) identified certain planktonic fora-minifera which include *Orbulina universa* and specimens of keeled *Globorotalia,* approximating to zones N.11 to N.12 of Banner & Blow (1965) and Clarke & Blow (1969). As the Daulo volcanic member also interfingers with the lower f-stage Asaro conglomerate member, its age is restricted to the lower f stage.

3.3 K-Ar DATING RESULTS

3.31 *Tarua Volcanic Member*

Samples were collected near the Sau River and the road section west of Kompiam pat-rol post (Fig. 8). The volcanics are part of a continuous marine succession which dips to the southwest. This is a typical section of olivine basalts of the Tarua Volcanic Mem-ber, and one in which there is unequalled stratigraphic control that limits the period of volcanism to the lower f stage. The measured ages of seven whole rocks and one pyroxene separate from the Tarua Volcanic Member are listed in Table 1. Agreement between replicate measurements is excellent.

The results generally show good internal consistency with the stratigraphy, as the samples (5630 and 5631) that yield the oldest ages (about 14 m.y.) occur towards the bottom of the member. The lower part of the Tarua Volcanic Member is separated from the e-stage sediments by a thin lower f-stage limestone bed, and, therefore, the 14 m.y. age may be close to the lower age limit of the lower f stage. A pyroxene (5630) age of 13.9 $\pm$ 3.4 m.y. is con-cordant with the whole-rock age, but it has a large error because of the high atmospheric argon contamination. The agreement be-tween the whole-rock and pyroxene ages indicates that they are minimum ages. A mean age of 13.3 $\pm$ 0.3 m.y. for a slightly more altered basalt (5636) from the Sau River is slightly younger than the other samples from the lowest part of the member,

16
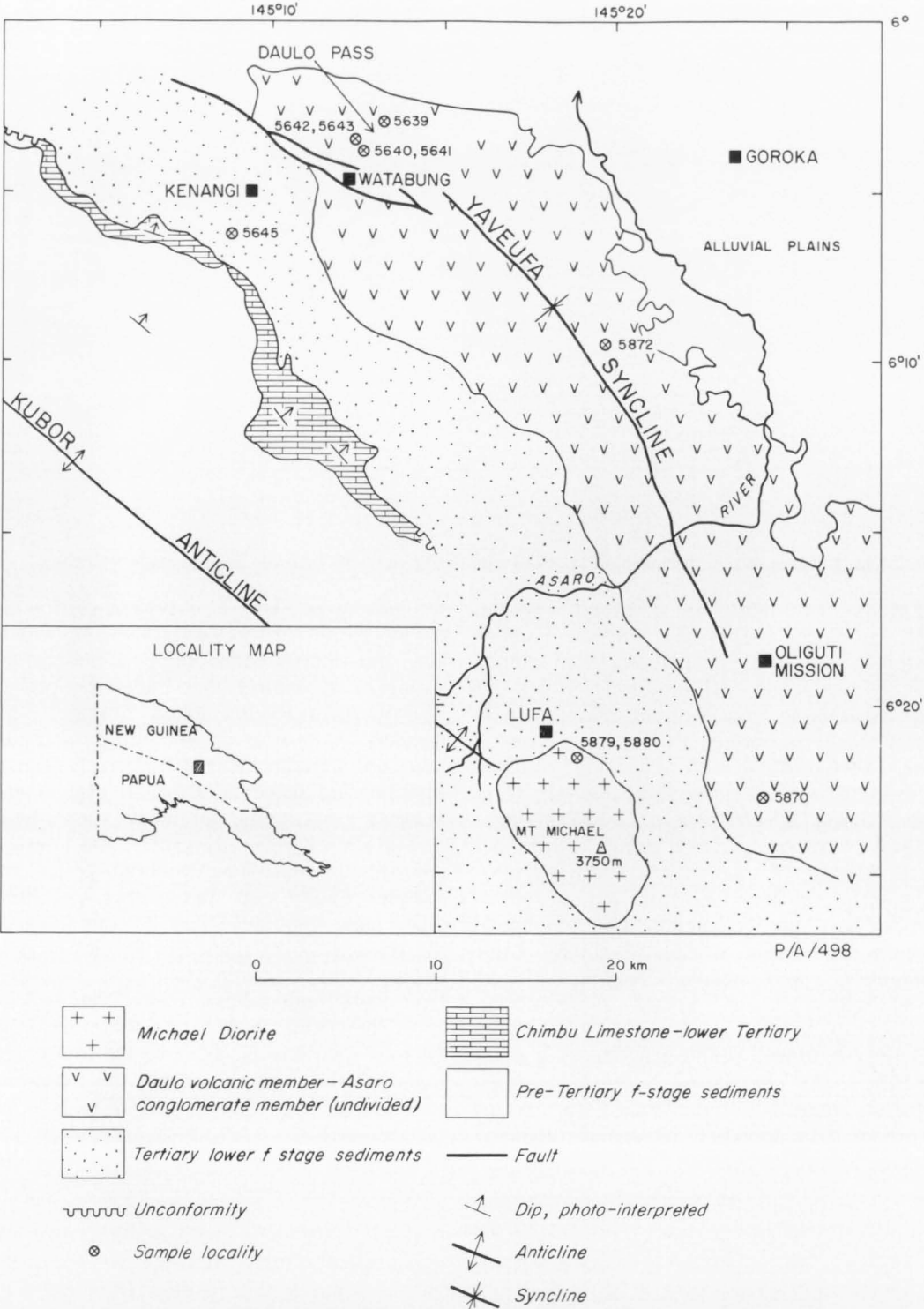
Fig. 10. Simplified geological map—Goroka area.

TABLE 1. K-AR AGES FOR THE TERTIARY LOWER *f*-STAGE VOLCANICS

No.	Sample	K %	$*Ar^{40}$ $x10^{-6} cm^3$ NTP/g	Ar^{40} %	Calculated age (m.y.)	Rock type and locality
Tarua Volcanic Member						
5630	Whole rock	0.760 } 0.759 0.758	0.419 0.411	35.8 36.9	13.8 ± 0.5 13.5 ± 0.5	Olivine basalts, road-cutting 6.4 km W of Kompiam
5630	Pyroxene	0.0398 } 0.0404 0.0410	0.023	2.4	13.9 ± 3.4	
5631	Whole rock	0.774 } 0.773 0.772	0.421 0.438	19.3 22.9	13.6 ± 0.6 14.1 ± 0.6	
5633	Whole rock	1.007 } 1.009 1.010	0.509 0.534	36.9 35.4	12.8 ± 0.4 13.2 ± 0.4	Olivine basalt, 8 km W of Kompiam
5634	Whole rock	0.913 } 0.918 0.922	0.475 0.481	40.9 21.2	13.0 ± 0.4 13.1 ± 0.6	Olivine basalt, 13 km W of Kompiam
5635	Whole rock	0.784 } 0.783 0.782	0.427	36.6	13.6 ± 0.4	Olivine basalt, Sau River, 9.5 km W of Kompiam
5636	Whole rock	1.277 } 1.280 1.282	0.671 0.684	50.1 42.3	13.1 ± 0.3 13.4 ± 0.4	Basalt, Sau River, 4.8 km W of Kompiam
5637	Whole rock	1.634 } 1.636 1.637	0.877	61.9	13.4 ± 0.3	Dolerite boulder from volcanic conglomerate, 13 km W of Kompiam
Karawari Conglomerate volcanics						
5648	Whole rock	1.681 } 1.680 1.678	0.973	79.8	14.5 ± 0.4	Pyroxene andesite, 8 km S of Imboin
5654	Whole rock	1.103 } 1.108 1.113	0.590 0.616	60.6 43.4	13.4 ± 0.4 13.9 ± 0.4	Hornblende andesite, 5 km S of Imboin
5654	Hornblende	0.270 } 0.271 0.272	0.187 0.186	38.7 30.6	17.2 ± 0.6 17.1 ± 0.8	
5654	Hornblende	0.268 } 0.268 0.267	0.303	54.2	28.2 ± 1.0	
Daulo volcanic member						
5639	Whole rock	5.700 } 5.712 5.723	2.917	56.3	12.4 ± 0.4	Brecciated lava
5640	Whole rock	6.128 } 6.121 6.114	2.911 2.991	63.0 58.0	11.9 ± 0.4 12.2 ± 0.5	Analcite basanite
5640	Analcite	3.566 } 3.551 3.536	1.630 1.467 1.723	64.4 40.5 44.9	11.5 ± 0.4 10.3 ± 0.4 12.1 ± 0.4	Daulo Pass section
5641	Whole rock	3.742 } 3.751 3.759	2.272 1.962	63.7 54.6	15.1 ± 0.4 13.1 ± 0.4	
5641	Pyroxene	0.0813 } 0.0824 0.0834	0.042	11.2	12.8 ± 0.7	
5642	Whole rock	2.445 } 2.450 2.454	1.110 1.046	75.0 55.4	11.4 ± 0.3 10.7 ± 0.3	Analcite basalt
5643	Whole rock	1.136 } 1.134 1.131	0.478 0.377 0.395 0.422	37.7 41.7 34.4 39.7	10.5 ± 0.3 8.3 ± 0.2 8.7 ± 0.3 9.1 ± 0.3	
5645	Whole rock	3.286 } 3.281 3.276	1.960 1.940	84.2 80.3	14.9 ± 0.4 14.8 ± 0.5	Trachyte, 3.2 km SW of Kenangi
5870	Whole rock	1.801 } 1.796 1.791	1.048	35.5	14.6 ± 0.6	Pyroxene andesite, 9 km S of Oliguti
5872	Whole rock	1.875 } 1.876 1.876	1.128	86.3	15.0 ± 0.5	Andesite, 20 km NW of Oliguti

but the rock may have lost some radiogenic argon because of slight alteration. The youngest mean ages of 13.0 ± 0.4 (5633) and 13.1 ± 0.5 (5634) were obtained for olivine basalts in the middle to upper parts of the member. A dolerite boulder (5637) from a conglomerate at the base of the overlying part of the Burgers Formation

gave an age of 13.4 ± 0.3 m.y., confirming that detritus from the Tarua Volcanic Member was the source material for the upper part of the Burgers Formation. Hence the Tarua Volcanic Member shows a spread in age from 13.0 to 13.9 m.y. It is possible that this spread covers the entire period of volcanism.

3.32 *Karawari Conglomerate volcanics*

Of 20 samples collected and examined from the Karawari Conglomerate volcanics, only two andesite samples were fresh enough for dating. Their localities, in the upper reaches of the Arafundi River, are shown in Figure 8, and results are given in Table 1; whole-rock mean ages are 14.5 ± 0.4 m.y. and 13.7 ± 0.4 m.y. The duplicate measurements agree to within experimental error, but there is no independent stratigraphic check on the dates. The agreement between the ages of the Tarua Volcanic Member and Karawari Conglomerate volcanics, and their inferred geological correlation, suggests that the latter have yielded reliable minimum ages. The apparent ages from the two separations of 5654 hornblende, however, are inconsistent, and are 20 to 100 percent higher than the whole-rock ages; the hornblende occurs in the rock as phenocrysts ranging from 1 to 20 mm in size. The poor reproducibility and the high apparent ages may be a result of the incorporation of various amounts of extraneous radiogenic argon from the environment into the hornblende phenocrysts when they crystallized at some depth before the magma erupted, but petrographic examination raises the possibility that some of the larger hornblende crystals may be xenocrysts rather than phenocrysts.

3.33 *Daulo volcanic member*

Samples of the Daulo volcanic member were collected from four widely spaced areas (Fig. 10), but, as the relation between most of the flows is not known, there is no superpositional control on the ages. Analyses of the volcanics were performed on a variety of rock types, and they show an apparent age spread of 7 m.y. (Table 1). However, only the oldest dates, from 14.5 to 15.0 m.y.,

are regarded as reliable ages. These include a trachyte sample (5645) dated at 14.9 ± 0.4 m.y., which probably marks the earliest outpourings of the Daulo volcanics; it comes from a flow (10 m thick) within the lower *f*-stage sediments and below the base of the defined Yaveufa Formation. The andesite (5870) was collected in the southern part of the formation, and its age (14.6 ± 0.6 m.y.) is close to that (15.0 ± 0.5) of a fresh andesite cobble (5872) from a conglomerate interbedded in the volcanics; the age of this cobble provides a possible maximum age for the conglomeratic sediments which are in the lower *f*-stage Asaro conglomerate member.

Most of the age determinations of samples near Daulo Pass (Fig. 10), however, are rejected as being too young to represent dates within the lower *f* stage in New Guinea. These samples, all of which contain analcite, alkali feldspar, and some devitrified glass, have apparent ages which range from 8.3 to 15.1 m.y. and probably reflect different degrees of argon leakage. Petrographically, all the Daulo Pass rocks are inferior for dating purposes, and they were analysed mainly on an experimental basis. Although these rocks are thought to be the youngest exposed of the Daulo lavas it is doubtful that the younger ages are meaningful. Results of replicate argon runs on several of them are poorly reproducible, apparently because the nature of the rocks led to sampling difficulties. Except for 5639, which is somewhat brecciated, the five Daulo Pass samples are petrographically similar to each other. They contain various proportions of phenocrysts of clinopyroxene, olivine, analcite, and plagioclase in a groundmass of interlocking potash feldspar, analcite, clinopyroxene, opaque oxide, needles of apatite, interstitial chlorite, sporadic amygdalar analcite, and interstitial patches of dusty brown devitrified glass. It is unlikely that all the argon loss can be attributed to the presence of devitrified glass, of which there are only small percentages in the samples analysed. McDougall, Allsopp, & Chamalaun (1966) reported little or no argon loss from basalts containing appreciable amounts of devitrified glass in Victoria, Australia. The alkali feld-

spar and analcite are primary minerals, and analcite has been found to be reliable elsewhere (McDougall & Wilkinson, 1967; Dasch, Armstrong, & Clabaugh, 1969); comparison of the whole-rock and mineral ages from 5640 (Table 1) does not point to argon loss from analcite as a plausible explanation. Argon leakage from alkali feldspar is probably the chief cause of the discrepancies found in the Daulo Pass samples. The young apparent ages and poor replication may also be related to potassium inhomogeneity between groundmass analcite and amygdalar analcite. Wilkinson (1962) has shown that amygdalar analcite is depleted in potassium with respect to analcite which occurs elsewhere in a rock. If this inhomogeneity can be generally applied to analcite basalts, then the potassium and radiogenic argon content of amygdalar analcite must be treated as a distinct phase, and rocks containing large amygdales could introduce serious sampling problems.

3.4 TERTIARY SUBDIVISIONS AND CORRELATIONS

The precise age limits of a geological event cannot be determined until the event itself and the preceding and succeeding intervals have been dated. Using the available field evidence, the dating of the lower *f*-stage volcanic suites in New Guinea has yielded reliable ages between 13 and 15 m.y. (Fig. 9), and it is suggested that the approximate age limits of this stage are 12.5 and 15 m.y. The general concordancy of the ages, particularly from the Tarua Volcanic Member, is interpreted as a date of eruption rather than one relating to a subsequent event.

Before comparing these results with Tertiary stages dated elsewhere in the world, it is desirable to outline the stratigraphic basis of Tertiary-stage nomenclature, firstly for the classical European sections and then for the East Indies.

3.41 *European Tertiary stages*

The basic subdivision of Lyell (1833, *in* Lyell, 1865) of the marine Tertiary of western Europe into Pliocene, Miocene, and Eocene was based on the percentage of living species of Mollusca found in the Tertiary sequences. The term 'Oligocene' was later proposed by Beyrich (1854) to include beds that were formerly classed partly as upper Eocene and partly as lower Miocene.

Since the latter part of the nineteenth century, the European Tertiary has been divided into several stages, and the present correlation difficulties start in the stratotype areas where these stages (Pontian, Tortonian, Helvetian, Langhian, Burdigalian, Aquitanian, etc.) were first defined. Although some of them contain minor breaks, the type sections of the stages were originally chosen for their abundance of the larger fossils, particularly Mollusca and Echinoidea (Glaessner, 1959). Unfortunately there are few continuous sections, and some of the sediments were deposited in brackish water. Hence there is a general paucity of planktonic fossils suitable for long-range correlation in the type sections (Drooger, 1956; Stainforth, 1960; Jenkins, 1965). In places, overlapping type sections of different environments cannot be properly correlated (cf. Glaessner, 1953, 1960; Jenkins, 1965). The situation was summarized by van der Vlerk (1959), who referred to 'the deplorable uncertainty surrounding European type localities'.

The subdivisions of the Tertiary period are much smaller than other subdivisions in the Phanerozoic, and any errors in correlation become magnified as they are applied to these short time divisions. Some populations of species are recognized as characteristic of particular Lyellian epochs, and it is by this method that the relation between the European Miocene stages and the Lyellian concept is deduced (Glaessner, 1953; Lipps, 1967; Clarke & Blow, 1969; Berggren, 1971); thus the Aquitanian and Burdigalian are generally regarded as lower Miocene; the middle Miocene comprises the Helvetian and Tortonian, which constitute the Vindobonian; and the Messinian, Sarmatian, and Pontian have upper Miocene affinities.

The exact correlation of the stages with the Lyellian epochs and the Oligocene is still much debated (Glaessner, 1953; Stainforth, 1960; Eames, Banner, Blow, & Clarke,

1962; Drooger, 1964; Banner & Eames, 1966). Blow (1969) believe that the 'problem of deciding what stages should be grouped together and placed into a particular system' reduces to a compromise between the biostratigraphic and geological utilitarian aspects. Although it is recognized that the positions of many of the boundaries are arbitrary, the assignment of stage names to epochs must be approved generally in order that correlations can be made throughout the world.

To help overcome the difficulties of Tertiary correlation, and instead of rejecting the conventional stages in Europe altogether, stratigraphers now correlate rocks that contain faunas more suitable for long-range correlation with the original stratotype. Hence, the admission and definitions of these parastratotypes, which contain fossil assemblages not wholly represented in the holostratotype, are now widely accepted; however, many of the relations are by no means unequivocal (Banner & Eames, 1966).

3.42 *East Indies letter stages*

When stratigraphers first tried to correlate the East Indies Tertiary sequence with the sequences in Europe there were no well defined fossil zones in existence. Consequently they turned to the next higher classification, the stage, as the basic unit for comparing and measuring geological time (Glaessner, 1943). However, the European Tertiary stages have proved to be difficult to recognize outside Europe (Jenkins, 1965; Adams, 1970).

Different approaches to the stratigraphic problems of the East Indies included the use of the 'percentages method' of living species of mollusca (Martin, 1921), which was analogous to that originated by Lyell in Europe. The present method of dividing the East Indies Tertiary was initiated by van der Vlerk & Umbgrove (1927), and was based solely on the assemblages of genera of tropical larger foraminifera and their stages of evolution in the local sequences. They introduced the letter-stages 'a' to 'f' and later 'g' to 'h', which were then tentatively assigned to the Tertiary epoch (Table 2).

TABLE 2. TENTATIVE CORRELATIONS OF LETTER STAGES AND TERTIARY EPOCHS (VAN DER VLERK, 1931)

Epoch	Letter stage
Pliocene	h
upper Miocene	upper f, g
lower Miocene	e, lower f
Oligocene	c, d
Eocene	a, b

This scheme is still useful for correlations within a limited area, but the letter stages are not generally applicable to long-range correlations (Glaessner, 1953; van der Vlerk, 1959).

The East Indies letter stages are based solely on assemblages of tropical larger foraminifera without reference to type sections, whereas the classical European Tertiary stages, which are based mainly on temperate-zone mollusca and (more recently) foraminifera, refer to type sequences; thus correlations between the two are difficult. However, the palaeontological and stratigraphic studies of Tan Sin Hok (1936, 1939), which are summarized by Glaessner (1943), established the letter stages on a firmer base, and enabled tentative correlations of these stages with the classical European stages. These correlations are set out in Table 3(a); they agree with those presented in van Bemmelen (1949) and Mohler (1949) except that the latter show the lower e stage as Aquitanian, and the uppermost part of the e stage as equivalent to the lower part of the Burdigalian. The stage names lower f and upper f are synonymous with the terms f_{1-2} and f_3 respectively.

During recent years the establishment of the planktonic foraminiferal zones has led to a modification of the correlations between the European and East Indies Tertiary stages (Table 3(b)). This more refined correlation of Banner & Blow (1965) and Clarke & Blow (1969) places the lower f stage between the planktonic foraminiferal zones $N.9$ and $N.12$. By comparing Table 3(b) with Table 3 (a) it is clear that the East Indies stages are now thought to be younger relative to the European chronology than they were before the establishment of the

European stages	East Indies letter stages
Pontian Messinian	g
'Tortonian' 'Helvetian'	upper f (f_3)
Burdigalian	lower f (f_{1-2})
Aquitanian	upper e
Oligocene stages	lower e
Eocene stages	a, b

Miocene Stages

TABLE 3(a)
Comparison between the East Indies letter stages and the European stages—modified after Tan Sin Hok (1936, 1939); van der Vlerk (1959); Eames, Banner, Blow, & Clarke (1962); Belford (1962); Banner & Eames (1966); Adams (1968).

European stages	Planktonic foraminiferal zones	East Indies letter stages
Messinian	N.18	g
Tortonian	N.17 N.16	
Serravallian	N.15 N.14 N.13 N.12	upper f
	N.11 N.10	lower f
Langhian	N. 9	
Burdigalian	N. 8 N. 7 N. 6	upper e
Aquitanian	N. 5 N. 4	

TABLE 3(b)
Comparison between the East Indies letter stages and the European stages—modified after Banner & Blow (1965); Clarke & Blow (1969); middle and upper Miocene European stages based on Cita & Blow (1969).

planktonic foraminiferal zones; thus the lower f stage is now equated with the lower Langhian of Clarke & Blow (1969) or upper Langhian-lower Serravallian of Cita & Blow (1969) and Berggren (1971), and both the Aquitanian and Burdigalian are now regarded as being equivalent to the upper e stage.

The palaeontological studies since 1965 (Table 3(b)), therefore, suggest some important changes to the earlier stratigraphic correlations (Table 3(a)) between the European stages and the East Indies letter stages. The lower f stage is equated with the Burdigalian in Table 3(a), but with the Langhian-Serravallian interval in Table 3(b). With reference to the Geological Society of London time scale (Funnell, 1964), the earlier correlations shown in Table 3(a) suggest an isotopic age of about 18 to 25 m.y. for the lower f stage, whereas the more recent correlation shown in Table 3(b) implies an age of 14 to 18 m.y. (Blow, 1969, fig. 20). It is clear that the limits of the lower f stage of about 12.5 and 15 m.y. suggested from the New Guinea data are considerably younger than expected on the basis of the presently accepted physical time scale. During the compilation of the Geo-logical Society of London time scale, relatively few physical age measurements were available on rocks in marine Tertiary sequences. Much reliance was placed on correlations of the terrestrial sequences of North America with worldwide marine sequences. These terrestrial sediments contain excellent mammalian faunas, which have been well dated by Evernden, Savage, Curtis, & James (1964) using interbedded lavas and tuffs. In view of the difficulties of correlating terrestrial and marine sequences, a review of the data presently available is necessary to determine whether the New Guinea results are consistent.

3.5 ISOTOPIC CORRELATIONS OF SOME TERTIARY STAGES

In this summary of the published and unpublished data, an attempt is made to convoke the age determinations on rocks which have good stratigraphic control. The relevant isotopically dated Miocene stages are placed against a linear scale in Figure 11 and the dates themselves are listed in Table 4. At first, only those ages that are related to marine sequences are considered. It is shown later that, if the accepted continental-marine corelations (Evernden et al.,

TABLE 4. K-Ar AGES RELEVANT TO THE MIOCENE TIME SCALE

Isotopic age (m.y.)	Stratigraphic position	Material dated	Reference	Locality
4.9 ± 0.4	Miocene-Pliocene boundary	Whole rock, biotite, hornblende	Gill & McDougall, 1973	Fiji
6 — 7	Miocene-Pliocene boundary	Biotite	Charlot et al., 1967	Morocco
9.5	Upper Miocene	Glauconite	Evernden et al., 1961	Kadenberge, Germany
9.8 — 11.7	Clarendonian	Sanidine, whole rock	Evernden et al., 1964	California
9.3 — 11.3	Upper f (f_3) stage	Hornblende, biotite, feldspar	Rodda et al., 1967	Fiji
11.4 ± 0.6	Mohnian	Glass	Dymond, 1966	Experimental Mohole, Guadalupe site
12.3 ± 0.4	Lower Luisian	Glass	Dymond, 1966	Experimental Mohole, Guadalupe site
13.0 ± 0.1	Waiauan to lower Tongaporutuan	Whole rock, anorthoclase	McDougall & Coombs, 1973	Dunedin Volcanics, New Zealand
13.7 — 14.5	Relizian-Luisian boundary	Plagioclase	Turner, 1970	California, Oregon, Washington
15.3	Saucesian-Relizian boundary	Plagioclase	Turner, 1970	California, Oregon, Washington
12.3 — 15.6	Barstovian	Whole rock, biotite, sanidine	Evernden et al., 1964	California
12.5 — 15	Lower f (f_{1-2}) stage	Whole rock, mineral	Page, this Bulletin	New Guinea highlands
15.4 ± 1.0	Hutchinsonian	Glauconite	Funnell, 1964—after Lipson, 1956, 1958	South Island, New Zealand
15.3 — 15.9	Upper Burdigalian	Whole rock	McDougall & Roche (unpublished)	Upper flow, Gergovie, France
15.2 ± 0.5	Altonian	Whole rock	Stipp, 1968	Northland, New Zealand
16.1 ± 0.3	Otaian to Altonian	Whole rock	Stipp, 1968	Northland, New Zealand
16.0 ± 1.0	Upper Burdigalian	Whole rock	Bout et al., 1966	Upper flow, Gergovie, France
16.2	Upper Burdigalian	Whole rock	McDougall & Roche (unpublished)	Côtes de Clermont, France
17,1	Hemingfordian	Biotite	Evernden et al., 1964	California
19.4 ± 1.2	Waitakian	Glauconite	Funnell, 1964—after Lipson, 1956, 1958	South Island, New Zealand
18.0 ± 1.0	Upper Stampian to Aquitanian	Whole rock	Bout et al., 1966	Gergovie Dyke, France
18.6 — 19.9	Upper Stampian to Aquitanian	Whole rock	McDougall & Roche (unpublished)	Gergovie Dyke, France
21.4 ± 0.3	Janjukian-Longfordian boundary	Whole rock	Abele & Page, 1974	Maude, Victoria, Australia
21.3 — 25.6	Arikareean	Whole rock, feldspar, biotite	Evernden et al., 1964	California
22.5	Zemorrian-Saucesian boundary	Plagioclase	Turner, 1970	California coast
23.1 ± 0.7	Upper Zemorrian	Plagioclase	Turner, 1970	California
23.3	Oligocene-Miocene boundary	Glassy shards	Selli & Tongiorgi, 1967	Bologna, Italy
26.5 ± 0.5	Lower to middle Janjukian	Whole rock	Abele & Page, 1974	Airey's Inlet, Victoria, Australia

1964, fig. 1) are adopted, the recent reliable isotopic dates from marine sequences would be incompatible with the physical time scale based on fossil mammals in western North America.

3.51 Europe

Direct age measurements from European marine stages are few, and most of the dates reviewed here were not available to von Koenigswald (1962) or to Funnell (1964), both of whom earlier summarized physical dates in the European Tertiary.

The Oligocene-Miocene boundary age determination of 23.3 m.y. in Bologna, Italy (Selli & Tongiorgi, 1967) is based on the K-Ar dating of glassy material in a volcanic ash interbedded with marl.

Stratigraphically controlled lower Miocene dykes and flows in Gergovie, France, have been dated by Bout, Frechen, & Lippolt (1966) and McDougall & Roche (unpublished). Michel (1953) suggested an Aquitanian age for the dykes, which intrude Stampian limestone, but according to Glangeaud (1957) their age is upper Stampian. Bout et al. (1966) determined an age of 18 ± 1 m.y. for the Gergovie Dyke. This is close to several concordant dates which have a mean of 19.5 m.y. (McDougall & Roche, unpublished). These age determinations may be applied to either Michel's (1953) or Glangeaud's (1957) interpretations of the stratigraphic age of the dykes.

Isotopic dating of an upper Burdigalian flow at Gergovie (upper flow) and another at Côtes de Clermont by Bout et al. (1966) and McDougall & Roche (unpublished) gave concordant ages of 15 to 16 m.y. These dates provide a minimum for the upper Burdigalian of France, and are consistent with the date of 19.5 m.y. for the stratigraphically older Gergovie Dyke.

Evernden, Curtis, Obradovich, & Kistler (1961) dated a glauconitic sandstone from a well near Kadenberge (25 km southwest of Stade), in West Germany, at 9.5 m.y. They regarded the date as being too young for the known upper Miocene stratigraphy '. . . when compared with dates for western USA'. From Figure 11 it is clear that 9.5 m.y. is a reasonable estimate for the age of the upper Miocene. A stratigraphically controlled age estimate for the Miocene-Pliocene boundary in Morocco is given as 6 to 7 m.y. by Charlot, Choubert, Faure-Muret, Hottinger, Marçais, & Tisserant (1967).

A few previously documented European dates are omitted from Table 4. They include a glauconite date of 25 m.y. from the 'Burdigalian' of the Vienna Basin, Austria (Evernden et al., 1961); the doubtful reliability of this estimate is discussed in detail by Lipps (1967) and Turner (1970). Another age estimate, that of Lippolt, Gentner, & Wimmenauer (1963) for the Burdigalian/Helvetian boundary as 17 m.y. in the Kaiserstuhl area of Germany, may be in accord with a 25 m.y. age for the base of the Burdigalian Stage, but this is too old when compared with more recent age data from elsewhere; the discrepancy may be partly because of some difficulties in correlating the Kaiserstuhl sequence, which has a vertebrate fauna, with the marine stages, but in addition, as pointed out by the authors themselves, there are discordances between their K-Ar data and the field evidence.

3.52 New Zealand

Two K-Ar glauconite dates and three whole-rock dates from the marine Miocene of New Zealand are included in Table 4. Using more recent decay constants, Funnell (1964) recalculated the glauconite data of Lipson (1956, 1958) giving ages of 19.4 m.y. for a sample within the Waitakian Stage and 15.4 m.y. for a sample within the Hutchinsonian Stage. Funnell considered the 15.4 m.y. date for the Hutchinsonian as being too young because this stage was at that time regarded as lowermost Miocene; when compared with other lower Miocene dates then available, 15.4 m.y. was clearly discrepant. More recently, however, the Hutchsinsonian Stage has been regarded as late lower Miocene (Jenkins, 1966; Hornibrook, 1968), and an age of 15.4 m.y. is in reasonable agreement with late early Miocene ages obtained in marine successions elsewhere (cf. Fig. 11). Stipp (1968) obtained a minimum whole-rock age of 16.1 m.y. for rocks within the Otaian-Altonian interval.

TIME SCALE m.y.	EPOCH	NEW ZEALAND	FIJI	NEW GUINEA	VICTORIA	CALIFORNIA	EUROPE	WESTERN U.S.A. MAMMAL 'AGES'
5	PLIOCENE		PLIOCENE 4·9	— — ? — —			— — ? — — 6-7	
			g STAGE	g STAGE		DELMONTIAN	MESSINIAN 9·5	HEMPHILLIAN
10		TONGAPORUTUAN	UPPER f STAGE 9·3 11·3	— — ? —		MOHNIAN 11·3	TORTONIAN	— — — — — 10 CLARENDONIAN
	MIOCENE	WAIAUAN 13·0		— — — 12·5		LUISIAN 12·4 13·7	SERRAVALLIAN	— — — — — 12 / 13
		LILLBURNIAN	LOWER f STAGE			RELIZIAN 14·5 15·3	LANGHIAN 15·6	BARSTOVIAN
15		ALTONIAN 15·2 HUTCHINSONIAN OTAIAN 15·4 } 16·1		15		15-16	BURDIGALIAN 16·2	17
20		WAITAKIAN 19·4	UPPER e STAGE		LONGFORDIAN	SAUCESIAN	AQUITANIAN 19·5	HEMINGFORDIAN 21
				— — — 21·4		22·5 23·1	23·3	ARIKAREEAN
25	OLIGOCENE				JANJUKIAN	ZEMORRIAN 26·5	STAMPIAN	26

← — — — — — — — — — — MARINE — — — — — — — — — — → | ← NON-MARINE →

M(S) 360

Fig. 11. Correlation of Miocene stages based on K-Ar ages. (Earlier correlations between the marine ages of Europe and the mammal ages of the western USA are indicated by pattern symbols.)

Each of the whole-rock and glauconite dates is based on a single age measurement. Therefore, until further physical dating of the New Zealand Miocene is undertaken, they must be regarded as tentative. Their questionable validity is highlighted by reference to two other glauconite dates (Lipson, 1956, 1958) of 21.1 ± 1.5 m.y. in the Waiauan (middle Miocene) and 22.0 ± 1.5 m.y. in the Duntroonian-Whaingaroan (lower to middle Oligocene); they have been recalculated (Funnell, 1964) as 19.9 m.y. and 20.8 m.y. respectively. Both dates are anomalous whether compared with the time scale based on fossil mammmals (Funnell, 1964) or that based on dated marine sequences.

Concordant dates of 13.0 m.y. have been obtained for stratigraphically controlled late Lillburnian to Waiauan (or possibly early Tongaporutuan) lavas of the Initial Eruptive Phase of the Dunedin Volcanics (McDougall & Coombs, 1973). Hornibrook (in Fleming,

1959, p. 429) points out that the New Zealand Waiauan Stage can be correlated with the East Indies upper f stage, and Jenkins (1966) and Hornibrook (1968) suggest that the Lillburnian-Waiauan interval is equivalent to the latter half of the middle Miocene. The 13 m.y. result thus provides a confident date for this part of the New Zealand Miocene.

3.53 Fiji

A limited amount of data relevant to the Miocene time scale is available from Fiji (Rodda, Snelling, & Rex, 1967). Tonalites of the Tholo Suite (which are dated between 9.3 and 11.3 m.y.) are overlain by probable upper f to early g-stage (middle to upper Miocene) sediments. This suggests a maximum age of 9 to 11 m.y. for the upper f stage in Fiji.

A recent estimate of 4.9 ± 0.4 m.y. for the Miocene-Pliocene boundary in Fiji (Gill & McDougall, 1973) provides an additional

data point on the physical time scale (Fig. 11) in this region of the world.

3.54 *Pacific Coast, USA*

Dating by Turner (1970) has provided a good check for the physical age of the Pacific Coast foraminiferal stages (Fig. 11). The isotopic ages for these Miocene stage boundaries are: Zemorrian-Saucesian, 22.5 m.y.; Saucesian-Relizian, 15.3 m.y.; Relizian-Luisian, 13.7 to 14.5 m.y.; and Luisian-Mohnian, less than 13 m.y. A tentative age of between 11.4 and 12.3 m.y. was given by Dymond (1966) for the Luisian-Mohnian boundary from his dating of glass shards. Berggren (1969b) has summarized Turner's (1970) dating, and has interpreted the physical ages in terms of the established planktonic foraminiferal zones. Using magnetic stratigraphy methods, Hays, Saito, Opdyke, & Burckle (1969) have given estimates for the ages of fossil zones in deep-sea cores from the equatorial Pacific. By extrapolation they conclude that the Miocene-Pliocene boundary in Italy has an age slightly greater than 4.5 m.y. Berggren (1969b) assigns an age of 5.5 m.y. to this boundary.

3.55 *Victoria, Australia*

Recent K-Ar dating in Victoria (Abele & Page, 1974) was undertaken specifically to gain further control on the dating of stratigraphic intervals in the lower Miocene and upper Oligocene. Concordant K-Ar ages were obtained for basalts which are stratigraphically controlled by planktonic foraminifera. A mean age of 21.4 ± 0.3 m.y. is reported for a basalt flow lying near the boundary of 'faunal unit 5' and 'faunal unit 6' of Carter (1964). Locally, this is the Janjukian-Longfordian Stage boundary, which is thought to correspond to the lowermost lower Miocene. Another age of 26.5 to 27 m.y. is reported for a basalt flow of early to mid-Janjukian (mid-Oligocene) age.

3.56 *Implications for East Indies letter stage time scale*

The correlations explicit in Figure 11 are based only on K-Ar ages for rocks which occur where there is good stratigraphic control. These ages and the rejection of earlier, poorly controlled ages suggest several revisions of the age boundaries of these marine stages.

In Figure 11 the relationship between the upper *f* stage dated in Fiji (Rodda et al., 1967) and the lower *f* stage dated in New Guinea implies that the lower *f*/upper *f* stage boundary is about 11.5 to 12.5 m.y. old. Figure 11 also shows that the lower *f* stage of New Guinea is equivalent to the Langhian-lower Serravallian interval of Europe, hence substantiating the recent stratigraphic correlations summarized in Table 3(b). The dated boundaries in Europe and New Guinea imply that both the Burdigalian and Aquitanian stages are probably equivalent to the upper *e* stage.

The relationship between the European and Californian marine stages is in accord with the stratigraphic interpretations of Lipps (1967). These correlations are discussed in more detail by Berggren (1969b). The correlation of the Aquitanian with the Saucesian gives an estimate for the base of the Aquitanian of 22 to 23 m.y., which corresponds to the Oligocene-Miocene boundary (cf. Selli & Tongiorgi, 1967). This agrees quite closely with the Victorian estimate of about 21.4 m.y. (Abele & Page, 1974).

3.6 COMPARISONS OF THE PHYSICAL AGES OF CONTINENTAL AND MARINE SUCCESSIONS

The range of dates obtained by Evernden et al. (1964) in the non-marine succession of western USA provides an internally consistent time scale for the mammalian chronology (Fig. 11). They summarized the vertebrate palaeontologists' provisional correlations of the land-mammal stages with the European and Pacific Coast marine stages. At that time little direct dating of the European marine stages had been done. Turner's (1970) dating of the Californian marine stages, and Lipp's (1967, 1968) correlations based on planktonic foraminifera and calcareous nannoplankton of the same stages with the European successions, permit more reliable age estimates to be assigned to the European stages. Berggren (1969b) proposed revisions within the Miocene which

are based on the Californian stage dates obtained by Turner (1970). The dating of the lower f stage of New Guinea, and the new dates obtained for the European Aquitanian and Burdigalian, confirm the recent correlations of worldwide marine stages (Clarke & Blow, 1969; Lipps, 1967) and substantiate the conclusions reached by Berggren (1969b, 1971) that the provisional correlations (cf. Evernden et al., 1964, fig. 1) of the non-marine mammalian stages with the European stages are discordant with the isotopic age data. The discordances are illustrated in Figure 11 by the pattern symbols, which represent the earlier stratigraphic correlations. The western USA mammal 'ages' are older than their supposed European correlatives: the base of the Aquitanian 'equivalent' (just below the Arikareean base) is 4.5 m.y. older in the mammalian chronology, and the Burdigalian 'equivalent' is about 7 m.y. older.

3.7 SUGGESTED EAST INDIES MIOCENE TIME SCALE

From the literature reviewed and the dating carried out on the Tertiary volcanics in New Guinea, a time scale is postulated for the relevant East Indies letter stages (Fig. 11). The limits of the upper e stage are thought to range from 22.5 m.y. to 15 m.y.; the lower f stage, 15 m.y. to 12.5 m.y.; the upper f stage, 12.5 m.y. to 9 m.y.; and the g stage, 9 m.y. to the top of the Miocene, about 5.5 m.y.

4. LATE PALAEOZOIC TO MESOZOIC PLUTONIC ACTIVITY

4.1 INTRODUCTION

K-Ar mineral and whole-rock ages and a smaller number of Rb-Sr ages have been measured on all the major intrusive bodies and some metamorphic rocks in part of the Main Cordillera of New Guinea (Plate 1). This section deals with the late Palaeozoic to Mesozoic plutonic activity, which occurred before or in the early stages of the development of the Papuan Geosyncline. In general the Tertiary plutons (see section 5) lie on the northeast (Pacific Ocean) side of the pre-Tertiary intrusive masses, but there is some overlapping of the younger onto the older intrusions.

The isotopic age data related to the Palaeozoic-Mesozoic history indicate periods of granitic intrusions in the Late Permian, the Late Triassic to Early Jurassic, and the mid-Cretaceous. The largest exposed area is the Kubor massif in the Kubor Range. The other Mesozoic plutonic rocks (the Strickland Granite, the Urabagga intrusives, the intrusives into the Bena Bena Formation, and the Mount Victor Granodiorite) crop out over a limited area, as they are covered by the younger sedimentary sequences.

4.2 KUBOR RANGE PLUTONIC ROCKS

The oldest-known rocks in Papua New Guinea, the Omung Metamorphics and Kubor Granodiorite, occupy the core of the Kubor Anticline, which is over 120 km long and 50 km across (Fig. 12). It was first mapped by Rickwood (1955), who believed that the granitic and metamorphic rocks in the core are unconformably overlain by an incomplete marine succession of Permian, Upper Jurassic, Cretaceous, Eocene, Oligocene, and Miocene sediments, with a maximum thickness exceeding 10 000 m. The region was folded in the Late Tertiary. Recent workers in the area (Bain et al., in press) confirmed the general structure as outlined by Rickwood (1955), and also mapped possible Triassic volcanics as part of the anticlinal sequence; Bain et al, however, believe that the Mesozoic-Cainozoic sediments have a maximum thickness of 6300 m.

The stratigraphic age of the Kubor Granodiorite is a matter of some debate. The Kubor batholith intrudes unfossiliferous low-grade metamorphosed sediments and volcanics of the Omung Metamorphics of unknown age. In several areas in the western and northeastern parts of the anticline, the granodiorite and metamorphics are unconformably overlain by the Kuta Formation (calcareous arkoses grading upwards into limestone), which is the lowest unit of the
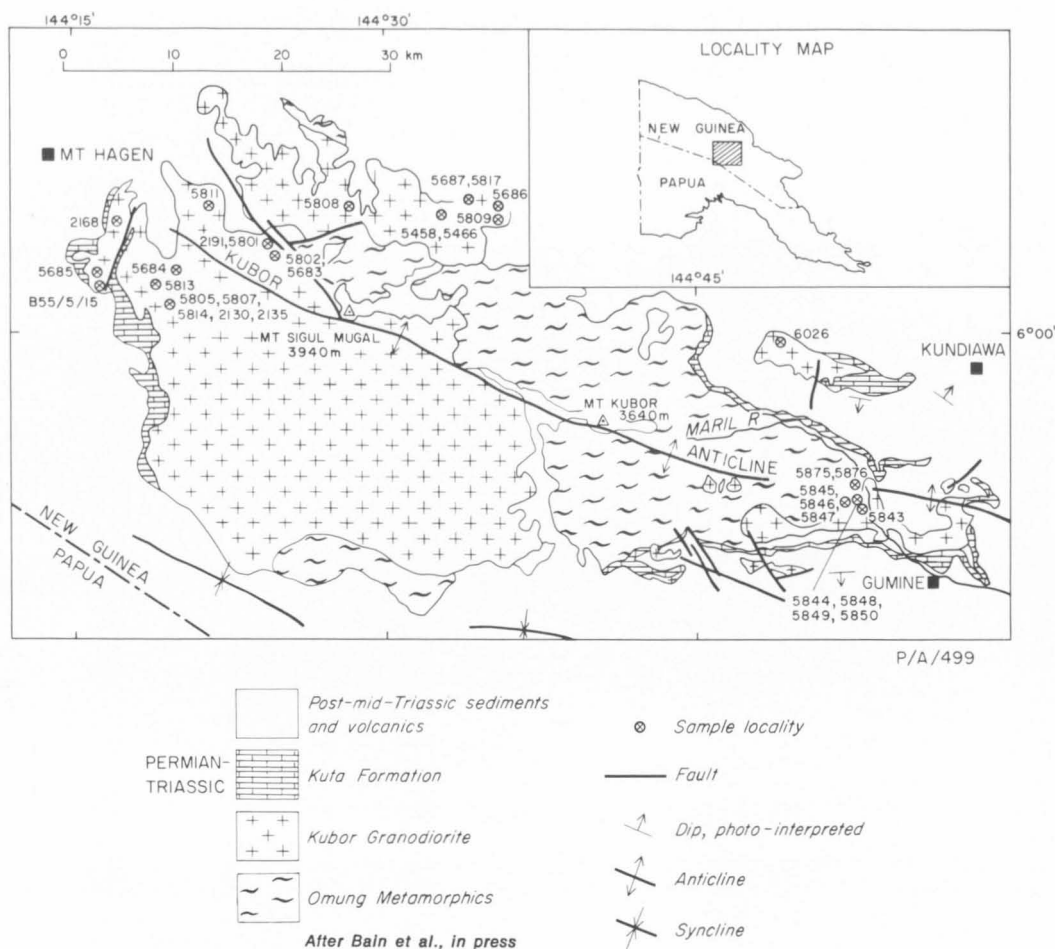
Fig.12. Simplified geological map—Kubor Range area.

Kubor Anticline succession. The age of the Kuta Formation thus provides an upper limit to the age of the Kubor Granodiorite. A Permian age for the foraminifera of the Kuta Formation was determined by Glaessner, Llewellyn, & Stanley (1950), and the Kubor Granodiorite has since been regarded as pre-Permian in age. However, the recent mapping and palaeontological examination of brachiopods from the Kuta Formation (K.S.W. Campbell, pers. comm.) have led to a review and possibly a slight modification of the age (Bain et al., in press). The brachiopods have affinities to both Permian and Triassic types and their age is considered to be close to that of the Permian-Triassic boundary. A full discussion is given by Bain et al., who conclude that the Kuta Formation may have rather broader age limits from Late Permian to Late Triassic.

The Kubor Granodiorite was sampled in areas only where it intrudes the Omung Metamorphics, which are briefly discussed before proceeding to the Kubor Granodiorite data.

4.21 Omung Metamorphics

Rickwood (1955) believed that these rocks represent the oldest sediments in Papua New Guinea, and McMillan & Malone (1960) subsequently correlated them with the metamorphics near Goroka. Fossils have never been found in the Omung Metamorphics, and, apart from a knowledge
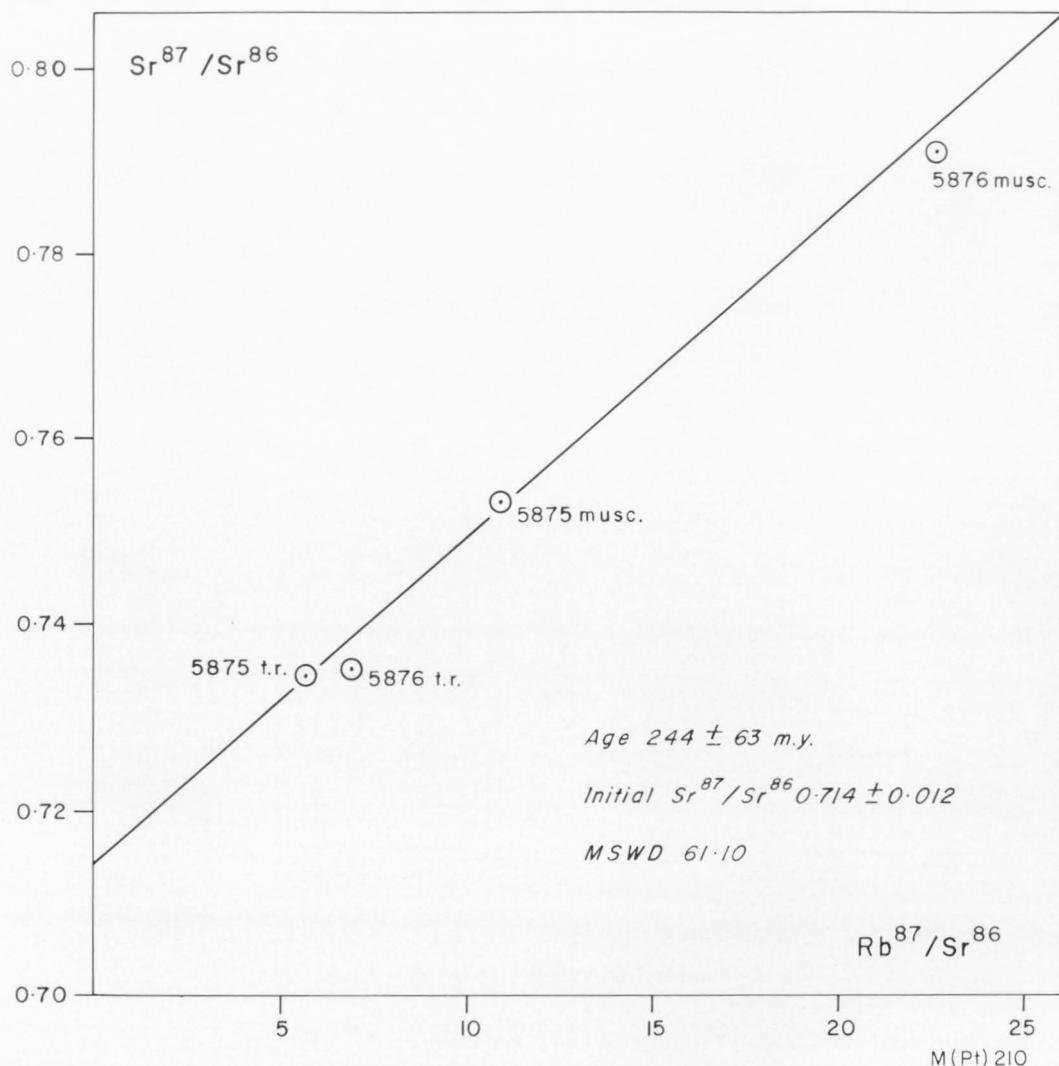
Fig. 13. Rb-Sr isochron for the Omung Metamorphics.

of the general rock types which Rickwood (1955) describes as 'mainly highly folded argillaceous rocks', no detailed mapping has yet been done. A minimum age estimate for the Omung Metamorphics is given by the age of the intrusive Kubor Granodiorite and the overlying Permian to Triassic Kuta Formation.

All the sediments and volcanics of the Omung Metamorphics have been regionally metamorphosed to greenschist facies, but this material was not dated. The intrusion of

granodiorite into the Omung Metamorphics has produced hornfels zones from a few tens to several hundred metres wide (Bain et al., in press). A number of clusthered samples of the hornfelses (only two of which were suitable for dating) were collected within a few metres of the granodiorite contact in the Maril River area northwest of Gumine (Fig. 12). The two samples that were dated are thoroughly recrystallized pelitic hornfelses and consist of a granoblastic aggregate of quartz, muscovite, plagioclase, graphite, and minor andalusite. Hence their ages

should relate to the time of the Kubor Granodiorite emplacement.

The K-Ar ages (Table 5) of two muscovite separates (5875 and 5876) from the hornfelsed Omung Metamorphics are in broad agreement at 211 ± 3 m.y. and 217 ± 4 m.y. The potassium values differ by 13 percent, and hence the age concordancy probably gives a reliable indication of the time when radiogenic argon began to be retained in the hornfelses following the emplacement of the Kubor Granodiorite.

The two muscovites and their corresponding whole rocks were also analysed by the Rb-Sr method. A plot of the data (Table 7 and Fig. 13) gives a Model III isochron (MSWD = 61.10) with an age of 244 ± 63 m.y. and initial Sr^{87}/Sr^{86} ratio of 0.714 ± 0.012. The large uncertainties in the age and initial ratio are due to the small number of data points and (evidently) to the inhomogeneous initial Sr^{87}/Sr^{86} ratios. It is possible to obtain two parallel isochrons: one by joining the 5875 muscovite and whole-rock points, the other by joining the 5876 muscovite and whole-rock points. The apparent initial ratios would then be 0.714 and 0.711, and the parallel isochron ages would become slightly older at 263 and 253 m.y. respectively.

Apart from indicating a late Palaeozoic to early Mesozoic event, these results do not permit a more precise age estimate for the time of the contact metamorphism. The results are discussed later in the light of the stratigraphic evidence and the isotopic data for the age of the Kubor Granodiorite.

4.22 Kubor Granodiorite

In mapping the Kubor Granodiorite, Bain et al. (in press) have shown that there are three main areas of outcrop, in which there are over 20 separate exposed masses that extend a total distance of 80 km from northwest to southeast (Fig. 12). Granodiorite and tonalite are the dominant rock types, but gabbro, diorite, adamellite, and dykes of pegmatite and aplite are present in places. The granodioritic rocks contain quartz, zoned oligoclase to andesine, perthitic alkali feldspar (orthoclase ± microcline), green hornblende, dark brown biotite, and accessory sphene, zircon, and apatite. Nearly all the samples collected show slight alteration or weathering, or both, producing sericitization of the feldspars and, in some, chloritization of biotite and hornblende. The last two minerals (when fresh) were separated from the granodiorites, and muscovite was separated from the pegmatites. They were used for the K-Ar dating study, and some of them, together with several aplite whole rocks, were subsequently used in the Rb-Sr analyses.

Granodiorite K-Ar ages. The K-Ar mineral ages for the Kubor Granodiorite are listed in Table 5, and the localities of the dated samples are plotted on the simplified geological map (Fig. 12). The hornblende and biotite ages range from 217 to 242 m.y., and the age histograms for both minerals (Fig. 14) have a strong peak between 220 and 225 m.y. The dates, which are internally concordant for each of the nine biotite-hornblende pairs, would normally be taken as strong evidence for the time of emplacement of the intrusion, with the 25 m.y. spread in the ages indicating a rather complex intrusive history. However, there is no geological evidence to support this, nor are the older dates restricted to any particular area.

K-Ar data for one plagioclase and two potash feldspar separates are also given in Table 5. One of the potash feldspar results (5809, 233 m.y.) agrees to within experimental error with the hornblende and biotite ages from the same rock, but 5809 plagioclase is clearly discrepant at 142 m.y. and must have lost some radiogenic argon. The anomalously young age of 170 m.y. for 5801 potash feldspar is probably the result of loss of argon, the diffusion of which may have been aided by the strongly perthitic nature of this sample. In reviewing the literature of diffusion of argon, Mussett (1969) concluded that lattice imperfections are the prime cause of argon escape in feldspars, but that the degree of perthitization (involving lattice imperfection) may or may not be related to the degree of argon loss. Both 5809 (233 m.y.) and 5801 (170 m.y.) potash feldspar are perthitic in the thin sections examined, and hence in these examples

TABLE 5. K-Ar AGES FOR THE KUBOR RANGE PLUTONIC ROCKS

No.	Sample	K %		$*Ar^{40}$ $x\ 10^{-6}\ cm^3$ NTP/g	$*Ar^{40}$ %	Calculated age (m.y.)
Omung Metamorphics hornfelses						
5875	Muscovite	7.425 / 7.430	7.428	66.119	95.8	211 ± 3
5876	Muscovite	8.396 / 8.328	8.362	76.811	96.6	217 ± 4
Kubor Granodiorite						
5458	Biotite	4.571 / 4.604	4.588	42.173	96.9	217 ± 4
	Hornblende	0.462 / 0.465	0.464	4.358	89.7	222 ± 4
5466	Biotite	6.898 / 6.866	6.882	65.635	96.4	225 ± 4
	Hornblende	0.400 / 0.400	0.400	3.775	88.1	223 ± 4
5801	Biotite	5.318 / 5.267	5.293	50.317	96.6	224 ± 6
	Hornblende	0.496 / 0.497	0.497	4.687	86.7	223 ± 6
	Potash feldspar	11.589 / 11.690	11.640	82.600	98.7	170 ± 4
5802	Hornblende	0.658 / 0.658	0.658	6.132	82.2	220 ± 6
5805	Biotite	6.267 / 6.264	6.266	58.794	96.4	222 ± 6
	Hornblende	0.495 / 0.490	0.493	4.720	91.8	226 ± 6
5807	Biotite	6.722 / 6.676	6.699	62.751	97.9	221 ± 6
	Hornblende	0.637 / 0.628	0.633	5.944	93.4	222 ± 6
5808	Biotite	5.330 / 5.351	5.342	53.305	96.2	235 ± 6
	Hornblende	0.492 / 0.496	0.494	5.056	75.0	241 ± 6
5809	Biotite	5.726 / 5.769	5.748	59.167	97.1	242 ± 6
	Hornblende	0.634 / 0.628	0.631	6.365	83.4	237 ± 9
	Potash feldspar	10.906 / 10.992	10.949	108.111	99.4	233 ± 9
	Plagioclase	1.118 / 1.126	1.122	6.597	73.3	142 ± 4
5811	Biotite	4.690 / 4.664	4.677	43.479	95.4	220 ± 6
	Hornblende	0.522 / 0.527	0.525	4.867	78.7	219 ± 9
5813	Biotite	6.417 / 6.439	6.428	59.667	98.2	219 ± 9
	Hornblende	0.613 / 0.609	0.611	5.976	94.0	230 ± 9
5814	Biotite	6.241 / 6.280	6.261	59.464	97.9	224 ± 6
5817	Hornblende	0.277 / 0.279	0.278	2.556	41.3	217 ± 11
6026	Biotite	6.486 / 6.446	6.466	65.433	97.7	238 ± 4

TABLE 5. K-Ar AGES FOR THE KUBOR RANGE PLUTONIC ROCKS—(cont.)

Kubor Granodiorite pegmatites

5843	Muscovite	8.653 8.612	8.633	80.322	97.0	220 ± 9
5844	Muscovite	8.610 8.513	8.562	80.841	90.6	223 ± 9
5845	Muscovite	8.666 8.668	8.667	80.582	97.7	220 ± 9
5846	Muscovite	8.516 8.534	8.525	81.398	94.3	225 ± 9
5847	Muscovite	8.485 8.509	8.497	79.125	97.8	220 ± 9
5848	Muscovite	8.534 8.539	8.537	85.795	91.7	236 ± 9
5849	Muscovite	8.425 8.417	8.421	79.104	89.7	222 ± 9
5850	Muscovite	8.435 8.487	8.461	80.448	90.7	224 ± 9

there is no direct correlation between degree of perthitization and percentage argon loss.

All the biotite and hornblende data for the Kubor Granodiorite were plotted on initial argon and isochron-type diagrams to see if any further information could be obtained. These graphical techniques will give the same ages as the normal K-Ar age calculations if the conventional assumptions (see Appendix 1) used to make the latter are valid for the particular set of data. If these assumptions do not hold, the graphical plot may result in a different pooled age, and may also give information on such values as the extraneous argon concentration and the initial Ar^{40}/Ar^{36} ratio.

Data from 11 of the biotites of the Kubor Granodiorites are plotted on an initial argon diagram (Fig. 15) and isochron diagram (Fig. 16). Results of each regression analysis are given in the respective graphical plots, with the errors quoted at the 95 percent confidence level. The initial argon plot gives a pooled age of 223 ± 20 m.y. (MSWD = 5.01); the intercept of the y axis is not statistically distinguishable from zero, and the pooled age is thus in agreement with the ages given by the conventional calculations. The argon isochron plot (Fig. 16) gives an age of 222 ± 10 m.y., with an initial Ar^{40}/Ar^{36} ratio of 429 ± 387, which is indistinguishable from that in atmospheric argon.

The initial argon and argon isochron plots for the hornblende samples are shown in Figures 17 and 18, and all the graphical results are summarized in Table 6. Although the scatter of the data is outside experimental error, the pooled ages of the biotite and hornblende data are concordant at about 230 m.y. The ages from the initial argon plots, although marginally higher, are not significantly different from those of the argon isochron plot. The scatter of the data points in both hornblende and biotite regressions, as shown by the MSWD values greater than unity, may indicate various concentrations or isotopic compositions of any initial argon, or it may be a result of differential losses of radiogenic argon or, indeed, a spread in age of the intrusion. These factors are considered at the end of this section.

The rather low potassium contents of the Kubor biotites, especially 5458 and 5811, are indicative of their partly chloritized nature, and it is perhaps surprising that the points fall anywhere near an isochron which shows an age that is in perfect agreement with the pooled hornblende age. Although the two most chloritized biotite samples (5458 and 5811) do give the youngest, conventionally calculated K-Ar ages, neither the biotites nor the hornblendes in general show any correlation between age and degree of chloritization. This finding is in agreement with the laboratory investigations by Kulp & Bassett (1961) and Kulp & Engels (1963), who found that the Ar^{40}/K^{40} ratio for biotite decreased by only 15 percent after a reduction (due to exchange
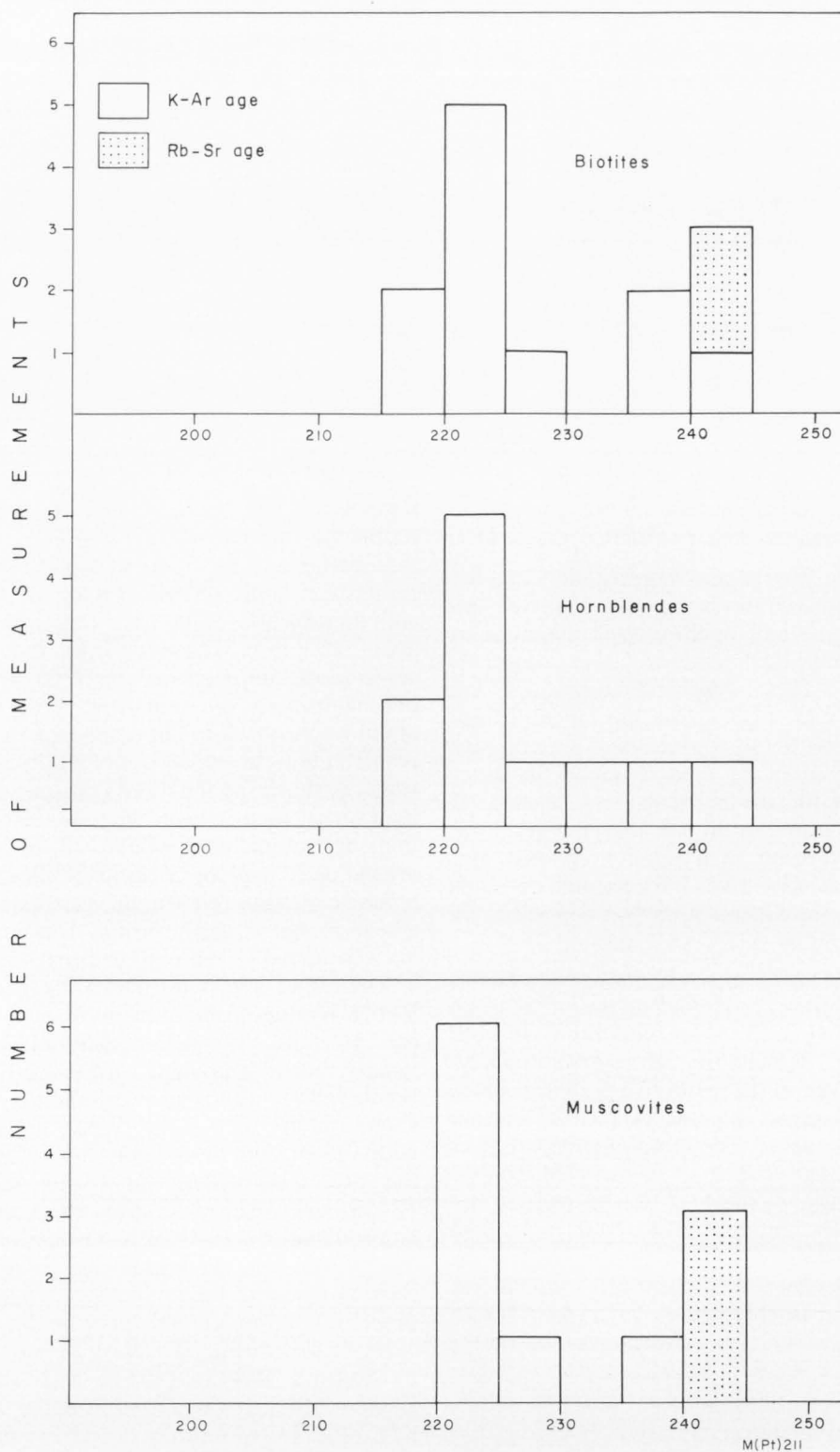
Fig. 14. Histograms of Kubor Granodiorite ages.
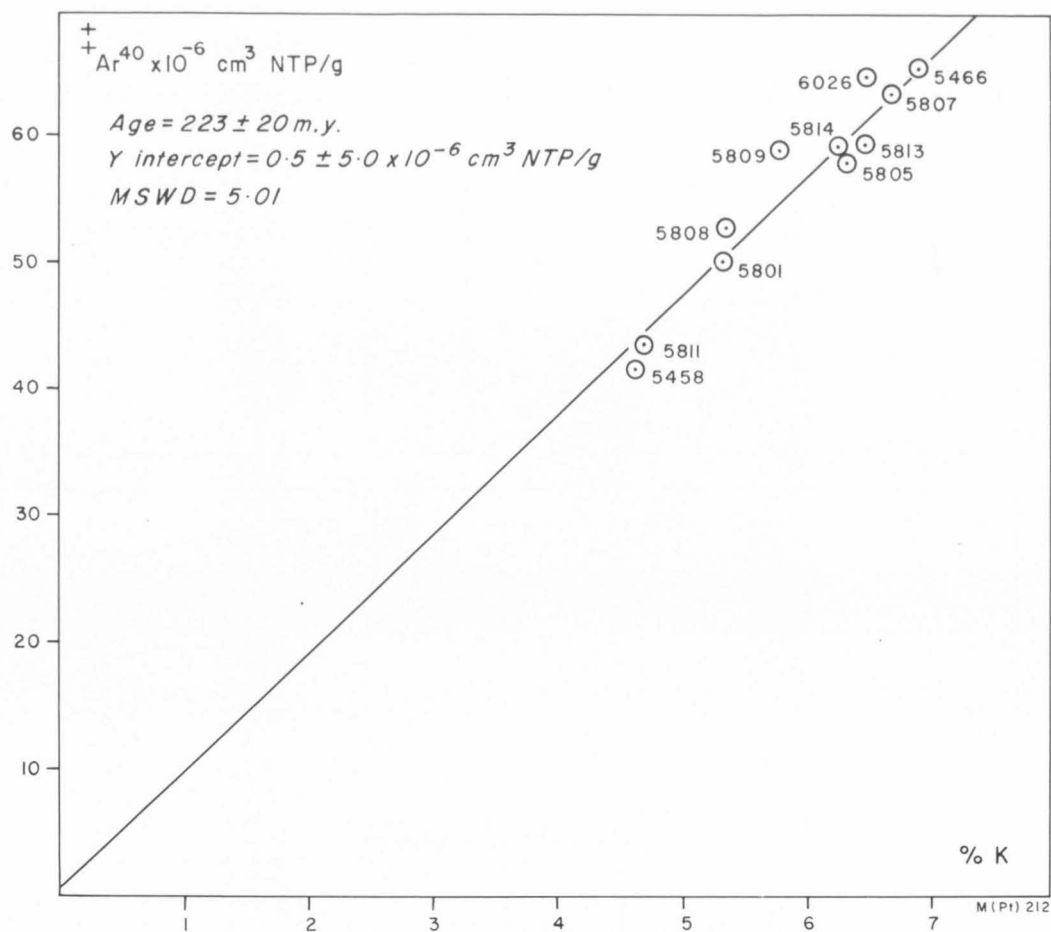
Fig. 15. Initial argon plot for the Kubor biotites.

TABLE 6. GRAPHICALLY OBTAINED K-Ar AGES FOR MINERALS FROM THE KUBOR
GRANODIORITE

Mineral	Pooled age (m.y.) from initial argon plot	Pooled age (m.y.) from argon isochron plot
Biotite	223 ± 20	222 ± 10
Hornblende	234 ± 14	226 ± 4
Muscovite	—	219 ± 7

with calcium or magnesium) of 85 percent in the potassium content.

Granodiorite Rb-Sr ages. Three of the Kubor Granodiorite biotites were analysed by the Rb-Sr method, and the analytical data and ages are given in Table 7. An initial Sr^{87}/Sr^{86} value of 0.704 (based on two whole-rock granodiorite unspiked Sr^{87}/Sr^{86} measurements) was used to calculate the ages. (Further whole-rock Rb-Sr age studies were not warranted because of the uniformly low Rb/Sr ratios ranging from about 0.05 to 1.0.) 5805 biotite has a Rb-Sr age of 243 m.y., which is virtually independent of choice of initial Sr^{87}/Sr^{86}. The age of 5808 is in close agreement with 5805, whereas the corresponding K-Ar dates are
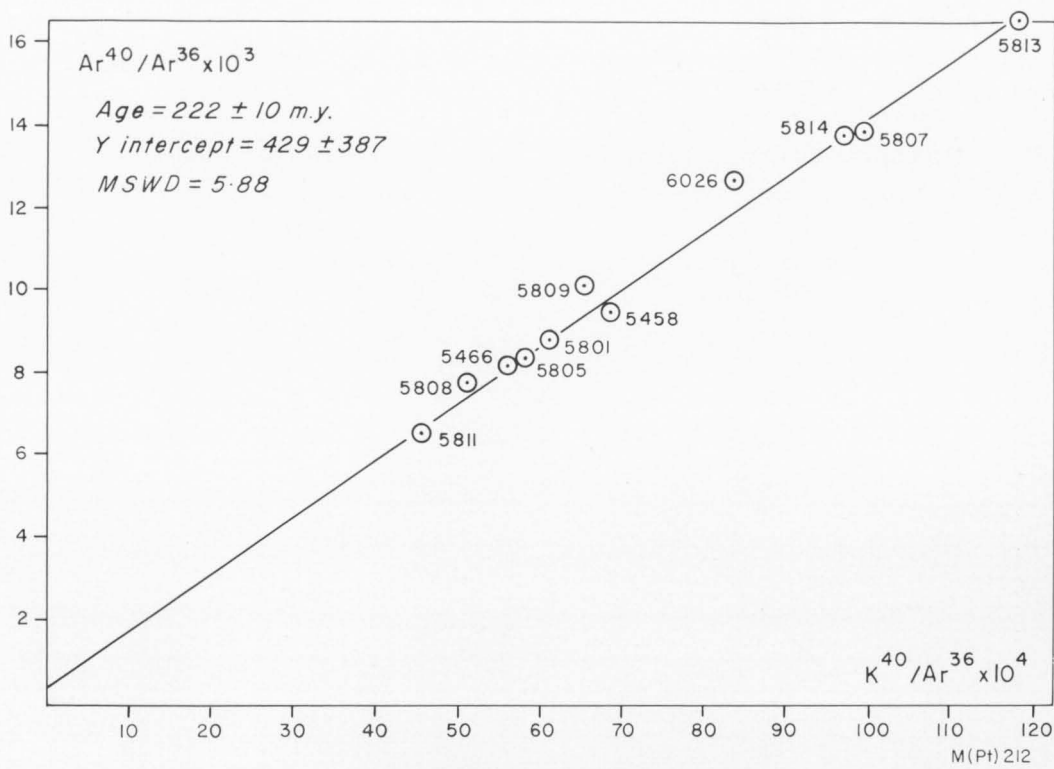
Fig. 16. Argon isochron for the Kubor biotites.
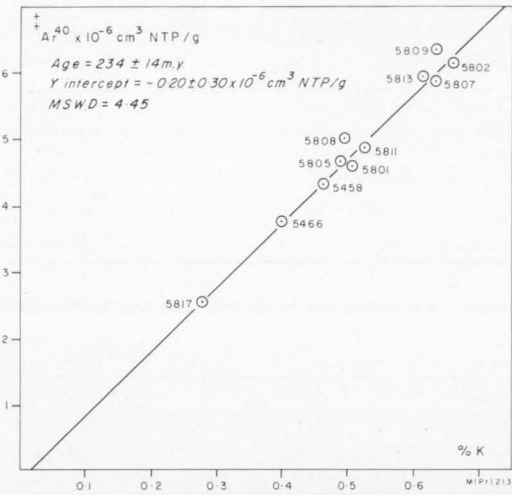
Fig. 17. Initial argon plot for the Kubor hornblendes.
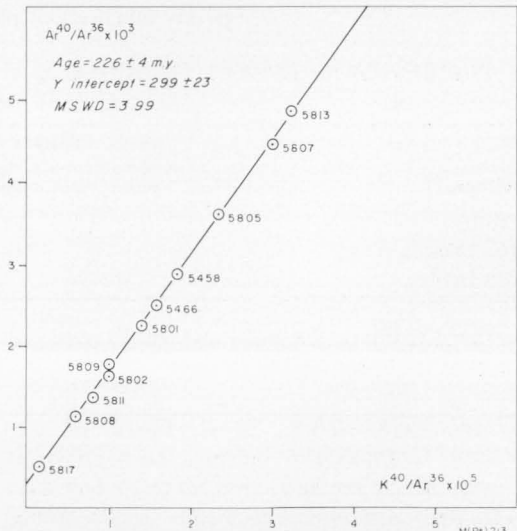
Fig. 18. Argon isochron for the Kubor hornblendes.

TABLE 7. Rb-Sr DATA FOR THE KUBOR RANGE PLUTONIC AND METAMORPHIC ROCKS

No.	Sample	Rb (ppm)	Sr (ppm)	Rb^{87}/Sr^{86}	Sr^{87}/Sr^{86}	** Sr^{87}/Sr^{86}	Rb-Sr age (m.y.)	K-Ar age (m.y.)
5875	Whole rock	122.5	62.3	5.695	0.7345			
	Muscovite	226.1	60.1	10.922	0.7538			211
5876	Whole rock	125.5	52.8	6.886	0.7348			
	Muscovite	282.5	36.2	22.693	0.7908			217
Granodiorites								
5458	Biotite	196.5	29.6	19.276	0.7638		225	217
5805	Biotite	355.8	6.5	167.608	1.2712		243	222
5808	Biotite	245.2	19.5	36.778	0.8289		244	235
2135	Whole rock	3.9*	231.4*			0.7044		
2191	Whole rock	11.2*	513.6*			0.7034		
Pegmatites								
5846	Muscovite	979.3	3.0	1401.319	5.4764		244	225
5848	Muscovite	1390.7	3.4	1973.157	7.3035		240	236
5849	Muscovite	1152.9	3.5	1404.526	5.3999		240	222
Aplites								
B55/	Whole rock	50.3	59.2	2.450	0.7098	0.7068		
5/15						0.7069		
2130	Whole rock	87.9	152.7	1.662	0.7088			
2168	Whole rock	6.6	67.5	0.2818	0.7056	0.7056		
5683	Whole rock	34.1	37.7	2.755	0.7134	0.7127		
5684	Whole rock	8.3	107.6	2.183	0.7106			
5685	Whole rock	93.8	65.1	4.166	0.7158	0.7154		
5686	Whole rock	123.2	286.8	1.241	0.7083			
5687	Whole rock	99.6	47.9	6.011	0.7186	0.7184		

* Approximate XRF measurement
** Measured value, unspiked run

significantly lower and are internally discordant. The sample with the lowest K-Ar age (5458) also has a lower Rb-Sr age than the others; it is quite chloritized, as indicated by the low potassium value of 4.6 percent. The differences between the K-Ar and Rb-Sr ages may be partly related to uncertainties in the Rb^{87} decay constant; this problem is discussed later.

Pegmatite K-Ar ages. Muscovite pegmatite dykes (0.3 to 4 m wide) intrude the eastern part of the Kubor Granodiorite within an area of 2 km^2 near the Maril River (Fig. 12). The K-Ar age data of eight muscovite separates are given in Table 5 and are summarized in the histogram (Fig. 14); their ages of 220 to 236 m.y. are close to the K-Ar ages determined on biotites and hornblendes from the granodiorite in other parts of the Kubor mass.

An initial argon plot of the muscovite data is not particularly useful because there is very little spread in the potassium contents. In an argon isochron plot (Fig. 19)

the pooled age is 219 ± 7 m.y. and the indicated initial Ar^{40}/Ar^{36} is 401 ± 122. This age derived from the isochron is younger than the conventionally calculated ages because the Ar^{40}/Ar^{36} intercept obtained in the plot is marginally higher than, but statistically indistinguishable from, that of atmospheric argon, 295.5. The 16 m.y. total spread of the muscovite pegmatite ages, and the pooled age of 219 ± 7 m.y. obtained by the isochron method, present an analogous situation to that of the biotite and hornblende data for the granodiorites. Because of the concordancy of the biotite /hornblende-pair ages, it was reasonable to interpret the age spread (from 217 to 242 m.y.) in terms of a complex intrusive history. The pegmatites, however, were collected from one restricted area, and on geological grounds it is unlikely that emplacement lasted for the 16 m.y. duration indicated by the data. It could be argued that the oldest age (236 m.y. for 5848) is the best minimum estimate for the date of emplacement, and that the younger dates are
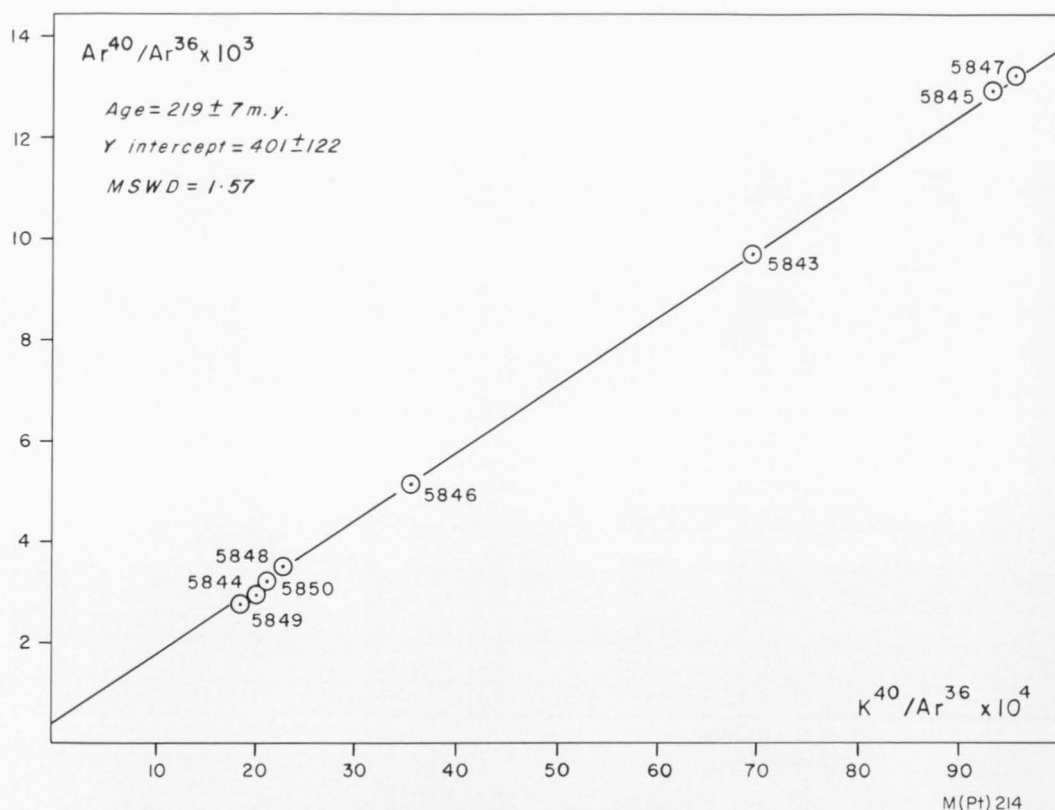
Fig. 19. Argon isochron for the Kubor muscovites.

reflecting a subsequent geological event during which there was partial loss of radiogenic argon from some of the muscovites. This would necessarily imply a similar explanation for the biotite and hornblende results.

Pegmatite Rb-Sr ages. The Rb-Sr ages of three muscovites from the Maril River pegmatites (Table 7) are consistent at 240 to 244 m.y. It will be remembered that Rb-Sr ages of 243 and 244 m.y. were obtained for two biotite samples from the granodiorite (cf. Fig. 14) and that an age of 244 ± 63 m.y. was obtained for the isochron regression of the hornfelses from the Omung Metamorphics. The consistency of the Rb-Sr ages provides strong evidence that this is the date of emplacement of the Kubor rocks. The Rb-Sr muscovite ages are clearly older than the discordant K-Ar ages measured on the same samples. This situation is again analogous to that found in the earlier comparison of the K-Ar and Rb-Sr biotite results.

Aplite whole-rock age data. That the history of intrusion of the Kubor Granodiorite may be even more complex is indicated by the Rb-Sr isochron results for several aplites. The aplites intrude the granodiorite in isolated veins and dykes throughout the body. They have a medium-grained granular texture and contain quartz, plagioclase, and potash feldspar, with rare biotite, chlorite, and opaque minerals. The aplite data (Table 7) are plotted on a Rb-Sr isochron (Fig. 20) and show considerable scatter about the straight line. The regression of seven data points (excluding B55/5/15) gives a Model II isochron (MSWD = 4.29) with an age of 177 ± 27 m.y. and an initial Sr^{87}/Sr^{86} ratio of 0.7051 ± 0.0007. The inclusion of B55/5/15 sharply increases the MSWD to
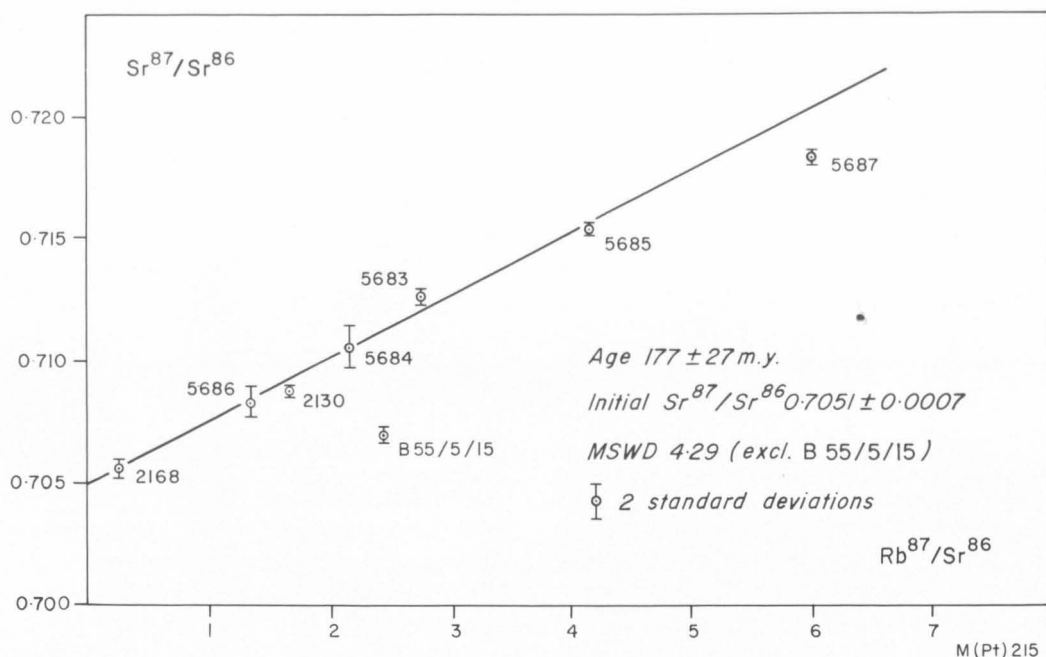
Fig. 20. Rb-Sr isochron for the Kubor aplites.

28.17 and a Model IV isochron (age 163 ± 76 m.y., initial ratio 0.705 ± 0.003) is obtained. For the Model II isochron, the scatter of results can be explained by either a complex aplite intrusive history or a subsequent loss of radiogenic strontium. The aplites were collected from widely separated areas throughout the Kubor Granodiorite, and, since the whole region was folded in the latter part of the Tertiary, either of the two explanations for the aplite Rb-Sr scatter is reasonable. It is perhaps significant that the regression of five aplite data points (excluding 5687, 5685, and B55/5/15) gives a Model I fit with an age of 201 ± 38 m.y. and initial Sr^{87}/Sr^{86} of 0.7047 ± 0.0009. This means that the errors can be wholly ascribed to experimental uncertainties, and that the five samples are probably cogenetic. The 201 ± 38 m.y. age is also not significantly different from either the K-Ar or Rb-Sr mineral ages for the granodiorites and pegmatites. The three points that do not fit the 201 m.y. isochron all give younger ages of 90, 170, and 180 m.y. (assuming the same initial Sr^{87}/Sr^{86}). Since selective updating of the whole rocks

is unlikely, the younger ages could represent later pulses of aplite intrusion.

The initial Sr^{87}/Sr^{86} ratio of 0.7051 ± 0.0007 for the seven Kubor aplites is clearly controlled by the point 2168, which gave identical values for both spiked and unspiked runs (Table 7). The present-day Sr^{87}/Sr^{86} ratios were also measured for two of the granodiorites (2135 and 2191) with low Rb/Sr ratios (Table 7) and, with corrections made for the small Sr^{87} enrichment, initial Sr^{87}/Sr^{86} ratios of 0.7042 and 0.7032 were obtained. These values are lower than the graphically obtained value of 0.7051 ± 0.0007 for the aplites, but, because of the previously mentioned uncertainties surrounding the aplite data, it is not clear whether the initial Sr^{87}/Sr^{86} values are significantly different.

4.23 Discussion of the Kubor Granodiorite ages

Table 8 summarizes all the age determinations made on the Kubor Granodiorite and associated hornfelses of the Omung Metamorphics. If the dates are regarded as those of emplacement, all but the Rb-Sr mica ages

TABLE 8. SUMMARY OF THE AGES FOR THE KUBOR RANGE PLUTONIC ROCKS

Unit	Sample	Pooled or average K-Ar age (m.y.)	Pooled or average Rb-Sr age (m.y.)
Omung Metamorphics hornfelses	Muscovite, whole rock	214	244 ± 63
Kubor Granodiorite	Biotite	222 ±10	244
	Hornblende	226 ± 4	
	Potash feldspar	233	
Pegmatites	Muscovite	219 ± 7	242
Aplites	7 whole rocks		177 ± 27
	(5 whole rocks)		(201 ± 38)

are inconsistent with (younger than) the stratigraphic control, which according to Rickwood (1955) determines that the granodiorites must be pre-Triassic (i.e. older than 235 m.y.). The stratigraphy of the area as outlined by Bain et al. (in press), however, allows more latitude and indicates that the Kubor Granodiorite may be as young as the Triassic; all the mineral ages would then be consistent with the stratigraphic interpretation.

From the internal concordance of the K-Ar biotite/hornblende-pair dates, and from the excellent agreement of the pooled K-Ar mineral data of 219 to 234 m.y., it would have been reasonable to conclude that this was the time of emplacement of the Kubor Granodiorite and, as noted above, this age would be consistent with the field evidence of Bain et al. (in press). However, the Rb-Sr mica ages of 244 m.y. and the Rb-Sr isochron age (244 m.y.) for the Omung Metamorphics suggest that there has been leakage of radiogenic argon from these rocks. The 244 m.y. Rb-Sr ages are believed to be the best estimates for the age of emplacement of the Kubor Granodiorite and, if the Permian-Triassic boundary is taken as 230 to 235 m.y. (Webb & McDougall, 1967), this emplacement can be regarded as Late Permian.

For the determination of the Rb-Sr dates, the Rb^{87} half-life of 5.0×10^{10} yr ($\lambda = 1.39 \times 10^{-11}yr^{-1}$; Aldrich, Wetherill, Tilton, & Davis, 1956) was employed. The Rb-Sr ages are lowered by about 14 m.y. if the 4.7×10^{10} yr half-life (($\lambda = 1.47 \times 10^{-11}yr^{-1}$; Kulp & Engels, 1963) is used, thus bringing the Rb-Sr ages closer to the K-Ar results.

From a comparison of K-Ar and Rb-Sr dates on undisturbed upper Palaeozoic granites in eastern Queensland, Webb (1967) concluded that the $1.47 \times 10^{-11}yr^{-1}$ Rb^{87} decay constant was the more appropriate 'geological' constant. Although the $1.47 \times 10^{-11}yr^{-1}$ value produces better concordancy for the Kubor Granodiorite results by reducing the average Rb-Sr-versus-K-Ar age difference from about 9 percent to 3 percent, other factors indicate updating of the K-Ar ages. This area has been folded since the granodiorite was emplaced, and any comparisons of the K-Ar and Rb-Sr ages would be biased towards accepting the shorter half-life of Rb^{87} because of the greater sensitivity of argon diffusion in response to geological events. It is, therefore, not appropriate to argue for either Rb^{87} half-life on the basis of the Kubor data, and the value of 5.0×10^{10} yr currently employed in this laboratory is adhered to.

The pooled biotite, hornblende, and muscovite K-Ar isochron ages are in the range 219 to 226 m.y., but, on the basis of the older Rb-Sr ages, the K-Ar ages do not reflect the Kubor Granodiorite emplacement. The few older K-Ar dates (5808, 5809, and 5848) of 235 to 242 m.y. are closer to the Rb-Sr mica ages of 244 m.y., but the general K-Ar age distribution tends to be smeared out either side of the 220 to 225 m.y. peak for the mineral separates (Fig. 14). The updated K-Ar age pattern may have occurred during one or more of the following events:

(i) Late Tertiary folding, which resulted in the Kubor Anticline;

(ii) Subsequent intrusion of the aplites;

(iii) Slow differential raising or lowering of the thermal gradients of the region, in such a manner as to delay cooling to below the threshold temperature for argon diffusion;

(iv) Burial metamorphism below the Mesozoic geosynclinal sediments.

The first explanation is realistic enough in terms of the observed geology, but one would perhaps expect to find far greater age discordance. Later aplite intrusion cannot be seriously considered for two reasons: firstly, the age derived from the Rb-Sr isochron for the aplites (Fig. 20) is somewhat ambiguous, and secondly, on the basis of field and laboratory argon retention studies (Hart, 1964; Hanson & Gast, 1967; Gerling, Leviskiy, & Morozova, 1963), the hornblendes from the updated granodiorites should have been more retentive than the biotites and, consequently, would have shown consistently older ages; this, however, is not so.

For the third possible explanation, slow raising of the regional thermal gradients after the Rb-Sr clock had been set at 244 m.y. would involve a delay of about 20 m.y. before temperatures were low enough for the radiogenic argon to be retained. For this model to be valid, the ages of the hornblendes would have to be older than those of the biotites. However, the K-Ar ages of each biotite-hornblende pair are indistinguishable at the 95 percent confidence level; this suggests that uplift was relatively rapid. Another reason for assuming that uplift was rapid is that, after the Kubor Granodiorite was emplaced in the Late Permian (244 m.y.), there was sufficient time for it and the Omung Metamorphics to be eroded before the Permian (Rickwood, 1955) or Permian/Triassic (Bain et al., in press) Kuta Formation was deposited. If 244 m.y. is the age of emplacement and if the overlying Kuta Formation is Permian, then an interval of only a few million years is allowed for the ensuing processes of uplift, erosion, and deposition. The epeirogenic history of the Kubor region is far more complex than here suggested, as the mapping of Rickwood (1955) and Bain et al. (in press) shows; the entire Kubor Granodiorite is not unconformably overlain by the Kuta Formation, but in places the time gaps, which are indicated by unconformity, extend to the Upper Jurassic (Maril Shale) and even to the Lower Cretaceous (Kondaku Tuffs).

The fourth and preferred alternative to explain the younger K-Ar dates of the biotites, hornblendes, and muscovites invokes differential heating of parts of the granodiorite and Omung Metamorphics; this could have been caused by burial metamorphism beneath the Mesozoic sediments, which have a maximum thickness of 5500 m (Bain et al., in press) on the northern flank of the Kubor Range near Kundiawa but are thinner in the Kubor Range itself. Both Edwards & Glaessner (1953) and Rickwood (1955) recorded diagenetic minerals such as laumontite, chlorite, calcite, and zeolites from the lower Cretaceous Kondaku Tuff. These minerals are characteristic of low-grade burial metamorphism and require temperatures of perhaps 200-300°C (Turner & Verhoogen, 1960) for their formation. Such temperatures must have been present also in the underlying Kubor plutonic rocks, and may have been sufficient to cause partial loss of radiogenic argon from the minerals without upsetting the Rb-Sr clock. Again the argument could be advanced that the hornblendes would be expected to have consistently higher ages than the biotites, as predicted from the contact metamorphic studies of Hart (1964), who found that hornblende was markedly more retentive under these conditions. However, low-grade regional metamorphism as here invoked probably acts for a far longer time (for example, over 10 m.y.) than the effects of a high-level intrusion (less than 2 m.y.), and the diffusion parameters of argon in hornblende and in biotite may not be significantly different over the longer period. This possibility was earlier raised by Kulp & Engels (1963) and Webb & McDougall (1968). The latter concluded a similar effect to explain the concordant K-Ar ages of their hornblende-biotite pairs, which they thought had probably lost argon because the ages were incompatible with inde-

pendent Rb-Sr ages. In addition, they stressed, and these points are relevant to the present study, that care is needed in the interpretation of K-Ar ages, and that a better understanding of the geological history of a region can be given when the K-Ar method is used in conjunction with the Rb-Sr method.

4.3 STRICKLAND GRANITE

In the headwaters of the Strickland River in northwest Papua (Plate 1) there are a few small outcrops of stratigraphically controlled Mesozoic granitic bodies. Oil companies who have mapped in this area (APC, 1961) believe that this granitic basement also underlies much of the region to the west. This is evidenced in a number of places in the Jurassic sequence by gritty arkoses and granitic conglomerate debris up to 250 m thick (Osborne, 1945).

In the Strickland Gorge the eroded surface of the granite is unconformably overlain by a thin basal conglomerate and ammonite-bearing sandstone sequence (BP Petroleum Development Australia Pty Ltd, pers. comm., 1970), which is Early to Middle Jurassic in age. One specimen of biotite granodiorite from this locality has been dated by the K-Ar method; the result is given in Table 9. The single boitite age of 222 ± 4 m.y. must be regarded as a minimum age of emplacement, and it is tempting to correlate this with the similar K-Ar biotite ages obtained for the Kubor Granodiorite. The overlying Mesozoic sediments are well

over 2000 m thick (Osborne, 1945), and it is therefore possible that the 222 m.y. K-Ar age has been updated as suggested for the Kubor Granodiorite K-Ar ages. It was pointed out earlier (2.3) that several oil-exploratory boreholes have bottomed in granitic rocks elsewhere in western Papua. A biotite separate from granite recovered from the Aramia No. 1 well was dated (by the K-Ar method) by J. R. Richards (*in* Harding, 1969) as 236 m.y., and it would not seem unreasonable to also provisionally correlate this occurrence with the Strickland River 'basement'. It is worth noting, however, that the granite outcrops farther south at Mabaduan (Plate 1) appear to be older at about 300 m.y. (Richards & Willmott, 1970).

4.4 URABAGGA INTRUSIVES

The Urabagga intrusives is the informal name for a number of small granodiorite-diorite bodies which range in size from 0.5 to 2 km across, and which have a restricted outcrop in the region west of Asaro (see Fig. 32). McMillan & Malone (1960) mapped these rocks as outliers of the 'Bismarck Granodiorite' (now referred to as the Bismarck Intrusive Complex) in the Goroka Formation. As mentioned earlier and discussed more fully in section 5, the age of the Bismarck Intrusive Complex has been a matter of much debate (Rickwood, 1955; McMillan & Malone, 1960; Dow & Dekker, 1964), but extensive isotopic dating (see 5.33) now shows it to be no older than mid-

TABLE 9. K-Ar AGES FOR THE STRICKLAND GRANITE, THE URABAGGA INTRUSIVES, AND THE INTRUSIVES INTO THE BENA BENA FORMATION

No.	Sample	K %		$*Ar^{40}$ $x10^{-6} cm^3$ NTP/g	$*Ar^{40}$ %	Calculated age (m.y.)
Strickland Granite						
5998	Biotite	6.436 6.476	} 6.456	60.806	98.9	222 ± 4
Urabagga intrusives						
5897	Hornblende	0.125 0.127	} 0.126	0.981	60.3	186 ± 8
5899	Whole rock	0.224 0.222	} 0.223	1.271 1.199	80.2 77.1	138 ± 5 130 ± 5
Intrusives into the Bena Bena Formation						
5836	Muscovite	7.742 7.770	} 7.756	7.100 7.167	71.9 76.5	22.8 ± 0.9 23.0 ± 0.4

TABLE 10. Rb-Sr DATA FOR THE URABAGGA INTRUSIVES

No.	Sample	Rb (ppm)	Sr (ppm)	Rb^{87}/Sr^{86}	Sr^{87}/Sr^{86}	* Sr^{87}/Sr^{86}
5887	Whole rock	140.3	3.7	112.440	1.0031	1.0010
5888	Whole rock	80.7	31.6	7.378	0.7362	0.7215
						0.7208
5973	Whole rock	12.1	30.3	1.148	0.7061	
5974	Whole rock	17.3	31.7	1.571	0.7063	
5975	Whole rock	5.5	311.8	0.051	0.7041	
5976	Whole rock	4.7	93.2	0.144	0.7038	
5977	Whole rock	15.9	70.3	0.655	0.7046	

* Measured value, unspiked run

Miocene. The Miocene ages, however, are in conflict with McMillan & Malone's (1960) stratigraphic evidence for the age of the Bismarck Intrusive Complex, viz. at Urabagga Hill (2 km west of Asaro), where granitic rocks (Urabagga intrusives) are unconformably overlain by Oligocene e-stage limestone. These restricted Oligocene sediments provide the only unequivocal stratigraphic control of any intrusive rocks in the region. The author sampled the granitic rocks underlying the Oligocene limestone at Urabagga Hill, but because of poor outcrop and deep weathering none was fresh enough for dating purposes. Another of the Urabagga intrusive bodies, 4 km to the northwest, provided several fresh samples (Fig. 32). This body intrudes low-grade metamorphics of the Goroka Formation (unknown age, but Palaeozoic according to McMillan & Malone, 1960) and is overlain by e-stage limestone. It contains a variable suite of rocks ranging from diorite to chloritized leucogranite, and is intruded by a number of dolerite and aplite dykes.

A hornblende from one of the diorites, and the mean of two whole-rock dolerites, gave discordant K-Ar ages of 186 m.y. and 134 m.y. respectively (Table 9). Rb-Sr analyses (Table 10) on 7 whole-rock samples from the mass have indicated a Model III isochron age of 190± 3 m.y., and an initial Sr^{87}/Sr^{86} ratio of 0.7029 ± 0.0009 (Fig. 21). The slope of the line is controlled by the very enriched aplite sample 5887, but a separate regression made without this data point also gives a Model III isochron with the age (176 ± 18 m.y.) and initial $Sr^{87}/$

Sr^{86} (0.7033 ± 0.0008) identical to within experimental error.

It would appear from the isotopic evidence that the Urabagga intrusives are not related to the Bismarck Intrusive Complex, but were emplaced between 180 and 190 m.y. ago in the Early Jurassic. The discordant K-Ar ages appear to have been updated by a subsequent event. The apparent age discrepancy (alluded to above) with the stratigraphic control at Urabagga Hill is rationalized if the plutonic rocks underlying the e-stage limestone are regarded as the same age as the intrusion 4 km to the northwest, here dated as Early Jurassic.

4.5 GNEISSIC GRANITIC ROCKS INTRUDING THE BENA BENA FORMATION

The Bena Bena Formation, east of Goroka, was first mapped by McMillan & Malone (1960), and was subsequently extended by Dow & Plane (1965). Pitt (1966) informally referred to the rocks as the 'Bismarck Metamorphics'. The formation consists of a variety of greenschist-facies metasediments (quartz-muscovite schist, green actinolite schist, and quartzite) occupying at least 600 km^2 in the Bismarck Ranges northwest of Kainantu. Dow & Plane (1965) suggested that the Bena Bena Formation might be correlated with the pre-Permian Omung Metamorphics (discussed in 4.21), which occur 100 km to the west. However, both formations are unfossiliferous, and the only stratigraphic control is for the parts of the Bena Bena Formation that are unconformably overlain by the Tertiary e-stage (lower Miocene) Nasananka Conglomerate (Dow & Plane, 1965). No
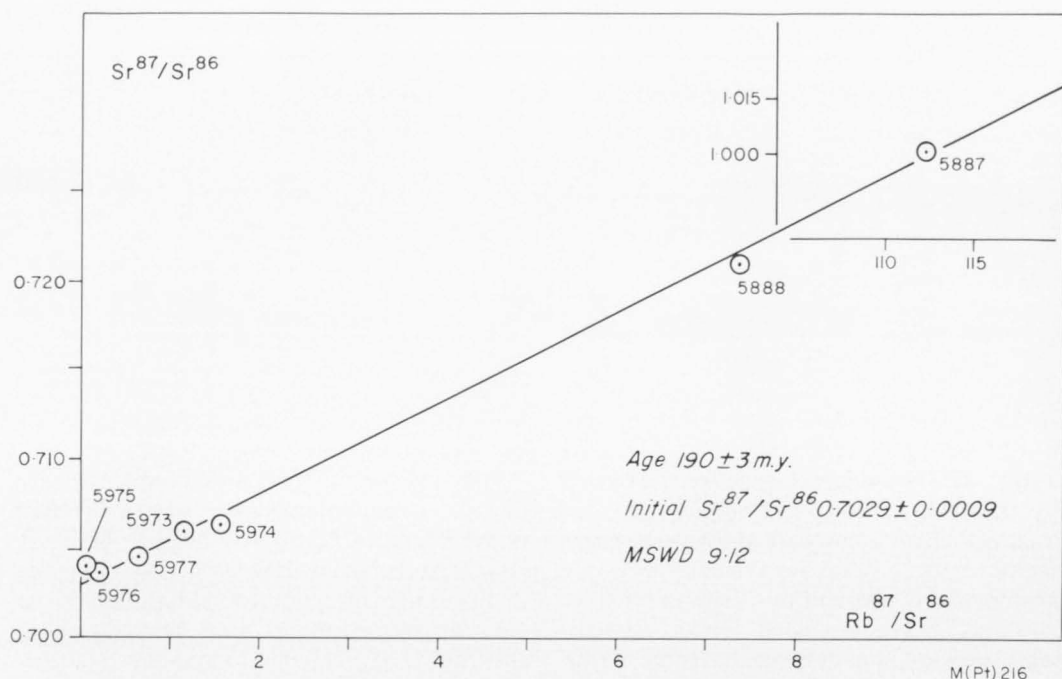
Fig. 21. Rb-Sr isochron for the Urabagga intrusives.

isotopic data have been obtained on the Bena Bena Formation.

Two rather distinctive gneissic granite bodies which intrude the Bena Bena Formation were mapped by McMillan & Malone (1960) and Dow & Plane (1965) in the region of the Karmantina River (Fig. 22). McMillan & Malone (1960) stated that these bodies are texturally and compositionally similar to other gneissic rocks which form small isolated outcrops elsewhere within the Bena Bena Formation. They interpreted these masses (the largest of which is 4 km across) as having intruded the Bena Bena Formation in the Palaeozoic and been subsequently affected in the regional metamorphism of the area. Dow & Plane (1965) regarded the gneissic granites as sills 'belonging to the Bismarck Granodiorite'; this, however, is a massive biotite-hornblende granodiorite and is distinct from these gneissic rocks. I remapped the largest gneissic granite body in the Karmantina River, and collected a suite of rocks (Fig. 22) for isotopic dating. The sampling was hampered by the weathered and crumbly

nature of most outcrops, and some samples were collected as boulders from restricted stream drainages.

Rb-Sr analyses were made on the gneissic granites and on one of the segregated biotite-rich schlieren (5690) from the mass (Table 11). The regression of the 13 gneissic granite whole-rock analyses indicates a large residual variance which cannot be attributed to experimental error. The geological scatter of points produces a Model IV isochron which has an age of 172 ± 27 m.y. and initial Sr^{87}/Sr^{86} of 0.712 ± 0.002 (Fig. 23). Further regression results were obtained using (i) only the eight samples collected in situ (173 ± 23 m.y.) and (ii) four samples collected close to each other (178 ± 40 m.y.). These regressions make little difference to the original isochron age of 172 ± 27 m.y. It does not seem unreasonable to regard this as the age of emplacement of the granitic body, which therefore provides a minimum estimate of Early Jurassic for the age of the Bena Bena Formation. Alternatively, the indicated Jurassic age may reflect a strong meta-
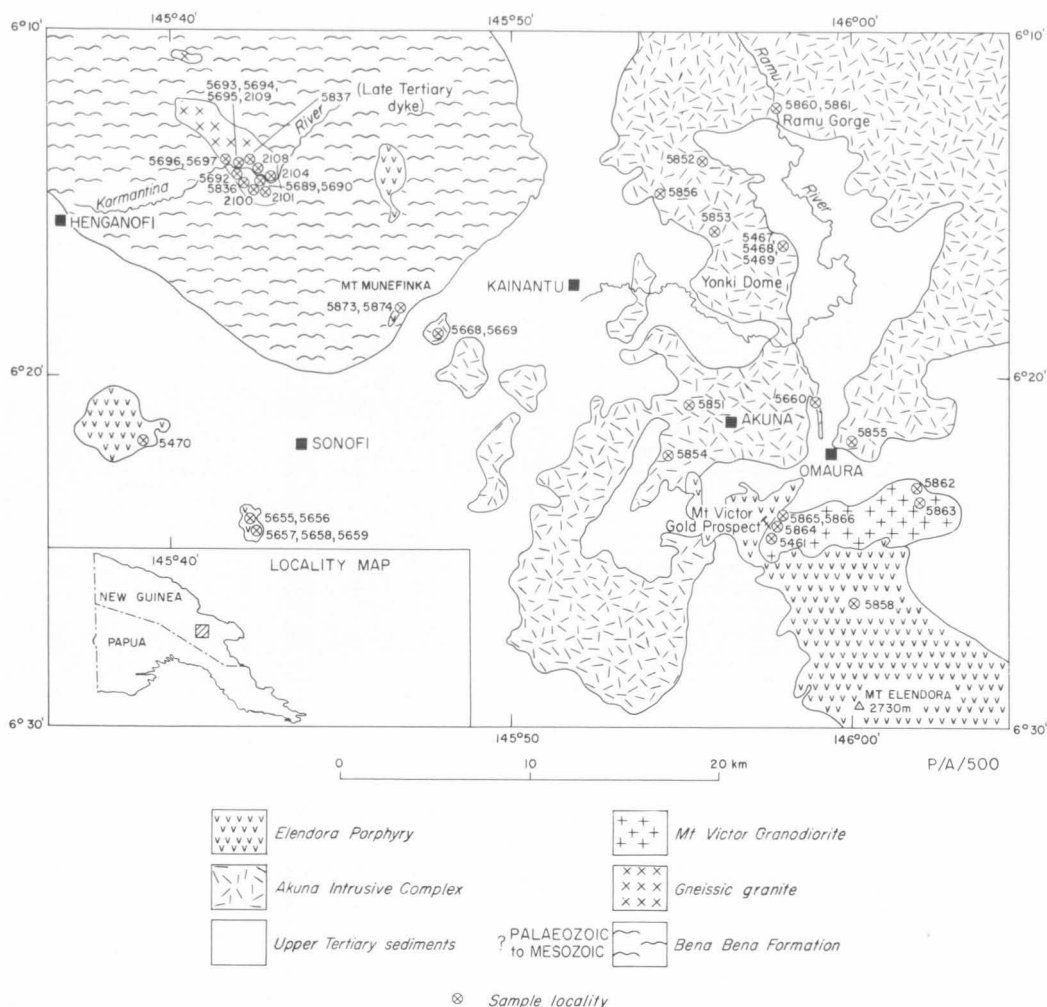
Fig. 22. Simplified geological map—Kainantu area.

morphic event. The large uncertainties in age and initial Sr^{87}/Sr^{86} are due to partial updating of some of the whole rocks and to incomplete isotopic homogenization. Another interpretation for the isochron plot would be a line passing through the sample points 5693 and 5697 and the four points near the origin; this would give an age, probably of emplacement, of about 220 m.y. (Early Triassic), and indicate that the remaining samples had been severely updated. However, there are no geological or petrographic grounds for rejecting these, for most of the samples are texturally and minera-

logically similar. Quartz (30%), and plagioclase (albite-oligoclase) and coarsely perthitic alkali feldspar (total, 50-70%), are the dominant minerals of the gneissic granites; epidote, andalusite, and fine-grained muscovite and biotite are also present. The micas have a rough preferred orientation and are most common in veins and cracks. The quartz and feldspars also show deformational features such as partial recrystallization at grain boundaries, strong undulose extinction, and kinked twin-planes. The texture of the fine-grained micas suggests that they recrystallized during the

TABLE 11. Rb-Sr DATA FOR THE GNEISSIC GRANITIC ROCKS INTRUDING THE BENA
BENA FORMATION

No.	Sample	Rb (ppm)	Sr (ppm)	Rb^{87}/Sr^{86}	Sr^{87}/Sr^{86}	Sr^{87}/Sr^{86} *
5689	Whole rock	43.9	45.3	2.806	0.7188	0.7186
5690	Whole rock	424.5	54.7	22.424	0.7228	
5692	Whole rock	136.6	24.5	16.161	0.7455	0.7445
5693	Whole rock	181.1	8.6	61.768	0.8990	
		180.8	8.7	61.334	0.8999	
5694	Whole rock	140.3	11.4	35.926	0.7878	0.7867
5695	Whole rock	14.7	65.0	0.654	0.7155	
5696	Whole rock	56.3	18.0	9.077	0.7340	
5697	Whole rock	141.3	27.0	15.195	0.7575	0.7563
5836	Whole rock	27.1	64.6	1.211	0.7121	
	Muscovite	246.9	32.2	22.205	0.7251	
2100	Whole rock	177.3	11.1	46.864	0.8253	
2101	Whole rock	99.5	17.7	16.284	0.7534	
2104	Whole rock	100.3	17.1	16.953	0.7437	
2108	Whole rock	26.9	74.0	1.049	0.7153	
2109	Whole rock	114.8	18.5	17.951	0.7527	

* Measured value, unspiked run
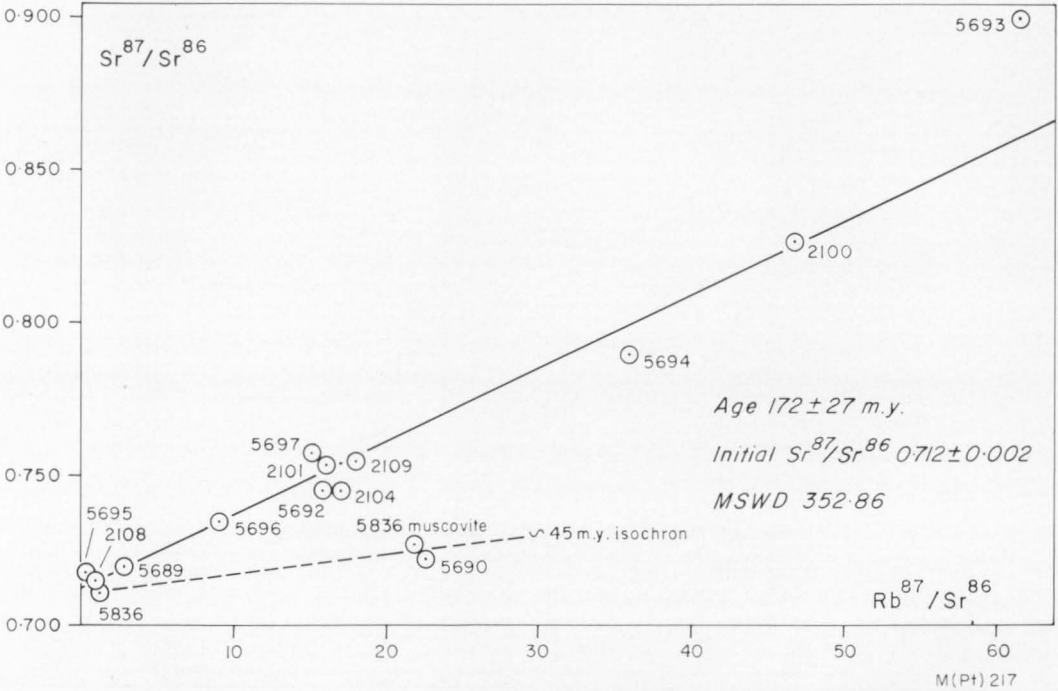
Fig. 23. Rb-Sr isochron for gneissic granites intruding the Bena Bena Formation.

regional metamorphism, and this is substantiated by the following Rb-Sr and K-Ar data for the mica phases.

The Rb-Sr analyses of the muscovite separate from 5836 and of the almost pure biotite-chlorite-tremolite rock (5690), which occurs as schlieren cutting the gneissic granite, show that the ages have clearly been updated with respect to the other whole-rock ages, and an 'event' about 45 m.y. ago is indicated (Fig. 23). Duplicate K-Ar analyses of the muscovite (Table 9) give an even younger age of 23 m.y. These limited data do not allow us to talk of an 'age of metamorphism', as the process is probably progressive and retrogressive over a period of

millions of years (cf. Armstrong, 1966). The discordance of the K-Ar and Rb-Sr muscovite ages for the Bena Bena intrusives contrasts with concordant K-Ar and Rb-Sr ages determined by Armstrong, Jäger, & Eberhardt (1966). Working on Alpine biotites, these authors were able to conclude either that there was a rapid cooling rate or that the temperature at which biotite changes from an open to a closed system is similar for Rb-Sr and K-Ar systems. In the present study, the closure of the Rb-Sr clock at about 45 m.y. can be regarded only as a minimum estimate for the metamorphism, whereas the younger K-Ar date indicates that the rock system remained at the depths where it was metamorphosed, or at least below the critical isotherm or 'metamorphic veil' (Armstrong, 1966) of argon diffusion, until about 23 m.y. ago. The K-Ar muscovite age may then be reflecting uplift of the region in the early Miocene. This is consistent with the geological evidence (McMillan & Malone, 1960; Dow & Plane, 1965), which indicates that in the early Miocene the Bena Bena Formation was a land surface, to the south of which was a shore-line and shallow-water deposition of the lower Miocene Nasananka Conglomerate.

In summary, the Rb-Sr and K-Ar data on one of the metamorphosed granitic bodies intruding the Bena Bena Formation indicates that the latter is at least as old as Early Jurassic, but that metamorphism may not have occurred until Tertiary time. It is unlikely that the Bena Bena Formation metamorphic rocks ('Bismarck Metamorphics' of Pitt, 1966) and the Omung Metamorphics are correlatives because the latter gives minimum ages related to the emplacement of the Kubor Granodiorite in the Late Permian. The Kubor Granodiorite is not metamorphosed (apart, perhaps, from burial effects), so it is clear that the Omung Metamorphics did not have a Tertiary metamorphic history. However, the age data do not preclude the possiblity that the Bena Bena Formation was regionally metamorphosed twice (i.e. at the same time as the Omung Metamorphics and then again in the

Early Tertiary), but more work would be needed to test this alternative.

4.6 MOUNT VICTOR GRANODIORITE

This mass crops out southeast of Kainantu (Fig. 22) and was first mapped by Mackay (1955), who considered it, together with most granitic rocks in the region, as Palaeozoic in age. Dow & Plane (1965) mapped the area in detail and showed that the Mount Victor Granodiorite is unconformably overlain by the Tertiary e-stage Nasananka Conglomerate, and is exposed in the core of an east-plunging anticline. The stratigraphy thus provides a definite pre-Miocene younger limit on the age of the Mount Victor Granodiorite, but there is no older limit. Dow & Plane (1965) suggested the mass might be correlated with the Morobe Granodiorite, 80 km to the southeast, or with the Bismarck Intrusive Complex, exposed 100 km to the northwest (see Plate 1). The Mount Victor Granodiorite and the two intrusives mentioned are petrographically similar, the dominant rock type being a biotite-hornblende granodiorite.

The K-Ar results for five biotites and four hornblendes from the Mount Victor Granodiorite are given in Table 12. Apart from 5461, the ages range from 89 to 95 m.y. All the rocks that were measured are granodiorites, except for 5866, which is a hornblende dolerite dyke intruding the granodiorite only 2 m away from sample 5865. The general concordance of the biotite and hornblende K-Ar dates at about 90 m.y. suggests that this (i.e. middle to Late Cretaceous) is the time of emplacement of the granodiorite. The two areas of Mount Victor Granodiorite represented by the samples dated are about 10 km apart (Fig. 22), and there is no difference in the ages.

The younger dates for 5461 of 77 and 80 m.y. (hornblende), and 88 m.y. (biotite), are not readily explained: a near-surface apophysis of the late Miocene Elendora Porphyry intrusion (see 5.32) may have updated the ages by reheating the sample. The Elendora Porphyry has intruded the Mount Victor Granodiorite and produced obvious contact metasomatic effects

TABLE 12. K-Ar AGES FOR THE MOUNT VICTOR GRANODIORITE

No.	Sample	K %		$*Ar^{40}$ $x10^{-6} cm^3$ NTP/g	$*Ar^{40}$ %	Calculated age (m.y.)
5461	Biotite	7.127 ⎱ 7.184 ⎰	7.156	25.632	95.7	88 ± 2
	Hornblende	0.610 ⎱ 0.611 ⎰	0.611	1.917 1.998	38.5 60.2	77 ± 2 80 ± 3
5862	Biotite	5.537 ⎱ 5.551 ⎰	5.544	21.003	93.7	93 ± 4
	Hornblende	0.439 ⎱ 0.439 ⎰	0.439	1.601	80.9	89 ± 4
5863	Biotite	6.461 ⎱ 6.412 ⎰	6.437	25.005	95.4	95 ± 4
5864	Biotite	6.943 ⎱ 6.958 ⎰	6.951	25.172	92.0	89 ± 4
5865	Biotite	7.120 ⎱ 7.099 ⎰	7.110	26.899	96.9	93 ± 4
	Hornblende	0.683 ⎱ 0.675 ⎰	0.679	2.550	59.0	92 ± 4
5866	Hornblende	0.809 ⎱ 0.805 ⎰	0.807	2.992	60.8	91 ± 4

close to the Mount Victor Gold Prospect to the west of sample 5461. If local reheating by the younger intrusion was responsible for argon loss from 5461 biotite and hornblende, the ages obtained do not conform to the well documented pattern found by Hart (1964). He made several K-Ar and Rb-Sr age determinations on different minerals as a function of distance from a Tertiary intrusion in a Precambrian region, and showed that hornblende was always far more argon-retentive than biotite. Perhaps the argon loss from 5461 resulted from local reheating during the deformation that resulted in the anticlinal structure of the area, but even so, one would expect the hornblende to have been more retentive. The area around 5461 would need to be dated in detail before any firm conclusions could be made.

The K-Ar evidence indicates the Mount Victor Granodiorite was emplaced 90 to 95 m.y. ago in the middle to Late Cretaceous. This age is consistent with the field evidence and so far represents the only known occurrence of Cretaceous plutonic activity in New Guinea.

5. TERTIARY PLUTONIC ACTIVITY AND METAMORPHISM IN THE NEW GUINEA MOBILE BELT

5.1 INTRODUCTION

The isotopic age data presented in the previous section indicate that emplacement of granites in the Central Highlands during the Mesozoic Era was only local and rather sporadic. Before discussing the geochronology of Tertiary plutonism and metamorphism, it is worthwhile recalling the sedimentary history of the developing Papuan Geosyncline. Sedimentation in the geosyncline during the Early Tertiary was the same as that during the late Mesozoic, but in the Oligocene there was emergence and local deposition of relatively shallow-water limestones. At the end of the Oligocene and in the early Miocene, widespread sedimentation recommenced, and the Papuan Geosyncline and Aure Trough were supplied with sediment derived from the rising land-masses within the New Guinea region. There was widespread volcanic activity throughout most of the Miocene, and some of these basic to andesitic lavas—where they are intercalated with fossiliferous sedimentary rocks—provide a basis for direct physical dating of part of the East Indies letter stage

time-scale (see 3.3). During the Miocene, and concomitant with the development of the Papuan Geosyncline, the region of the present-day Central Highlands became an elongate tectonically unstable belt, called by Dow et al. (1972) the New Guinea Mobile Belt. In this belt there is a complex system of faults and fault zones, many of which have vertical and horizontal displacements of thousands of metres (Dow et al., (1972). The Miocene Epoch was the climax to the tectonic development of the Main Cordillera of New Guinea, and the volcanism and major faulting of this time were accompanied at depth by widespread metamorphism and plutonic igneous activity.

The remainder of this chapter deals with the geological interpretation of the K-Ar and Rb-Sr dating results on several of the granodioritic to gabbroic intrusives and a smaller number of the metamorphic rocks from the New Guinea Mobile Belt. Plate 1 shows the general distribution of all the intrusive rocks. The oldest plutonic rocks (late Oligocene to early Miocene) in the belt are discussed first, and then the mid-Miocene belt of plutonic activity is described. The bulk of the geochronological work was carried out on the latter, and it is recorded in some detail.

5.2 Late Oligocene to Early Miocene Activity

The few K-Ar results indicating late Oligocene to early Miocene ages were determined for plutonic and metamorphic rocks from miscellaneous localities in the south Sepik and Ramu regions. Except for the Ambunti Metamorphics and the Kaindi Metamorphics, only one date has been determined for each mass, so the results should be regarded as tentative.

5.21 Intrusive rocks

Samples (5649 and 5970, Fig. 42) that were taken from two small unnamed hornblende diorite intrusions about 15 km apart in the lower Frieda River give concordant whole-rock and hornblende K-Ar ages of 22 to 25 m.y. (Table 13). At both localities lower f-stage (mid-Miocene) Wogamush Beds overlie the plutonic rocks, and hence the ages are consistent with the field evidence. The April Ultramafics appear to intrude or be faulted against the southern diorite mass in the Frieda River section (Fig.

TABLE 13. K-Ar AGES FOR INTRUSIVES AND METAMORPHICS IN THE SOUTH SEPIK REGION

No.	Sample	K %		$*Ar^{40}$ $x10^{-6} cm^3$ NTP/g	$*Ar^{40}$ %	Calculated age (m.y.)
Lower Frieda River intrusives						
5649	Whole rock	1.265 1.259	1.263	1.249	32.8	24.6 ± 0.8
5970	Hornblende	0.440 0.441	0.441	0.396	61.4	22.4 ± 0.4
Chambri Diorite						
5867	Biotite	7.944 7.920	7.932	6.519	76.8	20.5 ± 0.8
Ambunti Metamorphics						
5960	Muscovite	7.753 7.708	7.731	8.305	82.4	26.7 ± 0.5
5962A	Muscovite	7.557 7.571	7.564	8.092	71.6	26.6 ± 0.5
5967	Biotite	7.206 7.259	7.233	6.555	84.5	22.6 ± 0.4
5968	Hornblende	0.300 0.301	0.301	0.320	40.9	26.5 ± 0.6
Gwin Metamorphics						
71-898	Hornblende	0.0595 0.0602	0.0599	0.056	10.6	23.2 ± 2.8

42); thus the 22 to 25 m.y. diorite age, if accepted at face value, provides a maximum older estimate for the emplacement of this part of the April Ultramafics. The age of the highlands ultramafic rocks in general is considered later in 5.4. It is noted that the 22 to 25 m.y. hornblende diorite ages are distinctly older than the Frieda Porphyry intrusions (Page & McDougall, 1972a), which crop out about 20 km to the west.

The Chambri Diorite crops out in the Sepik swamps east of Ambunti. It intrudes the Ambunti Metamorphics, which are about 25 m.y. old (see later), and is overlain by Recent alluvium. The rocks have a definite flow foliation, shown by the alignment of plagioclase crystals. A single biotite K-Ar age of 20.5 ± 0.8 m.y. was determined for the Chambri Diorite, and this early Miocene date can be regarded as a tentative minimum for the emplacement of the mass. It will be seen later that the respective ages of the Ambunti Metamorphics (about 25 m.y.) and the intruding Chambri Diorite (about 20 m.y.) are internally consistent with the geologically mapped relations between the two masses.

Another late Oligocene to early Miocene K-Ar age was determined by Isotopes Incorporated (Continental Oil Company of Australia Pty Ltd, pers. comm., 1970) for a small microsyenite mass (at 144°38'E, 4° 54'S) near Annenberg Mission Station, on the Ramu River. There is no stratigraphic control on the intrusion, from which a whole-rock sample was dated as 22.7 ± 0.3 m.y.

5.22 Metamorphic rocks

Ambunti Metamorphics. Mapping of the sporadic outcrops over the Sepik River plains (Fig. 42) showed that much of this vast area is underlain by rocks known as the Ambunti Metamorphics (Dow et al., 1972). East of the April River, the metamorphics are greenschist-facies slates and phyllites; to the west, amphibolite-facies rocks (including quartz-garnet-muscovite gneiss, with or without kyanite and staurolite; biotite-staurolite schist; hornblende-diopside amphibolite; quartz-albite-muscovite schist, etc.) are developed. The stratigraphic age of the Ambunti Metamorphics is not known, but a younger limit is given by lower *f*-stage (mid-Miocene) sediments which unconformably overlie the metamorphic rocks in several places. Dow et al. (1972) suggested a probable Mesozoic age, and tentatively correlated the Ambunti Metamorphics with the Gwin Metamorphics, which crop out about 50 km to the west and have a supposed pre-Late Cretaceous age (Paterson & Perry, 1964). As pointed out by Dow et al. (1972), the stratigraphic relations for the Gwin Metamorphics indicated by Paterson & Perry (1964) are by no means unequivocal, and hence the younger age limit of Late Cretaceous is somewhat uncertain.

In this study only a few results were obtained for the Ambunti Metamorphics because of very limited outcrop and strong weathering. One area in the upper part of the May River was chosen for study (Fig. 42), and the K-Ar results are listed in Table 13; the mineral separates are from two muscovite-garnet schists (5960 and 5962A), a biotite-garnet-amphibole schist (5967), and an amphibolite (5968). The two muscovite samples and the hornblende give virtually identical ages of just over 26 m.y. (late Oligocene), and the apparent biotite age is 22.6 ± 0.4 m.y. One hornblende from an amphibolite in the Gwin Metamorphics (sample 71-898; lat. 4°28'S, long. 141° 14'E) gives a similar age of 23.2 m.y., thus helping to confirm the supposed correlation.

The three micas and the whole-rock schists from which they were separated were also analysed by the Rb-Sr method; the analyses are given in Table 14 and are plotted on a Rb-Sr isochron diagram (Fig. 24) in which the sample points are widely scattered and may reflect incomplete isotopic homogenization at the time of metamorphism. These differences between the initial Sr^{87}/Sr^{86} ratios are not unexpected, since the samples are from widely separated localities. If the minerals have remained closed systems since the last metamorphic event, one can extrapolate the mineral/ whole-rock join for each sample, in order to find the respective initial Sr^{87}/Sr^{86} ratios, and hence calculate the Rb-Sr mica ages.

TABLE 14. Rb-Sr DATA FOR THE AMBUNTI METAMORPHICS AND KAINDI
METAMORPHICS

No.	Sample	Rb (ppm)	Sr (ppm)	Rb^{87}/Sr^{86}	Sr^{87}/Sr^{86}
Ambunti Metamorphics					
5960	Whole rock	77.0	75.6	2.939	0.7077
	Muscovite	326.2	275.9	3.415	0.7080
5962A	Whole rock	119.0	159.0	2.160	0.7083
	Muscovite	383.1	268.1	4.127	0.7087
5967	Whole rock	39.0	179.3	0.628	0.7044
	Biotite	226.5	37.9	17.269	0.7101
Kaindi Metamorphics					
71-274	Whole rock	150.9	81.6	5.347	0.7206
71-275	Whole rock	32.4	183.0	0.512	0.7182
					0.7183*
71-276	Whole rock	163.3	42.9	10.999	0.7214
71-277	Whole rock	160.6	51.3	9.045	0.7209
71-278	Whole rock	145.1	38.4	10.936	0.7215
71-279	Whole rock	166.4	71.5	6.731	0.7207
71-280	Whole rock	172.1	51.0	9.751	0.7213
71-281	Whole rock	187.8	48.1	11.279	0.7220

* Sr^{87}/Sr^{86} measured directly, unspiked analysis.
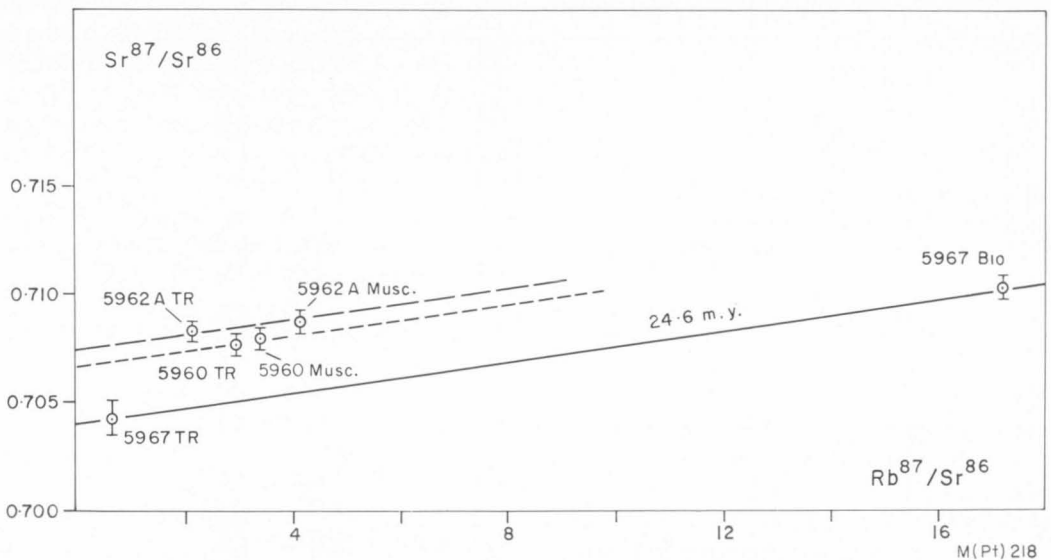
Fig. 24. Rb-Sr isochron for the Ambunti Metamorphics.

The resultant age from the two-point iso-chron for 5967 is 24.6 m.y. with an indicated initial Sr^{87}/Sr^{86} ratio of 0.7042. Although two lines approximately parallel to this isochron can be drawn through each muscovite/whole-rock pair, there are insufficient data to allow adequate interpretation. Taken at face value, however, the isochrons in Figure 24 imply that the metamorphic rocks began their post-metamorphic history with different initial Sr^{87}/Sr^{86} ratios; these range from 0.7042 (for 5967) to 0.7075 (for 5962A). It is stressed that this interpretation is tentative, and that further
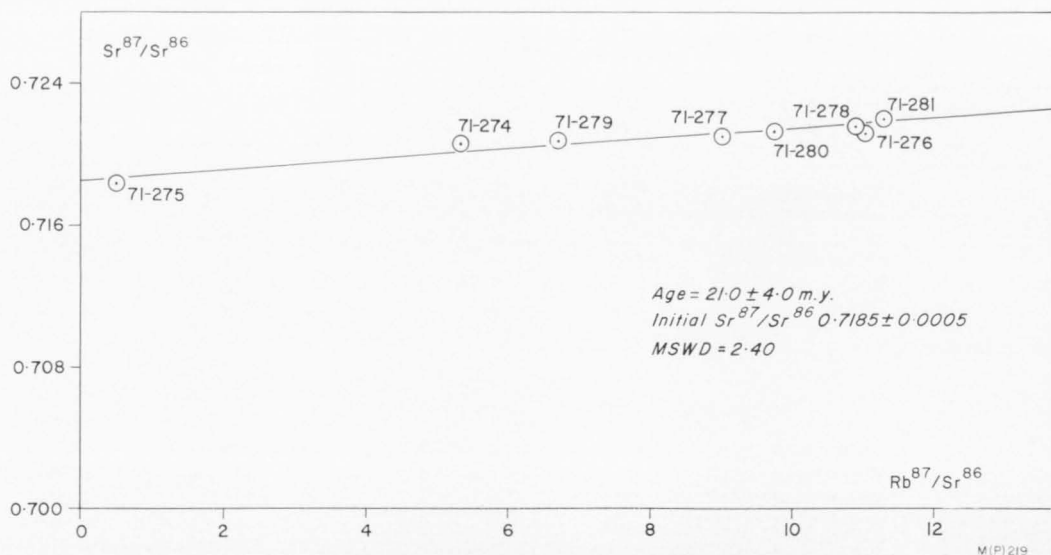
Fig. 25. Rb-Sr isochron for the Kaindi Metamorphics.

analyses of related samples of the schists would be necessary to obtain a reliable Rb-Sr isochron.

Even though the Ambunti Metamorphics are of variable rock type and may have had a complex metamorphic history, it is possible to make some conclusions about the probable meaning of the apparent ages. The excellent agreement between the K-Ar ages of the muscovites and hornblende suggests that the 26 m.y. age is significant, particularly as the potassium contents of the two minerals differ by a factor of 25. This age is interpreted as a minimum estimate for uplift of the area after regional metamorphism of the Ambunti Metamorphics. The K-Ar biotite age (5967) is 4 m.y. younger than the other K-Ar mineral ages; these data would be in accordance with a slow uplift in which the rocks were gradually raised to a cooler level in the crust where radiogenic argon began to accumulate simultaneously in the muscovite and hornblende, which formed closed systems at higher temperatures (about 4 m.y. earlier) than the biotite.

The difference between the K-Ar and Rb-Sr ages of 22.6 m.y. and 24.6 m.y. is negligible considering the uncertainties in the ages. Armstrong et al. (1966) found a similar pattern in 16 out of 18 comparisons

of K-Ar and Rb-Sr biotite ages from metamorphic rocks of the southern and central Alps. From independent data the authors concluded that the biotites were reflecting cooling (uplift) ages, and that the Rb-Sr versus-K-Ar concordancy was due to similar transition temperatures of biotite from an open to a closed system for both isotopic clocks. As stated above, the data, although limited, from the Ambunti Metamorphics would be consistent with such an interpretation.

The credibility of the youthful late Oligocene to early Miocene ages obtained for the Ambunti and Gwin Metamorphics is enhanced by the slightly younger ages that are obtained on the plutonic rocks (Chambri Diorite, 5.21; Frieda Porphyry, Page & McDougall, 1972a) which are known to intrude the metamorphics.

Kaindi Metamorphics. As part of the regional geochronological investigations in New Guinea, a suite of samples from the Cretaceous? Kaindi Metamorphics was sampled about 4 km west-northwest of Wau (Fig. 26). The geological background and structure of this metamorphic belt are discussed by Dow & Davies (1964) and Dow, Smit, & Page (1974). In the area sampled, the Kaindi Metamorphics are mainly quartz-

sericite-graphite schists and phyllites. Although later Pliocene porphyries intrude the metamorphics a few kilometres to the east and west of the area sampled, there are no apparent signs of contact metamorphism in the rocks studied. In thin section, the delicate micaceous schistosity is undisturbed. Because of their fine grainsize, K-Ar work on the minerals was not feasible, and a clustered group of samples for Rb-Sr whole-rock analysis was collected from across the entire area of one outcrop (10 m diameter), which was quite foliated with obvious slaty cleavage but had no recognizable primary bedding.

The 8 samples analysed (Table 14, Fig. 25) show a desirable dispersion in Rb^{87}/Sr^{86} ratios, and the isochron regression yields an age of 21.0 ± 4.0 m.y. and initial Sr^{87}/Sr^{86} ratio of 0.7185 ± 0.0005. This is a Model I isochron as the MSWD is not significantly greater than unity at the 5 precent level (using the statistical F test).

The age of 21 m.y. and the indicated high initial ratio must be reflecting the main metamorphic imprint on the rocks, because fossiliferous control elsewhere in the formation indicates that deposition took place at least as early as the Cretaceous. The 21 m.y. 'metamorphic age' corresponds to a time in the early Miocene, and is virtually indistinguishable from the K-Ar ages recorded on the Ambunti and Gwin Metamorphics in the south Sepik area.

The present Rb-Sr data do not provide any information about the number of episodes of metamorphism. The Model I isochron suggests that the 21 m.y. metamorphism was the major and probably the final metamorphic event, but it does not preclude the possibility that there was an earlier metamorphic history. Field evidence elsewhere in the metamorphic belt (Dow et al., 1974) suggests the presence of a mid-Early Tertiary (pre-*e* stage) metamorphism.

The early Miocene age of metamorphism for the Kaindi Metamorphics determined in this study is clearly a minimum value because of the possibility of updating by the nearby Pliocene intrusives in the Edie Creek area. However, if later updating had affected the isotopic system, one would not expect the samples to define a Model I isochron. If the early Miocene age is confined on metamorphic rocks elsewhere in the Owen Stanley Ranges, it will provide a more precise estimate, not only of the age of metamorphism, but also of the age of emplacement of the Papuan Ultramafic Belt. The two processes are thought to be closely related by Davies & Smith (1971), who have, in fact, suggested an early Eocene age.

5.3 MIDDLE AND LATE MIOCENE PLUTONIC ACTIVITY

The preceding discussion (5.2) based on reconnaissance dating in the south Sepik and Ramu regions demonstrated that Tertiary plutonic igneous and metamorphic activity was initiated in New Guinea in the late Oligocene to early Miocene. Rocks of this age were evidently the forerunners of widespread middle to late Miocene plutonic igneous activity, volcanism, and faulting of great magnitude. These plutonic and volcanic igneous rocks form a major part of the Main Cordillera.

Because of the rather limited stratigraphic evidence for the age of the widespread batholiths, most observers in the Central Highlands believed (until recently) that they constituted the basement complex upon which the Tertiary geosynclinal sediments developed. It is true that there are a few small 'basement' intrusives of late Palaeozoic to Mesozoic age in the Highlands, as demonstrated by the stratigraphic evidence and isotopic dates outlined in section 4. In the absence of stratigraphic restraints on plutonic rocks elsewhere, the ages of many intrusives were extrapolated from the known age of the nearest 'basement' intrusives. This led to the general misconception that much of the plutonic igneous activity in New Guinea took place in Mesozoic or Palaeozoic times.

A large number of KAr and Rb-Sr age measurements were made on the individual granodiorite, diorite, and minor gabbro plutons of the New Guinea Mobile Belt in an attempt to elucidate the intrusive history. The granitic belt is over 700 km long in Papua New Guinea alone (Plate 1), and since the intrusions are completely massive
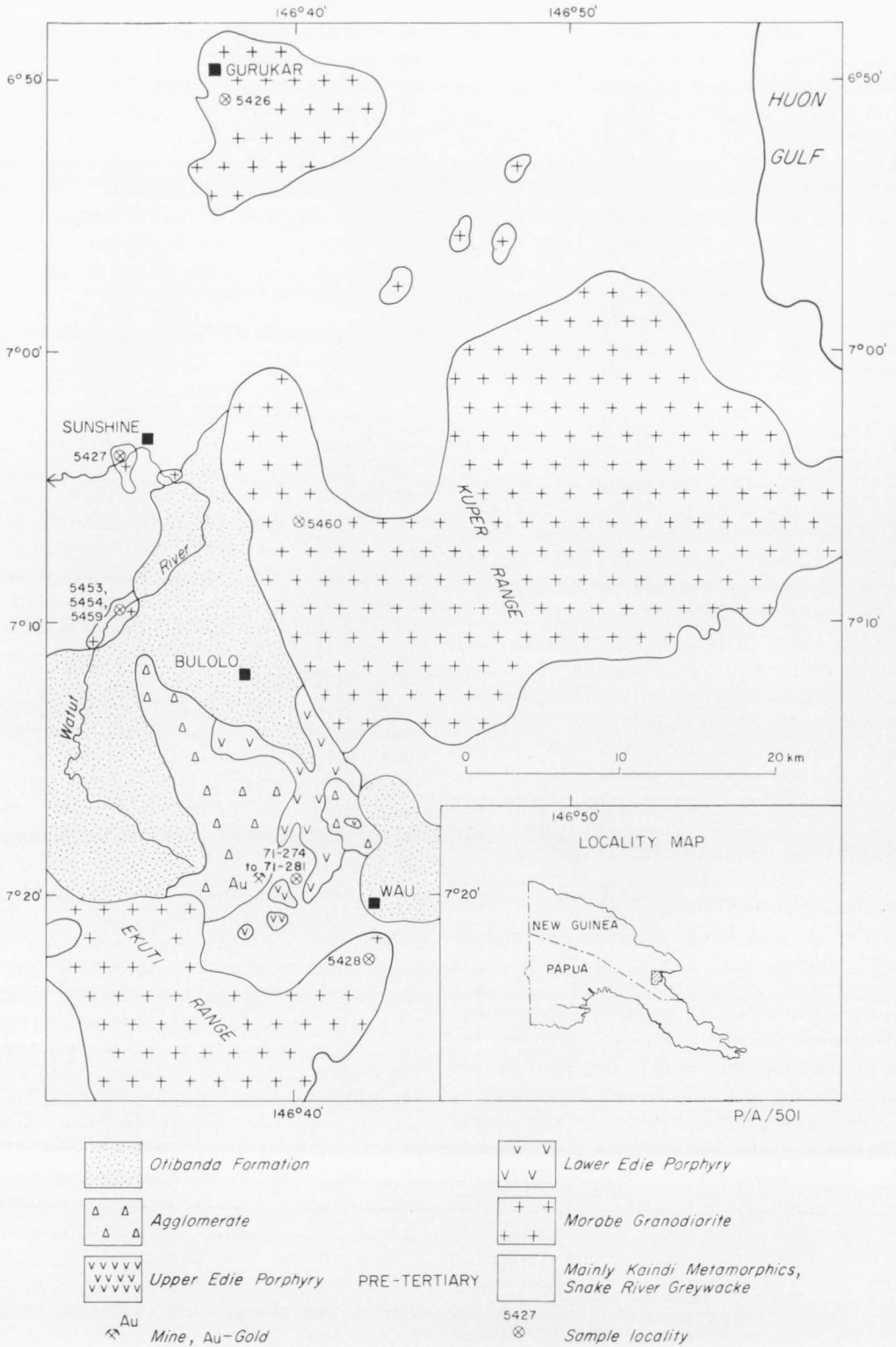
Fig. 26. Simplified geological map—Morobe area.

TABLE 15. K-Ar AGES FOR THE MOROBE GRANODIORITE

No.	Sample	K %		$*Ar^{40}$ $x10^{-6}$ cm^3 NTP/g	$*Ar^{40}$ %	Calculated age (m.y.)
5426	Biotite	7.597 7.632	7.615	3.939	80.1	12.9 ± 0.2
	Hornblende	0.588 0.588	0.588	0.343	26.5	14.6 ± 0.5
5427	Biotite	7.551 7.555	7.553	4.044 3.932	62.4 70.1	13.4 ± 0.3 13.0 ± 0.2
	Hornblende	0.783 0.777	0.780	0.465	58.7	14.9 ± 0.3
5428	Biotite	7.512 7.544	7.528	3.267	87.6	11.0 ± 0.2
	Hornblende	1.064 1.056	1.060	0.523	51.7	12.3 ± 0.3
5460	Hornblende	0.554 0.559	0.557	0.281	50.5	12.6 ± 0.3
5453	Biotite	7.854 7.833	7.844	4.209	53.7	13.4 ± 0.2
5454	Biotite	7.555 7.548	7.552	4.027	68.7	13.3 ± 0.2
	Hornblende	0.474 0.478	0.476	0.256	37.0	13.5 ± 0.6
5459	Biotite	7.511 7.552	7.532	4.079	80.2	13.5 ± 0.2
	Hornblende	0.605 0.600	0.603	0.353	47.8	14.6 ± 0.3

and transgressive bodies (except where emplacement was fault-controlled) it is reasonable to assume they are of high-level, post-tectonic origin. Various names have been applied to the plutonic rocks by BMR regional mapping parties, and it is found convenient to discuss the isotopic age data in five sections that correspond to major areas from east to west in the Central Highlands intrusive belt.

5.31 Morobe Granodiorite

The Morobe Granodiorite is the name given by Fisher (1944) to a number of large and several small granodiorite plutons in the Morobe District southwest of Lae (Fig. 26). Noakes (1938), Fisher (1944), and Mackay (1955) stated that the rocks are mainly granodiorite and adamellite with differentiates of monzonite, diorite, hornblendite, and pegmatite developed at the margins. The Morobe Granodiorite intrudes the Kaindi Metamorphics and the Cretaceous Snake River Greywacke (Dow & Davies, 1964), and a separate intrusion farther west is overlain by the Miocene Langimar Beds (Fisher, 1944; Dow, 1967); the exact age

of the Langimar Beds is uncertain as the Miocene microfauna are not distinctive enough for further definition. Lake beds of the Pliocene Otibanda Formation (Plane, 1967) also overlie the Morobe Granodiorite in many areas.

Biotite and hornblende K-Ar ages (Table 15) have been measured on some of the granodiorite intrusions, and the sample localities are shown in Figure 26. The intrusion surrounding Gurukar village, and the two small bodies sampled just west of Sunshine and in the Watut River, give a consistent pattern with five biotite ages at about 13 m.y., and all hornblende ages at about 14 m.y. One sampled dated from each of the Ekuti Range and Kuper Range masses (5428 and 5460) gives hornblende and biotite ages 2 m.y. younger than the other bodies.

K-Ar data for the Morobe Granodiorite are plotted on initial argon and argon isochron diagrams in Figures 27 to 29. The data points from the Ekuti and Kuper Range masses were not considered in the regressions, because both K-Ar and Rb-Sr
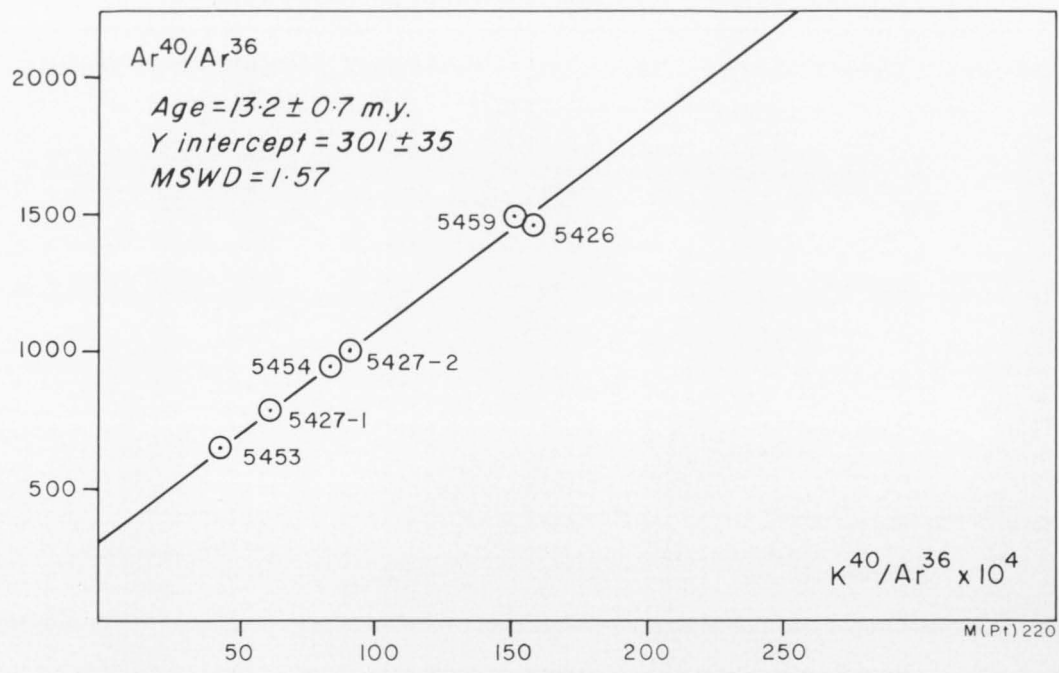
Fig. 27. Argon isochron for the Morobe biotites.
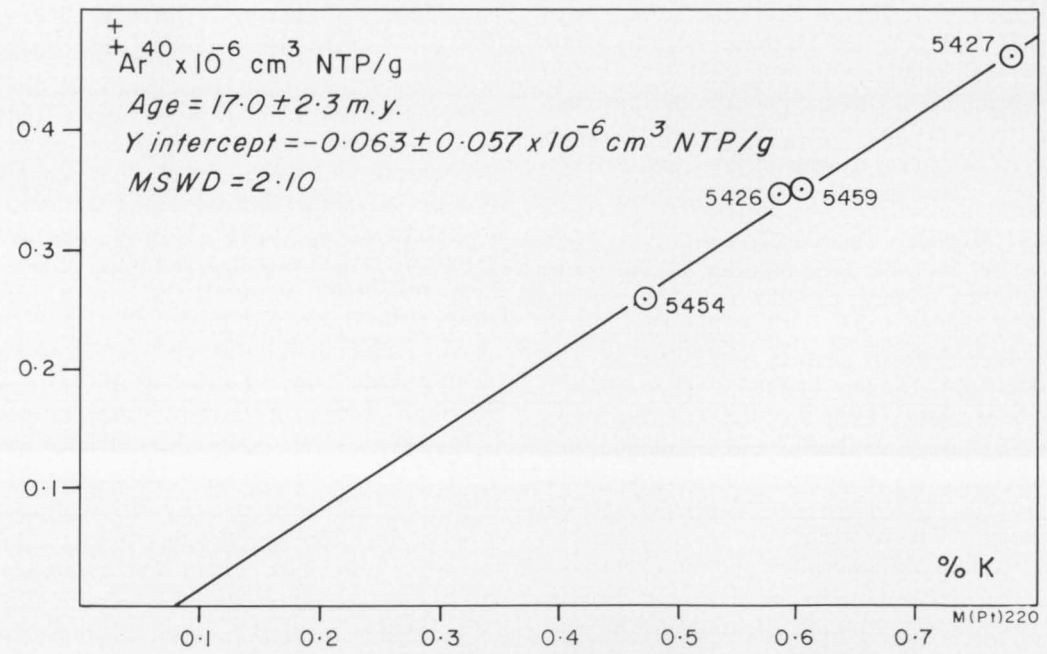
Fig. 28. Initial argon plot for the Morobe hornblendes.
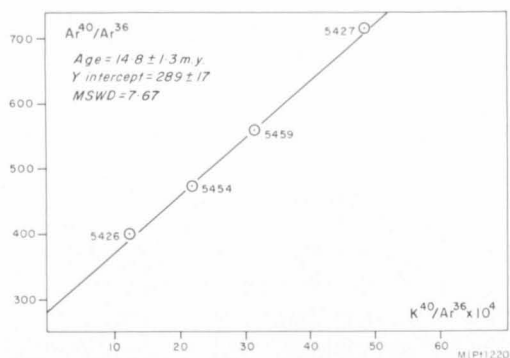
Fig. 29. Argon isochron for the Morobe hornblendes.

ages (see later) indicate that these are slightly younger masses. Results of each regression analysis are given in the respective graphical plots with the errors quoted at the 95-percent confidence level. The ages from the initial argon and isochron plots are not distinguishable from the conventionally calculated ages, and, within the uncertainties quoted, no extraneous argon appears to be present in the hornblendes or biotites.

Table 16 gives Rb-Sr data for three biotites and whole rocks from the Morobe Granodiorite. The granodiorites have rather low Rb/Sr ratios and hence are not amenable to independent age determination. Their present-day Sr^{87}/Sr^{86} values (equal to initial Sr^{87}/Sr^{86}) provide a basis for calculating the Rb-Sr biotite ages, which are shown and also compared with the K-Ar ages in the right-hand column in Table 16. The three Rb-Sr biotite ages are 0.9 to 1.7 m.y. older than the respective K-Ar ages, and such differences cannot be accounted for

by any experimental or Rb^{87} half-life uncertainties. The Rb-Sr biotite results confirm the relative K-Ar ages on the individual intrusions. In each of 5426, 5427, and 5428 the Rb-Sr biotite and K-Ar hornblende ages are close. This consistency is good evidence that the Gurukar, Sunshine, and Watut bodies were emplaced between 14 and 14.5 m.y. ago (i.e. in the mid-Miocene) and the other two masses (Ekuti and Kuper Range) about 12 to 13 m.y. ago.

The constant age difference of 1 to 2 m.y. between the K-Ar and Rb-Sr biotite results can be interpreted probably in terms of the uplift and cooling history of the stocks after they were emplaced. The 1 to 2 m.y. gap may be the time interval during which the rocks crystallized (when radiogenic argon began to accumulate in the hornblende, and radiogenic strontium began to accumulate in the biotite) and were raised to cooler levels in the crust (when radiogenic argon began to accumulate in the biotite). Such an interpretation is more or less in accordance with Hart's (1964) findings in his study of mineral age variations across a plutonic contact zone. He demonstrated that for a given distance from the pluton, the order of argon and strontium retentivity was: hornblende (K-Ar), biotite (Rb-Sr), and the least retentive was biotite (K-Ar). As pointed out by Hart (1964), this order may change under different environmental conditions, and, for the Morobe Granodiorite, it would appear that hornblende (K-Ar) and biotite (Rb-Sr) became closed systems at about the same temperature.

TABLE 16. Rb-Sr DATA FOR THE MOROBE GRANODIORITE

No.	Sample	Rb (ppm)	Sr (ppm)	Rb^{87}/Sr^{86}	Sr^{87}/Sr^{86}	Rb-Sr age (m.y.)	K-Ar age (m.y.)
5426	Whole rock	73.3	678.3	0.312	0.7048		
	Biotite	503.2	21.0	69.244	0.7181	13.8	12.9
	Hornblende						14.6
5427	Whole rock	44.9	602.9	0.215	0.7043		
	Biotite	462.9	17.2	77.654	0.7199	14.5	13.2
	Hornblende						14.9
5428	Whole rock	49.3	897.2	0.159	0.7047		
	Biotite	462.5	9.7	137.543	0.7289	12.7	11.0
	Hornblende						12.3

It was noted earlier that Armstrong et al. (1966) observed concordant biotite Rb-Sr and K-Ar ages on regionally metamorphosed rocks in the southern and central Alps, and that a similar situation existed in the Ambunti Metamorphics (5.22). From these results it would seem that argon and strontium behave similarly under conditions of regional metamorphism, but in terms of the emplacement of granites and contact metamorphism the Rb-Sr system in biotite is closed earlier (at higher temperatures) than the K-Ar system. The well documented conclusion that hornblende is more argon-retentive than biotite is also demonstrated by the Morobe Granodiorite data and, as will be seen later, this is a common phenomenon in most of the New Guinea Miocene intrusives.

5.32 Intrusives in the Kainantu and Mount Michael areas

For convenience, the intrusives in the Kainantu and Mount Michael areas are informally grouped to include over 25 large and small Tertiary masses (Plate 1). In the past, the intrusions have been assigned various names based on locality, mineralogy, and texture, but there is very little stratigraphic control on their ages, and so it is considered best to discuss these bodies in relation to the isotopic dating results.

Akuna Intrusive Complex. Formerly the Akuna Dolerite of Dow & Plane (1965), the Akuna Intrusive Complex (Grainger & Tingey, 1976) includes several gabbroic intrusives up to 10 km across in the area east of Kainantu (Fig. 22). Dow & Plane (1965) described the rocks as porphyritic dolerites containing phenocrysts of augite and plagioclase in a groundmass of augite, plagioclase, and iron minerals, with or without biotite and olivine. Mackay (1955) and McMillan & Malone (1960) noted intermediate differentiates in the Yonki Dome mass, and Read (1967) mapped a granodiorite mass, which is here included in the Akuna Intrusive Complex, near the Ramu River Gorge. Mackay (1955) stated that gabbroic rocks intrude the granodiorite north of Yonki Dome. I noted doleritic rocks

similar to the Akuna Intrusive Complex about 8 km southwest of Kainantu (5668 and 5669). Dow & Plane (1965) mapped this body as part of the Aifunka Volcanics, which they assumed were Pliocene in age; but there was no fossil evidence or any strong stratigraphic argument for such an age. The Akuna Intrusive Complex intrudes Tertiary *e*-stage (lower Miocene) Omaura Greywacke, and is intruded by the Elendora Porphyry (see later), thus providing a younger age limit for the Akuna Intrusive Complex. Dow & Plane (1965) suggested that the Akuna Intrusive Complex is the intrusive counterpart of volcanics in the Tertiary lower *f*-stage (mid-Miocene) Lamari conglomerate member of the Yaveufa Formation, and therefore inferred that it was probably also lower *f*-stage in age.

Seventeen mineral and whole-rock K-Ar measurements were made on samples from various localities (Fig. 22) within the Akuna Intrusive Complex and related rocks. The data and ages are listed in Table 17. Four of the eight whole rocks (5660, 5851, 5854, and 5855) were dolerites sampled near Akuna and Omaura villages, and ages of between 14 and 16.5 m.y. are indicated. The two dolerite ages from the Yonki Dome mass (5852 and 5853) are 15.5 ± 0.6 m.y. and 13.2 ± 0.6 m.y. The latter sample is somewhat altered, and the young age may indicate some loss of radiogenic argon. The dolerites (5668 and 5669) mapped as part of the Aifunka Volcanics by Dow & Plane (1965) show an age spread of 14.2 to 16.7 m.y., similar to that for the main Akuna Intrusive Complex.

The K-Ar mineral ages for the Akuna Intrusive Complex (Table 17) were measured on the basic, intermediate, and acidic rocks that occur towards the margins of the Yonki Dome intrusion. The Ramu Gorge samples (5860 and 5861) are granodiorites from near the intrusive contact with the Omaura Greywacke. In general the mineral ages cannot be distinguished from the dolerite whole-rock ages and (with the exception of 5861 hornblende) both show a similar spread. Four of the biotite ages are

TABLE 17. K-Ar AGES FOR INTRUSIVES IN THE KAINANTU-MOUNT MICHAEL AREA

No.	Sample	K %		$*Ar^{40}$ $x10^{-6} cm^3$ NTP/g	$*Ar^{40}$ %	Calculated age (m.y.)
Akuna Intrusive Complex						
5660	Whole rock	1.562 1.570	1.566	0.930	26.3	14.8 ± 0.5
5668	Whole rock	0.659 0.654	0.657	0.440	48.4	16.7 ± 0.7
5669	Whole rock	0.713 0.709	0.711	0.405	50.4	14.2 ± 0.6
5851	Whole rock	1.200 1.195	1.198	0.802 0.799	35.7 25.0	16.7 ± 0.7 16.6 ± 0.3
5852	Whole rock	0.390 0.385	0.388	0.241	49.3	15.5 ± 0.6
5853	Whole rock	0.474 0.478	0.476	0.252	51.2	13.2 ± 0.6
5854	Whole rock	1.361 1.373	1.367	0.799	61.2	14.6 ± 0.6
5855	Whole rock	1.381 1.391	1.386	0.828	50.7	14.9 ± 0.3
5467	Biotite	6.434 6.494	6.464	3.450	78.3	13.5 ± 0.2
	Hornblende	0.552 0.550	0.551	0.360	13.3	16.3 ± 0.8
5468	Biotite	7.616 7.612	7.614	4.707	85.0	15.4 ± 0.6
5469	Biotite	7.740 7.718	7.729	4.138	73.0	13.4 ± 0.2
5856	Biotite	7.750 7.748	7.749	4.605	62.8	14.8 ± 0.6
5860	Biotite	7.566 7.628	7.597	4.022	81.2	13.2 ± 0.5
5861	Biotite	6.996 6.967	6.982	3.786	72.5	13.5 ± 0.5
	Hornblende	0.676 0.670	0.673	0.259	25.0	9.6 ± 0.5
Elendora Porphyry						
5837	Hornblende	1.278 1.278	1.278	0.509	40.1	10.0 ± 0.4
5858	Hornblende	0.674 0.676	0.675	0.215	40.9	8.0 ± 0.3
5873	Hornblende	0.577 0.572	0.575	0.169 0.172	26.1 23.0	7.4 ± 0.3 7.5 ± 0.4
5874	Hornblende	0.607 0.611	0.609	0.236 0.248	43.1 18.3	9.7 ± 0.4 10.1 ± 0.5
Intrusives near Sonofi village						
5470	Hornblende	0.527 0.529	0.528	0.261	36.5	12.4 ± 0.5
5655	Whole rock	0.637 0.627	0.632	0.230	21.0	9.1 ± 0.3
5656	Whole rock	1.029 1.028	1.029	0.333	44.3	8.1 ± 0.2
5657	Whole rock	0.765 0.758	0.762	0.249	41.8	8.2 ± 0.2
	Hornblende	0.392 0.395	0.394	0.125	34.1	7.9 ± 0.2
	Clinopyroxene	0.0401 0.0396	0.0399	0.034	7.4	21.1 ± 2.6

TABLE 17. K-Ar AGES FOR INTRUSIVES IN THE KAINANTU-MOUNT MICHAEL AREA—(cont.)

No.	Sample	K %		$*Ar^{40}$ $x10^{-6} cm^3$ NTP/g	$*Ar^{40}$ %	Calculated age (m.y.)
5658	Whole rock	1.087 1.087 }	1.087	0.311	31.3	7.2 ± 0.2
	Hornblende	0.392 0.387 }	0.390	0.129	12.8	8.2 ± 0.5
5659	Whole rock	0.937 0.923 }	0.930	0.267	22.8	7.2 ± 0.3
Michael Diorite						
5879	Hornblende	0.635		0.182	20.6	7.2 ± 0.2
5880	Hornblende	0.412 0.416 }	0.414	0.105 0.122	23.3 15.7	6.3 ± 0.3 7.4 ± 0.2
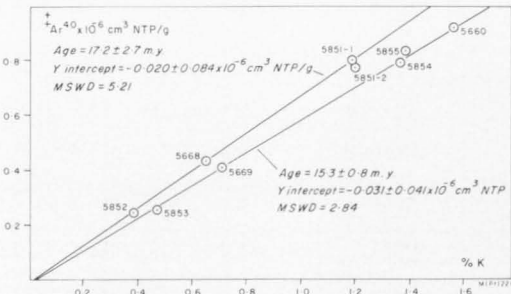
Fig. 30. Initial argon plot for Akuna whole rocks.
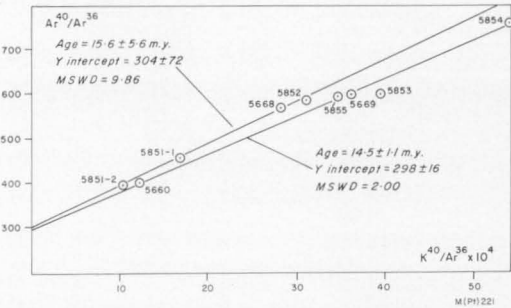
Fig. 31. Argon isochron for Akuna whole rocks.

about 13.5 m.y. and two others, from localities about 8 km apart, are about 15 m.y. The hornblende age for 5861 is 4 m.y. lower than the biotite age; the reason for the general discordancy of the results is not immediately explicable.

Graphical plots of the Akuna Intrusive Complex whole-rock data (Figs. 30 and 31) suggest that there may be two separate ages of about 15 and 17 m.y. The points show considerable scatter about the straight lines

and, within the uncertainties quoted, there is no indication of extraneous argon in the samples. It is possible that the ages represent a somewhat complex intrusive history in the area, but there is no apparent correlation between age and rock type. Perhaps the spread is due to partial updating of some of the rocks. The southern Akuna Intrusive Complex mass is intruded by the Elendora Porphyry; it is conceivable that the latter is more widespread beneath the Akuna Intrusive Complex, and that its heating effects have been the cause for loss of argon from parts of the mass.

Elendora Porphyry. Intrusives grouped in the Elendora Porphyry crop out in many places in the Kainantu area (Fig. 22). These hornblende microdiorite bodies were shown to be later than the Tertiary lower *f*-stage 'Lamari Conglomerate' (now part of the Yaveufa Formation) by Dow & Plane (1965), who regarded them as Pliocene in age. The Elendora Porphyry corresponds to the 'late Tertiary hypabyssal rocks' mapped by McMillan & Malone (1960).

The K-Ar ages for the Elendora Porphyry are listed in Table 17. The hornblende sample dated from north of Mount Elendora (5858) has a K-Ar age of 8.0 ± 0.3 m.y. The samples from Mount Munefinka (5873 and 5874) give discordant duplicated ages of about 7.5 and 10 m.y., and the fourth hornblende date of 10.0 ± 0.4 m.y. is from a dyke (5837) that intrudes the gneissic granite of the Bena Bena Formation.

About 8 km west of Sonofi, a hornblende microdiorite body (5470) shown as Aifunka Volcanics by Dow & Plane (1965) intrudes the Tertiary e-stage sediments, and a hornblende age of 12.4 ± 0.5 m.y. was determined. A number of K-Ar measurements were made on another small porphyritic hornblende microdiorite mass which intrudes the Tertiary lower f-stage Lamari conglomerate member of the Yaveufa Formation in the Faiantina River 6 km southwest of Sonofi village, and these results (5655 to 5659) are also given in Table 17. The five whole-rock and two hornblende results form a fairly consistent age group of about 7 to 9 m.y., which is good evidence that this is the probable age of emplacement of the mass. The anomalously high age of 5657 clinopyroxene is probably due to the presence of extraneous radiogenic argon, whose effect is emphasized by the low potassium content (0.04%). As with the other dated hornblende microdiorites in the Kainantu region, the measured ages of this mass are completely consistent with the field observations.

Taken at face value the hornblende and whole-rock ages indicate that most of the Elendora Porphyry microdiorites were emplaced between 7 and 9 m.y. ago, during the late Miocene. This was well after the time of Akuna Intrusive Complex emplacement, and, as previously suggested, the younger intrusions may have been responsible for updating and causing the observed age spread in the Akuna Intrusive Complex.

Michael Diorite. The Michael Diorite (Bain et al., in press) forms a prominent mountain peak at the eastern end of the Kubor Range about 60 km west-southwest of Kainantu. It is a hypabyssal intrusive body consisting of several bosses and sills described as 'microporphyritic hornblende diorites'. Rickwood & Kent (1956) believed that the rocks intruded Cretaceous sediments, but Bain et al. (in press) demonstrated that the mass intrudes sediments as young as Tertiary lower f stage (middle Miocene). Hornblende was dated from two microdiorites (Table 17) that were sampled along the road southeast of Lufa patrol post (Fig. 10). It would appear that these rocks were emplaced 6 to

7 m.y. ago in the late Miocene, and that the Michael Diorite belongs to the same age group as the several microdiorite masses near Kainantu.

5.33 *Bismarck Intrusive Complex*

The Bismarck Intrusive Complex (Bain et al., in press) is the amended name of the Bismarck Granodiorite, an elongate northwest-trending batholith (65 km by 25 km) with a number of smaller bodies around its eastern margin (Fig. 32). It is composed predominantly of granodiorite with minor gabbro and diorite, and crops out over a considerable area of the rugged Bismarck Range. Many of the peaks are over 3000 m above sea level and some, such as Mount Wilhelm (4510 m above sea level), show evidence of Pleistocene glaciation (Peterson, 1970).

Rickwood (1955) and McMillan & Malone (1960) mapped part of the Bismarck mass and, because of its lithological similarity to the Kubor Granodiorite about 50 km to the southwest, they considered that it was also of Palaeozoic age. With further mapping of the area, however, Dow & Dekker (1964) showed that the Bismarck mass intrudes the Upper Triassic Kana Formation (renamed Kana Volcanics by Dow et al., 1972). On the basis of questionable stratigraphic evidence, Dow & Dekker (1964) believed that the batholith was overlain by Jurassic sediments, and hence they concluded that the mass was emplaced in the latest Triassic or earliest Jurassic. However, the only unequivocal stratigraphic control on the age was beyond the southeast end of the main Bismarck mass, at Urabagga Hill, where a small outcrop of granitic rock is unconformably overlain by Oligocene *Nummulites* limestone (Fig. 32). McMillan & Malone (1960) extrapolated the undisputed unconformable relationship at Urabagga Hill and stated that the whole of the Bismarck 'batholith is certainly older than the Oligocene'. Such an extrapolation clearly depends on the assumption that the main Bismarck mass and the outcrop at Urabagga Hill are the same age. It was shown in 4.4 that the Urabagga Hill intrusion is most probably the same age as the nearby intrusion (4 km

60
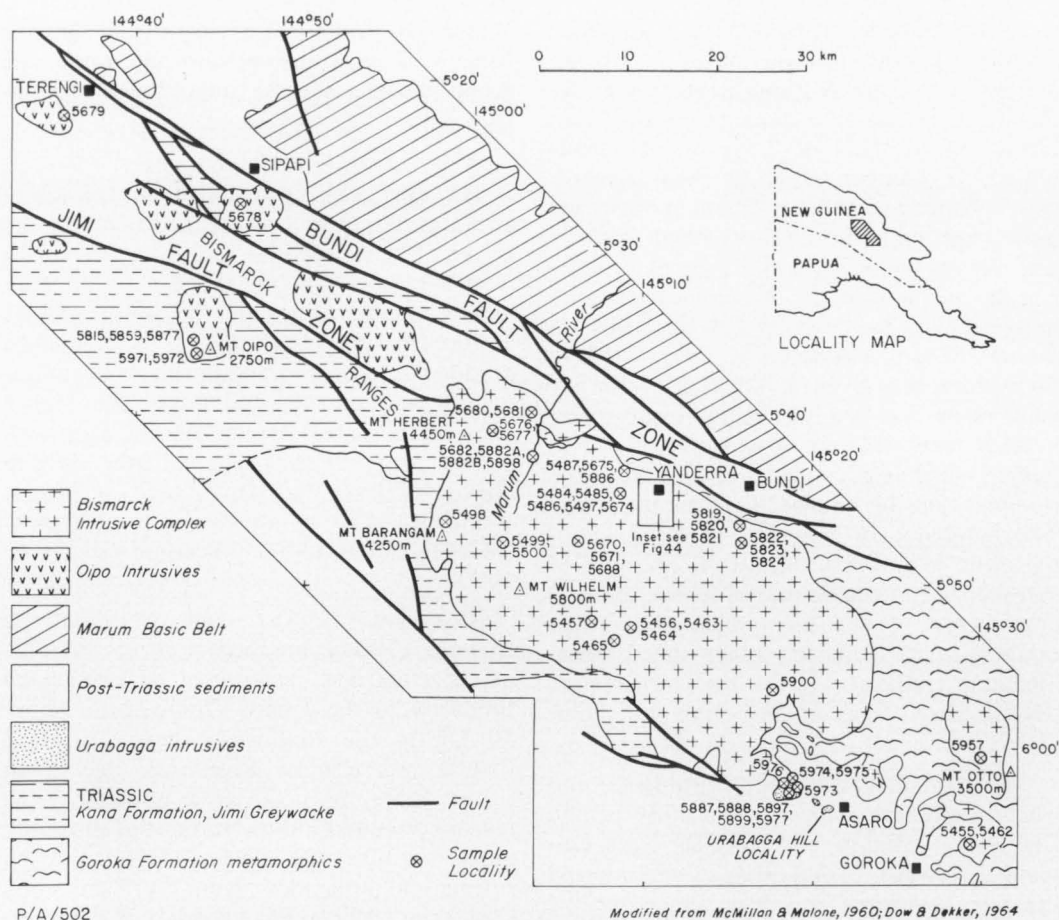
Fig. 32. Simplified geological map—Bismarck Range area.

northwest of Urabagga Hill), which was dated as Early Jurassic (180 to 190 m.y.). It is reiterated that the only unquestionable stratigraphic control on the age of the main mass of the Bismarck Intrusive Complex is that it intrudes, and is therefore younger than, the Upper Triassic Kana Volcanics (Dow & Dekker, 1964); there is no conclusive younger limit for the age.

Previous Rb-Sr age for the Bismarck Intrusive Complex. A Rb-Sr biotite age of 194 m.y. for a sample of the Bismarck Intrusive Complex (981) from Yanderra village was determined by V. M. Bofinger and acknowledged by Dow & Dekker (1964). As stressed by Bofinger (*in* Dow & Dekker, 1964) the 194 m.y. age was quite prelim-

inary. The single age determination was consistent with, and used as substantive evidence for, the Mesozoic stratigraphic age of the batholith interpreted by Dow & Dekker (1964).

After the results of several more K-Ar and Rb-Sr determinations (all giving ages of the order of 10 to 15 m.y., i.e. mid-Miocene) on minerals from further samples of the Bismarck Intrusive Complex by the present author (see below), it became clear that the preliminary 194 m.y. age was quite anomalous. An analysis of the same biotite separate (981) was repeated, and the 194 m.y. age duplicated perfectly, but no K-Ar analysis of the same biotite was possible because all of it was consumed. However,

TABLE 18. K-Ar AGES FOR THE BISMARCK INTRUSIVE COMPLEX

No.	Sample	K %		$*Ar^{40}$ $x10^{-6} cm^3$ NTP/g	$*Ar^{40}$ %	Calculated age (m.y.)
Wilhelm-Marum area						
5456	Biotite	7.492 7.493	7.493	3.042	60.0	10.1 ± 0.2
	Hornblende	0.540 0.545	0.543	0.283	36.0	13.1 ± 0.4
	Plagioclase	0.552 0.545	0.549	0.243	23.1	11.1 ± 0.6
5457	Biotite	7.753 7.753	7.753	3.683	82.5	11.9 ± 0.2
	Hornblende	0.748 0.749	0.749	0.375	49.4	12.5 ± 0.3
5463	Biotite	7.706 7.713	7.710	3.950	73.3	12.8 ± 0.4
	Hornblende	0.513 0.513	0.513	0.270	38.3	13.1 ± 0.5
5464	Biotite	7.608 7.665	7.637	3.592	82.9	11.8 ± 0.2
	Hornblende	0.683 0.683	0.683	0.340	26.5	12.4 ± 0.5
5465	Hornblende	0.378 0.382	0.380	0.166 0.149 0.137	30.6 25.2 28.0	10.9 ± 0.4 9.8 ± 0.4 9.0 ± 0.4 } 9.9 ± 0.4
5497	Biotite	6.658 6.669	6.664	3.163	79.0	11.9 ± 0.3
	Potash feldspar	10.384 10.349	10.367	4.243	57.1	10.2 ± 0.3
	Plagioclase	0.0210 0.0230	0.0220	0.614	49.5	595 ± 29
5498	Hornblende	0.301 0.302	0.302	0.171	28.1	14.1 ± 0.5
5499	Biotite	7.410 7.413	7.412	3.405	66.2	11.5 ± 0.3
5500	Biotite	7.319 7.357	7.338	3.514	76.3	11.9 ± 0.3
5670	Biotite	7.575 7.589	7.582	3.654	77.0	12.0 ± 0.3
	Hornblende	0.580		0.297	15.7	12.8 ± 0.7
5671	Biotite	7.349 7.376	7.363	3.549	58.6	12.0 ± 0.3
	Hornblende	0.599 0.599	0.599	0.297	55.9	12.4 ± 0.3
5676	Biotite	7.240 7.244	7.242	3.599 3.572	66.3 63.7	12.4 ± 0.3 12.3 ± 0.5
	Hornblende	0.479 0.480	0.480	0.289	31.6	15.1 ± 0.4
5677	Hornblende	0.477 0.476	0.477	0.333	46.1	17.4 ± 0.5
5680	Hornblende	0.491 0.496	0.494	0.244	30.3	12.3 ± 0.5
5681	Biotite	7.650 7.729	7.690	3.652	87.5	11.9 ± 0.5
	Hornblende	0.676 0.670	0.673	0.302 0.314	52.2 49.2	11.2 ± 0.5 11.6 ± 0.2
5682	Biotite	7.600 7.546	7.573	3.367	73.8	11.1 ± 0.3
	Hornblende	0.397 0.398	0.398	0.214	19.8	13.5 ± 0.6

TABLE 18. K-Ar AGES FOR THE BISMARCK INTRUSIVE COMPLEX—(cont.)

No.	Sample	K %		$*Ar^{40}$ $x10^{-6}\,cm^3$ NTP/g	$*Ar^{40}$ %	Calculated age (m.y.)
Goroka/Mount Otto area						
5455	Biotite	5.880 5.786 }	5.833	2.545	57.4	10.9 ± 0.2
	Hornblende	0.566 0.574 }	0.570	0.257	27.6	11.3 ± 0.3
5462	Biotite	7.092 7.057 }	7.075	2.499	72.7	8.8 ± 0.2
	Hornblende	0.492 0.492 }	0.492	0.213	21.2	10.8 ± 0.5
5957	Biotite	5.788 5.777 }	5.783	1.973	47.8	8.5 ± 0.1

Fig. 33. Histograms of Bismarck Intrusive Complex ages.

K-Ar ages were determined in duplicate on hornblende and potash feldspar from sample 981, and, in addition, two more separate crushings (981A and 981B) of the original

granodiorite (involving mineral separations of biotite, hornblende, and potash feldspar) were made in an attempt to clarify the anomalies. These and other anomalous age results, all from the area north of Yanderra village, are discussed later (see pp. 71-74). In short, it has been concluded that the original single age determination of 194 m.y. quoted by Dow & Dekker (1964) was analytically reliable but quite anomalous.

Because of the controversy regarding the age of the Bismarck Intrusive Complex, this body was studied in considerably more detail than any of the other intrusives in the New Guinea Mobile Belt. It was hoped that the interpretations of the Bismarck Intrusive Complex K-Ar and Rb-Sr mineral and whole-rock ages would enable a better understanding of the young ages determined on other masses in this apparently very juvenile intrusive belt.

K-Ar ages in the Wilhelm-Marum area. Hornblendes, biotites, and feldspars separated from both granodiorites and diorites were sampled from many localities within the Bismarck body (Fig. 32). Results from the main mass of the Bismarck Intrusive Complex between Mount Wilhelm and the Marum River (the Wilhelm-Marum area) are discussed first. These have ages (Table 18) in the range 10 to 15 m.y., and the age histograms (Fig. 33) show a strong peak at about 12 m.y. For most samples, biotite and hornblende pairs were measured, and, of the nine pairs, six show a consistent age dif-
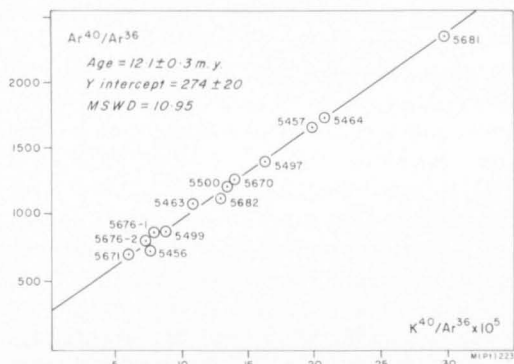
Fig. 34. Argon isochron for the Bismarck biotites.
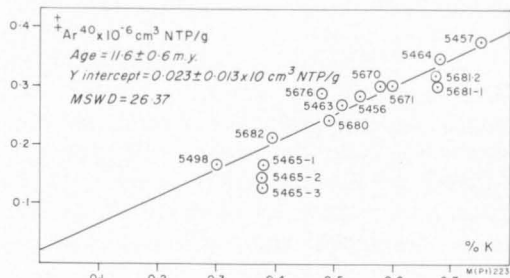
Fig. 35. Initial argon plot for the Bismarck hornblendes.
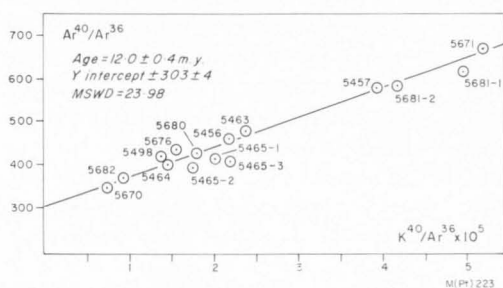
Fig. 36. Argon isochron for the Bismarck hornblendes.

ference of less than 1 m.y.; with one exception, the biotite gives the younger age. This is also reflected in the histogram peaks (Fig. 33) and in the calculated mean ages of 11.78 ± 0.26 m.y. for 12 biotites, compared with 12.72 ± 0.78 m.y. for 12 hornblendes (excluding 5677); the errors quoted are 2 SD of the mean. The 1 m.y. age difference might reflect slow cooling of the Bismarck intrusion such that radiogenic argon began to accumulate in hornblende about 1 m.y. before biotite became a closed system. The mean hornblende age of 12.7 m.y. is

regarded as the best minimum estimate for the time of emplacement of the body. The higher age of the hornblende 5677 is not considered in the pooled ages, for the sample was a xenolith in the granodiorite. Another discrepant age is given by 5497 plagioclase; it may result from incorporation of extraneous radiogenic argon at the time of crystallization; note the low potassium content (0.02%).

Initial argon and argon isochron diagrams of the Wilhelm-Marum data were drawn up to investigate further the use of such plots and to see if any additional information could be derived. Figure 34 is an isochron diagram for the Wilhelm-Marum biotites. The regression analysis result is given with the errors quoted at the 95-percent confidence limits. Replicate argon data are plotted individually but only a mean value was used in the regression analyses. The graphically obtained age of 12.1 ± 0.3 m.y. is in good agreement with the mean of 11.8 m.y. from the conventionally calculated ages, and, as the Ar^{40}/Ar^{36} intercept is not distinguishable from 295.5, no extraneous argon is indicated. No initial argon plot of the biotite data is given because of the small spread in the potassium values. The initial argon and isochron plots for the hornblendes (Figs. 35 and 36) give indicated ages of 11.6 ± 0.6 and 12.0 ± 0.4 m.y. respectively. The graphically obtained ages are slightly less than the mean of the conventional ages of 12.7 m.y., and result from the positive intercept in the initial argon plot and the high initial Ar^{40}/Ar^{36} in the isochron plot. These intercepts suggest the presence of extraneous argon in the hornblendes.

The approximate concentration of the indicated initial argon in the hornblendes can be calculated using the intercepts from both graphs (cf. Roddick & Farrar, 1971). From equation (9) (see Appendix 1, p. 107), the radiogenic Ar^{40} intercept on the initial argon diagram can be expressed as: Ar_i^{36} (I—295.5), where I is equal to the

initial Ar^{40}/Ar^{36}. Then, from Figure 35:
$$Ar_i^{36} (I—295.5) = 0.23 \times 10^{-6} \text{ cm}^3 \text{ NTP/g}$$

and from the isochron diagram (Fig. 36):
$$I = 303$$
Thus
$$Ar_i^{36} = \frac{0.023 \times 10^{-6}}{(303 - 295.5)} = 3.1 \times 10^{-9} \text{ cm}^3 \text{ NTP/g}$$
and
$$Ar_i^{40} = Ar_i^{36} \, I = 0.939 \times 10^{-6} \text{ cm}^3 \text{ NTP/g}$$

Taken at face value, the graphical plots, therefore, indicate that each hornblende had an initial Ar^{40} concentration of about 0.9×10^{-6} cm^3 NTP/g. However, this estimate is quite unrealistic, for in only three of the hornblende measurements did the total Ar^{40} exceed 1.0×10^{-6} cm^3 NTP/g. The conclusion must be that one or both of the graphical plots of the argon data cannot be applied to the Bismarck hornblendes, because some of the underlying assumptions are not fulfilled; the possible reasons for this will be discussed further below.

For the K-Ar dating of young rocks and minerals, such as the Bismarck Intrusive Complex, a limiting factor in the use of the isochron plot will be contamination by atmospheric argon after the system was closed (see Appendix 1, p. 104). As pointed out by McDougall et al. (1969) and by Hayatsu & Carmichael (1970), the addition of such atmospheric argon to the samples will result in a scatter on the isochron plot, unless the initial ratio is equal to the present atmospheric Ar^{40}/Ar^{36} ratio (cf. Appendix 1, Fig. B). Hayatsu & Carmichael (1970) concluded that, in their series of measurements on very low-grade metamorphosed Palaeozoic rocks from Nova Scotia, Canada, more than 90 percent of the Ar^{36} came from the samples themselves. For the Bismarck Intrusive Complex, an estimate of the contamination from the laboratory or extraction line, or both, can be made by comparing the total volume of atmospheric Ar^{40} in the runs with the volume obtained in blank runs. Under normal operating conditions in this laboratory the argon extraction blank in terms of total atmospheric Ar^{40} is about 1×10^{-7} cm^3 NTP/g (I. McDougall, pers. comm.); when special precautions are employed the average blank obtained is 5×10^{-8} cm^3 NTP/g. On the

basis of a blank of 1×10^{-7} cm^3 NTP/g, the present measurements on the 12 Bismarck hornblendes show that the proportions of non-radiogenic Ar^{40} resulting from laboratory contamination is of the order of 10 percent, but three samples (5456, 5457, and 5671) may have 20 to 30 percent contamination. For the 12 analysed Bismarck biotites, the proportion of non-radiogenic Ar^{40} from laboratory contamination was generally about 20 percent, with only three samples (5456, 5499, and 5671) between 10 and 15 percent. In the isochron plot, such contamination causes smearing of the points towards 295.5 on the Ar^{40}/Ar^{36} axis, if the initial Ar^{40}/Ar^{36} is not equal to that of present-day atmospheric argon. The extent of the smearing of the data points depends on the amount of contamination, and the scatter will cause the MSWD in the regression analysis to be greater than unity, as observed in the Bismarck hornblende and biotite results. If any of the other assumptions, such as constant initial argon concentration (for the initial argon plot) and constant Ar^{40}/Ar^{36} (in both initial argon and isochron plot), are not met, then the scatter introduced will be reflected in an MSWD value greater than unity, and it becomes difficult to interpret the results meaningfully or with any confidence. Also, a real age spread or variable loss of radiogenic Ar^{40} will upset the isochron model, and it is felt that these may be significant for the Bismarck hornblende data. For the biotites, however, all except one of the conventionally calculated ages are in the narrow range 11.0 to 12.8 m.y., and hence the isochron plot (with no indicated extraneous argon) gives a figure in the same range. Even for the biotites, the high MSWD of 10.95 indicates that probably not all assumptions of the model are met, and the graphically obtained age could be fortuitous.

It can be concluded that the use of argon isochron and initial argon plots may not be particularly helpful in analysing mineral data from young rocks. The conditions of the plots are not fulfilled for the Bismarck Intrusive Complex data because the sampled area of about 1200 km^2 probably has finite

TABLE 19. Rb-Sr DATA FOR THE BISMARCK INTRUSIVE COMPLEX

No.	Sample	Rb (ppm)	Sr (ppm)	Rb^{87}/Sr^{86}	Sr^{87}/Sr^{86}	Sr^{87}/Sr^{86} **	Rb-Sr age (m.y.)	K-Ar age (m.y.)
Granodiorites								
5455	Biotite	387.9	15.6	71.785	0.7138		9.7	10.9
	Whole rock	37*	504*			0.7041		
5456	Biotite	245.0	20.3	34.778	0.7092		10.6	10.1
	Whole rock	41*	535*			0.7041		
5497	Biotite	373.6	11.3	95.275	0.7211		13.0	11.9
	Potash feldspar	255.6	480.2	1.536	0.7050			10.2
	Whole rock	73*	448*			0.7040		
5492	Whole rock	61.0	585.1	0.301	0.7027	0.7035		
5670	Whole rock	97.2	458.4	0.612	0.7039			
5672	Whole rock	71.2	374.1	0.549	0.7042	0.7042		
5674	Whole rock	112.3	239.8	1.351	0.7041	0.7041		
5675	Whole rock	100.5	289.6	1.002	0.7042	0.7042		
5882A	Whole rock	142.3	170.3	2.412	0.7041	0.7039		
5882B	Whole rock	49.7	412.8	0.347	0.7038			
981A	Whole rock	42.5	880.1	0.139	0.7036			
5493	Whole rock	46.8	702.1	0.192	0.7036	0.7036		
5673	Whole rock	30.2	378.0	0.231	0.7039	0.7037		
						0.7040		
Aplites								
5482	Whole rock	107.4	105.2	2.947	0.7044	0.7042		
5483	Whole rock	208.1	35.4	16.973	0.7079	0.7073		
5484	Whole rock	99.2	287.5	0.996	0.7038	0.7038		
5485	Whole rock	159.2	18.2	25.258	0.7080	0.7079		
5486	Whole rock	138.6	12.5	32.020	0.7086	0.7091		
5487	Whole rock	100.2	33.0	8.766	0.7056	0.7055		
5688	Whole rock	238.0	170.7	4.024	0.7054			
		239.2	171.3	4.025	0.7047	0.7046		
5884	Whole rock	67.9	275.6	0.711	0.7044	0.7038		
5885	Whole rock	57.9	288.0	0.580	0.7036	0.7040		
5886	Whole rock	125.5	60.3	6.048	0.7066	0.7051		
5898	Whole rock	82.4	237.9	0.999	0.7039	0.7040		
5900	Whole rock	81.1	28.7	8.167	0.7046	0.7048		
						0.7045		
5957	Whole rock	136.0	26.5	14.799	0.7061	0.7062		
	Biotite	608.9	24.4	71.998	0.7130		9.3	8.5
		599.7	24.2	71.706	0.7124		9.0	

** Measured value, unspiked run

* Approximate XRF measurement

age differences, as well as inhomogeneous initial argon concentration and Ar^{40}/Ar^{36} values. Where these factors exist, the two-error regression analysis of McIntyre et al. (1966) applied to the data does not necessarily give the correct slope; the indicated uncertainties of the regression could also be wrong, as the variances applied to individual data points in the isochron plot may not be realistic. Because of all these difficulties, interpretation of the Bismarck argon data is best considered in the light of the conventionally calculated ages as represented on the histograms in Figure 33.

Rb-Sr biotite ages in the Wilhelm-Marum area. Several biotites from the Bismarck Intrusive Complex were analysed by the Rb-Sr method; the data for two of them (5456 and 5497) from the Wilhelm-Marum area

are included in Table 19; the K-Ar biotite ages which are 0.5 and 1.1 m.y. lower, are also listed for comparison. The younger K-Ar and Rb-Sr ages of 5456 may be a result of slight mineralization—veins of pyrite and minor chalcopyrite—of the rock that was sampled. The initial Sr^{87}/Sr^{86} ratios used to calculate the Rb-Sr biotite ages of 5456 and 5497 are based on their respective whole-rock measurements of the present-day Sr^{87}/Sr^{86} values.

K-Ar and Rb-Sr ages of the Bismarck Intrusive Complex between Goroka and Mount Otto. Two separate intrusions were mapped by McMillan & Malone (1960) as outliers at the eastern end of the main Bismarck mass between Goroka and Mount Otto (Fig. 32). Two granodiorite samples (5455 and 5462) from the southern mass give biotite and hornblende K-Ar ages between 8.8 and 11.3 m.y. (Table 18); the biotites again give the younger apparent ages. The Rb-Sr age of 5455 biotite is 9.7 m.y. (Table 19), which is just outside the experimental uncertainties of the K-Ar measurement. A biotite from an aplitic sample (5957) from the northern intrusion yields a K-Ar age of 8.5 ± 0.1 m.y. (Table 18) and well duplicated Rb-Sr ages of 9.0 and 9.3 (Table 19). From these limited data it would appear that the intrusions between Goroka and Mount Otto cooled below the respective threshold temperatures for rentention of radiogenic argon and strontium about 2 to 3 m.y. after the main mass of the Bismarck Intrusive Complex in the Wilhelm-Marum area (cf. Fig. 33). The Goroka/Mount Otto bodies may well be younger intrusions.

Rb-Sr whole-rock data. To enable a better understanding of the relatively young K-Ar and Rb-Sr mineral ages determined on the Bismarck Intrusive Complex, and indeed on several other plutons throughout the New Guinea Mobile Belt, further Rb-Sr work was undertaken to obtain a whole-rock isochron for the Bismarck Intrusive Complex, and thereby to establish an unequivocal age for the mass. Unfortunately the granodiorites and diorites of the mass have low and ·uniform Rb/Sr ratios and, alone, are not very

suitable for Rb-Sr dating. The aplitic dykes intrusive into the granodiorites proved to have a wide range of Rb/Sr ratios, and 13 samples were analysed. The assumption initially made, and later tested, is that the aplites are cogenetic with, and have about the same age as, the granodiorites they intrude. The aplites analysed came from many areas throughout the entire outcrop of the Bismarck Intrusive Complex; these are shown on the general locality map (Fig. 32) and the more detailed Yanderra map (Fig. 41).

The Rb-Sr analytical data for the 13 aplites (Table 19) are plotted in Figure 37. The Sr^{87}/Sr^{86} ratios were determined from both spiked and unspiked runs, between which there is generally excellent agreement. A y variance of 0.05 x 10^{-6} was used in the regression analysis of Figure 37, and a Model I isochron with an age of 12.3 ± 1.0 m.y. and initial Sr^{87}/Sr^{86} of 0.7038 ± 0.0002 fitted. The errors quoted are at the 95 percent confidence limits. The MSWD of 1.48 is not significantly different from unity at the 5 percent level (using the statistical F test) and indicates that all errors can be attributed to the experimental uncertainties. The Model I whole-rock aplite isochron provides good evidence that the age of 12.3 ± 1.0 m.y. is geologically meaningful and is probably the time of emplacement of the aplite dykes. This age also provides a firm minimum estimate for emplacement of the Bismarck Intrusive Complex.

Ten granodiorite whole-rock samples from widespread localities within the Bismarck mass were analysed (Table 19) to test whether the aplites and granodiorites can be regarded as cogenetic. As earlier mentioned, the granodiorites are poorly enriched and, as a result, the slope of the Model I isochron (Fig. 38) that fitted the data has large uncertainties. However, the young indicated age of 12.7 ± 17.4 m.y. supports the other mineral and aplite data. The indicated initial Sr^{87}/Sr^{86} from the granodiorites of 0.7037 ± 0.0002 is almost identical with the aplite value. Thus the aplites and granodiorites may well be cogenetic, and the data in the two isochrons
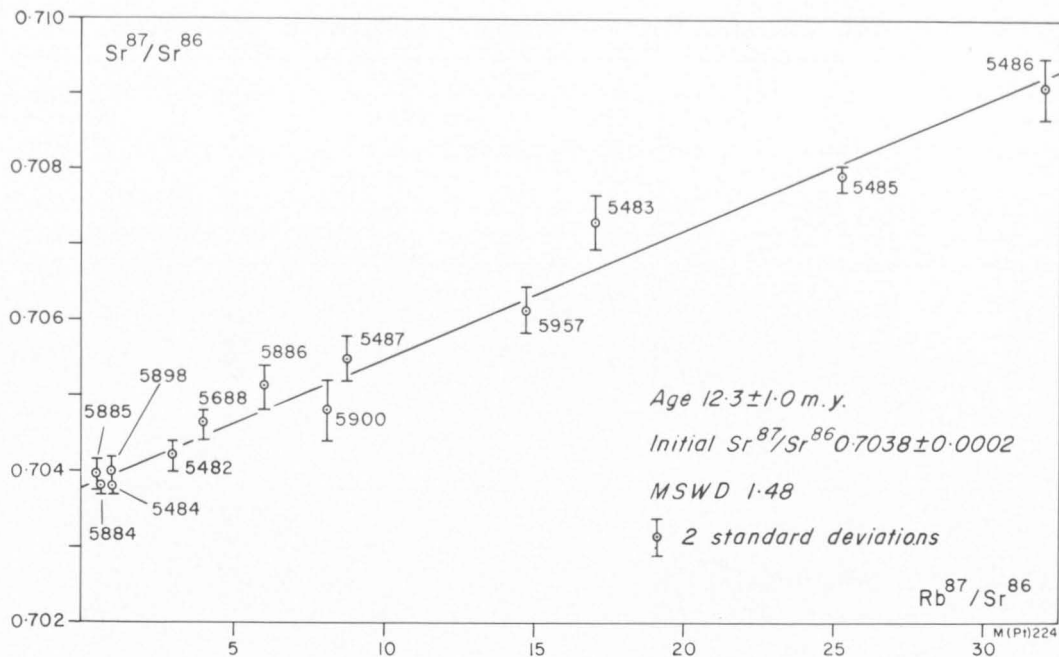
Fig. 37. Rb-Sr isochron for the Bismarck aplites.
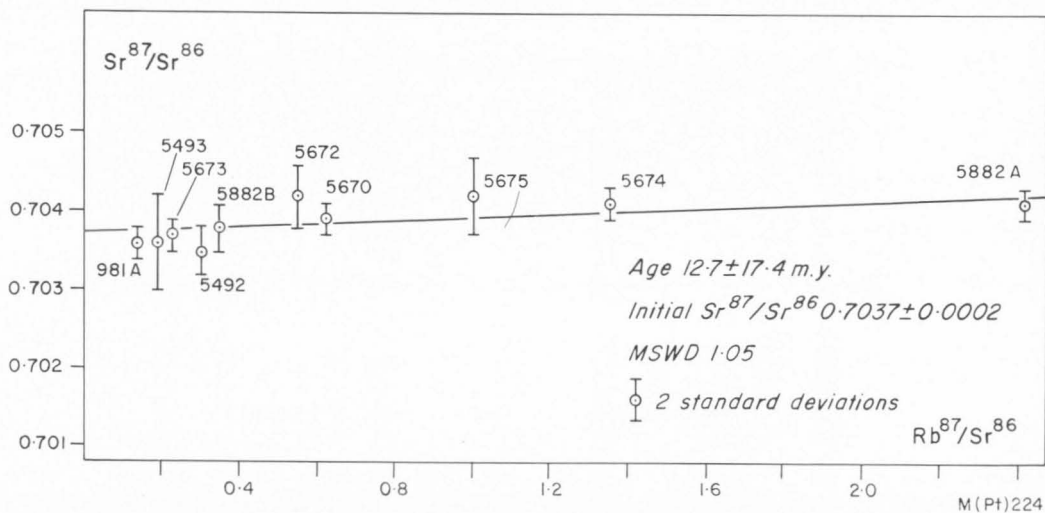
Fig. 38. Rb-Sr isochron for the Bismarck granodiorites.

(Figs. 37 and 38) can be validly combined. When this is done, the 23 whole-rock samples define a Model I isochron (MSWD 1.10) with an age of 12.4 ± 0.8 m.y. and initial Sr^{87}/Sr^{86} of 0.7037 ± 0.0001. This must be regarded as the best age estimate for the emplacement of the Bismarck Intrusive Complex and aplites, and it is noted

that it is close to the mean K-Ar hornblende age for the granodiorite of 12.7 ± 0.8 m.y.

Muscovite pegmatite ages. Several muscovite pegmatite dykes from 0.3 to 1.5 m wide were found in two areas about 4 km and 6 km south of Bundi (Fig. 32). At the northern locality, they crop out near the

TABLE 20. K-Ar AGES FOR THE BISMARCK MUSCOVITE PEGMATITES

No.	Sample	K %		$*Ar^{40}$ $x10^{-6} cm^3$ NTP/g	$*Ar^{40}$ %	Calculated age (m.y.)
5819	Muscovite	7.474 7.478	} 7.476	2.563 2.458	66.7 22.0	8.6 ± 0.2 8.2 ± 0.3
5820	Muscovite	7.230 7.186	} 7.208	2.518	59.1	8.7 ± 0.2
5821	Muscovite	7.416 7.457	} 7.437	2.682	40.0	9.0 ± 0.3
5822	Muscovite	7.820 7.806	} 7.813	2.667	58.1	8.5 ± 0.2
5823	Muscovite	7.457 7.421	} 7.439	2.953	66.9	9.9 ± 0.4
5824	Muscovite	7.668 7.657	} 7.663	2.636	57.7	8.6 ± 0.3
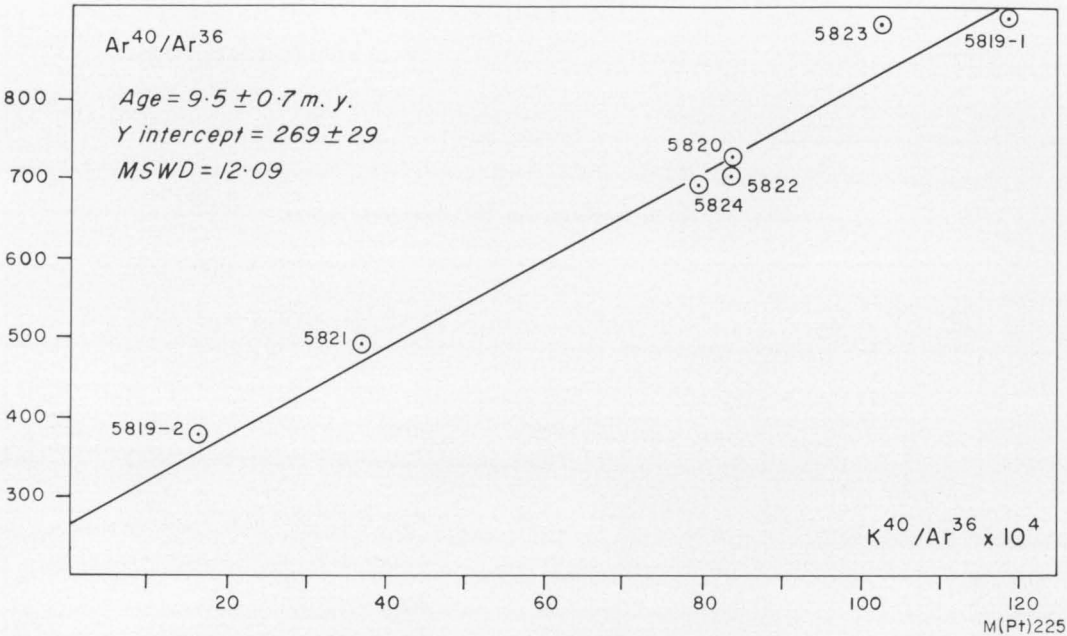
Fig. 39. Argon isochron for the Bismarck muscovite pegmatites.

margin between the Bismarck Intrusive Complex and the Mesozoic to Palaeozoic Goroka Formation.

The K-Ar results for six separated muscovites are listed in Table 20. Five of the ages are between 8.2 and 9.0 m.y., and the sixth (5823) is slightly older at 9.9 ± 0.4 m.y. These are minimum emplacement ages for the pegmatites. The argon isochron plot of the data (Fig. 39) indicates a pooled age of 9.5 ± 0.7 m.y. for the six samples. Although the duplicate argon runs are plot-ted individually in Figure 39, only a mean value was used in the regression analysis. The duplicate runs on 5819 indicate that the slope of the isochron is heavily controlled by variable contamination from atmospheric argon. The MSWD of 12.09 is also an indication that the assumptions of the plot are not fulfilled, and hence acceptance of the pooled age is perhaps not justified. The data were not plotted on an initial argon diagram because of the small potassium variation.

TABLE 21. Rb-Sr DATA FOR THE BISMARCK MUSCOVITE PEGMATITES

No.	Sample	Rb (ppm)	Sr (ppm)	Rb^{87}/Sr^{86}	Sr^{87}/Sr^{86}
5820	Whole rock	75.9	126.1	1.737	0.7087
	Muscovite	241.6	66.5	10.485	0.7097
5821	Whole rock	38.2	43.3	2.545	0.7088
	Muscovite	213.2	68.7	8.969	0.7095
5822	Whole rock	45.7	38.2	3.455	0.7098
	Muscovite	267.2	69.9	11.035	0.7112
5823	Whole rock	98.8	94.9	3.007	0.7085
	Muscovite	222.3	61.2	10.489	0.7098
5824	Whole rock	88.9	94.0	2.673	0.7091
	Muscovite	217.9	64.4	9.765	0.7100
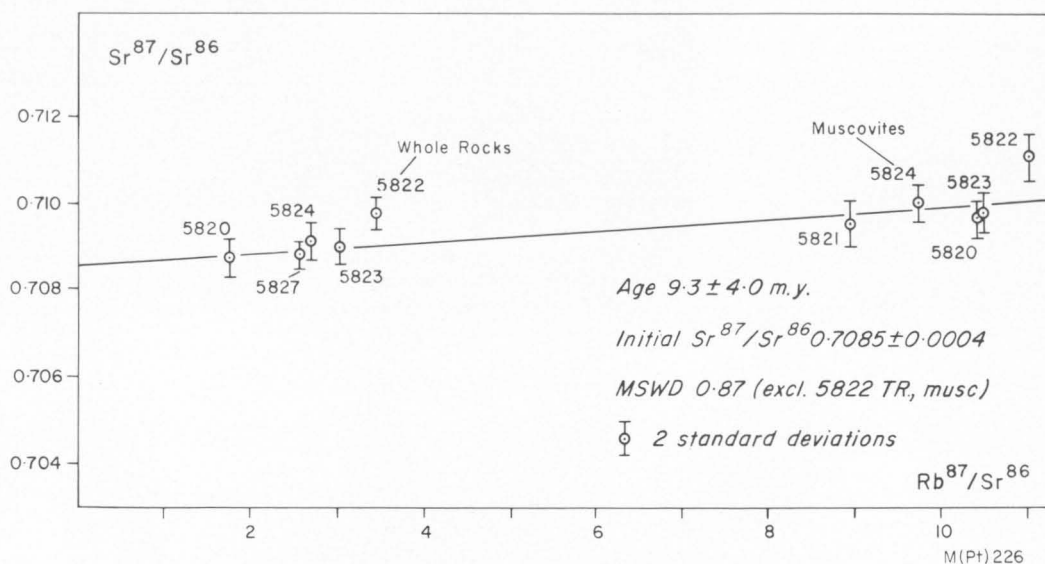
Fig. 40. Rb-Sr isochron for the Bismarck muscovite pegmatites.

Five of the pegmatites were chosen for Rb-Sr muscovite and whole-rock analyses, and data for these are given in Table 21. No independent muscovite ages can be determined from the data because of the low Rb/Sr ratios. The Rb-Sr data are plotted in Figure 40, and regression of the 10 points gives a Model IV isochron (MSWD = 4.71) with an age of 10.9 ± 7.5 m.y. and initial Sr^{87}/Sr^{86} of 0.7085 ± 0.0006. The Model IV isochron suggests that the extent to which the analyses lie outside experimental error can be attributed to a combination of variation in the initial Sr^{87}/Sr^{86} and elemental redistribution, or real age differences. Inspection of the data on the isochron diagram (Fig. 40) shows that the large uncertainties are mainly due to the scatter of the muscovite and whole-rock points of sample 5822. When this sample is deleted from the regression a Model I isochron with an age of 9.3 ± 4.0 m.y. and initial Sr^{87}/Sr^{86} of 0.7085 ± 0.0004 is obtained. The age still has a large error because of the relatively low enrichments in Sr^{87}/Sr^{86}, and perhaps also because the muscovite and whole-rock points lie in two separate clusters on the isochron diagram. The rejection of 5822 appears to be justified since the MSWD is significantly reduced from 4.71 to 0.87. It would be possible to fit a parallel two-point 'isochron' through 5822 muscovite and whole rock, and the indicated initial Sr^{87}/Sr^{86} of such a line would be 0.7092.
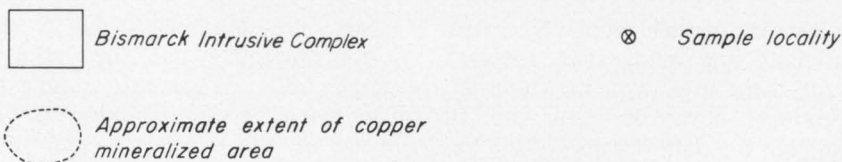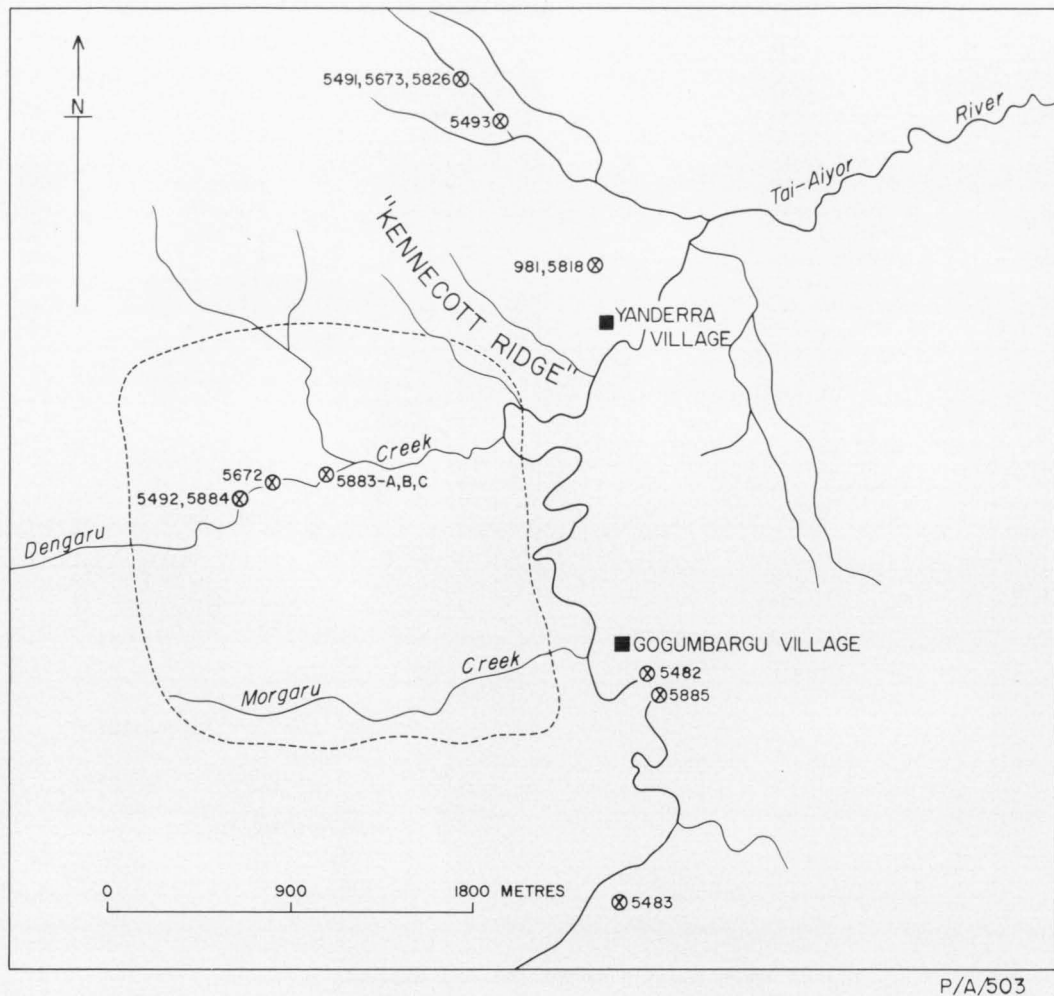
Fig. 41. Yanderra village area and copper prospect.

Although there is a large uncertainty in the age determined from the Rb-Sr isochron, the indicated value of 9.3 m.y. is in reasonable agreement with K-Ar muscovite ages of 8 to 9 m.y. The general concordancy by both methods is strong evidence that the Bismarck pegmatites were intruded about 9 m.y. ago, about 3.5 m.y. after the main emplacement of the Bismarck Intrusive Complex. Unlike the aplites, which have the same age and initial Sr^{87}/Sr^{86} (0.7037) as the granodiorite and are probably differentiates of it, the pegmatites have a much higher initial Sr^{87}/Sr^{86} of at least 0.7085. If the pegmatites are differentiates of the granodiorite magma, then they have been contaminated by strontium with a higher Sr^{87}/Sr^{86} ratio. The pegmatites were found to intrude

TABLE 22. K-Ar AGES FOR THE BISMARCK INTRUSIVE COMPLEX—NORTH YANDERRA AREA

No.	Sample	K %		$*Ar^{40}$ $x10^{-6}\,cm^3$ NTP/g	$*Ar^{40}$ %	Calculated age (m.y.)
981	Hornblende	0.539 0.535	} 0.537	0.274 0.264	32.2 39.4	12.8 ± 0.3 12.3 ± 0.5
	Potash feldspar	11.080 11.020	} 11.050	12.359 12.073	84.2 93.8	27.8 ± 0.9 27.2 ± 0.9
981A	Biotite	5.859 5.708	} 5.784	1.949	24.1	8.4 ± 0.4
	Hornblende	0.531 0.537	} 0.534	0.227 0.249	20.4 32.0	10.6 ± 0.5 11.7 ± 0.5
	Potash feldspar	11.425 11.402	} 11.414	3.968	62.2	8.7 ± 0.3
981B	Biotite	8.157		470.499	99.5	1073 ± 76
	Hornblende	0.546 0.546	} 0.546	0.250 0.253	29.8 45.1	11.4 ± 0.4 11.6 ± 0.4
	Potash feldspar	11.460 11.450	} 11.455	3.968	79.8	8.7 ± 0.3
5491	Hornblende	0.564 0.565	} 0.565	0.252	42.6	11.2 ± 0.3
5493	Biotite	4.448		9.919	57.5	55 ± 1
	Hornblende	0.555 0.556	} 0.556	0.238	33.2	10.7 ± 0.4
5818	Hornblende	0.527 0.527	} 0.527	0.229	35.4	10.8 ± 0.6
5826	Whole rock	0.789 0.799	} 0.794	0.316	33.4	10.0 ± 0.3

the granodiorite within metres of the metamorphic rocks of the Palaeozoic or Mesozoic Goroka Formation, and it is possible that the metamorphic rocks were contaminants which had been well mixed at depth with the pegmatitic liquids. As the pegmatites have a small volume, uniform mixing could have taken place rapidly. Incomplete mixing, however, would give rise to different initial Sr^{87}/Sr^{86} in parts of the magma, and would explain the results of the analysis of sample 5822.

Anomalous granodiorite ages in the area north of Yanderra village. Numerous K-Ar and Rb-Sr measurements were made on the granodiorite and feldspar porphyry intrusions near Yanderra village and Yanderra Copper Prospect, which are close to the northern boundary of the Bismarck Intrusive Complex (Figs. 32 and 41). It was hoped that the anomalous 194 m.y. Rb-Sr age which had been reported by Dow & Dekker (1964) from the area north of Yanderra village would be resolved, and that something of the relative ages of emplacement of

the Bismarck mass and the subsequent copper mineralization in the Yanderra Copper Prospect would be learnt. The isotopic data regarding the mineralization are only briefly outlined here (cf. Fig. 33), but are more fully discussed by Page & McDougall (1972a).

Plane (1965) studied the Yanderra area in some detail and regarded the micrograno-diorite porphyries, generally called feldspar porphyries, as Pliocene in age. They clearly intrude the more massive Bismarck Intrusive Complex, and it is thought that they have introduced the copper and gold mineralization into the area. Bordering the Bismarck Intrusive Complex 1 km to the north of Yanderra (Fig. 32) is a belt of metamorphic rocks of the Goroka Formation, which according to Dow & Dekker (1964), is probably Mesozoic or Palaeozoic in age. That the metamorphic rocks of this belt are at least as old as Early Jurassic was also suggested by the previously discussed (4.5) isotopic study in relation to the Bena Bena Formation to the southeast.

TABLE 23. Rb-Sr DATA FOR THE BISMARCK INTRUSIVE COMPLEX—NORTH YANDERRA AREA

No.	Sample	Rb (ppm)	Sr (ppm)	Rb^{87}/Sr^{86}	Sr^{87}/Sr^{86}	** Sr^{87}/Sr^{86}	Rb-Sr age (m.y.)	K-Ar age (m.y.)
981	Biotite	549.0	4.8	332.360	1.6039		194	
	Biotite	567.3	10.1	169.343	1.1627		195	
	Potash feldspar	232.3	875.3	0.766	0.7051	0.7079		27.6
	Whole rock	48.0	761.7	0.181	0.7018			
	Hornblende							12.6
981A	Biotite	367.2	17.4	60.981	0.7126		10.9	8.4
	Biotite	409.7	13.7	86.375	0.7161		10.5	
	Potash feldspar	233.5	885.8	0.761	0.7046			8.7
	Whole rock	42.5	880.1	0.139	0.7036			
	Hornblende							11.2
981B	Biotite	468.1	7.2	258.072	4.5500		1064	1073
	Biotite	475.9	7.2	266.142	4.6356		1055	
	Biotite	469.7	7.3	255.664	4.5740		1080	
	Potash feldspar	233.3	882.5	0.763	0.7040	0.7067		8.7
	Chlorite	41.4	62.1	1.921	0.7040			
	Chlorite (30 % biotite)	285.0	42.4	19.396	0.7063			
	Hornblende							11.5
5493	Biotite	309.5	31.0	28.852	0.7275		60	55
	Biotite	308.3	29.5	30.238	0.7309		65	
	Whole rock	46.8	702.1	0.192	0.7036	0.7036		
	Hornblende							10.7
5673	Whole rock	30.2	378.0	0.231	0.7039	0.7037 / 0.7040		
5818	Biotite	413.3	9.7	123.760	0.7214		10.0	
	Chlorite	106.9	28.1	10.989	0.7052		7.7	
	Whole rock	541*	745.4*			0.7040		
	Hornblende							10.8

** Measured value, unspiked run
* Approximate XRF analysis

The area of igneous rocks north of Yanderra village (Fig. 41) is now considered. As stated earlier, this is the locality of sample 981, which gave a 194 m.y. Rb-Sr biotite age (Dow & Dekker, 1964). Samples 981, 981A, and 981B were prepared from the same specimen of the Bismarck Intrusive Complex which had been originally collected by Mr M. D. Plane. Five more samples, including 5818 from as near possible to the locality from which 981 was sampled, were collected in the area north of Yanderra village. In general, this area is not mineralized except for occasional pyrite veining, but several small feldspar porphyries intrude the Bismarck Intrusive Complex, which is quite xenolithic in places.

The K-Ar and Rb-Sr data for rocks from the north Yanderra area are presented and compared in Tables 22 and 23. It is appropriate to look first at sample 981 and the other two fractions of the original field sample, 981A and 981B. The 194 m.y. Rb-Sr age of 981 is now duplicated, confirming the analytical reliability, but a K-Ar determination could not be made, as 981 biotite was used up. The K-Ar ages of 981 hornblende and potash feldspar are quite discordant at about 12 and 27 m.y. respectively, but it is noted that 12 m.y. is the approximate age of the Bismarck Intrusive Complex determined elsewhere within this mass. Further gross discordancy is seen in the mineral ages of the fraction 981B; the Rb-Sr and K-Ar biotite ages of over 1000 m.y. must be regarded as completely unreal in terms of the known geology, because the Bismarck mass is known to intrude Upper Triassic sediments. Note that 981B hornblende is consistent with the other hornblende K-Ar

ages of between 11 and 13 m.y. The third fraction 981A gives reasonably concordant dates between 8 and 11 m.y. by Rb-Sr and K-Ar methods on biotite, hornblende, and potash feldspar.

One definite conclusion that can be made from these data is that the original biotite-hornblende granodiorite collected in the field is extremely heterogeneous, particularly with regard to the biotite content. This cannot be seen in hand specimen, but in 981B it appears possible that two generations of biotite can be distinguished in thin section: one is a perfectly fresh biotite and the other is partly to completely chloritized. The thin section of 981 was not available, but in 981A almost all the biotite has some degree of chloritization.

Three chlorite concentrates from the Yanderra rocks were prepared to investigate the effect of rubidium depletion, through chloritization, on the Rb-Sr ages. The Rb-Sr analyses of two impure chlorites from 981B and one from 5818 are given in Table 23, and indicate that, although there has been alkali loss, and gain in strontium, in the breakdown of biotite to chlorite, no anomalous enrichment in Sr^{87} is apparent. Ovchinnikov, Yunikov, & Mettikh (1961) investigated the composition and structure of naturally hydrated biotites from the Buldym deposit in the USSR, and found that, with decreasing potassium (ionic radius 1.33 A) due to lattice replacement by H_3O^+ ions (ionic radius 1.35 A), rubidium was removed to such a degree that the potassium/rubidium ratio changed from 90 to 450. They also showed that the Ar^{40}/K^{40} ratio remained essentially constant even in highly altered biotites; this was confirmed in the laboratory alteration studies of Kulp & Bassett (1961) and Kulp & Engles (1963). For the 981 sample, preferential loss of potassium or rubidium, or both, cannot account for the huge age discordances. 981B is quite a pure biotite, with 8.1 percent potassium, and clearly cannot have lost much potassium; because the K-Ar and Rb-Sr ages are concordant, loss of rubidium as described by Ovchinnikov et al. (1961) is also most unlikely.

Although it is highly unlikely that the sample became contaminated during mineral separation in the laboratory, it can never be ruled out completely. Another possible explanation for the anomalous biotite ages is that the granodiorite sampled in the field contained a highly radiogenic biotite-rich xenolith or number of xenocrysts. The granodiorite contains many xenoliths in places, and, although none was apparent in any part of sample 981, some may have been broken up and dispersed in the magma, which solidified before the foreign xenolithic materials were uniformly mixed with it. Lack of homogenization is invoked to explain the entirely different ages obtained for the biotite from the three fractions, and also the apparently normal, non-radiogenic Sr^{87}/Sr^{86} values of the whole rocks. The lack of enrichment in the whole rocks is due to swamping of the radiogenic component by the high concentration of common strontium in the whole rock; a calculation shows that the Sr^{87}/Sr^{86} enrichment due to 2 percent biotite (4.8 ppm strontium) in 981 whole rock (761.7 ppm strontium) is 0.00011.

There was ample opportunity for the granodiorite to incorporate blocks or perhaps crystals of highly radiogenic micaeous material from the Mesozoic or Palaeozoic Goroka Formation, which consists of biotite-andalusite schists and slates as well as other varieties of metamorphic rocks (Dow & Dekker, 1964). These metamorphics crop out only 1 km north of Yanderra and could be much closer at depth. Implicit in the above interpretation of the anomalous Yanderra ages is the possibility that the Goroka Formation metamorphics contain Precambrian material. Further isotopic study of the metamorphics would be required to test this hypothesis.

Further K-Ar and Rb-Sr ages (Tables 22 and 23) have been measured on four granodiorites and one dolerite from north of Yanderra village to find a geologically realistic age for the rocks or to determine just how widespread the phenomena affecting sample 981 might be. The three hornblendes (5491, 5493, and 5818) give concordant K-Ar ages

from 10.7 to 11.2 m.y., and the dolerite (5826) intrusive into granodiorite gives a whole-rock age of 10.0 ± 0.3 m.y. A Rb-Sr age of about 10 m.y. was determined on 5818 biotite, and this is also in reasonable agreement with the hornblende K-Ar ages. However, the biotite K-Ar age of 5493 is quite aberrant at 55 ± 1 m.y., which is somewhat less than the equally anomalous duplicated Rb-Sr ages of 60 and 65 m.y. on the same sample. Like sample 981, sample 5493 contains no obvious xenoliths, but in view of all the other isotopic data on the Bismarck Granodiorite, the biotite ages of 55 to 65 m.y. have to be disregarded. The discovery of this second anomalous biotite sample about 800 m from the locality of 981 (Fig. 41) strengthens the suggestion that some of the biotite occurs as xenocrysts. The present-day Sr^{87}/Sr^{86} ratio measured on 5493 whole rock is 0.7036 ± 0.0003, and there is excellent agreement between the spiked and unspiked runs. This value, as for 981 whole rock, is perhaps lower than expected, but can again be rationalized in that the rock contains only 3 percent biotite; the enrichment in the whole rock of Sr^{87}/Sr^{86} from this biotite is less than 0.00004.

In addition to the dating of the granodiorites north of Yanderra, several K-Ar and Rb-Sr ages (Page & McDougall, 1972a) have been measured on the mineralized granodiorites and porphyries which crop out about 2 to 3 km southwest of Yanderra (Fig. 41). These data are not entirely relevant to the age of the Bismarck Intrusive Complex, for they represent a special case where there was localized mineralization after the intrusion of the main part of the batholith. For present purposes it is sufficient to refer to the general histograms in Figure 33, which summarize the K-Ar ages for both the mineralization (southeast Yanderra) and the intrusion of the Bismarck mass in the three areas in which it was studied.

Discussion of the Bismarck Intrusive Complex age data. Table 24 summarizes the K-Ar and Rb-Sr ages determined for the Bismarck Intrusive Complex in the different areas of study. The spread of the mineral

and whole-rock ages is large, from about 7 to 13.5 m.y., and this is attributed to a complex emplacement and cooling history for the batholith over a wide area, of which at least 1500 km² is now exposed. To a certain extent it is possible to unravel the large age spread by examining the ages of the various rock types from individual regions within the mass.

The best estimate for the initial post-emplacement cooling of the Bismarck Intrusive Complex is given by the aplite and granodiorite whole-rock Rb-Sr isochron data yielding an age of 12.4 ± 0.8 m.y., and by the mean K-Ar age of 12.7 m.y. for the hornblendes of the Wilhelm-Marum area. These results provide an unambiguous mid-Miocene age for the emplacement of the main part of the batholith. The biotite K-Ar ages from the Wilhelm-Marum area are commonly about 1 m.y. younger than the ages of the respective hornblendes, and average 11.8 m.y. This 1 m.y. age difference can be interpreted as the interval that followed the closure of the hornblende system to argon diffusion and during which the rocks were raised to a cooler level in the crust where radiogenic argon began to accumulate in the biotite. This interpretation is concordant with the generally accepted belief that hornblende is one of the most argon-retentive minerals, and biotite considerably less so. This is based both on laboratory measurements, which show that hornblende has a consistently higher activation energy for argon diffusion (cf. Mussett, 1969), and on the earlier-mentioned field retention studies of Hart (1964) and Hanson & Gast (1967). The few biotite Rb-Sr ages in the Wilhelm-Marum area of the Bismarck Intrusive Complex are variable, but are in general agreement with the hornblende K-Ar results.

The complexity of the emplacement or the cooling history, or both, of the Bismarck Intrusive Complex is indicated by the K-Ar and Rb-Sr mineral ages for samples from the Goroka/Mt Otto region and from near Yanderra; they are 2 to 5 m.y. younger than the ages from the Wilhelm-Marum area (Fig. 33). The pegmatite K-Ar and Rb-Sr ages at 8 to 9 m.y. may represent the final

TABLE 24. POOLED AGES FOR THE BISMARCK INTRUSIVE COMPLEX

Rock type	General locality	Sample	No. of samples	K-Ar age m.y.	Rb-Sr age m.y.
Granodiorite, diorite	Wilhelm-Marum	Biotite	12	11.8	10.6 — 13.0
Granodiorite, diorite	Wilhelm-Marum	Hornblende	12	12.7	
Granodiorite, diorite	Wilhelm-Marum	Feldspar	2	10.7	
Granodiorite	Goroka/Mt Otto	Biotite	2	8.5 — 10.9	9.4
Granodiorite	Goroka/Mt Otto	Hornblende	2	11.1	
Granodiorite	Widely separated	Whole rock	10		12.7 $\pm$ 17.4
Aplite	Widely separated	Whole rock	13		12.3 $\pm$ 1.0
Aplite + granodiorite	Widely separated	Whole rock	23		12.4 $\pm$ 0.8
Pegmatite	Bundi	Muscovite	6	8.9	
Pegmatite	Bundi	Muscovite, whole rock	8		9.3 $\pm$ 4.0
Granodiorite	North Yanderra	Biotite	2	8.4	10.4
		Biotite	2	Anomalous	
Granodiorite	North Yanderra	Hornblende	4	11.0	
Granodiorite	Southwest Yanderra	Biotite	4	7.0	7.6 — 13.5
Granodiorite	Southwest Yanderra	Hornblende	2	10.0, 11.8	
Granodiorite	Southwest Yanderra	Feldspar	2	7.0, 9.8	

stage of the intrusive history of the Bismarck Intrusive Complex.

Questions could still be raised about the validity of assuming that the apparent ages (i.e. the times of closure of the systems) are those of emplacement rather than those of some subsequent geological event, such as regional metamorphism or uplift. Throughout this study, it was felt that if such questions could be resolved with reference to the data from the Bismarck mass, then it would be justifiable to suppose that other similar, consistent, Miocene ages determined elsewhere in the New Guinea Mobile Belt reflect ages of emplacement. The following observations lead to the conclusion that the Bismarck Intrusive Complex ages are related to magmatic emplacement and cooling rather than any metamorphic updating:

(a) The mid-Miocene ages are consistent with the stratigraphic control, which, however, has a large degree of latitude for the Bismarck Intrusive Complex.

(b) In the Central Highlands, several intrusive bodies (e.g. Kubor Granodiorite, Urabagga intrusives, Mount Victor Granodiorite—4.2, 4.4, 4.6) that were known to be 'old' on stratigraphic grounds yielded late Palaeozoic or Mesozoic isotopic ages which are consistent with the field evidence. If the young Bismarck ages were produced by updating through regional metamorphism, then other intrusives such as the Kubor, Mount Victor and Urabagga bodies would be expected to have been updated considerably too.

(c) The age of 12.4 $\pm$ 0.8 m.y. determined from the Rb-Sr Model I isochron for the 23 aplites and granodiorites from widely separated localities throughout the Bismarck mass represents the time that these rocks first cooled after differentiating from an isotopically homogeneous magma which had an initial Sr^{87}/Sr^{86} of 0.7037 $\pm$ 0.0001. It will be seen in section 6 that a similar initial Sr^{87}/Sr^{86} value is found in almost all of the New Guinea igneous rocks and, indeed, in most other areas of the circum-Pacific Belt. The concordance of the ages determined from the whole-rock Rb-Sr isochron and the Rb-Sr biotite analyses is further evidence that the ages are reflecting initial magmatic cooling rather than any subsequent metamorphism.

(d) The recognition of small age differences within the Bismarck Intrusive Complex results (e.g. hornblende ages in the Wilhelm-Marum area at 12.7 m.y.; mineralized granodiorites at southwest Yanderra, 7 to 10 m.y.; pegmatites, 8 to 9 m.y.) enables the definition of subareas, which are clearly quite acceptable, and even predictable, on geological grounds; this again confirms the reality of the ages in terms of magmatic rather than metamorphic processes.

(e) That the mid-Miocene ages are magmatic rather than metamorphic is also suggested by the excellent agreement between the hornblende K-Ar analyses (in the Wilhelm-Marum area) and the aplite-granodiorite Rb-Sr isochron age of about 12.5 m.y.

The total age spread of about 5 m.y. in the Bismarck Intrusive Complex data may be taken as an approximate maximum estimate for the length of time for the whole of the batholith to cool below about 200°C; this is the temperature below which argon is retained in most minerals. An approximate average rate of uplift can be obtained by assuming that the general ages reflect closed systems at 200°C and that the geothermal gradients average 30°C/km; for parts of the Bismarck mass now over 4000 m above sea level, an uplift rate of about 1 mm/year is indicated. This figure is of the same order as that obtained from the dating of uplifted Recent coral terraces on the north coast of New Guinea (Veeh & Chappell, 1970), and may indicate that uplift has been more or less constant since the Miocene.

5.34 Oipo Intrusives

In the northwest part of the Bismarck Range (Fig. 32) several small stocks from 2 to 7 km² in area were mapped by Dow & Dekker (1964) and Bain (1967) as the Oipo Intrusives. These plutonic rocks have intruded Tertiary e-stage sediments known as the Asai Shale (Bain, 1967), and they crop out intermittently over a distance of 70 km along the general trend of the Bundi and Jimi Fault Zones. Even within one body the compositions of the rocks are extremely

variable, and range from pyroxenite to granodiorite. Dow & Dekker (1964) reported gabbro and granodiorite as the predominant rock types, but Bain's (1967) mapping of the northwestern bodies revealed only gabbroic rocks. The complexity of the rock types and general range of composition in the Oipo Intrusives is similar to that found in the Marum Basic Belt, to the north and east (Fig. 32). Dow & Dekker (1964) found evidence of the Marum Basic Belt intruding Tertiary e-stage sediments, and it is suggested here that the Oipo Intrusives and the Marum Basic Belt intrusives could be cogenetic. No isotopic study has been undertaken in the Marum Basic Belt.

The K-Ar dating results from three bodies of the Oipo Intrusives are presented in Table 25, and the localities of the dated samples are shown in Figure 32. The hornblende and biotite ages of two coarse-grained hornblende gabbro samples (5815 and 5859) and one biotite diorite sample (5877) from the Mount Oipo stock are in the range 14.8 to 16.3 m.y. Concordant biotite and hornblende ages of 15.3 ± 0.4 m.y. and 15.6 ± 0.7 m.y. were determined for a sample (5678) from the mass south of Sipapi village, and two ages of about 18 m.y. were given by a sample (5679) of microdiorite from the intrusion near Terengi village. One other hornblende age of 16.1 m.y. was determined on the Kimil Diorite body (Plate 1), which intrudes Jurassic strata about 20 km southwest of Mount Oipo (Bain et al., in press); this age is similar to that of the Oipo Intrusives and it is possible that the two are comagmatic. Further work will be necessary to delineate the full history of the Oipo Intrusives but, as the present data are quite consistent with the stratigraphic control, the apparent mid-Miocene ages are interpreted as good minimum estimates for the time of emplacement. It would appear that the Oipo rocks were emplaced and cooled below the necessary temperature for retention of argon some 2 to 5 m.y. earlier than the Bismarck Intrusive Complex.

The relative ages of the Oipo Intrusives at 15 to 18 m.y. and the Bismarck Intrusive

TABLE 25. K-Ar AGES FOR THE OIPO INTRUSIVES

No.	Sample	K %		$*Ar^{40}$ $x10^{-6}\ cm^3$ NTP/g	$*Ar^{40}$ %	Calculated age (m.y.)
Mount Oipo stock						
5815	Hornblende	1.342 1.332 }	1.337	0.855	74.2	16.0 ± 0.6
5859	Hornblende	1.370 1.379 }	1.375	0.814	83.0	14.8 ± 0.6
5877	Biotite	6.880 6.804 }	6.842	4.481	83.5	16.3 ± 0.6
Sipapi stock						
5678	Biotite	7.419 7.423 }	7.421	4.549	57.7	15.3 ± 0.4
	Hornblende	0.375 0.376 }	0.376	0.235	42.4	15.6 ± 0.7
Terengi stock						
5679	Hornblende	0.297 0.295 }	0.296	0.211	37.3	17.8 ± 0.5
	Plagioclase	0.212 0.212 }	0.212	0.157	35.1	18.4 ± 0.6
Kimil Diorite stock						
6029	Hornblende	0.427 0.431 }	0.429	0.277	40.7	16.1 ± 0.4

Complex at 12 to 13 m.y. provide some constraint on the age of the several large faults in the Jimi and Bundi Fault Zones (Dow & Dekker, 1964), which are major lineaments of the northern boundary of the New Guinea Mobile Belt. The northwestern part of the Bismarck Intrusive Complex abuts against and obliterates the Jimi Fault (Fig. 32), whose activity had probably ceased by the time the granodiorite was emplaced in the mid-Miocene. The Oipo Intrusives cut across, and are controlled by, the en echelon faults of the Bundi Fault Zone, which Dow & Dekker (1964) concluded is still active. It seems that the Bundi Fault Zone has been active from at least 17 m.y. ago to the present day.

5.35 Maramuni Diorite

Large areas of granodioritic to gabbroic intrusives occur farther northwest in the New Guinea Mobile Belt, in the region between the Burgers Mountains and the Sepik River (Fig. 42). This area of the Central Range was mapped by Dow et al. (1972), and is one of the most isolated and rugged regions in New Guinea. The Maramuni Diorite crops out on the northern fall of the ranges, and consists of three large

plutons up to 20 km wide, as well as scores of smaller intrusives. The three batholithic bodies are elongated in a northwest direction, and their emplacement has been at least partly controlled by the similarly oriented Karawari and Maramuni Fault Zones. The intrusions east of the Maramuni Fault are grouped by Dow et al. (1972) as the Yuat intrusives, and the large body south of the Karawari Fault and the many apophyses to the west are called the Karawari intrusives.

Yuat intrusives. There is very little stratigraphical control on the age of the Yuat intrusives, except that in the northwest they intrude the Upper Cretaceous to Lower Tertiary Salumei Formation. Only a small number of samples were available from the Yuat intrusives and these have been dated by the K-Ar method. Dow et al. (1972) described the rocks as predominantly hornblende-biotite microgranodiorite with minor diorite phases. With the exception of 5473 hornblende (which is rather badly altered) the three biotite and two hornblende ages of the north Yuat body (Table 26) are concordant at 14 m.y. The clinopyroxene, 5676, gives a much older age of about 20 m.y., and is assumed to have incorporated
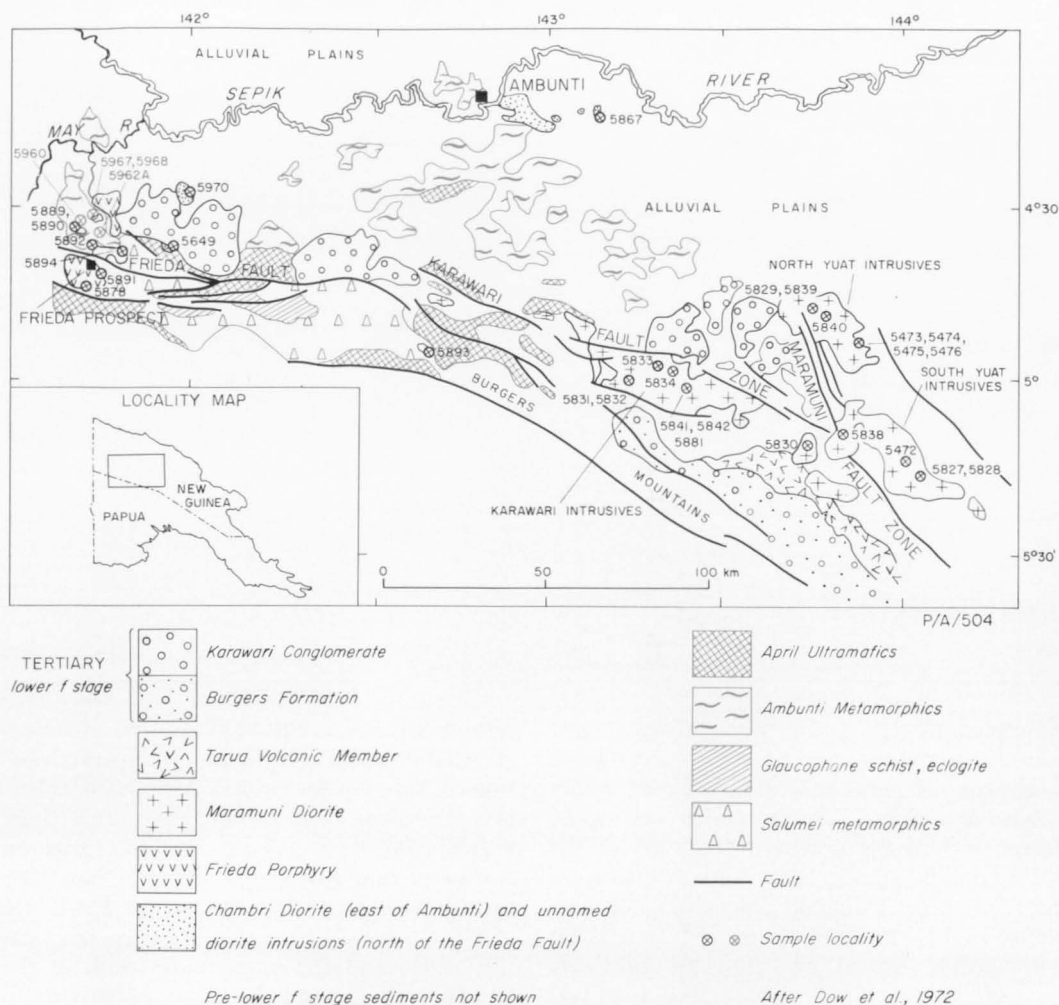
Fig. 42. Simplified geological map—south Sepik area.

extraneous radiogenic argon. The agreement of the biotite and hornblende K-Ar dates provides strong evidence that this is the time of emplacement of the north Yuat body.

Significantly younger ages of between 11.2 and 12.5 m.y. (Table 26) were determined on all but one of the granodiorites from the south Yuat body (Fig. 42). The poor reproducibility of the duplicate runs on 5472 hornblende could not be reconciled, and this result cannot be seriously considered in the interpretation.

Karawari intrusives. The age of the Karawari intrusives to the west (Fig. 42) is given by their intrusive relationship with the Ter-

tiary *e*-stage Pundugum Formation and the inferred unconformable relationship with the overlying Tertiary lower *f*-stage Karawari Conglomerate (Dow et al., 1972). However, Dekker & Faulks (1964) considered that parts of the Karawari intrusives postdate the lower *f*-stage Tarua Volcanic Member, and hence there is no unequivocal younger limit for their age. Dow et al. (1972) described the Karawari intrusives as pyroxene-quartz gabbros, porphyritic quartz diorites, and anorthite gabbros. Extreme local relief in the area of these intrusives prevented close sampling, and most of the dated rocks were collected as float from streams of restricted drainage. That the numerous rock types are

TABLE 26. K-Ar AGES FOR THE MARAMUNI DIORITE

No.	Sample	K %		$*Ar^{40}$ $x10^{-6}\,cm^3$ NTP/g	$*Ar^{40}$ %	Calculated age (m.y.)
North Yuat body						
5473	Hornblende	0.262 0.264	0.263	0.197 0.176	23.7 12.5	18.7 ± 0.9 16.7 ± 1.1
5474	Hornblende	0.373 0.366	0.370	0.209	44.3	14.2 ± 0.6
5475	Biotite	6.770 6.780	6.775	3.869	78.3	14.2 ± 0.5
5476	Clinopyroxene	0.274 0.276	0.275	0.248 0.205	21.3 11.6	22.5 ± 0.8 18.6 ± 1.2
5829	Biotite	6.988 6.993	6.991	3.929	75.5	14.0 ± 0.5
5839	Biotite	7.297 7.298	7.298	4.144	83.7	14.2 ± 0.6
5840	Hornblende	0.426 0.426	0.426	0.238	19.5	14.0 ± 0.7
South Yuat body						
5472	Biotite	6.694 6.722	6.708	3.161	68.8	11.8 ± 0.2
	Hornblende	0.377 0.378	0.378	0.396 0.220	33.3 27.7	26.1 ± 1.0 14.6 ± 0.4
5827	Biotite	6.990 7.075	7.033	3.157	54.3	11.2 ± 0.4
	Hornblende	0.399 0.394	0.397	0.197	25.2	12.4 ± 0.6
5828	Biotite	6.674 6.737	6.706	3.046	64.4	11.4 ± 0.4
	Hornblende	0.286 0.286	0.286	0.144	19.9	12.5 ± 0.6
5838	Hornblende	0.328 0.330	0.329	0.149	28.9	11.3 ± 0.5
Karawari intrusives						
5830	Hornblende	0.200 0.200	0.200	0.119	27.4	14.8 ± 0.7
5831	Hornblende	0.230 0.232	0.231	0.119	12.3	12.8 ± 1.0
5832	Hornblende	0.287 0.287	0.287	0.157	35.1	13.6 ± 0.6
5833	Hornblende	0.398 0.400	0.399	0.164 0.160	40.0 12.9	10.3 ± 0.4 10.1 ± 0.6
5834	Hornblende	0.806 0.840	0.823	0.354	46.6	10.7 ± 0.5
5841	Hornblende	0.635 0.636	0.636	0.355	59.2	14.0 ± 0.6
5842	Hornblende	0.288 0.289	0.289	0.175	29.2	15.1 ± 0.7
5881	Hornblende	0.940 0.951	0.946	0.507	60.1	13.4 ± 0.5
5893	Hornblende	0.304 0.318	0.311	0.127	25.2	10.2 ± 0.5

reflecting the complexity of intrusion of the mass is seen in the relatively large spread of the K-Ar ages (Table 26), which range from 10 to 15 m.y. A sample of a hornblendite (5881, consisting of 95 percent hornblende) yielded a K-Ar age of 13.4 ± 0.5 m.y., with-

in the range of the diorite ages. As the sampling control is rather poor, detailed interpretation of these data is not feasible. It is possible that the Karawari intrusives had a complex intrusive history over the 5 m.y. period indicated by the data. This would be

consistent with the field evidence as different parts of the intrusives appear to antedate and postdate the lower *f*-stage rocks (cf. Dekker & Faulks, 1964; Dow et al., 1972).

The mid-Miocene ages of the Karawari intrusives overlap the ages of 13 to 14 m.y. determined on andesitic lavas from the Tarua Volcanic Member (3.31) a few kilometres to the south (Fig. 42). The initial Sr^{87}/Sr^{86} ratios for samples from the Tarua Volcanic Member and Karawari intrusives (see section 6) are uniformly low, between 0.7036 and 0.7040. The similar ages and initial strontium isotopic compositions, therefore, support the proposal of Dow et al. (1972) that the Tarua Volcanic Member is cogenetic with, and the volcanic counterpart of, the Karawari intrusives.

Comparison of the Yuat and Karawari intrusives. Differences in the mean trace-metal (copper, nickel, and silver) contents of the Yuat and Karawari intrusives were invoked by Dow et al. (1972) as evidence that the two intrusives could have either been formed from different magmas or, alternatively, could represent the same magma which had been differentially contaminated by country rock. The Karawari intrusives, which contain numerous rock types, are certainly more complex than the Yuat intrusives, which consist essentially of only one rock type, granodiorite. Although the south Yuat body appears to be 1 to 2 m.y. younger than the north Yuat body, the other ages determined on the Karawari and Yuat intrusives completely overlap and would probably not support an hypothesis appealing to two different magmas. The initial Sr^{87}/Sr^{86} ratios indicated by two samples of the Karawari intrusives (see section 6) are 0.7036 and 0.7037. If there had been contamination (other than to a minor degree) of the Karawari intrusives by the country rock, a significantly higher value for the initial ratio might be expected.

5.4 SUMMARY OF TERTIARY PLUTONIC ACTIVITY AND METAMORPHISM

The ages of the Tertiary plutonic and metamorphic rocks in the Central Highlands have in the past been known only within very wide limits. Some of the plutonic rocks had been proved to have intruded Lower Tertiary sedimentary sequences of the Papuan Geosyncline, but for others the youngest intruded country rocks had been shown to be as early as Mesozoic. A compilation of the Tertiary isotopic ages from all the major plutonic bodies and some of the metamorphic rocks of the Central Highlands is given in Table 27. The ages quoted are considered to be the best estimates for the main phases of emplacement of the plutons in areas sampled. The data included in Table 27 are only those that have been discussed in this section; several porphyry intrusions of intermediate composition also fit into the Late Tertiary age category, but they are of minor areal extent; they are referred to in Page & McDougall (1972a).

The first sign of Tertiary tectonic activity, as shown by the mineral and whole-rock K-Ar and Rb-Sr ages throughout the Central Highlands, was that of metamorphism and minor dioritic intrusion in the south Sepik and Ramu regions between 20 and 25 m.y. ago in the late Oligocene to early Miocene. The majority of the plutonic rocks of the Central Highlands were intruded between 12 and 15 m.y. ago in middle Miocene time, and there are a few small stocks near Kainantu which indicate middle to late Miocene ages. These Miocene plutons are known to be exposed over at least 6500 km^2 of the Central Highlands, and they are arranged in an arcuate, roughly northwest-trending belt, the New Guinea Mobile Belt, (Dow et al., 1972), which is over 700 km in length (cf. Plate 1). The pulse of plutonic activity between 12 and 15 m.y. ago in the mid-Miocene played an important part in the development of the New Guinea Mobile Belt. The emplacement of many of these intrusive batholiths appears to have been partly controlled by the major northwest-trending fault systems. Dow & Bain (1970) and Dow et al. (1972) showed that at about this time (mid-Miocene) there were also extensive outpourings of lava in a discontinuous chain along much of the length of the New Guinea Mobile Belt. The known stratigraphic control and physical ages deter-

TABLE 27. COMPILATION OF AGES OF PLUTONIC ROCKS IN THE NEW GUINEA MOBILE BELT

	K-Ar age (m.y.)	Rb-Sr age (m.y.)
Sepik-Ramu Plains intrusives	20-25	
Ambunti Metamorphics	26-27	25
Gwin Metamorphics	23	
Kaindi Metamorphics		21
Morobe Granodiorite	12, 14	13, 14.5
Akuna Intrusive Complex	15, 17	
Elendora Porphyry	7-12	
Michael Diorite	6-7	
Bismarck Intrusive Complex	12.5	12.5
Oipo Intrusives	15, 18	
Maramuni Diorite	10-15	

mined on the volcanics (section 3) certainly indicate that they were approximate time-equivalents of the mid-Miocene intrusives 12 to 15 m.y. ago. However, the exact nature of the volcanic/intrusive relations, especially on petrological criteria, is not yet clear.

One of the lesser-known elements of the Tertiary intrusive activity in the New Guinea Mobile Belt is that of the emplacement of the many ultramafic bodies of the region. The major units (Plate 1) are the Marum Basic Belt (Fig. 32) of about 500 km² in the Ramu area, and the April Ultramafics of over 1000 km² in the south Sepik area (Fig. 42). The ultramafic bodies are elongated parallel to the regional structural trend, and they range from small serpentinite lenses to large masses of dunite and pyroxenite up to 50 km in length. In the south Sepik region the ultramafics are locally associated with glaucophane schists and eclogites (Ryburn, 1970; Dow et al., 1972). The field evidence, although equivocal, suggests that tectonic emplacement of the ultramafic rocks took place in the early to mid-Miocene along the major fault zones of the New Guinea Mobile Belt (Dow et al., 1972). No general isotopic study was undertaken on the ultramafic rocks, but some supporting evidence for the early to mid-Miocene age is derived from the small diorite mass (Fig. 42) apparently intruded by ultramafics in the lower Frieda River (5.21);

the diorite (5649) was dated as 25 m.y. (Table 13), thus providing a tentative maximum age for the emplacement of the ultramafics in this area. One other sample relevant to the age of the ultramafic rocks is the hornblendite rock (5881) from the region of the Karawari River; a K-Ar age of 13.4 m.y. for the hornblendite (Table 26) is similar to those obtained for other parts of the Karawari intrusives. It does not seem unreasonable to conclude that the ultramafic rocks of the Central Highlands were emplaced about the same time, and were related to the same peak of tectonism as the mid-Miocene granodiorite intrusives of the New Guinea Mobile Belt.

The close association of the major tectonic processes of faulting, volcanism, and plutonism over a relatively narrow time span of a few million years in the mid-Miocene can be correlated with the waning phases and even the culmination of the Papuan Geosyncline sedimentary history in the Central Highlands. As pointed out by Dow et al. (1972) there are no identifiable upper Miocene or later geosynclinal sedimentary successions anywhere in this region. This proposed relation between tectonic activity and cessation of geosynclinal sedimentation in the mid-Miocene implies a common catastrophic cause for the two effects. Such possibilities are explored in the consideration of the overall development of the island of New Guinea later in this Bulletin.

6. CONTINENTAL GROWTH AND STRONTIUM ISOTOPES IN IGNEOUS ROCKS

6.1 INTRODUCTION

It was shown earlier that plutonism and volcanism in New Guinea occurred mainly in the late Palaeozoic, the Mesozoic, and in the latter part of the Cainozoic (cf. Plate 1). The Cainozoic igneous rocks of the New Guinea Mobile Belt in particular are closely related in space and time to the development of the Papuan Geosyncline. This Tertiary tectonic setting, together with the present-day island-arc-type seismicity and volcanicity in north New Guinea and the New Britain arc regions, can possibly be viewed in terms of the concept of continental growth (Wilson, 1952; Taylor & White, 1965; Taylor, 1967; Mitchell & Reading, 1969; Coney, 1970; Dewey & Horsfield, 1970). A model of continental formation in which there are continual major additions of new material to the crust was first proposed by Hurley, Hughes, Faure, Fairbairn, & Pinson (1962) by tracing the development of radiogenic Sr^{87} in the crust. In this section, stontium-isotope data for some of the New Guinea plutonic and volcanic rocks are presented; comparison of this data with that determined for other rocks from oceanic, island-arc, and continental regions allows certain restrictions to be placed on the genesis of the New Guinea igneous rocks.

6.2 CONTINENTAL GROWTH

Several authors (Gilluly, 1955; Wasserburg, 1966; Taylor, 1967) have pointed out that, as continents are being constantly eroded, continental accretionary processes are necessary in order to maintain regions of positive relief over long periods of time. Allowing for isostatic uplift and the slowing rates of erosion as base level is approached, Taylor (1967) calculated that a period of only 30 to 50 million years would be necessary to remove the mountainous areas on the Earth's present surface.

The concept of continental growth is accomplished by a series of orogenies deforming the sediments which had previously accumulated in basins bordering the nucleus. The genesis and role of calc-alkaline volcanism and plutonism as a complementary means of adding to the continental crust in this type of environment have been discussed by Taylor & White (1965), Hamilton (1966), Green & Ringwood (1966, 1968), Taylor, Kaye, White, Duncan, & Ewart (1969), Ringwood (1969), Christensen (1970), and Dickinson (1970). It is generally agreed that the calc-alkaline suite may originate by at least a two-stage process involving the transformation of basalt to eclogite or amphibolite; and this in turn undergoes partial melting (with or without sediment mixing) to produce an andesitic magma. Such a process is believed to be occurring today near the Benioff zone in descending lithospheric plates around the periphery of the Pacific Ocean.

Geochronological and geochemical data within and near the margins of continents are pertinent to the question of continental growth, or accretion. Hurley et al. (1962) and Hart (1969) pointed out that tectonic belts in North America are progressively younger towards the continental margins, and thus generally provide strong support for the growth concept. Webb & McDougall (1968) related age patterns of granitic rocks in the Tasman Geosyncline to the hypothesis that this region represents the eastward growth of the Australian continent. In New Guinea we may also be seeing the process of continental growth, or accretion, taking place, and this may in time result in a northward addition to the Australian mass (cf. Glaessner, 1950).

6.3 STRONTIUM-ISOTOPE DATA FROM NEW GUINEA IGNEOUS ROCKS

While considering the continental growth concept in New Guinea, it would be desirable to establish whether this geologically young terrain represents the addition of new material, or is in fact the metamorphic product of older, pre-existing provinces (e.g., the Tasman Geosyncline). The application of strontium-isotope studies to the problems of the origin of igneous rocks was initially proposed by Hurley et al. (1962) and Faure

TABLE 28. Sr^{87}/Sr^{86} RATIOS, AND RUBIDIUM AND STRONTIUM CONCENTRATIONS IN IGNEOUS ROCKS FROM NEW GUINEA

Rock unit	Sample no.	Rb* (ppm)	Sr* (ppm)	Sr^{87}/Sr^{86} (measured**)		Corrected or indicated initial Sr^{87}/Sr^{86}
PRE-TERTIARY INTRUSIVES						
Kubor Granodiorite	2135	3.9	231.4	0.7044 0.7044	0.7044	0.7042
	2191	11.2	513.6	0.7035 0.7033	0.7034	0.7032
	7 aplites					0.7051
Urabagga intrusives	7 aplites, diorites					0.7029
Mount Victor Granodiorite	5461	81.9	632.0	0.7046 0.7042	0.7044	0.7039
MIOCENE INTRUSIVES						
Morobe Granodiorite	5453	35.1	839.4	0.7039 0.7040	0.7040	0.7040
	5459	33.9	845.2	0.7044 0.7044	0.7044	0.7044
Akuna Intrusive Complex	5660	60.8	396.1	0.7055 0.7055	0.7055	0.7054
	5851	34.8	588.7	0.7041 0.7040	0.7041	0.7041
	5854	43.4	444.3	0.7047 0.7046	0.7047	0.7046
Bismarck Intrusive Complex	23 aplites, granodiorites					0.7037
	5883A	57.7	562.2	0.7039 0.7038	0.7039	0.7038
	5883B	69.0	402.4	0.7039 0.7039	0.7039	0.7038
	5883C	17.8	629.8	0.7037 0.7039	0.7038	0.7038
	4 muscovite pegmatites					0.7085
Oipo Intrusives	5971	63.0	951.9	0.7040 0.7040	0.7040	0.7040
	5972	128.5	581.2	0.7041 0.7041	0.7041	0.7040
Maramuni Diorite	5833	22.0	297.9	0.7036 0.7035	0.7036	0.7036
	5841	6.5	834.0	0.7037 0.7037	0.7037	0.7037
MIOCENE VOLCANICS						
Tarua Volcanic Member	5630	16.8	379.4	0.7040 0.7038 0.7042	0.7040	0.7040
	5631	19.1	380.3	0.7036 0.7036	0.7036	0.7036
	5634	23.1	444.9	0.7039 0.7040	0.7040	0.7040
Karawari Conglomerate volcanics	5654	53.7	453.9	0.7038 0.7038	0.7038	0.7037
Daulo volcanic member	5641	183.9	1016.6	0.7047 0.7046	0.7047	0.7046
	5645	64.4	1059.2	0.7043 0.7040	0.7042	0.7042

* Approximate XRF analysis
** Unspiked run, average SD ~ 0.0002; mean Sr^{87}/Sr^{86} for E and A standard 0.70811 (see Appendix 1, p. 111)

& Hurley (1963). Because the rubidium/strontium ratios found in crustal sialic material are higher than those in the upper mantle, these authors suggested that magma formed from the fusion or assimilation of old continental crust should have measurably higher Sr^{87}/Sr^{86} than magma derived from the upper mantle. The present-day Sr^{87}/Sr^{86} in the upper mantle as indicated by young oceanic basalts, which are believed to be derived from this region, is about 0.703 to 0.704 (data summarized by Gast, 1967). On the other hand continental volcanic rocks are usually more radiogenic and have a wider range from 0.703 to upwards of 0.711 (Gast, 1967). The higher Sr^{87}/Sr^{86} values are usually interpreted as indicating various degrees of crustal contamination.

The majority of the Central Highlands plutonic and volcanic rocks are part of the calc-alkaline suite, which is relatively common throughout the circum-Pacific region (Dow et al., 1972). Theories of the genesis of calc-alkaline rocks invoke various degrees of partial melting of the crust or upper mantle with or without assimilation of some crustal component. The study of strontium isotopes may thus provide a measure of the importance of the crustal-versus-mantle processes in the genesis of the New Guinea igneous rocks.

Sr^{87}/Sr^{86} measurements for at least one sample from each major intrusive and volcanic body in the Central Highlands are listed in Table 28, together with the initial Sr^{87}/Sr^{86} ratios of the intrusive rocks which have been dated by the Rb-Sr method (from sections 4 and 5). The present-day Sr^{87}/Sr^{86} ratios were measured for the whole-rock samples and corrected for age where necessary to give the initial Sr^{87}/Sr^{86} ratios. Localities of the analysed samples are shown on the respective geological maps in the earlier sections. Of the pre-Tertiary intrusive rocks, the initial Sr^{87}/Sr^{86} ratios range from 0.7029 to 0.7051; because these data are limited it is not possible to draw any firm conclusions from them alone. The initial Sr^{87}/Sr^{86} values in the Miocene intrusives of the New Guinea Mobile Belt are more

closely grouped, and average 0.7041 ± 0.00015 (SD of mean). Sr^{87}/Sr^{86} values of 0.7038 measured on three strongly mineralized granodiorites (5883 A, B, C) from the Yanderra Copper Prospect are indistinguishable from the normal granodiorite values. The much higher indicated initial Sr^{87}/Sr^{86} ratio (0.7085) of the pegmatites from the Bismarck Intrusive Complex (5.33) has probably resulted from local crustal contamination, and this value is not considered in the average. The range of values of Sr^{87}/Sr^{86} obtained in the Miocene volcanic rocks is 0.7036 to 0.7046; the average is 0.7040 ± 0.00014 (SD).

The initial Sr^{87}/Sr^{86} ratios in the New Guinea igneous rocks reveal:
(a) no significant change in the isotopic composition of the source of the intrusive rocks during the Permian through to the Miocene;
(b) almost constant isotopic composition (~ 0.7041) of the intrusive rocks along the length of the New Guinea Mobile Belt (i.e., independent of the age of the intruded basement);
(c) that the average initial Sr^{87}/Sr^{86} of the Miocene volcanics (0.7040) is not distinguishable from that of the Miocene intrusive rocks (0.7041);
(d) that, except for the Bismarck pegmatites, there is no isotopic evidence of contamination of any of the intrusive or volcanic rocks by old (radiogenic) crustal material.

6.4 DISCUSSION

The simplest interpretation is that the majority of the New Guinea igneous rocks have been no more affected by crustal strontium than has the average oceanic basalt, and that they might reasonably be expected to have been derived from the upper mantle. It is noted that the Sr^{87}/Sr^{86} values of the igneous rocks of the Central Highlands (Table 28) are almost indistinguishable from the values obtained for the Quaternary volcanic rocks at Talasea, New Britain (Peterman, Lowder, & Carmichael, 1970), and at other Quaternary volcanic centres in the New Guinea region (Page & Johnson, 1974). Recent workers on strontium iso-

topes in calc-alkaline rocks from other island-arc and Cainozoic orogenic environments (Pushkar, 1968; Hedge & Knight, 1969; Gill, 1970; Hedge, Hildreth, & Henderson, 1970) have also found initial Sr^{87}/Sr^{86} values close to 0.704, which indicates there is a magma source with uniform Sr^{87}/Sr^{86} throughout the circum-Pacific regions studied. One exception may be the New Zealand andesites, where the average value of Sr^{87}/Sr^{86} is significantly higher at 0.7055 (Ewart & Stipp, 1968); but the authors concluded that the primary magma had incorporated various amounts of greywacke country rock before eruption.

The similarity of strontium isotopic compositions of volcanics in island arcs and oceanic islands was noted earlier; the average Sr^{87}/Sr^{86} ratio in both of these environments is close to 0.704. This is significantly higher than that (0.702 to 0.703 so far reported) for the low-potassium tholeiitic basalts from mid-oceanic ridges (Tatsumoto, Hedge, & Engel, 1965; Hedge & Peterman, 1970) and may, therefore, reflect mantle heterogeneity or 'radiogenic contamination' by the assimilation of sediments of the island arcs and oceanic islands. Limited comparitive data of lead isotopes in both island arcs and abyssal basalts (Armstrong, 1968; Tatsumoto, 1969; Armstrong & Cooper, 1971) also suggest that oceanic sediments are mixed with mantle material

to form calc-alkaline magmas. However, trace-element studies (Taylor et al., 1969), as well as the remarkable constancy of the average Sr^{87}/Sr^{86} at 0.704 throughout most island-arc regions, point to little or no involvement of oceanic sediments in calc-alkaline genesis. If oceanic sediments (present-day Sr^{87}/Sr^{86} of 0.704 to 0.743, Dasch, 1969) or eugeosynclinal greywackes (initial Sr^{87}/Sr^{86} of 0.706 to 0.714; Peterman, Hedge, Coleman, & Snavely, 1967) were significant contributors to partial melts, a much greater variation in Sr^{87}/Sr^{86} in the calc-alkaline island-arc rocks would be expected.

Apart from negating the wholesale addition of sialic material to the primary magma that formed the New Guinea igneous rocks, it is beyond the present scope to investigate further the hypotheses of calc-alkaline petrogenesis. Current theories invoke fractional crystallization of basalt (Bowen, 1928), limited basalt-sediment mixing (Armstrong, 1968), and the two-stage process (the transformation of basalt to eclogite, then the partial melting of eclogite) of calc-alkaline series evolution (Green & Ringwood, 1968). It appears that the igneous rocks of the Central Highlands may represent addition to the crust, at Australia's northern continental margin, of material which was chiefly, if not entirely, derived from the upper mantle.

7. SUMMARY OF RESULTS

The geological interpretations of the geochronology results, and an outline of some of the more general aspects and problems of K-Ar and Rb-Sr dating in young orogenic belts such as New Guinea, are synthesized below.

7.1 RESULTS

(i) K-Ar dating of stratigraphically controlled lavas in the Central Highlands has enabled the first direct physical subdivision of the relative time scale of the East Indies letter stages. From the New Guinea dating and literature review, the suggested East Indies Miocene time scale is:

g stage	5.5	to 9	m.y.
upper f stage	9	to 12.5	m.y.
lower f stage	12.5	to 15	m.y.
upper e stage	15	to 22.5	m.y.

(ii) The geochronological data for the New Guinea intrusive rocks are summarized in a histogram of ages (Fig. 43) and a notional 'intrusive activity' diagram (Fig. 44). In the histogram, each reliable K-Ar mineral age determination on intrusive rocks is plotted. In addition, the K-Ar ages of several mineralized intrusives (Page & McDougall, 1972a, b) are also plotted. For the Bena Bena gneissic granites and Ura-
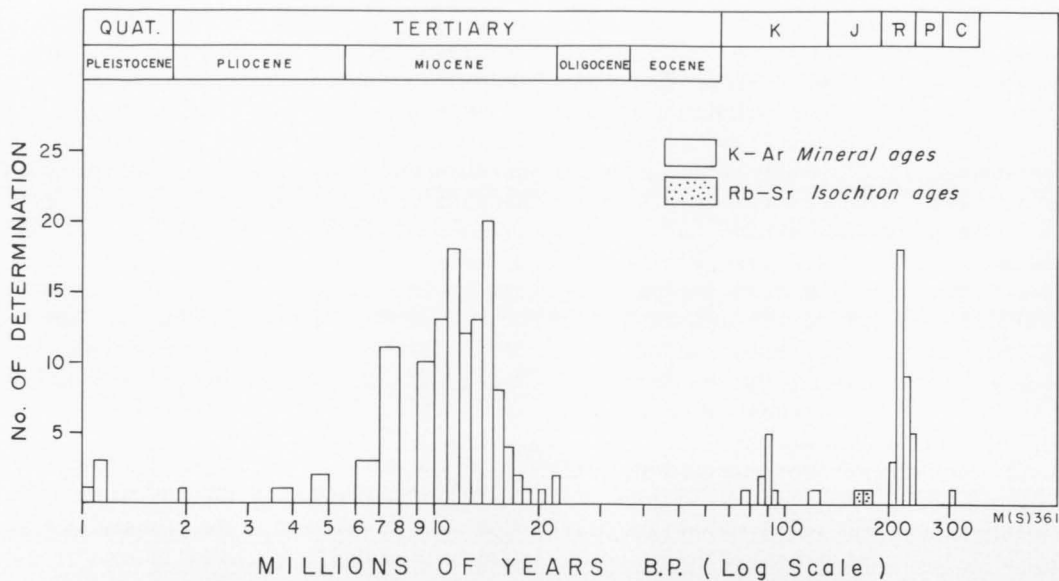
Fig. 43. Histogram of ages of New Guinea intrusive rocks.
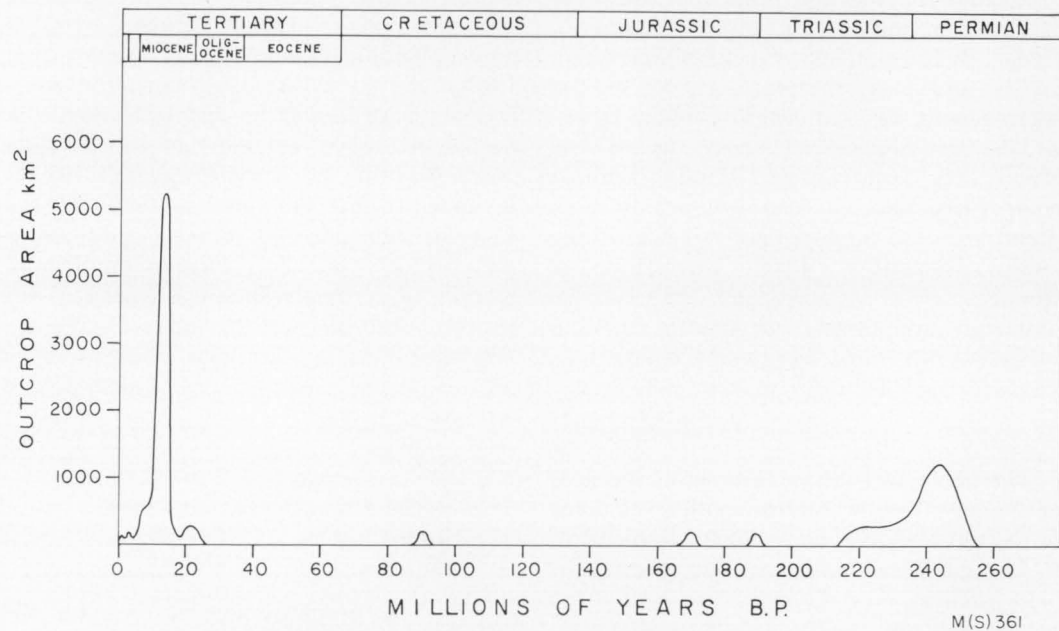
Fig. 44. Activity of plutonic igneous rocks in New Guinea.

bagga intrusives (170-190 m.y.), the best age estimate was the Rb-Sr isochron, and each of these is indicated as one determination. Because the general distribution of the peaks is similar in both plots (Figs. 43 and 44), it is considered that the sampling has been representative and the age determina-

tions provide a reasonably complete picture of the intrusive history in the Central Highlands. The geological and geochronological studies thus show that:

(a) Granitic intrusion was of limited extent and occurred rather sporadically during the late Palaeozoic and the Mesozoic.

(b) A rather dramatic increase in intrusive activity took place in the Miocene, and reached a climax between 10 and 15 m.y. ago in the mid-Miocene; this late orogenic activity in the New Guinea Mobile Belt is identifiable with the waning stages of the development of the Papuan Geosyncline and with the beginning of the main mountain building in the Central Highlands.

Limited data in four metamorphic terrains in the highlands (the Bena Bena Formation, Ambunti Metamorphics, Gwin Metamorphics, and Kaindi Metamorphics) do not discriminate between ages of metamorphism and ages of uplift, but the general tectonic setting suggests that the mid-Tertiary ages obtained are close to the times of metamorphism.

(iii) The ages of emplacement and mineralization of several metalliferous deposits in New Guinea and Bougainville Island (Page & McDougall, 1972a, b) indicate that the related magmatic events are all mid-Miocene or younger. It is clear that the high-level intrusives of the young island-arc orogenic environment may be of considerable economic interest

(iv) The strontium isotopic study of the New Guinea igneous rocks reveals a constant initial Sr^{87}/Sr^{86} composition of 0.7041 ± 0.00015 (SD). This value is not distinguishable from those determined for rocks from oceanic islands and other circum-Pacific orogenic and island-arc environments. The strontium isotopic data on the New Guinea igneous rocks are therefore consistent with derivation of magma chiefly from upper mantle sources, with little or no contamination by crustal material enriched in Sr^{87}.

7.2 GENERAL FEATURES OF THE GEOCHRONOLOGICAL STUDY

The following is a summary of general aspects of the K-Ar and Rb-Sr dating techniques as found in sections 3, 4, and 5.

7.21 Relative argon retentivities

The rate at which argon diffuses in minerals has been examined in many field and laboratory studies (summarized in Mus-sett, 1969) which show that argon diffuses from minerals at rates that depend on the degree of crystal imperfections and the relative activation energies in the lattice. Diffusion of argon from rocks and minerals can be detected in laboratory experiments above about 300°C, and, by extrapolation, may occur in the geological environment at temperatures as low as 200°C, or even lower. Differential argon diffusion is recognized in the New Guinea ages determined for hornblende, biotite, and feldspar from the one sample. Among the young intrusives dated by the K-Ar method in section 5, it was generally found that ages determined for hornblende are 1 to 2 m.y. greater than those for biotite, and that the few feldspar ages are equal to or less than the biotite ages. The biotite-hornblende age pattern reflects the cooling history of the intrusive in which argon began to be retained in hornblende at an earlier time (higher temperature) than in biotite. For the late Palaeozoic and Mesozoic intrusives, hornblende and biotite K-Ar ages generally showed excellent agreement; any discordant effects caused by the cooling history of the intrusive would have been marked by experimental errors.

The few perthitic alkali feldspars dated in this study have ages slightly younger than the accompanying ferromagnesian minerals, probably because perthitization of potash feldspar produces lattice imperfections which are believed to enhance argon diffusion (Mussett, 1969). The predictable effect of chloritization (again involving lattice imperfections) in some of the Kubor Granodiorite rocks (4.2) was to lower the biotite or hornblende age. The most chloritized samples gave the lowest ages, although no general correlation between age and the degree of chloritization was found.

7.22 Comparison of K-Ar and Rb-Sr ages

Comparison of Rb-Sr and K-Ar ages for micas from the Miocene intrusive rocks (section 5) shows that the K-Ar ages are commonly about 1 to 2 m.y. less than the Rb-Sr ages. Hornblende dated by the K-Ar method closely corresponds to the Rb-Sr mica age for the same rock. As the ages are

TABLE 29. EXCESS Ar⁴⁰ IN MINERALS FROM SOME NEW GUINEA INTRUSIVES

Text reference	Sample		Excess Ar^{40} $(x10^{-6}\ cm^3$ $NTP/g)$
5.32	5657	Clinopyroxene	0.02
5.33	5497	Plagioclase	0.58
5.35	5476	Clinopyroxene	0.07

consistent with the stratigraphic control, and the Miocene intrusives are not apparently deformed, it is again concluded that the age pattern may be reflecting the cooling history of the intrusive in which the diffusion of argon from hornblende, and of radiogenic strontium from mica, ceased at about the same time (temperature), 1 to 2 m.y. before the cessation of argon diffusion from mica.

That argon diffuses more readily than strontium in response to geological processes is seen in the consistently lower, but wider-ranging, K-Ar ages compared with the Rb-Sr ages in the Permian Kubor Granodiorite. An analogous situation is found in the younger K-Ar ages obtained for micas from the Yanderra copper-mineralized area (Page & McDougall, 1972a), where the use of both dating methods has provided a better understanding of the geological history.

7.23 Extraneous argon

Extraneous argon was recognized in a few samples whose apparent ages contrasted with those for related samples. The most common type is excess argon, which is that incorporated within minerals at the time of their crystallization owing to a high partial pressure of Ar^{40} in the magma (Damon, 1968). This was found mainly in minerals with a low potassium content, such as pyroxene and some plagioclase samples. The approximate amounts of excess radiogenic Ar^{40} that have been calculated using the ages given by related samples in the individual areas are given in Table 29. These quantities of excess argon are generally similar to those reported by Livingston, Damon, Mauger, Bennett, & Laughlin (1967) in feldspars from Tertiary plutons in Arizona.

Inherited argon (Damon, 1968) contained within xenoliths or xenocrysts included in the magma was also encountered

in a few samples in this study. The most obvious examples are the samples 981, 981B, and 5493 from the Bismarck Intrusive Complex north of Yanderra village (see 5.33). Inherited argon was also invoked in a hornblende sample from the Karawari Conglomerate volcanics (3.32).

It is perhaps surprising that the effects of extraneous argon are not more widespread in K-Ar dating, because in subcrustal conditions, where the rocks are generated, copious amounts of radiogenic Ar^{40} must be present. Any excess argon in the relatively potassium-rich minerals, such as biotite and hornblende, would usually be swamped by the greater proportions of true radiogenic argon. Nevertheless, the newly developed K-Ar isochrons are a useful approach to test for extraneous argon in a given suite of rocks.

7.24 K-Ar isochrons

The interpretation of several sets of K-Ar mineral and whole-rock data using graphical isochron diagrams was investigated in the course of this study. Where there were sufficient data points, this approach (after McDougall et al., 1969; Hayatsu & Carmichael, 1970) provided a means of testing for the presence of extraneous argon in either whole rocks or different minerals from an intrusion. In nearly all the rock suites tested no extraneous argon was indicated within the statistical uncertainties of the results, and thus calculated K-Ar ages are deemed more reliable. A few of the pooled ages from the argon isochron diagrams were shown to be erroneous because of small differences in age of the rocks sampled over a large outcrop area, inhomogeneous initial argon concentration and Ar^{40}/Ar^{36} values, and, in part, post-closure contamination of the samples with atmospheric argon; thus

some of the underlying assumptions of the plots were not met.

7.25 Rb-Sr whole-rock and mineral ages

The Rb-Sr method used in conjunction with the K-Ar method enabled a more complete picture of the geological history to be obtained. Concordant Rb-Sr mica ages determined for the Kubor Granodiorite (4.22) provided the best estimate of the age of emplacement of this body, because the low-grade burial metamorphic effects (with temperatures inferred to be 200° to 300°C) evidently did not upset the Rb-Sr clock. Rb-Sr mica ages for the Miocene intrusives are related to the cooling history, which was shown to correspond closely to the time of emplacement. As noted previously, the several examples of concordant Rb-Sr biotite and K-Ar hornblende ages for the same intrusive rock sample indicate that

the respective minerals and isotopic systems were closed at similar temperatures.

Many of the New Guinea intrusives have low and rather uniform Rb/Sr ratios, and hence Rb-Sr whole-rock isochrons could be used for rock samples from only a few areas. The study of the Bismarck Intrusive Complex has shown that meaningful ages from Rb-Sr whole-rock isochrons can be obtained for young intrusives if there is suitable material and mass-spectrometer precision. The young age derived from the isochron for the Bismarck Intrusive Complex gives the time the whole-rock systems cooled after differentiating from an isotopically homogeneous magma. The few Rb-Sr biotite ages are equal to or younger than the age derived from the isochron, and reflect the lower temperatures at which the Rb-Sr system became closed in the mineral.

8. SPECULATIONS ON REGIONAL TECTONICS

The geophysical and geological studies of the world's oceans and seismic belts in the last few years have led to a new appraisal of geological features on land. In particular, an important corollary of the plate-tectonic theory accounts for orogenic belts of mountain building as the narrow elongate junction between moving lithospheric plates at a given time (Dewey & Bird, 1970). The marine magnetic data south of Australia, for example (Le Pichon & Heirtzler, 1968), indicate that the Australian Plate has separated from Antarctica and has been moving north since the Early Tertiary (Fig. 45). Worldwide and regional seismic studies (Barazangi & Dorman, 1969; Denham, 1969) previously discussed in 2.2 show that New Guinea is today part of the northern edge of the Australian Plate (cf. Figs. 3 and 4). Along much of this edge, the plate is today being partly thrust into east-west crustal sinks or subduction zones of the type presently associated with active trenches. The New Britain-Bougainville and Java-Sumatra Trenches are associated with north-dipping Benioff zones, and the Weber Deep is associated with a west-dipping Benioff zone at which compression between the

plates is absorbed. Where continents are part of the northern margin of the Australian Plate, the earthquake pattern is rather diffuse, and a complex mountain-building system is present (e.g. New Guinea and the Himalayas).

The extent to which plate tectonics has influenced the Tertiary geological history of New Guinea is best investigated by attempting to correlate the observed geology with given tectonic models. As a basic premise, Papua New Guinea can be considered as a zone of interaction or subduction between the north-moving Australian Plate and the west-moving Pacific Plate. Le Pichon (1968) computed that differential west-southwest strike-slip motion between these two plates is 9 to 11 cm/year, and the half-rate of northward sea-floor spreading from the Australia-Antarctica Ridge is about 3 cm/year. Because there is no 'sink' around Antarctica, it is necessary to postulate that the Australia-Antarctica Ridge is itself migrating north, and that the Australian Plate is moving north at 6 cm/year. Le Pichon (1968) concluded from a global synthesis that the major 'sinks' at the northern part of the Australian Plate have
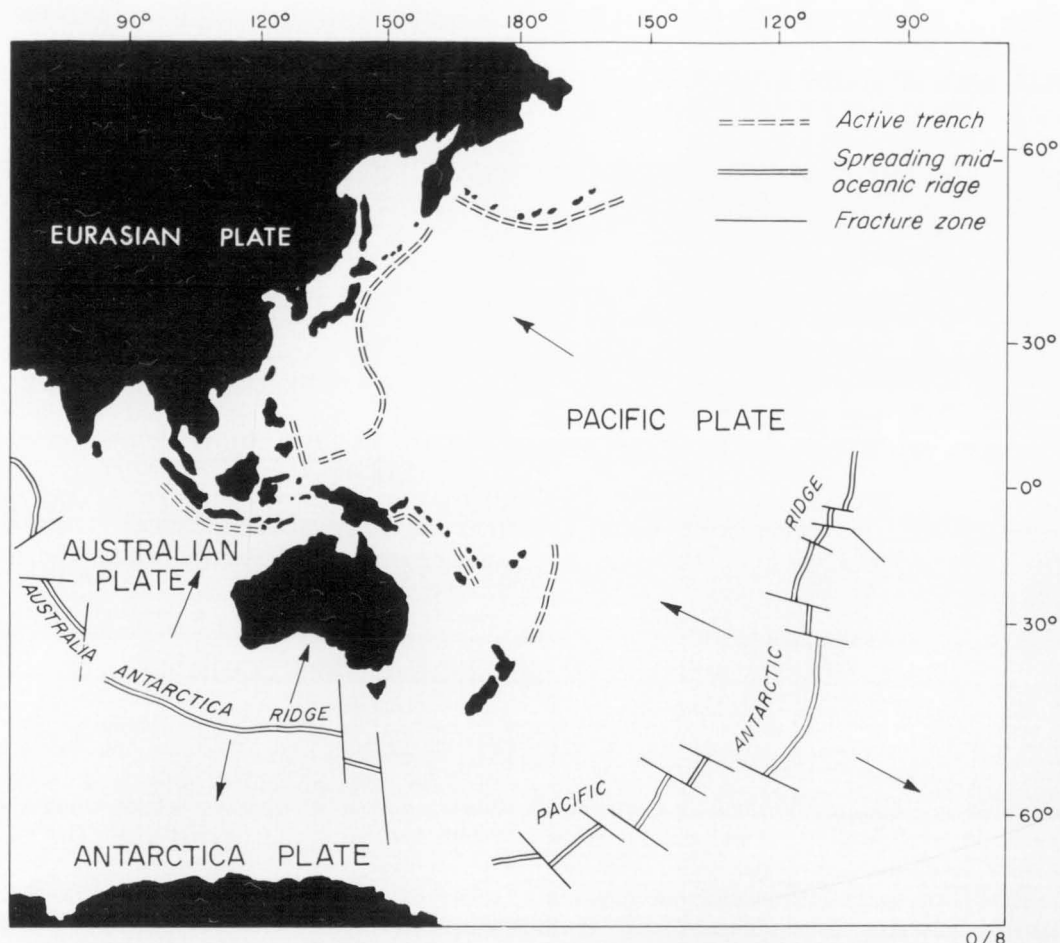
Fig. 45. Present-day features of the plate tectonic model around Australia.

been in existence for periods several times longer than the life of the present mid-oceanic ridges. Thus the New Britain and Java Trenches have probably been active sites for the consumption of the Australian Plate at least since the Early Tertiary. Relative to the present position (Fig. 45) of the Indonesian-Melanesian volcanic arc, New Guinea appears to have intersected and moved across the east-west-trending Indonesian-Melanesian subduction zone during the last 15 to 20 m.y. (cf. Figs. 45 and 46; spreading data from Heirtzler et al., 1968). The assumption underlying Figure 46 is that the Indonesian-Melanesian arc has had little north-south movement since the Miocene, and that Antarctica is also fixed.

A number of recent workers (Hamilton, 1969; Dickinson, 1970; Moores, 1970) have argued that granitic batholith belts represent the plutonic phase of arc volcanism, and that some such belts may be identifiable with fossil subduction zones. The Miocene magmatic front represented by the intrusives and volcanics in the New Guinea Mobile Belt (Plate 1) is partly in accord with such an interpretation. On the basis of this model, the triggering mechanism for the Miocene intrusive belt could have been the collision of New Guinea with the Indonesian-Melanesian subduction zone; according to the model illustrated by Figures 45 and 46, the postulated collision would have taken place in the Miocene. Predict-
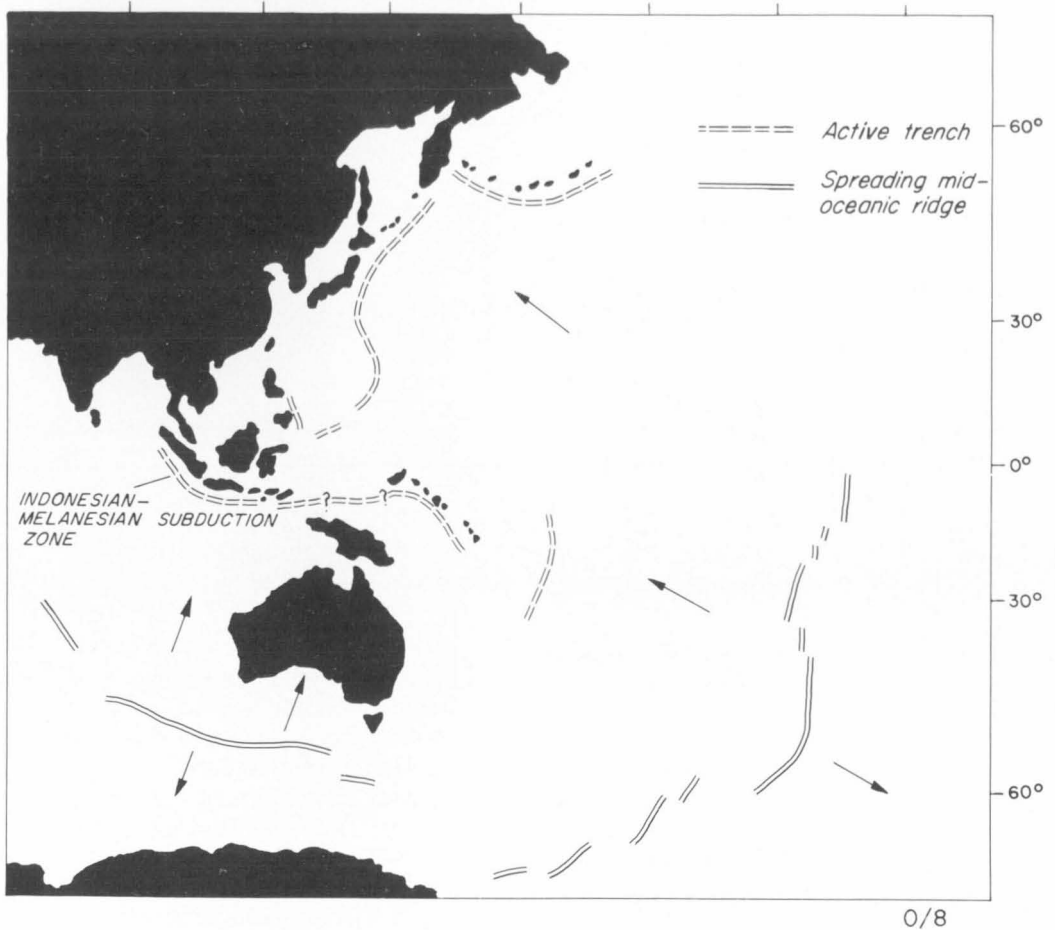
Fig. 46. Approximate situation of Australia and New Guinea about 20 m.y. ago.

ably, the sedimentation in the Papuan Geosyncline also ended in Miocene time, and major uplift of the region began. The above model may also explain the presence of elongate ultramafic pods and glaucophane schist complexes which occur in the New Guinea highlands (Dow et al. 1972) and in Irian Jaya (Visser & Hermes, 1962). Blake, Irwin, & Coleman (1969), Dewey & Horsfield (1970), Hamilton (1970), and Moores (1970) consider that such metamorphic belts and ultramafic complexes may closely represent the ancient fossilized sites of lithosphere consumption.

The nature and orientation (polarity) of the Tertiary subduction zone and the site of lithosphere consumption remain speculative, but there would appear to be two general alternatives; either a south-dipping or north-dipping Benioff zone could have existed. If there was a south-dipping Benioff zone (dipping under New Guinea) in the Tertiary (Fig 47-A), then the Australia-New Guinea 'continent' may have overridden it (Fig. 47-B) in a manner analogous to that of the western North American continent, which is thought to have overridden a trench in the late Mesozoic (Hamilton, 1969). Before it overrode the Benioff zone, New Guinea would have been a western Pacific island arc which was associated with the generation of calc-alkaline magma from the region of the Benioff zone in the descending Pacific Plate.

A LOWER MIOCENE

B MIOCENE TO PRESENT DAY

Oceanic Crust

Continental Crust

Upper Mantle

Intermediate-basic
volcanic rocks

Intermediate-basic
intrusive rocks

Westward moving
Pacific Plate

Lithosphere
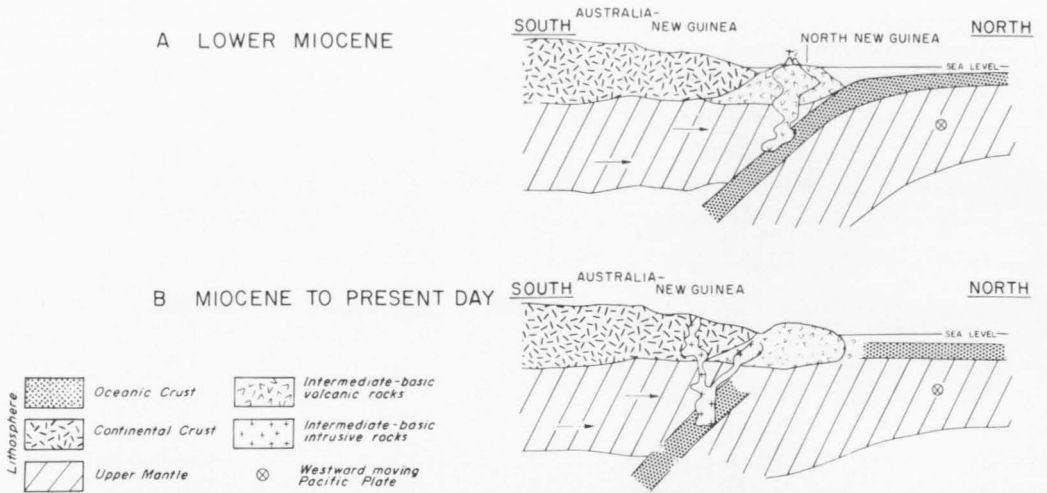
P/A/505

Fig. 47. Cross-sections of hypothetical south-dipping Benioff zone in New Guinea.

The other and preferred alternative is that a north-dipping Benioff zone may have operated during the Tertiary (as it is today in the active Java-Sumatra and New Britain Trenches), and consumption of oceanic lithosphere would have taken place ahead of the north-moving Australia-New Guinea continental mass (Fig. 48-A). This model is preferred because it is consistent with the present-day polarity of the Indonesian-Melanesian Benioff zones, and it may be used to explain the absence of both a deep oceanic trench and present-day calc-alkaline volcanism (on the basis of its supposed origin) in New Guinea; volcanism is restricted to the offshore islands of the New Britain Arc to the north and east, where no continental interaction has occurred.

With their relative distribution, ages, and low Sr^{87}/Sr^{86} ratios, the Miocene plutonic rocks of the Central Highlands may represent the eroded root of the Miocene volcanic belt, which was described by Dow et al. (1972) and Dow & Bain (1970). Because of the relatively abrupt development and short duration of this igneous activity (see section 3), the rocks are probably not typical of those developed in island-arc environments. It is considered more likely that the dramatic but short-

lived Miocene plutonic and volcanic activity was caused by the convergence of, and climaxed by, the ultimate collision between the northward-moving Australian continent and the Indonesian-Melanesian subduction zone. Dewey & Horsfield (1970) and Dewey & Bird (1970) postulated that New Guinea represents a mid-Tertiary Australian continent/island-arc collision. This is consistent with the model presented here, and, as outlined in section 2, it is conceivable that the basement volcanic rocks of the coastal range of north New Guinea represent a pre-Miocene volcanic arc that was an active part of the Indonesian-Melanesian Arc at that time.

A Miocene north-dipping Benioff zone between southern New Guinea and what is now the North Coast Range coastal range is postulated (Fig. 48-A). Carey (1938) noted the long topographic depressions of the Meervlakte-Sepik-Ramu-Markham regions, between the North Coast Range and the Main Cordillera, and he drew attention to the possibility that the depression may be the westward expression of the New Britain Trench. This major elongate depression may represent the overridden or fossilized trench (subduction zone) which lay north of the Australia-New Guinea continent in pre-Miocene times. Another possibility is that

A LOWER TERTIARY NEW GUINEA

B MIOCENE NEW GUINEA

C PRESENT-DAY NEW GUINEA
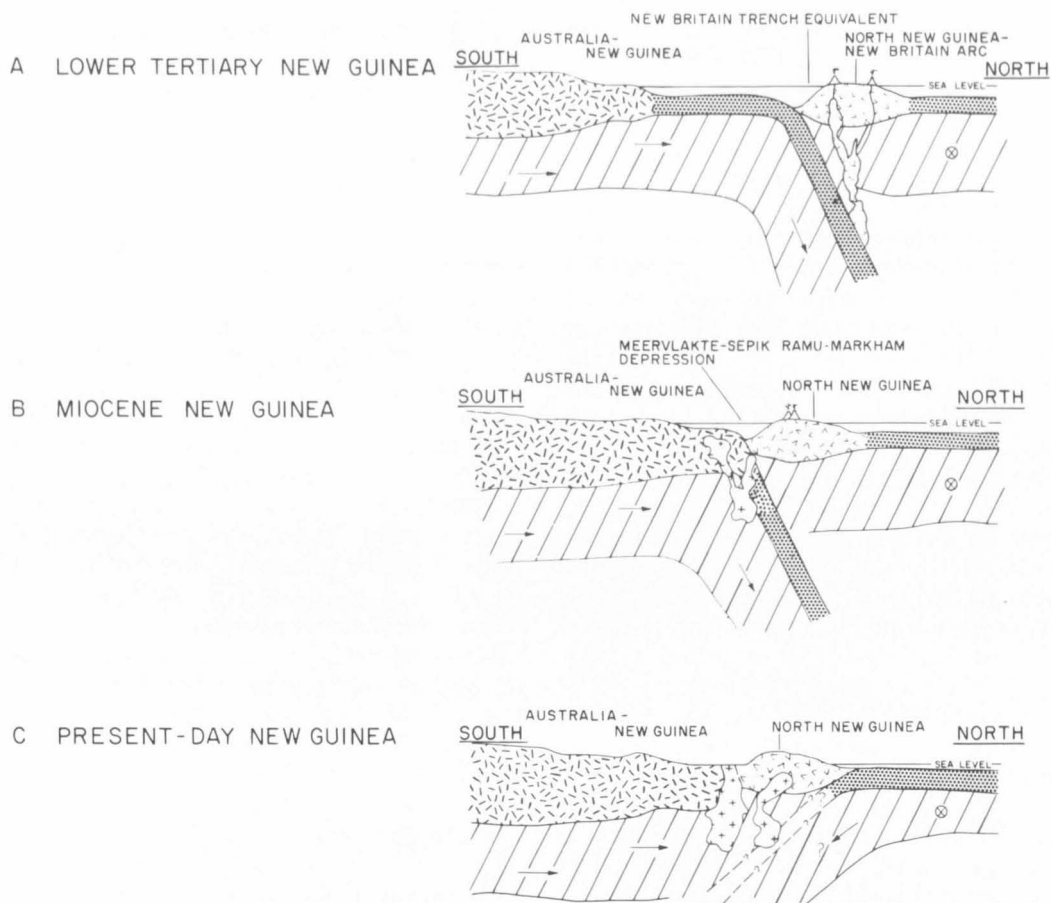
P/A/505

Fig. 48. Cross-sections of hypothetical north-dipping Benioff zone in New Guinea.

the ultramafic and blueschist facies complexes in the Central Highlands represent the approximate site of lithosphere consumption, but, until further detailed mapping and geochemistry are carried out, these suggestions remain entirely speculative.

As discussed in section 6, calc-alkaline magmas are believed to be generated near the Benioff zone in the descending lithospheric plate. The development of massive Miocene calc-alkaline rocks in New Guinea as a result of the postulated collision between the Australia-New Guinea continent and either the Indonesian-Melanesian subduction zone or the island arc of North New Guinea, or both, requires magma generation on the continental (southern) side of the subduction zone (Fig. 48-B),

that is, on the side opposite to that of the north-dipping descending plate. Because this mechanism of magma generation is somewhat different from that believed to occur at or above the Benioff zone in normal calc-alkaline island-arc environments, it might be expected that detailed petrological study of the Miocene plutonic rocks in New Guinea will reveal a rather different character than the usual calc-alkaline series.

The present-day diffuse seismic pattern for the New Guinea mainland (Denham 1969; Johnson, 1970) may be explained by the 'flipping' models discussed by McKenzie (1969), Dewey & Horsfield (1970), Dewey & Bird (1970), and Moores (1970). As the leading edge of the north-moving Australian continent, Miocene New Guinea could have

attempted to underthrust the proposed North New Guinea-New Britain island arc (Fig. 48-B); this is today happening in New Britain and Java. However, buoyancy of the Australia-New Guinea continental mass would prevent much underthrusting. The diffuse earthquake pattern beneath the New Guinea mainland may result from continued plate convergence, which would lead to interfingering with crumpling, overlap, and mountain-building near the plate junction. The 'flipping' model (McKenzie, 1969) predicts that the arrested continental underthrusting would lead to a change in the direction of thrusting, such that lithosphere would begin to be consumed from the oceanic side (Fig. 48-C). That this model may be valid is supported by earthquake focal mechanisms (Fitch, 1970; Johnson & Molnar, 1972) which indicate underthrusting of the Pacific Plate beneath northwestern New Guinea.

One complexity in the island-arc tectonics of the New Guinea region comes from the accumulating evidence that the island of New Guinea may have been rotated sinistrally from a position east of Queensland to its present position north of Australia. This concept originated with du Toit (1937), and gained support from Carey (1958) as part of his Melanesian Shear System. Tectonic analysis of the southwest Pacific (Cullen, 1970), and consideration of structural alignments and lithological comparisons between New Guinea and Queensland (Rod, 1966), have also supported anticlockwise rotation of New Guinea. The

geology of Papua (Davies & Smith, 1971) also lends support to the rotation hypothesis. Recent seismic refraction and bathymetric studies in the Coral Sea (Ewing, Hawkins, & Ludwig, 1970; Gardner, 1970) suggest that the Coral Sea Basin is normal oceanic crust on which an average of only 1.5 km of sediment has been deposited. Using conservative sedimentation rates, Gardner (1970) concluded that this basin formed no earlier than late Eocene to early Oligocene. Analysis of magnetic data (Falvey, quoted by Gardener, 1970) reveals a fan-shaped distribution of linear magnetic anomalies with an extrapolated apex in the Gulf of Papua. Thus, the magnetic data also support anticlockwise rotational movement of New Guinea with respect to the Queensland coast. Tentative palaeomagnetic results from New Guinea (Green & Pitt, 1967) are consistent with the postulated anticlockwise rotation of the island. It seems likely that the various west-northwest-trending sinistral transcurrent fault zones throughout New Guinea (Krause, 1965; Dow et al., 1972) may have accommodated some of the stress associated with the rotational movement. It is noted that rotation of New Guinea in the manner described could well account for the development of the Papaun Ultramafic Belt (Davies, 1968) as an overthrust sheet of oceanic crust upon the sinistrally rotated Papuan peninsula. Comparisons of palaeomagnetic and further dating studies between the Central Highlands, North Coast Range, New Britain, and Papua are needed to test these ideas further and help resolve the geological history of this complex region.

9. REFERENCES

ABELE, C., & PAGE, R. W., 1974—Stratigraphic and isotopic ages of Tertiary basalts at Maude and Airey's Inlet, Victoria, Australia. *Proc. roy. Soc. Vic.*, 86(2), 143-50.

ADAMS, C. G., 1968—A revision of the foraminiferal genus *Austrotrillina* Parr. *Bull. Brit. Mus. (nat. Hist.) Geol.*, 16, 73-97.

ADAMS, C. G., 1970—Tropical Indo-Pacific zonation based on larger foraminifera. *Bull. Brit. Mus. (nat. Hist.) Geol.*, 19.

ALDRICH, L. T., WETHERILL, G. W., TILTON, G. R., & DAVIS, G. L., 1956—Half life of Rb87. *Phys. Rev.*, 103, 1045-7.

ALDRICH, L. T., & WETHERILL, G. W., 1958—Geochronology by radioactive decay. *Ann. Rev. nucl. Sci.*, 8, 257-98.

ARMSTRONG, R. L., 1966—K-Ar dating of plutonic and volcanic rocks in orogenic belts. *In* SCHAEFFER, O. A., & ZAEHRINGER, J., (*Eds*)— POTASSIUM-ARGON DATING. *New York, Springer-Verlag*, 117-33.

ARMSTRONG, R. L., 1968—A model for the evolution of strontium and lead isotopes in a dynamic earth. *Geophys. Rev.*, 175-99.

ARMSTRONG, R. L., & COOPER, J. A., 1971—Lead isotopes in island arcs. *Bull. volcanol.*, 35(1), 27-63.

ARMSTRONG, R. L., JAEGER, E., & EBERHARDT, P., 1966—A comparison of K-Ar and Rb-Sr ages on Alpine biotites. *Earth planet. Sci. Lett.*, 1, 13-9.

ARRIENS, P. A., & COMPSTON, W., 1968—A method for isotopic ratio measurement by voltage peak switching, and its application with digital output. *Int. J. Mass Spectrom. Ion Phys.*, 1, 471-81.

APC, 1961—The geological results of petroleum exploration in Western Papua 1937-1961. *J. geol. Soc. Aust.*, 8, 1-133.

BAIN, J. H. C., 1967—Schrader Range, New Guinea—reconnaissance geology. *Bur. Miner. Resour. Aust. Rec.* 1967/94 (unpubl.).

BAIN, J. H. C., 1973—A summary of the main structural elements of Papua New Guinea. *In* COLEMAN, P. J., (*Ed.*)—THE WESTERN PACIFIC: ISLAND ARCS, MARGINAL SEAS, GEOCHEMISTRY. *Perth, Univ. W. Aust. Press*, 147-61.

BAIN, J. H. C., MACKENZIE, D. E., & RYBURN, R. J., in press—Geology of the Kubor Anticline, Central Highlands of New Guinea. *Bur. Miner. Resour. Aust. Bull.* 155.

BANDY, O. L., 1964—Cenozoic planktonic foraminiferal zonation. *Micropaleontology*, 10, 1-17

BANDY, O. L., 1966—Restrictions of the 'Orbulina' datum. *Micropaleontology*, 12, 79-86.

BANDY, O. L., & INGLE, J. C., 1970—Neogene planktonic events and radiometric scale, California. *Geol. Soc. Am. spec. Pap.* 124, 131-72.

BANNER, F. T., & BLOW, W. H., 1965—Progress in the planktonic foraminiferal biostratigraphy of the Neogene. *Nature*, 208, 1164-6.

BANNER, F. T., & EAMES, F. E., 1966—Recent progress in world-wide stratigraphical correlation. *Earth-Sci. Rev.*, 2, 157-79.

BARAZANGI, M., & DORMAN, J., 1969—World seismicity maps compiled from ESSA, coast and geodetic survey, epicenter data, 1961-1967. *Bull seim. Soc. Am.*, 59, 369-80.

BECKINSALE, R. D., & GALE, N. H., 1969—A reappraisal of the decay constants and branching ratio of K40. *Earth planet. Sci. Lett.*, 6, 289-94.

BELFORD, D. J., 1962—Miocene and Pliocene planktonic foraminifera, Papua-New Guinea. *Bur. Miner. Resour. Aust. Bull.* 62.

BERGGREN, W. A., 1969a—Rates of evolution in some Cenozoic planktonic foraminifera. *Micropaleontology*, 15, 351-65.

BERGGREN, W. A., 1969b—Cenozoic chronostratigraphy, planktonic foraminiferal zonation and the radiometric time scale. *Nature*, 224, 1072-5.

BERGGREN, W. A., 1971—Neogene chronostratigraphy, planktonic foraminiferal zonation and the radiometric time scale. *Geol. Soc. Hungary Bull.* 101, 162-9.

BEYRICH, H. E. von, 1854—Ueber die Stellung der hessischen Tertiärbildungen. *Kgl. preuss. Akad. Wiss., Berlin, Monatsber.*, Nov. 1854, 664-6.

BLAKE, M. C., Jr, IRWIN, W. P., & COLEMAN, R. G., 1969—Blueschist-facies metamorphism related to regional thrust faulting. *Tectonophysics*, 8, 237-46.

BLOW, W. H., 1969—Late middle Eocene to Recent planktonic foraminiferal biostratigraphy. *Proc. 1st int. Conf., planktonic microfossils, Geneva, 1967*, 199-422. *Leiden, E. J. Brill*.

BOUT, P., FRECHEN, J., & LIPPOLT, H. J., 1966—Datations stratigraphiques et radiochronologiques de quelques coulées basaltiques de Limagne. *Revue d'Auvergne*, 80, 207-31.

BOWEN, N. L., 1928—THE EVOLUTION OF THE IGNEOUS ROCKS. *Princeton, Princeton University Press*.

BROOKS, J. A., 1969a—Rayleigh waves in southern New Guinea: II. A shear velocity profile. *Bull. seism. Soc. Am.*, 59, 2017-38.

BROOKS, J. A., 1969b—Rayleigh wave dispersion studies of crustal and upper mantle structure in New Guinea. *Ph.D. thesis, Univ. of Tasmania, Hobart* (unpubl.).

BROOKS, J. A., & RIPPER, I. D., 1966—Proposed investigations of crustal structure in New Guinea. *Bur. Miner. Resour. Aust. Rec.* 1966/33 (unpubl.).

BURNETT, D. S., LIPPOLT, H. J., & WASSERBURG, D. J., 1966—The relative isotopic abundance of K40 in terrestrial and meteoritic samples. *J. geophys. Res.*, 71, 1249-69.

CAREY, S. W., 1938—The morphology of New Guinea. *Aust. Geogr.*, 3, 3-31.

CAREY, S. W., 1958—The tectonic approach to continental drift. *Continental Drift Symp., Univ. of Tasmania*, 177-355.

CAREY, S. W., 1965—Tectonics of New Guinea (abstr.). *38th ANZAAS Congr., Hobart*.

CARTER, A. N., 1964—Tertiary foraminifera from Gippsland, Victoria and their stratigraphic significance. *Geol. Surv. Vic. Mem.* 23, 1-154.

CASEY, R., 1964—The Cretaceous Period. *In* HARLAND, W. B., SMITH, A. G., & WILCOCK, B. (Eds.)—The Phanerozoic time-scale. *Quart. J. geol. Soc. Lond.*, 120S, 193-202.

CHARLOT, R., CHOUBERT, G., FAURE-MURET, A., HOTTINGER, L., MARÇAIS, J., & TISSERANT, D., 1967—Note au sujet de l'age isotopique de la limite Miocène-Pliocène au Maroc. *C. R. Acad. Sci. Paris* 264, 222-4.

CHRISTENSEN, N. I., 1970—Composition and evolution of the oceanic crust. *Marine Geol.*, 8, 139-54.

CITA, M. B., & BLOW, W. H., 1969—The biostratigraphy of the Langhian, Serravallian and Tortonian stages in the type sections in Italy. *Riv. ital. paleont.*, 75, 549-603.

CLARKE, W. J., & BLOW, W. H., 1969—The interrelationships of some late Eocene, Oligocene and Miocene larger foraminifera and planktonic biostratigraphic indices. *Proc. 1st int. Conf., planktonic microfossils, Geneva, 1967*, 82-97. Leiden, E. J. Brill.

COMPSTON, W., ARRIENS, P. A., VERNON, M. J., & CHAPPELL, B. W., 1970—Rubidium-strontium chronology and chemistry of lunar material. *Science*, 167, 474-6.

COMPSTON, W., CHAPPELL, B. W., ARRIENS, P. A., & VERNON, M. J., 1969—On the feasibility of NBS 70a K feldspar as a Rb-Sr age reference sample. *Geochim. cosmoshim. Acta*, 33, 753-7.

COMPSTON, W., LOVERING, J. F., & VERNON, M. J., 1965—The rubidium-strontium age of the Bishopville aubrite and its component enstatite and feldspar. *Geochim. cosmochim. Acta*, 29, 1085-99.

CONEY, P. J., 1970—The geotectonic cycle of the new global tectonics. *Bull. geol. Soc. Am.*, 81, 739-48.

CONNELLY, J. B., 1974—A structural interpretation of magnetometer and seismic profiler records of the Bismarck Sea, Melanesian Archipelago. *J. geol. Soc. Aust.*, 21(4), 459-70.

COOPER, J. A., 1963—The flame photometric determination of potassium in geological materials used for potassium-argon dating. *Geochim. cosmochim. Acta*, 27, 525-46.

COOPER, J. A., MARTIN, I. D., & VERNON, M. J., 1966—Evaluation of rubidium and iron bias in flame photometric potassium determination for K-Ar dating. *Geochim. cosmochim. Acta*, 30, 197-205.

CRESPIN, I., & BELFORD, D. J., 1957—Micropalaeontology of rock samples from the Central Highlands, New Guinea. *Bur. Miner. Resour. Aust. Rec.* 1957/91 (unpubl.).

CRESPIN, I., & STANLEY, G. A. V., 1965—Palaeontological investigations, Papua and New Guinea. A revision of the list in BMR Rep. 20, with additions to the end of 1965. *Bur. Miner. Resour. Aust. Rec.* 1965/186 (unpubl.).

CULLEN, D. J., 1970—A tectonic analysis of the south-west Pacific. *NZ J. Geol. Geophys.*, 13, 7-20.

CURTIS, J. W., 1973a—The spatial seismicity of Papua New Guinea and the Solomon Islands. *J. geol. Soc. Aust.*, 20(1), 1-20.

CURTIS, J. W., 1973b—Plate tectonics of the Papua-New Guinea-Solomon Islands region. *J. geol. Soc. Aust.*, 20(1), 21-36.

DALRYMPLE, G. B., & LANPHERE, M. A. 1969—POTASSIUM-ARGON DATING. San Francisco, Freeman.

DAMON, P. E., 1968—Potassium-argon dating of igneous and metamorphic rocks with applications to the Basin ranges of Arizona and Sonora. *In* HAMILTON, E. J., & FARQUHAR, R. M. (Eds.)—RADIOMETRIC DATING FOR GEOLOGISTS. New York, Interscience, 1-71.

DASCH, E. J., 1969—Strontium isotopes in weathering profiles, deep-sea sediments and sedimentary rocks. *Geochim. cosmochim. Acta*, 33, 1521-52.

DASCH, E. J., ARMSTRONG, R. L., & CLABAUGH, S. E., 1969—Age of Rim Rock Dike swarm, Trans-Pecos, Texas. *Bull. geol. Soc. Am.*, 80, 1819-24.

DAVID, T. W. E., ed. BROWNE, W. R., 1950—THE GEOLOGY OF THE COMMONWEALTH OF AUSTRALIA (3 volumes). London, Arnold.

DAVIES, H. L., 1968—Papuan Ultramafic Belt. *23rd int. geol. Congr.. Prague*, 209-20.

DAVIES, H. L., 1971—Peridotite-gabbro-basalt complex in eastern Papua: an overthrust plate of oceanic mantle and crust. *Bur. Miner. Resour. Aust. Bull.* 128.

DAVIES, H. L., & SMITH, I. E., 1971—Geology of eastern Papua. *Bull. geol. Soc. Am.*, 82, 3299-312.

DEKKER, F. E., & FAULKS, I. G., 1964—The geology of the Wabag area, New Guinea. *Bur. Miner. Resour. Aust. Rec.* 1964/137 (unpubl.).

DENHAM D., 1968—Thickness of the Earth's crust in Papua-New Guinea and the British Solomon Islands. *Aust. J. Sci.*, 30, 277.

DENHAM, D., 1969—Distribution of earthquakes in the New Guinea-Solomon Islands region. *J. geophys. Res.*, 74, 4290-9.

DEWEY, J. F., & BIRD, J. M., 1970—Mountain belts and the new global tectonics. *J. geophys. Res.*, 75, 2725-47.

DEWEY, J. F., & HORSFIELD, B., 1970—Plate tectonics, orogeny and continental growth. *Nature*, 225, 521-5.

DICKINSON, W. R., 1970—Relations of andesites, granites and derivative sandstones to arctrench tectonics. *Rev. Geophys. Space Phys.*, 8, 813-60.

DOW, D. B., 1967—Lower Watut River, New Guinea—reconnaissance geology. *Bur. Miner. Resour. Aust. Rec.* 1967/73 (unpubl.).

DOW, D. B., 1969—Post-Palaeozoic volcanism in New Guinea (abstr.). *Geol. Soc. Aust. spec. Publ.* 2, 203.

DOW, D. B., & BAIN, J. H. C., 1970—A Miocene volcanic arc in New Guinea (abstr.). *42nd ANZAAS Congr., Port Moresby*.

DOW. D. B., & DAVIES, H. L., 1964—The geology of the Bowutu Mountains, New Guinea. *Bur. Miner. Resour. Aust. Rep.* 75.

DOW, D. B., & DEKKER, F. E., 1964—The geology of the Bismarck Mountains, New Guinea. *Bur. Miner. Resour. Aust. Rep.* 76.

DOW, D. B., & PLANE, M. D., 1965—The geology of the Kainantu Goldfields. *Bur. Miner. Resour. Aust. Rep.* 79.

Dow, D. B., Smit, J. A. J., Bain, J. H. C., & Ryburn, R. J., 1972— Geology of the south Sepik region, New Guinea. *Bur. Miner. Resour. Aust. Bull.* 133.

Dow, D. B., Smit, J. A. J., & Page, R. W., 1974 —Wau, Papua New Guinea—1:250 000 Geological Series. *Bur. Miner. Resour. Aust. explan. Notes* SB/55-14.

Doyle, H. A., & Webb, J. P., 1963—Travel times to Australian stations from Pacific nuclear explosions in 1958. *J. geophys. Res.*, 68, 1115-20.

Drooger, C. W., 1956—Transatlantic correlation of the Oligo-Miocene by means of foraminifera. *Micropaleontology*, 2, 183-92.

Drooger, C. W., 1964—Problems of mid-Tertiary stratigraphic interpretation. *Micropaleontology*, 10, 369-74.

Drooger, C. W., 1966—Zonation of the Miocene by means of planktonic foraminifera—a review and some comments. *Proc. III sess. Comm. Medit. Neocene Strat.*, Berne, 1964, 40-50. *Leiden, E. J. Brill.*

du Toit, A. L., 1937—our wandering continents. *Edinburgh, Oliver and Boyd.*

Dymond. J. R., 1966—Potassium-argon geochronology of deep-sea sediments. *Science*, 152, 1239-41.

Eames, F. E., Banner, F. T., Blow, W. H., & Clarke, W. J., 1962—fundamentals of mid-tertiary stratigraphical correlation. *Camb. Univ. Press.*

Edwards, A. B., & Glaessner, M. F., 1953— Mesozoic and Tertiary sediments from the Waghi Valley, New Guinea. *Proc. roy. Soc. Vic.*, 64, 93-118.

Engels, J. C., & Ingamells, C. O., 1970—Effect of the sample inhomogeneity in K-Ar dating. *Geochim. cosmochim. Acta*, 34, 1007-18.

Ernst, W. G., 1970—Tectonic contact between the Franciscan Melange and the Great Valley Sequence—crustal expression of a late Mesozoic Benioff zone. *J. geophys. Res.*, 75, 886-901.

Evernden, J. F., & Curtis, G. H., 1965—The potassium-argon dating of the late Cenozoic rocks in East Africa and Italy. *Curr. Anthrop.*, 6, 343-85.

Evernden, J. F., Curtis, G. H., Obradovich, J., & Kistler, R., 1961—On the evaluation of glauconite and illite for dating sedimentary rocks by the potassium-argon method. *Geochim. cosmochim. Acta*, 23, 78-99.

Evernden, J. F., Savage, D. E., Curtis, G. H., & James, G. T., 1964—Potassium-argon dates and the Cenozoic mammalian chronology of North America. *Amer. J. Sci.*, 262, 145-98.

Ewart, A., & Stipp, J. J., 1968—Petrogenesis of the volcanic rocks of the central North Island, New Zealand, as indicated by a study of Sr^{87}/Sr^{86} ratios and Sr, Rb, K, U and Th abundances. *Geochim. cosmochim. Acta*, 32, 699-736.

Ewing, M., Hawkins, L. V., & Ludwig, W. J., 1970—Crustal structure of the Coral Sea. *J. geophys. Res.*, 75, 1953-62.

Faure, G., & Hurley, P. M., 1963—The isotopic composition of strontium in oceanic and continental basalts: application to the origin of igneous rocks. *J. Petrol.*, 4, 31-50.

Finlayson, D. M., & Cull, J. P., 1973—Structural profiles in the New Britain–New Ireland region. *J. geol. Soc. Aust.*, 20(1), 37-48.

Fisher, N. H., 1944—Outline of the geology of the Morobe Goldfields. *Proc. roy. Soc. Qld*, 55(4), 51-8.

Fitch, T. J., 1970—Earthquake mechanisms and island arc tectonics in the Indonesian-Philippine region. *Bull. seism. Soc. Am.*, 60, 565-91.

Fleming, C. A., (Ed.), 1959—Oceania, Fascicule 4: New Zealand. *Lex. strat. int., CNRS, Paris.*

Francis, E. H., & Woodland, A. W., 1964—The Carboniferous Period. *In* Harland, W. B., Smith, A. G., & Wilcock, B. (Eds.)—The Phanerozoic time scale. *Quart. J. geol. Soc. Lond.*, 120S, 221-32.

Frechen, J. von, & Lippolt, H. J., 1965—Kalium-argon-daten zum alter des laacher vulkanismus, der Rheinterrassen und der Eiszeiten. *Eiszeitalter und Gegenwart*, 16, 5-30.

Funnell, B. M., 1964—The Tertiary Period. *In* Harland, W. B., Smith, A. G., & Wilcock, B. (Eds.)—The Phanerozoic time scale. *Quart. J. geol. Soc. Lond.*, 120S, 179-91.

Furumoto, A. S., Hussong, D. M., Campbell, J. F., Sutton, G. H., Malahoff, A., Rose, J. C., & Woollard, G. P., 1970—Crustal and upper mantle structure of the Solomon Islands as revealed by seismic refraction survey of November-December, 1966. *Pacif. Sci.*, 24, 315-32.

Gardner, J. V., 1970—Submarine geology of the western Coral Sea. *Bull. geol. Soc. Am.*, 81, 2599-614.

Gast, P. W., 1967—Isotope geochemistry of volcanic rocks. *In* Hess, H. H., & Poldevaart, A., (Eds.)—basalts, vol. 1. *New York, Interscience.*

Gerling, E. K., Levskiy, L. K., & Morozova, I. M., 1963—On the diffusion of radiogenic argon from minerals. *Gechem. int.*, 6, 551.

Gill, J. B., 1970—Geochemistry of Viti Levu, Fiji, and its evolution as an island arc. *Contr. Miner. Petrol.*, 27, 179-203.

Gill, J. B., & McDougall, I., 1973—Biostratigraphic and geological significance of Miocene-Pliocene volcanism in Fiji. *Nature*, 241, 176-80.

Gilluly, J., 1955—Geological contrasts between continents and ocean basins. *Geol. Soc. Am. spec. Pap.* 62, 7-11.

Glaessner, M. F., 1943—Problems of stratigraphic correlation in the Indo-Pacific region. *Proc. roy. Soc. Vic.*, 55, 41-80.

Glaessner, M. F., 1950—Geotectonic position of New Guinea. *Bull. Am. Assoc. Petrol. Geol.*, 34, 856-81.

Glaessner, M. F., 1952—Geology of Port Moresby, Papua. *Sir Douglas Mawson anniv. Vol., Univ. Adelaide*, 63-86.

Glaessner, M. F., 1953—Time-stratigraphy and the Miocene epoch. *Bull. geol. Soc. Am.*, 64, 647-58.

Glaessner, M. F., 1959—Tertiary stratigraphic correlation in the Indo-Pacific region and Australia. *J. geol. Soc. India*, 1, 53-67.

Glaessner, M. F., 1960—West-Pacific stratigraphic correlation. *Nature*, 186, 1039-40.

GLAESSNER, M. F., 1967—Time scales and Tertiary correlations. *In* Tertiary correlations and climatic changes in the Pacific. *11th Pacif. Sci. Congr., Tokyo, 1966, Symposium 25,* 1-5.

GLAESSNER, M. F., LLEWELLYN, K. M., & STANLEY, G. A. V., 1950—Fossiliferous rocks of Permian age from the Territory of New Guinea. *Aust. J. Sci.,* 13, 24-5.

GLANGEAUD, L., 1957—Les éruptions souslacustres d'âge stampien supérieur du plateau de Gergovie. *C.R. Acad. Sci. Paris,* 245(3), 338.

GRAINGER, D. J., & TINGEY, R. J., 1976—Markham, Papua New Guinea—1:250 000 Geological Series. *Bur. Miner. Resour. Aust. explan. Notes* SB/55-10.

GREEN, R., & PITT, R. P. B., 1967—Suggested rotation of New Guinea. *J. Geomag. Geoelect.,* 19, 317-21.

GREEN, T. H., & RINGWOOD, A. E., 1966—Origin of the calc-alkaline igneous rock suite. *Earth planet. Sci. Lett.,* 1, 307-16.

GREEN, T. H., & RINGWOOD, A. E., 1968—Genesis of the calc-alkaline igneous rock suite. *Contr. Miner. Petrol.,* 18, 105-62.

GUTENBURG, B., & RICHTER, C. F., 1954—SEISMICITY OF THE EARTH, 2nd ed. *Princeton, Princeton Univ. Press.*

HAMILTON, E. I., 1965—APPLIED GEOCHRONOLOGY. *London, Academic Press.*

HAMILTON, W., 1966—Origin of the volcanic rocks of eugeosynclines and island arcs. *Geol. Surv. Canada Pap.* 66-15, 348-56.

HAMILTON, W., 1969—Mesozoic California and the underflow of Pacific mantle. *Bull. geol. Soc. Am.,* 80, 2409-30.

HAMILTON, W., 1970—Tectonic map of Indonesia —a progress report. *US geol. Surv. open File Rep.* (IR) IND-5.

HANSON, G. N., & GAST, A. W., 1967—Kinetic studies in contact metamorphic zones. *Geochim. cosmochim. Acta,* 31, 1119-53.

HARDING, R. R., 1969—Catalogue of age determinations on Australian rocks, 1962-1965. *Bur. Miner. Resour. Aust. Rep.* 117.

HARRISON, J., 1969—Review of the sedimentary history of the island of New Guinea. *APEA J.,* 9, 41-8.

HART, S. R., 1964—The petrography and isotopic-mineral age relations of a contact zone in the Front Range, Colorado. *J. Geol.,* 72, 493-525.

HART, S. R., 1969—Isotope geochemistry of crust-mantle processes. *In* HART, P. J. (Ed.)— GEOPHYSICAL MONOGRAPH 13: THE EARTH'S CRUST AND UPPER MANTLE. *Washington, Am. geophys. Un.,* 58-62.

HAYATSU, A., & CARMICHAEL, C. M., 1970—K-Ar isochron method and initial argon ratios. *Earth planet. Sci. Lett.,* 8, 71-6.

HAYS, J. D., SAITO, T., OPDYKE, N. D., & BURCKLE, L. H., 1969—Pliocene-Pleistocene sediments of the equatorial Pacific: their paleomagnetic, biostratigraphic, and climatic record. *Bull. geol. Soc. Am.,* 80, 1481-514.

HEDGE, C. E., HILDRETH, R. A., & HENDERSON, W. T., 1970—Strontium isotopes in some Cenozoic lavas from Oregon and Washington. *Earth planet. Sci. Lett.,* 8, 434-8.

HEDGE, C. E., & KNIGHT, R. J., 1969—Lead and strontium isotopes in volcanic rocks from northern Honshu, Japan. *Geochem. J.,* 3, 15-24.

HEDGE, C. E., & PETERMAN, Z. E., 1970—The strontium isotopic composition of basalts from the Gordo and Juan de Fuca Rises, northeastern Pacific Ocean. *Contr. Miner. Petrol.,* 27, 114-20.

HEIRTZLER, J. R., DICKSON, G. O., HERRON, E. M., PITMAN, W. C., & LE PICHON, X., 1968— Marine magnetic anomalies, geomagnetic field reversals, and motions of the ocean floor and continents. *J. geophys. Res.,* 73, 2119-36.

HESS, H. H., 1948—Major structural features of the western North Pacific, an interpretation of H.O. 5485 bathymetric chart, Korea to New Guinea. *Bull. geol. Soc. Am.,* 59, 417-45.

HORNIBROOK, N. de B., 1968—A handbook of New Zealand microfossils (Foraminifera and Ostracoda). *NZ Geol. Surv. Handbook, NZ Dept Sci. indust. Res. Inf. Ser.,* 62.

HOWARTH, M. K., 1964— The Jurassic Period. *In* HARLAND, W. B., SMITH, A. G., & WILCOCK, B., (Eds.)—The Phanerozoic time scale. *Quart J. geol. Soc. Lond.,* 120S, 203-5.

HURLEY, P. M., HUGHES, H., FAURE, G., FAIRBAIRN, H. W., & PINSON, W. H., 1962—Radiogenic strontium-87 model of continent formation. *J. geophys. Res.,* 67, 5315-34.

ISACKS, B., & MOLNAR, P., 1971—Distribution of stresses in descending lithosphere from a global survey of focal-mechanism solutions of mantle earthquakes. *Rev. Geophys. Space Phys.,* 9, 103-74.

ISACKS, B., OLIVER, J., & SYKES, L. R., 1968— Seismology and the new global tectonics. *J. geophys. Res.,* 73, 5855-99.

JAKES, P., & WHITE, A. J. R., 1969—Structure of the Melanesian arcs and correlation with distribution of magma types. *Tectonophysics,* 8, 223-36.

JENKINS, D. G., 1965—Planktonic foraminifera and Tertiary intercontinental correlations. *Micropaleontology,* 11, 265-77.

JENKINS, D. G., 1966—Planktonic foraminifera datum planes in the Pacific and Trinidad Tertiary. *NZ J. Geol. Geophys.,* 9, 424-7.

JOHNSON, R. W., 1970—Seismicity in the Bismarck Volcanic Arc. *Bur. Miner. Resour. Aust. Rec.* 1970/35 (unpubl.).

JOHNSON, T., & MOLNAR, P., 1972—Focal mechanisms and plate tectonics of the southwest Pacific. *J. geophys. Res.,* 77, 5000-32.

KRAUSE, D. C., 1965—Submarine geology north of New Guinea. *Bull. geol. Soc. Am.,* 76, 27-42.

KRAUSE, D. C., WHITE, W. C., PIPER, D. J. W., & HEEZEN, B. C., 1970—Turbidity currents and cable breaks in the western New Britain Trench. *Bull. geol. Soc. Am.,* 81, 2153-60.

KULP, J. L., & BASSETT, W. H., 1961—The base exchange effects on potassium-argon and rubidium-strontium isotopic ages. *Ann. N.Y. Acad. Sci.,* 91, 225-6.

KULP, J. L., & ENGELS, J., 1963—Discordances in K-Ar and Rb-Sr isotopic ages. *In* RADIOACTIVE DATING. *Vienna, International Atomic Energy Agency.*

LANPHERE, M. A., & DALRYMPLE, G. B., 1967—K-Ar and Rb-Sr measurements on P-207, the USGS interlaboratory standard muscovite. *Geochim. cosmochim. Acta*, 31, 1091-4.

LE PICHON, X., 1968—Sea-floor spreading and continental drift. *J. geophys. Res.*, 73, 3661-97.

LE PICHON, X., & HEIRTZLER, J. R., 1968—Magnetic anomalies in the Indian Ocean and sea-floor spreading. *J. geophys. Res.*, 73, 2101-18.

LIPPOLT, H. J., GENTNER, W., & WIMMENAUER, W., 1963—Altersbestimmung nach der kalium-argon-methode an tertiären Eruptivgesteinen Südwestdeutschlands. *Jh. geol. Landesamt Baden-Württemburg*, 6, 507-38.

LIPPS, J. H., 1967—Planktonic foraminifera, intercontinental correlation and age of California mid-Cenozoic microfaunal stages. *J. Paleont.*, 41, 994-9.

LIPPS, J. H., 1968—Mid-Cenozoic calcareous nannoplankton from western North America. *Nature*, 218, 1151-2.

LIPSON, J., 1956—K-A dating of sediments. *Geochim. cosmochim. Acta*, 10, 149-51.

LIPSON, J., 1958—Potassium-argon dating of sedimentary rocks. *Bull. geol. Soc. Am.* 69, 137-50.

LIVINGSTON, D. E., DAMON, P. E., MAUGER, R. L., BENNETT, R., & LAUGHLIN, A. W., 1967—Argon 40 in cogenetic feldspar-mica mineral assemblages. *J. geophys. Res.*, 72, 1361-75.

LYELL, C., 1865—ELEMENTS OF GEOLOGY. London, John Murray.

MCDOUGALL, I., 1966—Precision methods of potassium-argon age determination on young rocks. *In* METHODS AND TECHNIQUES IN GEOPHYSICS, 2. London, Interscience, 279-304.

MCDOUGALL, I., ALLSOPP, H. L., & CHAMALAUN, F. H., 1966—Isotopic dating of the Newer Volcanics of Victoria, Australia, and geomagnetic polarity epochs. *J. geophys. Res.*, 71, 6107-18.

MCDUOGALL, I., & CHAMALAUN, F. H., 1969—Isotopic dating and geomagnetic polarity studies on volcanic rocks from Mauritius, Indian Ocean. *Bull. geol. Soc. Am.*, 80, 1419-42.

MCDOUGALL, I., & COOMBS, D. S., 1973—Potassium-argon ages for the Dunedin volcano and outlying volcanics. *NZ J. Geol. Geophys.*, 16, 179-88.

MCDOUGALL, I., POLACH, H. A., & STIPP, J. J., 1969—Excess radiogenic argon in young subaerial basalts from the Auckland volcanic field, New Zealand. *Geochim. cosmochim. Acta*, 33, 1485-520.

MCDOUGALL, I., & WILKINSON, J. F. G., 1967—Potassium-argon dates on some Cainozoic volcanic rocks from northeastern New South Wales. *J. geol. Soc. Aust.*, 14, 225-34.

MCINTYRE, G. A., BROOKS, C., COMPSTON, W., & TUREK, A., 1966—The statistical assessment of Rb-Sr isochrons. *J. geophys. Res.*, 71, 5459-68.

MACKAY, N. J., 1955—Geological report on a reconnaissance of the Markham and upper Ramu drainage systems, New Guinea. *Bur. Miner. Resour. Aust. Rec.* 1955/25 (unpubl.).

MACKENZIE, D. E., & CHAPPELL, B. W., 1972—Shoshonitic and calc-alkaline lavas from the highlands of Papua New Guinea. *Contr. Miner. Petrol.*, 35, 50-62.

MCKENZIE, D. P., 1969—Speculations on the consequences and causes of plate motions. *Geophys. J. Roy. astr. Soc.*, 18, 1-32.

MCMILLAN, N. J., & MALONE, E. J., 1960—The geology of the eastern central highlands of New Guinea. *Bur. Miner. Resour. Aust. Rep.* 48.

MARCHANT, S., 1969—A photogeological assessment of the petroleum geology of the northern New Guinea Basin north of the Sepik River, Territory of New Guinea. *Bur. Miner. Resour. Aust. Rep.* 130.

MARTIN, K., 1921—The age of the Tertiary sediments of Java. *B. P. Bishop Museum spec. Publ.* 7, 754-65.

MICHEL, R., 1953—Contribution a l'étude petrographique des pépérites et du volcanisme tertiare de la Grande Limagne. *Publ. Fac. Sci., Clermont Ferrand.*

MITCHELL, A. H., & READING, H. G., 1969—Continental margins, geosynclines and ocean floor spreading. *J. Geol.*, 77, 629-46.

MOHLER, W. A., 1949—Über das vorkommen von *Alveolina* und *Neoalveolina* in Borneo *Ecl. geol. Helvet.*, 41(1948), 321-9.

MOORES, E., 1970—Ultramafics and orogeny, with models of the US Cordillera and the Tethys. *Nature*, 228, 837-42.

MUSSETT, A. E., 1969—Diffusion measurements and the potassium-argon method of dating. *Geophys. J. Roy. astr. Soc.*, 18, 257-303.

MUSSETT, A. E., & DALRYMPLE, G. B., 1968—An investigation of the source of air argon contamination in K-Ar dating. *Earth planet. Sci. Lett.*, 4, 422-6.

NICOLAYSEN, L. O., 1961—Graphic interpretation of discordant age measurements on metamorphic rocks. *Ann. N.Y. Acad. Sci.*, 91, 198-206.

NIER, A. O., 1950—A redetermination of the relative abundances of the isotopes of carbon, nitrogen, oxygen, argon and potassium. *Phys. Rev.*, 77, 789-93.

NOAKES, L. C., 1938—Preliminary geological report on the Upper Watut area. *New Guinea Admin. Rep.* (unpubl.).

OSBORNE, N., 1945—The Mesozoic stratigraphy of the Fly River headwaters, Papua. *Proc. roy. Soc. Vic.*, 56, 131-49.

OSBORNE, N. A., 1966—Petroleum geology of Australian New Guinea. *Proc. 8th Comm. Min. metall. Cong.*, 5, 99-112.

OVCHINNIKOV, L. N., YUNIKOV, B. A., & METTIKH, L. I., 1961—Composition and structure of hydromicas from the Buldym deposit. *Trudy Gorno-Geol. Inst., Akad. Nauk SSSR, Ural. Filial*, 56, 3-18 (in Russian).

PAGE, R. W., 1971—The geochronology of igneous rocks in the New Guinea region. *Ph.D. thesis, Aust. Nat. Univ., Canberra* (unpubl.).

PAGE, R. W., & JOHNSON, R. W., 1974—Variation of Sr^{87}/Sr^{86} ratios in Quaternary volcanic rocks from the New Guinea-Solomon Islands region. *Lithos*, 7(2), 91-100.

PAGE, R. W., & McDOUGALL, I., 1972a—Ages of mineralization of gold and porphyry copper deposits in the New Guinea highlands. *Econ. Geol.*, 67, 1034-48.

PAGE, R. W., & McDOUGALL, I., 1972b—Geochronology of the Panguna porphyry copper deposit, Bougainville Island, New Guinea. *Econ. Geol.*, 67, 1065-74.

PATERSON, S. J., & KICINSKI, F. M., 1956—An account of the geology and petroleum prospects of the Cape Vogel Basin, Papua. *Bur. Miner. Resour. Aust. Rep.* 25, 47-70.

PATERSON, S. J., & PERRY, W. J., 1964—The geology of the upper Sepik-August River area, New Guinea. *J. geol. Soc. Aust.*, 11, 199-212.

PETERMAN, Z. E., HEDGE, C. E., COLEMAN, R. G., & SNAVELY, P. D., Jr, 1967—Sr^{87}/Sr^{86} ratios in some eugeosynclinal sedimentary rocks and their bearing on the origin of granitic magma in orogenic belts. *Earth planet. Sci. Lett.*, 2, 433-9.

PETERMAN, Z. E., LOWDER, G. G., & CARMICHAEL, I. S. E., 1970—Sr^{87}/Sr^{86} ratios of the Talasea Series, New Britain, Territory of New Guinea. *Bull. geol. Soc. Am.*, 81, 39-40.

PETERSON, J. A., 1970—Aspects of the morphology and distribution of glacial landforms of the Mt. Wilhelm area, Eastern Highlands. *42nd ANZAAS Congr., Port Moresby.*

PITT, R. P. B., 1966—Tectonics in central Papua and the adjoining part of New Guinea. *Ph.D. thesis, Univ. Tasmania, Hobart* (unpubl.).

PLANE, M. D., 1965—Geological investigation of the Yanderra copper prospect, Madang District, New Guinea. *Bur. Miner. Resour. Aust. Rec.* 1965/114 (unpubl.).

PLANE, M. D., 1967—Stratigraphy and vertebrate fauna of the Otibanda Formation, New Guinea. *Bur. Miner. Resour. Aust. Bull.* 86.

PUSHKAR, P., 1968—Strontium isotope ratios in volcanic rocks of three island arc areas. *J. geophys. Res.*, 73, 2701-14.

READ, J. R. L., 1967—Preliminary geological report on the proposed development of the upper Ramu River Gorge, New Guinea, for hydro-electric power. *Bur. Miner. Resour. Aust. Rec.* 1967/142 (unpubl.).

RICHARDS, J. R., & WILLMOTT, W. F., 1970—K-Ar age of biotites from Torres Strait. *Aust. J. Sci.*, 32, 369.

RICKWOOD, F. K., 1955—The geology of the Western Highlands of New Guinea. *J. geol. Soc. Aust.*, 2, 63-82.

RICKWOOD, F. K., 1968—The geology of western Papua. *APEA J.*, 8, 51-61.

RICKWOOD, F. K., & KENT, P. E., 1956—Report on the Pio-Purari survey, 1955. *APC Rep. LW* (unpubl.).

RINGWOOD, A. E., 1969—Composition of the crust and upper mantle. *In* HART, P. J., (Ed.)— GEOPHYSICAL MONOGRAPH 13: THE EARTH'S CRUST AND UPPER MANTLE. *Washington, Am. geophys. Un.*, 1-17.

ROD, E., 1966—Clues to ancient Australian geosutures. *Ecl. geol. Helvet.*, 59, 849-83.

RODDA, P., SNELLING, N. J., & REX, D. C., 1967— Radiometric age data on rocks from Viti Levu, Fiji. *NZ J. Geol. Geophys.*, 10, 1248-59.

RODDICK, J. C., 1970—The geochronology of the Tulameen and Hedley Complexes British Columbia. *Ph.D. thesis, Queen's University, Ontario* (unpubl.).

RODDICK, J. C., & FARRAR, E., 1971—High initial argon ratios in hornblendes. *Earth planet. Sci. Lett.*, 12, 208-14.

ROSE, J. C., WOOLLARD, G. P., & MALAHOFF, A., 1968—Marine gravity and magnetic studies of the Solomon Islands. *In* KNOPOFF, L., DRAKE, C. L., & HART, P. J. (Eds.)—GEOPHYSICAL MONOGRAPH 12: THE CRUST AND UPPER MANTLE OF THE PACIFIC AREA. *Washington, Am. geophys. Un.*

RYBURN, R. J., 1970—Glaucophane schist facies metamorphism in New Guinea (abstr.). *42nd ANZAAS Congr., Port Moresby.*

SANTO, T., 1963—Division of the Pacific area into seven regions in each of which Rayleigh waves have the same group velocities. *Bull. Earthq. Res. Inst., Univ. Tokyo*, 41, 719-41.

SANTO, T., 1970—Regional study on the characteristic seismicity of the world. Part IV: New Britain Island region. *Bull. Earthq. Res. Inst., Univ. Tokyo*, 48, 127-43.

SCOTT, G. H., 1968—Globigerinoides in the Aquitanian-Burdigalian of S.W. France. *Proc. IV Sess. Comm. Medit. Neogene Strat., Bologna, 1968*, 271-6.

SELLI, R., & TONGIORGI, E., 1967—Report of the working group: Absolute age. *4th Congr. Comm. Medit. Neogene Strat., Bologna*, 1-6 (mimeographed).

SHIELDS, W. R., GARNER, E. L., HEDGE, C. E., & GOLDICH, S. S., 1963—Survey of Rb^{85}/Rb^{87} ratios in minerals. *J. geophys. Res.*, 68, 2331-4.

SMITH, A. G., 1964—Potassium-argon decay constants and age tables. *In* HARLAND, W. B., SMITH, A. G., & WILCOCK, B., (Eds.)—The Phanerozoic time scale. *Quart. J. geol. Soc. Lond.*, 120S, 129-41.

SMITH, J. G., 1965—Orogenesis in western Papua and New Guinea. *Tectonophysics*, 2, 1-27.

SOLOMON, S., & BIEHLER, S., 1969—Crustal structure from gravity anomalies in the southwest Pacific. *J. geophys. Res.*, 74, 6696-701.

STAINFORTH, R. M., 1960—Current status of trans-Atlantic Oligo-Miocene correlation by means of planktonic foraminifera. *Rév. Micropaleont.*, 2, 219-30.

STIPP, J. J., 1968—The geochronology and petrogenesis of the Cenozoic volcanics of North Island, New Zealand. *Ph.D. thesis, Aust. Nat. Univ., Canberra* (unpubl.).

ST JOHN, V. P., 1967—The gravity field in New Guinea. *Ph.D. thesis, Univ. Tasmania, Hobart* (unpubl.).

TAN SIN HOK, 1936—Over verschillende paleontologische criteria voor de geleding van het Tertiair. *Ing. Ned. Indie*, 3(iv), 173-9.

TAN SIN HOK, 1939—Remarks on the letter-classification of the East Indian Tertiary. *Ing. Ned. Indie*, 6(iv), 98-101.

TATSUMOTO, M., 1969—Lead isotopes in volcanic rocks and possible ocean-floor thrusting beneath island arcs. *Earth planet. Sci. Lett.*, 6, 369-76.

TATSUMOTO, M., HEDGE, C. E., & ENGEL, A. E. J., 1965—Potassium, rubidium, strontium, thorium, uranium, and the ratio of strontium-87 to strontium-86 in oceanic tholeiitic basalt. *Science*, 150, 886-8.

TAYLOR, S. R., 1967—The origin and growth of continents. *Tectonophysics*, 4, 17-34.

TAYLOR, S. R., KAYE, M., WHITE, A. J. R., DUNCAN, A. R., & EWART, A., 1969—Genetic significance of Co, Sr, Ni, Sc, and V content of andesites. *Geochim. cosmochim. Acta*, 33, 275-86.

TAYLOR, S. R., & WHITE, A. J. R., 1965—Geochemistry of andesites and the growth of continents. *Nature*, 208, 271-3.

THOMPSON, J. E., 1957—The Papuan Ultrabasic Belt with particular reference to economic aspects. *Bur. Miner. Resour. Aust. Rec.* 1957/77 (unpubl.).

THOMPSON, J. E., 1967—A geological history of eastern New Guinea. *APEA J.*, 7, 83-93.

THOMPSON, J. E., & FISHER, N. H., 1965—Mineral deposits of New Guinea and Papua and their tectonic setting. *Bur. Miner. Resour. Aust. Rec.* 1965/10 (unpubl.).

TURNER, D. L., 1970—Potassium-argon dating of Pacific Coast Miocene foraminiferal stages. *Geol. Soc. Am. spec. Pap.* 124, 91-130.

TURNER, F. J., & VERHOOGEN, J, 1960—IGNEOUS AND METAMORPHIC PETROLOGY. *New York, McGraw-Hill.*

VAN BEMMELEN, R. W., 1949—THE GEOLOGY OF INDONESIA, IA. *The Hague, Govt Printing Office.*

VAN DER VLERK, I. M., 1931—Cainozoic Amphineura, Gastropoda, Lamellibranchiata, Scaphopoda. *Leid. geol. Mededel.*, 5, 206-96.

VAN DER VLERK, I. M., 1959—Problems and principles of Tertiary and Quaternary stratigraphy. *Quart. J. geol. Soc. Lond.*, 115, 49-63.

VAN DER VLERK, I. M., & UMBGROVE, J. H. F., 1927—Tertiaire gidsforaminiferen van Nederlandsch Oost-Indie. *Wetensch. Mededel.*, 6.

VEEH, H. H., & CHAPPELL, J., 1970—Astronomical theory of climatic change: support from New Guinea. *Science*, 167, 862-5.

VERBEEK, A. A., & SCHREINER, G. D. L., 1967—Variations in $K^{39}:K^{41}$ ratio and movement of potassium in a granite-amphibolite contact region. *Geochim. cosmochim. Acta*, 31, 2125-33.

VISSER, W. A., & HERMES, J. J., 1962—Geological results of the exploration for oil in Netherlands New Guinea. *Verh. K. Ned. geol.-mijnb. Genoot., geol. Ser. Decl. XX.* special number.

VON DER BORCH, C. C., 1969—Submarine canyons of southeastern New Guinea: seismic and bathymetric evidence for their modes of origin. *Deep Sea Res.*, 16, 323-8.

VON KOENIGSWALD, G. H. R., 1962—Potassium-argon dates for the Upper Tertiary. *Proc. K. Ned. Akad. Wetensch.*, ser. B, 65, 31-4.

WASSERBURG, G. J., 1966—Geochronology, and isotopic data bearing on development of the continental crust. *Adv. Earth Sci.*, 431-59.

WATTS, M. D., 1969—Sepik River helicopter gravity survey, TPNG, 1968. *Bur. Miner. Resour. Aust. Rec.* 1969/124 (unpubl.).

WEBB, A. W., 1967—The geochronology of the igneous rocks of eastern Queensland. *Ph.D. thesis, Aust. Nat. Univ., Canberra* (unpubl.).

WEBB, A. W., & McDOUGALL, I., 1967—Isotopic dating evidence on the age of the Upper Permian and Middle Triassic. *Earth planet. Sci. Lett.*, 2, 483-8.

WEBB, A. W., & McDOUGALL, I., 1968—The geochronology of the igneous rocks of eastern Queensland. *J. geol. Soc. Aust.*, 15, 313-46.

WIEBENGA, W. A., 1973—Crustal structure of the New Britain-New Ireland region. *In* COLEMAN, P. J., (Ed.)—THE WESTERN PACIFIC: ISLAND ARCS, MARGINAL SEAS, GEOCHEMISTRY. *Perth, Univ. W. Aust. Press*, 163-77.

WILKINSON, J. F. G., 1962—Mineralogical, geochemical and petrogenetic aspects of an analcite-basalt from the New England district of New South Wales. *J. Petrol.*, 3, 192-214.

WILSON, J. T., 1952—Orogenesis as the fundamental geological process. *Trans. Am. geophys. Un.*, 33, 444-9.

WORDEN, J. M., 1970—Weathering of Australian granitic rocks: a study of the variations in trace elements and isotopic ratios. *Ph.D. thesis, Aust. Nat. Univ., Canberra* (unpubl).

YORK, D., BASKI, A. K., & AUMENTO, F., 1969—K-Ar dating of basalts dredged from the North Atlantic (abstr.). *Trans. Am. geophys. Un.*, 50, 353.

YOUNG, G. A., 1963—Northern New Guinea Basin reconnaissance aeromagnetic survey 1961. *Bur. Miner. Resour. Aust. Rec.* 1963/117 (unpubl.).

APPENDIX 1. METHODS

When this project was begun in 1967, only 4 isotopic dates had been recorded in Papua New Guinea. Using a number of samples of intrusive rocks collected by D. B. Dow and R. R. Harding, the initial approach taken in the laboratory was to apply the Rb-Sr dating method. After preliminary X-ray fluorescence (XRF) exmination, it was clear that the common intrusive rock types, granodiorite and diorite, generally had low Rb-Sr ratios ($\leqslant 0.1$). This finding, together with the area's youthfulness, which became evident after preliminary K-Ar analyses, indicated that a major Rb-Sr project on the rocks would not be feasible. The K-Ar technique seemed the most useful method to help unravel the complex history of this juvenile orogenic belt, provided that the anticipated problem of argon loss from the recently uplifted rocks could be monitored and the results interpreted in a geologically meaningful way. The bulk of this work, then, is concerned with K-Ar dating, but the Rb-Sr method was later used on suitable rocks, and the results generally confirm those of the K-Ar analyses.

Selection and preparation of samples

Thin sections were first examined under a petrological microscope. For the plutonic rocks, alteration which had not been noted in the field rarely restricted sample selection in the laboratory. Many of the basic to intermediate volcanic rocks that appeared fresh in the field had to be rejected for dating work, usually because of groundmass alteration.

For whole-rock K-Ar dating of volcanic rocks the -100 BS aliquot (for potassium analysis) was split from jaw-crushed, chip-size fragments (for argon extraction) of one of the following size ranges: $-10 + 14$ BS, $-6.4 + 4.8$ mm, or $-4.8 + 3.2$ mm.

For mineral separation from coarser-grained plutonic rocks, about 2 to 5 kg of the rock was put through steel jaw crushers in two stages, and then through a steel disc mill until it passed 18 BS mesh; from this an aliquot was split and ground in a tungsten carbide 'Siebe' mill for a whole-rock (-100 BS) sample. The remainder of the sample was screened, and the required size fraction was separated for mineral concentrating using a 'Carpco' magnetic separator. The benefication of the mineral concentrate to more than 98 percent purity was achieved through one or more of the following procedures: further rolling and screening to remove any composite grains, flotation in high specific-gravity liquids, and magnetic separation with a 'Cook' electromagnetic separator. To remove any trace of heavy liquids, the mineral separate was cleaned ultrasonically with distilled water, and then washed in acetone. Most of the minerals used were in the range $-18 + 60$ BS for biotites, and $-85 + 120$ BS for hornblendes and feldspars.

The general age equation. The fundamental equation for any radioactive decay relies on the empirical fact that the rate of decay per unit time is proportional to the number of atoms present, i.e. $dP/dt = -\lambda P$, where $\qquad$ (1)

P is the number of parent atoms present at time t

P_o is the number of parent atoms present at time zero

D is the number of daughter atoms present at time t

λ is the decay constant (fraction decaying per year).

Integrating (1) between time $= O$, and time $= t$ (present), gives:

$$P = P_o e^{-\lambda t}$$

Now $\qquad P_o = P + D$

Therefore $P = (P + D) e^{-\lambda t}$

$$e^{\lambda t} = 1 + D/P$$

$$t = \frac{1}{\lambda \ln (1 + D/P)} \qquad (2)$$

This is the general age equation applicable to any isotopic dating method.

THE K-AR DATING METHOD

K-Ar decay scheme. Decay of the radioactive potassium isotope, K^{40}, is through a branching process (Fig. A) of electron capture and γ —emission to Ar^{40} (decay constant λ_e), and β —decay to Ca^{40} (decay constant $\lambda\beta$). The K-Ar dating method employs only the $K^{40} \rightarrow Ar^{40}$ branch, and the fraction of K^{40} which yields Ar^{40} can be expressed as $\dfrac{\lambda_e}{\lambda_e + \lambda_\beta}$, where $\lambda = \lambda_e + \lambda_\beta$.

The general age equation (2) now becomes:

$$t = \frac{1}{\lambda \ln \left[1 + {}^*Ar^{40}/Kr^{40} \left\{ \frac{\lambda_e + \lambda_\beta}{\lambda_e} \right\} \right]} \qquad (3)$$

or ${}^*Ar^{40} = \left[\dfrac{\lambda_e}{\lambda_e + \lambda_\beta} \right] K^{40} (e^{\lambda t} - 1) \qquad (4)$

where K^{40} is the present-day abundance, and ${}^*Ar^{40}$ is radiogenic argon abundance produced within time t.

In addition to the indirect decay of K^{40} to Ar^{40} by electron capture and γ-ray emission, Beckinsale & Gale (1969) have demonstrated two weak direct transitions: one by electron capture, the other by positron emission (dashed lines, Fig. A). *K-Ar decay constants.* As an extension of their discovery of the two weak direct transitions in the decay of K^{40} to the Ar^{40} ground state,
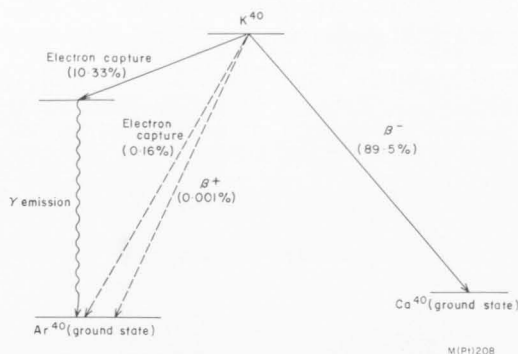
Fig. A. Radioactive decay scheme of K^{40}.

Beckinsale & Gale (1969) amended the decay constants used in the calculation of K-Ar ages. These, however, were not adopted for this study; instead, the following decay constants and natural isotopic abundances were used:

$$\lambda_e = 0.585 \times 10^{-10} yr^{-1}$$ Aldrich &
$$\lambda_\beta = 4.72 \times 10^{-10} yr^{-1}$$ Wetherill (1958)

K^{40} = 1.19 × 10^{-2} atom. percent of total potassium

Ar^{40} = 99.60 atom. percent of atmospheric argon

Ar^{38} = 0.063 atom. percent of atmospheric argon ⎬ Nier (1950)

Ar^{36} = 0.337 atom. percent of atmospheric argon

Application and assumptions of the K-Ar method. With the known decay constants and an accurate analysis of $*Ar^{40}$ and K^{40}, one can calculate a K-Ar age. In the past, the K-Ar method has been applied to many classes of rocks covering almost the whole of geological time. The method is particularly useful in dating rocks from about 100 000 years to a few hundred million years old, for which range the other dating methods are commonly difficult to apply in practice. A K-Ar age will record the time of crystallization or homogenization of a rock if the following assumptions, which must be evaluated in each particular study undertaken, are met:

(i) The mineral or rock remains a *closed system* after crystallization, i.e. there must be no gain or loss of K^{40} or Ar^{40} except by radioactive decay: the $*Ar^{40}$ must be retained quantitatively in the lattices of the minerals. It is well known that argon diffuses out of rocks and may be lost from the system at temperatures above 150-200°C. Some minerals, such as some of the alkali feldspars, appear to lose argon even at lower temperatures. Many laboratory experiments have been carried out to determine the argon diffusion characteristics of minerals; details of such experiments have recently been summarized by Mussett (1969). In general, the experimental data remain somewhat ambiguous, at least partly because the experiments fall short of duplicating the long-term and variable effects of a geological environment. Geological studies (Hart, 1964; Hanson & Gast, 1967) involving age determinations of various minerals at different distances from intrusive contacts have provided the most convincing evidence for different diffusion rates of argon from the various minerals. In geologically active terrains such as New Guinea, it is not unexpected that several examples of differential argon loss patterns are recognized. Evidence given earlier in this Bulletin shows that, during uplift and cooling of a batholith, hornblende retains argon at higher temperatures than biotite. Under burial metamorphic conditions, however, the argon retentivities of biotite and hornblende sometimes appear to be similar (cf. Webb & McDougall, 1968).

(ii) At the time of crystallization (t = O) the *sample loses any pre-existing* $*Ar^{40}$. When magmas are generated from older rocks, substantial amounts of pre-existing radiogenic argon are likely to be contained within the magma. Damon (1968) defined this *extraneous argon* as being either (a) inherited argon (Ar^{40} produced by radioactive decay and retained in a mineral from an earlier period in its history) or (b) excess argon (Ar^{40} occluded within a mineral owing to a high pressure in the magma). For the K-Ar method of dating to be viable, this extraneous argon must be lost from the system before final crystallization and cooling. Evidence is now accumulating (Damon, 1968; McDougall, Polach, & Stipp, 1969; Roddick, 1970) that this assumption is not always met. Clearly if the assumption is not fulfilled then measured ages will be too old.

(iii) *Argon, other than that produced by in situ radioactive decay of* K^{40} *since crystallization, has the composition of present-day atmospheric argon* (i.e. $Ar^{40}/Ar^{36} = 295.5$), for which a correction can be made in the calculation of radiogenic argon. Until recently it was generally believed that the measured atmospheric argon contamination was acquired in field, laboratory, or extraction procedures. However, there is now evidence (Frechen & Lippolt, 1965; Mussett & Dalrymple, 1968) that much so-called 'atmospheric contamination' has been held tightly within the rock or mineral since its inclusion at the time of crystallization or homogenization. Clearly, assumption (iii) will not be met if this 'initial argon' has an Ar^{40}/Ar^{36} composition other than 295.5.

Generally, these assumptions are tested by the analysis of either a number of related samples from one rock unit, or two or more minerals separated from the one rock specimen. Should the results agree, the consistency may be taken as evidence that the K-Ar ages are geologically meaningful. Another test of the reliability of K-Ar
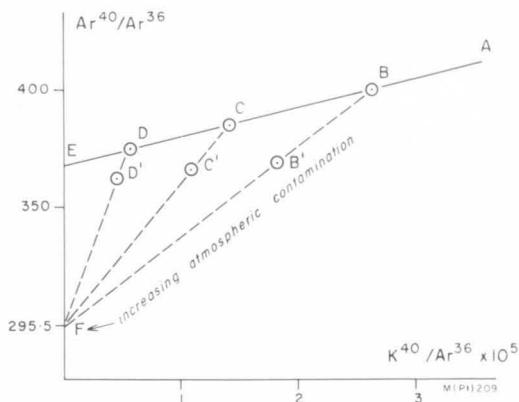
Fig. B. Diagram illustrating the isochron plot of K-Ar data.

dating is to compare the K-Ar ages with those determined by another dating technique, such as the Rb-Sr method, for the same samples. A summary of such comparisons is given by Dalrymple & Lanphere (1969), and many examples of similar approaches have been presented earlier in this Bulletin.

Graphical representation of K-Ar data
Argon isochron diagram. A recent development in the analysis of K-Ar data is the introduction of the isochron diagram, analogous to that used in Rb-Sr work. Ideally, plotting of data on the argon isochron diagram allows a more direct test of assumptions (ii) and (iii) above. In this type of diagram, Ar^{40}/Ar^{36} and K^{40}/Ar^{36} ratios for a given suite of cogenetic rocks are plotted against one another (McDougall et al., 1969; York, Baski, & Aumento, 1969; Hayatsu & Carmichael, 1970).

Derivation of the argon isochron equation is as follows:

$$Ar_t^{40} = {}^*Ar^{40} + Ar_a^{40} + Ar_i^{40} \tag{5}$$

Combining equations (4) and (5) and dividing by Ar_t :

$$(Ar^{40}/Ar^{36})_t = \left(\frac{\lambda_e}{\lambda_e + \lambda_\beta}\right)(e^{\lambda t} - 1) \, K^{40}/Ar_t^{36} + Ar_a^{40}/Ar_t^{36} + Ar_i^{40}/Ar_t^{36} \tag{6}$$

where ${}^*Ar^{40}$ = radiogenic Ar^{40} produced in the rock by in situ decay of K^{40} since crystallization or homogenization

Ar_a^{40} = contamination from the atmosphere after closure of the system

Ar_i^{40} = non-radiogenic argon initially in the rock

Ar_t^{40} = total Ar^{40} in the rock

Ar_t^{36} = $Ar_i^{36} + Ar_a^{36}$

If we define $Ar_a^{36}/Ar_t^{36} = f$ (i.e. the proportion of Ar^{36} that is atmospheric and added after closure of the system), then:

$$1 - f = Ar_i^{36}/Ar_t^{36}$$

Rewriting equation (6):

$$(Ar^{40}/Ar^{36})_t = \left(\frac{\lambda_e}{\lambda_e + \lambda_\beta}\right)(e^{\lambda t} - 1) \, K^{40}/Ar_t^{36} + (Ar_a^{40}/Ar_a^{36}) \, Ar_a^{36}/Ar_t^{36} + (Ar_i^{40}/Ar_i^{36}) \, Ar_i^{36}/Ar_t^{36}$$

$$= \left(\frac{\lambda_e}{\lambda_e + \lambda_\beta}\right)(e^{\lambda t} - 1) \, K^{40}/Ar_t^{36} + (Ar^{40}/Ar^{36})_a f + (Ar^{40}/Ar^{36})_i (1 - f)$$

If for the moment we assume that f is zero (i.e. there is no atmospheric argon contamination in the field after crystallization or in the laboratory) the equation becomes:

$$(Ar^{40}/Ar^{36})_t = \left(\frac{\lambda_e}{\lambda_e + \lambda_\beta}\right)(e^{\lambda t} - 1) \, K^{40}/Ar_t^{36} + (Ar^{40}/Ar^{36})_i \tag{7}$$

This is the equation of a straight line of the form $y = mx + c$

where $\quad y = (Ar^{40}/Ar^{36})_t$

$\qquad x = K^{40}/Ar_t^{36}$

slope, $m = \left(\frac{\lambda_e}{\lambda_e + \lambda_\beta}\right)(e^{\lambda t} - 1)$

intercept, $c = (Ar^{40}/Ar^{36})_i$

Hence, ideally, the results from a suite of co-genetic rocks plotted on an Ar^{40}/Ar^{36}-versus-K^{40}/Ar^{36} diagram will lie on a straight line (AE, Fig. B), the slope of which will be proportional to the time since the system was closed. The intercept, E, may be equal to, less than, or greater than that of atmospheric argon (295.5) and is the common value of Ar^{40}/Ar^{36} ($\sim$ 370 in Fig. B) contained within the rocks (B, C, and D) at the time of crystallization or homogenization.

Applying the conventional assumptions of K-Ar dating to Figure B, the 'age' calculated for sample D (i.e. slope of line DF) would be greater than the age calculated for C, and so on. Such a scatter of 'ages' would clearly be erroneous because the non-radiogenic argon does not have the composition of atmospheric Ar^{40}/Ar^{36}.

An example of an argon isochron plot was given by Hayatsu & Carmichael (1970) for a group of rocks which was formed in the Cambrian and subsequently isotopically homogenized about 400 m.y. ago in the Devonian. Their initial Ar^{40}/Ar^{36} ratio was 488, significantly higher than 295.5, and effectively indicated the presence of what is commonly called excess or extraneous argon.

In practice, the Ar_a^{40}, that component of Ar^{40} from the atmosphere absorbed onto the rock after closure of the system or introduced by sample handling in the laboratory, will always be present, but ideally it will be so low in amount relative to that contained in the rocks, as to be negligible in terms of equation (5). This appears to be so in the example given by Hayatsu & Carmichael (1970), who considered that more than 90 percent of the Ar^{36} had come from the samples. In dealing with young basalts from Auckland, however, McDougall et al. (1969) found that atmospheric argon contamination was of overriding importance. The effect of atmospheric argon contamination can be seen from Figure B. If F is the $Ar^{40}/$

Ar^{36} ratio in the atmosphere, then the addition of different amounts of atmospheric argon to each of B, C, and D causes the sample points to move down the isochron diagram along lines that join them to F; hence the simple relationship of equation (7) does not now hold. Points B', C', and D' thus generated may give an apparent isochron (B'C'D'), and both the slope and intercept would be incorrect. Where the initial ratio is equal or close to 295.5, any atmospheric contamination will have very little effect on the slope or intercept in the isochron diagram.

It is clear from the discussion above that the use of the argon isochron diagram will only be successful when (i) the complication due to subsequent atmospheric argon contamination is negligible, and (ii) the $(Ar^{40}/Ar^{36})_i$ in all the cogenetic samples is the same. Some of the New Guinea data have been examined using this approach.

Initial argon diagram. One other type of argon plot, the initial argon diagram, has been used to help determine whether extraneous argon is present, and to find the pooled age of a cogenetic suite of samples. In this diagram, $\ddagger Ar^{40}$ is plotted against potassium for each sample in the suite. If the conventional assumptions of the K-Ar method are met, then, as seen in equation (4):

$$*Ar^{40} = \left(\frac{\lambda_e}{\lambda_e + \lambda_\beta}\right) K^{40} (e^{\lambda t} - 1)$$

This is the equation of a straight line of the form $y = mx$, and a suite of cogenetic samples will lie on a straight line AB through the origin, with the slope proportional to their age (Fig. C).

If, however, some extraneous radiogenic argon has remained in the rocks (through incomplete outgassing of pre-existing Ar^{40}) the following more general equation (after Roddick, 1970), which introduces the normal correction for atmospheric argon, can be derived:

$$\ddagger Ar^{40} = Ar_i^{40} - 295.5\ Ar_i^{36}$$

Combining this with equations (4) and (5):

$$\ddagger Ar^{40} = \left(\frac{\lambda_e}{\lambda_e + \lambda_\beta}\right)(e^{\lambda t} - 1)\ K^{40} + Ar_i^{40} + Ar_a^{40} - 295.5\ Ar_i^{36}$$

Now $Ar_i^{36} = Ar_a^{36} + Ar_i^{36}$

Therefore:

$$\ddagger Ar^{40} = \left(\frac{\lambda_e}{\lambda_e + \lambda_\beta}\right)(e^{\lambda t} - 1)\ K^{40} + Ar_i^{40} + Ar_a^{40} - 295.5\ (Ar_a^{36} + Ar_i^{36})$$

If $I = Ar_i^{40}/Ar_i^{36}$, then:

$$\ddagger Ar^{40} = \left(\frac{\lambda_e}{\lambda_e + \lambda_\beta}\right)(e^{\lambda t} - 1)\ K^{40} + I\ Ar_i^{36} + 295.5\ Ar_a^{36} - 295.5\ Ar_a^{36} - 295.5\ Ar_i^{36}$$

(8)

$$= \left(\frac{\lambda_e}{\lambda_e + \lambda_\beta}\right)(e^{\lambda t} - 1)\ K^{40} + Ar_i^{36}(I - 295.5)$$

$\ddagger Ar^{40} =$ alleged radiogenic argon, all of which may or may not have been produced by in situ decay of K^{40}.

This is again a straight line equation of the form

$$y = mx + c$$

where $y = \ddagger Ar^{40}$

$$x = K^{40}$$

$$\text{slope, } m = \left(\frac{\lambda_e}{\lambda_e + \lambda_\beta} \right) (e^{\lambda t} - 1)$$

$$\text{intercept, } c = Ar_i^{36}(I - 295.5) \qquad (9)$$

Alternatively, $c = Ar_i^{40} - 295.5 \; Ar_i^{36}$

Equation (8) indicates that a suite of cogenetic samples with constant Ar_i^{36} and Ar_i^{40} will fall on a straight line CD (Fig. C), irrespective of the earlier conventional assumptions (ii) and (iii) of the K-Ar method outlined above. Note that the intercept at C is the value of extraneous argon common to all the samples on CD. If I is greater than 295.5, then a positive intercept will result, indicating that extraneous argon may be present. A negative intercept would suggest the presence of primordial Ar^{36}. If the straight line passes through the origin, the assumptions have been fulfilled.

Hayatsu & Carmichael (1970) applied their K-Ar data to the initial argon diagram, which indicated (i) the presence of extraneous Ar^{40} of 0.55×10^{-10} mole/g, and (ii) homogenization of the argon isotopic system about 400 m.y. ago. This age and the indication of extraneous argon were also found in the Ar^{40}/Ar^{36}-versus-K^{40}/Ar^{36} isochron plot, confirming that the assumptions of the graphical techniques were met in their study. Several sets of data from New Guinea have been examined in this manner.

Statistical regression of the graphical plots. The least-squares regression method of McIntyre, Brooks, Compston, & Turek (1966) was applied to each of the graphical argon plots in this study. This method makes allowance for experimental error in both co-ordinates, and permits an objective test of the goodness of fit of the straight line. The coefficients of variation (CV) of *Ar^{40} and K^{40} used in the regression were 2.0 percent and 0.3 percent respectively; these values result from a consideration of the precision of the measurements (see Table A). The values of CV of Ar^{40}/Ar^{36} and K^{40}/Ar^{36} used were 0.5 percent and 1.5 percent respectively; these were based on pooled estimates of the precision in individual runs. The y variance in each regression was determined by using an approximate average y for the data set; a standard deviation from the above CV could then be computed.

The goodness of fit of a set of data points is given by the weighted sums of squares of the residuals from the fitted line: if this value, known as the mean square of weighted deviates (MSWD), is unity or less, then the scatter of points is accountable in terms of experimental error. If MSWD is significantly greater than
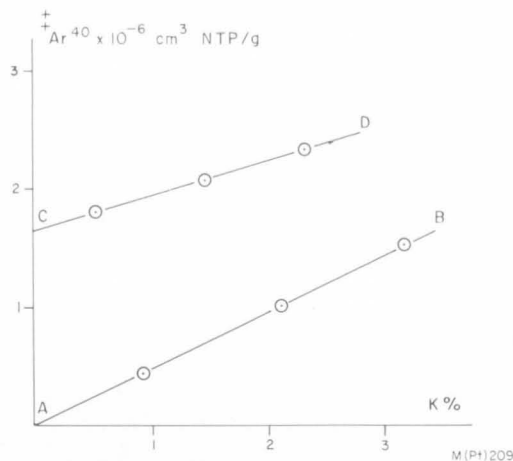
Fig. C. Diagram illustrating the initial argon plot of K-Ar data.

unity at the 5 percent level (using the statistical F test), then the assumptions of the graphical methods (viz. (i) in initial argon diagrams there must be a closed system, and the concentration of Ar_i^{40} and Ar_i^{36} must be constant in all samples; (ii) in argon isochron diagrams there must be a closed system, $(Ar^{40}/Ar^{36})_i$ must be constant for each sample, and post-closure atmospheric contamination must be negligible) are probably not met, and the regression analysis result may be incorrect.

Potassium analysis

Potassium was determined as total potassium by flame photometry (Cooper, 1963; Cooper, Martin, & Vernon, 1966), and the percentage of K^{40} was calculated from its known atomic abundance in the element. Nier (1950) determined the atomic abundance of K^{40} as 0.0119 atom. percent. Although in some unusual geochemical environments the atomic abundance of K^{40} has been found to be somewhat variable (Verbeek & Schreiner, 1967), the assumption of constant K^{40} at 0.0119 atom. percent is believed to be accurate to within ± 1 percent (Burnett, Lippolt, & Wasserburg, 1966), and is adopted here in preference to Beckinsdale & Gale's (1969) value of 0.0118 atom. percent.

Precision and accuracy of potassium measurements. All potassium determinations were done in duplicate, except for those mineral samples that were insufficient for separate dissolutions. An estimate of the precision of potassium determination can therefore be obtained from the results obtained during this study, and is summarized in Table A. Using all the analysed micas (19 biotites and 6 muscovites) from the Bismarck Intrusive Complex (5.33) a CV of a single measurement of 0.26 percent is obtained; all 23 hornblende potassium analyses from the same mass give a pooled CV of 0.32 percent. Whole-rock potassium analyses of 20 samples from the Tertiary volcanics (3.3) give a pooled CV of 0.28 percent. These

TABLE A. K-Ar PRECISION ESTIMATES BASED ON REPLICATE MEASUREMENTS

Sample	K measurement		$*Ar^{40}$ measurement		Overall precision (CV) for a single age
	No. of replicates	CV for a single measurement	No. of replicates	CV for a single measurement	
Whole rocks	20	0.28	12	1.74	1.76
Micas	25	0.26	5	2.42	2.43
Hornblendes, ($*Ar^{40} > 20\%$)	23	0.32	8	2.26	2.28
Hornblendes, ($*Ar^{40} > 12\%$)	23	0.32	14	3.65	3.67

figures for precision are close to the average for the ANU/BMR isotope laboratory of 0.30 percent.

Comparisons between flame-photometric potassium analyses done in this laboratory, and other techniques and potassium analyses obtained elsewhere, enabled Cooper (1963) to report an agreement to within 1 percent of the average values determined elsewhere. Repeated potassium analyses of the USGS standard-muscovite (P-207) over the last few years (Webb, 1967; McDougall, 1970, pers. comm.) agree with the interlaboratory average reported by Lanphere & Dalrymple (1967), and indicate no detectable drift in accuracy in this laboratory during this time.

Argon analysis. Argon was measured by isotope dilution using Ar^{38} as a spike. The argon extraction process utilizes a high-vacuum glass system in which a rock or mineral sample is fused; the

evolved gases are allowed to mix with a suitably calibrated amount of Ar^{38} spike, and the resulting gas mixture is purified by removing the active gases, after which the sample of argon gas is taken off the line. For this study, measurement of the relative quantities of Ar^{36}, Ar^{38}, and Ar^{40} in the gas sample was carried out in a Reynolds-type glass mass spectrometer of 60° sector and 11.4-cm (4.5-inch) radius of curvature. The apparatus, techniques, and corrections to be applied in argon extraction and mass spectrometry are fully described by McDougall (1966).

The calculation of the amount of radiogenic argon in a sample is made from the mass spectrometer Ar^{40}/Ar^{38} (40/38) and Ar^{38}/Ar^{36} (38/36) ratios corrected for memory, orifice, and discrimination effects. The volume of radiogenic argon ($*Ar^{40}$) is given by the following relationship:

$$*Ar^{40} = Ar^{38} \left\{ (40/38)_m - (40/38)_s - \frac{1 - (38/36)_m (36/38)_s}{(38/36)_m (36/38)_a - 1} \left[(40/38)_a - (40/38)_m \right] \right\}$$

where Ar^{38} = Ar^{38} content of spike (cm^3 NTP)
subscript m = measured ratio
subscript s = spike ratio
subscript a = atmospheric argon ratio

The term underlined in the above equation is the correction for atmospheric argon contamination. $*Ar^{40}$ can now be substituted into the general age equation (4) to calculate the K-Ar age.

Precision and accuracy of K-Ar measurements

The precision given to an age determination is a measure of the reproducibility if the analysis is repeated one or more times. Therefore, the best way to obtain a statistically valid precision estimate is to compare replicate measurements. Another way of determining the precision involves a statistical breakdown of each component step of the age determination. Page (1971) considers these two approaches with reference to the New Guinea results. Firstly, duplicate potassium and argon runs (with moderate air argon contamination) result in an overall precision for a single age of round 1.8 percent at the 68 percent confidence level; this is in close agreement with the precision determined in other recent studies in this laboratory (McDougall & Chamalaun, 1969).

Secondly, the errors that have accumulated in the separate steps of the K-Ar analysis are combined to obtain an 'experimental error', or estimate of the precision of each K-Ar age determination; in this study typical values of the total experimental error are of the order of 1.5 percent, which is quite similar to estimates based on replicate measurements, and the individual errors of each step are therefore regarded as realistic values.

The error of each age measurement quoted in this study is two standard deviations (2 SD), which is usually close to the 95 percent confidence limits.

THE Rb-Sr DATING METHOD

Rb^{87} decays by β-emission to Sr^{87}, and the general age equation (2) can be rewritten:

$$t = \frac{1}{\lambda \ln (1 + *Sr^{87}/Rb^{87})} \quad (10)$$

where $*Sr^{87}$ = the number of atoms of radiogenic strontium formed up to the present day, and Rb^{87} = the number of atoms of Rb^{87} left at the present day. Knowledge of the decay constant (λ), the amount of $*Sr^{87}$ produced, and the amount of residual Rb^{87} enables the age of a rock or mineral to be calculated. As in the K-Ar method,

the basic assumption is that the parent and daughter isotopes have occupied a closed chemical system since the geological event that produced them.

Because $*Sr^{87}/Rb^{87}$ is a very small number, we can approximate and rewrite equation (10) as:

$$\lambda t = *Sr^{87}/Rb^{87}$$
$$= (Sr_p^{87} - Sr_i^{87})/Rb^{87} \qquad (11)$$

where subscripts p and i are the present-day and initial values respectively;

i.e. $\lambda t = Sr^{86}/Rb^{87} (R_p - R_i)$ $\qquad$ (12)

where R_p and R_i are the present-day and initial (i.e. date of rock formation) Sr^{87}/Sr^{86} ratios respectively. Upon measurement of Rb^{87}, Sr^{86}, and R_p (with an assumed or estimated R_i and known decay constant, λ) the age of the rock or mineral sample can be calculated. Isotope dilution analysis for Rb^{87} and Sr^{86} requires the addition of an internal standard (spike) into the sample, so that, from the mass ratios measured in a mass spectrometer, the absolute amounts of the isotope can be calculated by comparison with the spike. R_p is measured directly or calculated from the respective mass ratios.

The Rb-Sr isochron. The value R_i cannot be directly measured, and must therefore be either assumed or estimated. An assumption of R_i is valid in an age determination if the sample is well enriched in $*Sr^{87}$ (i.e. high R_p in equation (12)). This is because Sr^{87}/Sr^{86} in common strontium in all crustal rocks is of the order of 0.70, and the age determination of samples with a high R_p will be almost independent of any slight uncertainty of, or deviation from, 0.70. This is often applicable to Rb-Sr mica ages.

For whole-rock samples with low R_p (as mostly applies in this study) the Rb-Sr age is markedly dependent on the value of the assumed R_i. For such samples, data from cogenetic rocks or minerals, or both, have to be studied, for they are considered to have had the same R_i. A graphical method (after Nicolaysen, 1961) is then used to represent the Rb-Sr age data and to extrapolate the common R_i (initial Sr^{87}/Sr^{86} ratio) of the suite of samples. The derivation of the graphical plot is as follows: by combining equations (11) and (12),

$$*Sr^{87}/Rb^{87} = Sr^{86}/Rb^{87} (R_p - R_i)$$
$$R_p = *Sr^{87}/Rb^{87} (Rb^{87}/Sr^{86}) + R_i$$

and this is the equation of a straight line ($y = mx + c$), where:

slope, $m = *Sr^{87}/Rb^{87}$ (proportional to age)

intercept, $c = R_i$ (the initial Sr^{87}/Sr^{86} ratio)

Rb^{87}/Sr^{86} is the independent variable.

In this method the analytical data, Rb^{87}/Sr^{86} and R_p, for a cogenetic suite are graphically plotted, and if the basic assumptions are met, the suite will plot on an isochron. This line is fitted statistically by the least-squares method of analysis (McIntyre et al., 1966). As for the graphical regression of argon data, the goodness of fit of the supposed cogenetic samples to an isochron is given by the mean square of weighted deviates (MSWD). In the Model I isochron (in which all error is assumed to be experimental) of McIntyre et al. (1966) the limit to the value of MSWD is placed at 1. When MSWD is significantly greater than unity at the 5 percent level (using the statistical F test), 'geological effects' (e.g. loss of $*Sr^{87}$ through metamorphism, or real differences in age or R_i between samples) are invoked. For Rb-Sr work, different models of distribution of such effects are used, and the calculation is repeated up to three times to determine which model is the most appropriate. Model II assigns the effects to variation in Sr^{87}/Sr^{86}, which it relates proportionally to Rb^{87}/Sr^{86} (applicable to cogenetic samples that have undergone slight redistribution of Sr^{87}). Model III assumes that primary variation in Sr^{87}/Sr^{86} is independent of Rb^{87}/Sr^{86} (widely applicable to metamorphic rocks, and even to samples from widely distributed igneous rocks of the same suite). Model IV is a combination of Models II and III.

The statistical fit of a Rb-Sr isochron to a suite of cogenetic samples requires prior estimates for the experimental precision of the Rb^{87}/Sr^{86} and Sr^{87}/Sr^{86} co-ordinates. The variance of Rb^{87}/Sr^{86} assumed by McIntyre et al. (1966), 25.51 x 10^{-6}, has been used in the present study. For the Sr^{87}/Sr^{86} co-ordinate, the variance of 0.10 x 10^{-6}, which is based on replicate data by Arriens & Compston (1968), has been used. Use of these values is justified because all analyses took place using the same mass spectrometer under similar conditions in the same laboratory. Recent work by Dr. W. Compston (pers. comm.) under better-controlled conditions indicates a lower Sr^{87}/Sr^{86} variance of 0.066 x 10^{-6} for spiked runs, and 0.05 x 10^{-6} for unspiked runs; these values were used in the study of the Bismarck Intrusive Complex (5.33). The uncertainties in ages and intercepts of Rb-Sr whole-rock and mineral data throughout the study are given at the 95 percent confidence level.

Rb^{87} decay constant. There is still considerable doubt about the exact half-life, and hence the decay constant, of Rb^{87}. An account of the conflicting geological and physical determinations used to determine the half-life is given by Hamilton (1965), who states that the value certainly lies between 4.7 and 5.3 x 10^{10} years. Webb (1967) followed Kulp & Engels (1963) in preferring a value for λ of 1.47 x $10^{-11}yr^{-1}$, based on age comparisons by the Rb-Sr and K-Ar methods. The value used here, 1.39 x $10^{-11}yr^{-1}$, is that currently used in this laboratory; the value of 1.47 x $10^{-11}yr^{-1}$, which depresses a Rb-Sr age by about six percent, was discarded at the meeting of the IUGS Subcommission on Geochronology in September 1974.

Selection of samples

A prospective suite of samples for Rb-Sr analy-

sis was first examined macroscopically and microscopically for its general suitability. The rock powders or mineral concentrates were then analysed by semiquantitative XRF to determine the total rubidium and total strontium, and hence the Rb/Sr ratio. With this data a suite of samples showing a spread of Rb/Sr ratio was chosen for isotope dilution analyses, and the same data also enabled the optimum spiking quantities for the isotope dilution to be determined.

The XRF analysis employed a Phillips PW 1540 spectrometer with molybdenum tube, lithium fluoride crystal, scintillation counter, and digital recorder. Each sample was loosely pressed onto 'Mylar' film in the sample holder and exposed to the X-rays. Rubidium and strontium peaks as well as background counts were monitored for 20 seconds each. A standard sample was used to check accuracy and machine drift. Corrections for dead time, background, and tail effects were applied and the data were reduced in a computer program written by Dr P. A. Arriens.

Chemical preparation for Rb-Sr analysis

The chemical preparation of a concentrated spiked rubidium and spiked or unspiked strontium sample used here was principally as described by Compston, Lovering, & Vernon (1965). 0.5 g of sample was weighed into a tared platinum dish and dissolved in 7 ml hydrofluoric acid, which was evaporated on a water-bath. 5 ml water, 5 ml hydrofluoric acid, and 1-2 ml perchloric acid were then added. The hydrofluoric acid was again evaporated, and the perchloric acid was fumed to dryness on a gently warmed hot-plate. 5 ml 2.5N hydrochloric acid was added and evaporated, and the sample was then dissolved in 25 ml 2.5N hydrochloric acid. This was completely transferred to a 'Parafilm'-covered tared Pyrex beaker and, before final cooling, allowed to mix thoroughly on the hot-plate. Appropriate amounts of the solution, to provide about 8 μg of strontium and 15 μg of rubidium, were separately measured into beakers; the strontium aliquot was placed in a beaker containing 0.4 μg of Sr^{84} spike (or for well enriched samples, a 'double' spike of Sr^{84} and Sr^{86}), and the rubidium aliquot was placed in a beaker containing 10 μg of Rb^{87} spike. After drying, the aliquots were dissolved in 5 ml of hydrochloric acid (2.5N for strontium, 1N for rubidium), and any residues were centrifuged. The aliquots were then concentrated through cation exchange columns (employing Dowex 50W-X8, 200-400 mesh) with hydrochloric acid of the same respective strengths. The rubidium and strontium columns were previously calibrated by monitoring the path of a radioactive tracer of Sr^{85} or Rb^{86} passed through the columns. 90 percent of the samples of strontium and rubidium could be concentrated in this way. After slow evaporation, the strontium and rubidium samples were taken up, each in one drop of water, and transferred in a Pyrex pipette to the two rhenium side filaments

of the triple filament assemblies of the mass spectrometer source.

The above procedure applied to most of the Rb-Sr analyses. For Rb-Sr analyses of micas, however, the practice was to take smaller quantities of sample, about 0.25 g. Although this meant using less strontium (sometimes as little as 1 μg), it had the advantage of reducing the large amounts of rubidium in the strontium ion exchange column. Another departure, for the unspiked strontium analyses, was to load the ion exchange columns so that approximately 20 μg of strontium was handled.

Contamination levels

In general, corrections have not been made for chemical and instrumental contamination of the rubidium and strontium analyses. Previous investigations by Compston et al. (1965) and Compston, Chappell, Arriens, & Vernon (1969) have shown that, for the relatively high levels of rubidium and strontium used, contamination is negligible compared with other sources of error, if normal precautions are taken. Compared with past and other recent blanks measured in the same laboratory, the levels of rubidium and strontium contamination in total blanks that I have analysed (Table B) reveal the general improvement in reagent purities between 1965 and 1971; these results justify the omission of blank corrections.

Rb-Sr mass spectrometry

Most rubidium mass spectrometer runs were performed on the MS-X machine (built in the Department of Geophysics and Geochemistry, ANU, Canberra), and a few analyses were made on a Metropolitan-Vickers MS2-SG machine. Both have a 15.2-cm (6-inch)-radius, 90°-sector tube, and use a magnet-switching technique with a 10^{11}-ohm resistor in the Cary 31 electrometer. The MS-X was operated at 6kV, the MS2-SG at 2kV.

Strontium (spiked and unspiked) runs were made with a Nuclide Analysis Associate's (NAA) 30.4-cm (12-inch)-radius, 60°-sector machine, employing 6kV accelerating voltage. For the first analyses, peaks were changed by voltage switching in a steady magnetic field (Arriens & Compston, 1968). The NAA machine was subsequently modified to employ a semi-automatic magnet-switching device. For each machine, the ion current at the collecter was measured with a Cary 31 vibrating-reed electrometer; output was digitized with a voltage-to-frequency converter and a counter and digital recorder, and was monitored by chart recorder.

For rubidium runs, at least 12 comparisons of each pair of mass units (85 and 87) were made. Independent measurements were made for each side filament (operated at less than 1.0 amp, with centre filament at 2.5 amp) so that a weighted mean ratio could be calculated. The Rb^{85}/Rb^{87} value in natural rubidium has been taken as 2.600 (Shields, Garner, Hedge, & Goldich, 1963).

TABLE B. RUBIDIUM AND STRONTIUM TOTAL BLANK LEVELS, INCLUDING ION
EXCHANGE PROCESS

Quantity	Compston et al. (1965)	Compston & Vernon (pers. comm., 1967)	Worden (1970)	This study
Rubidium (μg/dissolution)	0.012 0.014 0.007	0.012 0.007	0.010 0.008	0.004 0.003
Strontium (μg/dissolution)	0.09 0.15 0.054	0.055 0.056	0.016 0.017	0.029 0.025

For strontium runs, it was usual to run both side filaments (at about 1.0 amp, but sometimes up to 2.2 amp, and centre filament at 4.0 amp) concurrently. Strontium data were not taken until the Rb^{85} had fallen to less than 3 percent of the Sr^{87} peak, thus ensuring that Rb^{87} was less than 1 percent of Sr^{87}. The ratio sets measured in spiked strontium runs were 88/86, 86/84, 88/86, 87/86, and 88/86. Double-unspiked strontium runs, giving duplicate measurements of 87/86 for each strontium separation, were measured as follows: 88/86, 87/86, 88/86, 87/86, and 88/86. This procedure, with at least 13 comparisons of each ratio, permits precise 'beam-curvature' and 'drift' corrections.

To estimate the linear background under the peaks, twenty zero measurements were taken before and after the runs. As the acquisition of rubidium data involves the measurement of only one isotopic ratio, fewer corrections are necessary. For strontium, a dynamic zero correction, which is obtained by alternately switching from the largest peak to background, allows for any lag in electrometer response (Arriens & Compston, 1968). Another electrometer correction, based on standard data of Dr P. A. Arriens (pers. comm.), was applied to account for slight non-linearity

between electrometer ranges. A mass spectrum was drawn at the end of each run by slow magnet-scanning so that any 'tail' corrections due to the largest 88 peak could be applied to the observed ratios; commonly, these were about 0.013 percent under the 87 peak and 0.005 percent under the 86 peak.

The normalization procedure (written into a computer program devised by Dr P. A. Arriens) relates the measured Sr^{88}/Sr^{86} ratio with an assumed value for the sample of 8.3752. Three unspiked measurements of Eimer and Amend strontium carbonate standard gave me the following values of Sr^{87}/Sr^{86}:

$$\left. \begin{array}{l} 0.70804 \\ 0.70814 \end{array} \right\} \quad 0.70809$$

$$\left. \begin{array}{l} 0.70811 \\ 0.70817 \end{array} \right\} \quad 0.70814$$

$$\left. \begin{array}{l} 0.70810 \\ 0.70811 \end{array} \right\} \quad 0.70811$$

The mean value, 0.70811, is in excellent agreement with previously quoted values from the NAA machine in this laboratory of 0.70813 ± 0.00015 (Arriens & Compston, 1968) and 0.70810 (Compston, Arriens, Vernon, & Chappell, 1970).

APPENDIX 2: SAMPLES USED

Listed below for each sample analysed is the ANU number, field number, rock type, and text-figure reference. The ANU number is that used throughout the text. Up to 5660, the ANU number has the prefix 'GA'. After 5660, the following applies to the ANU number: from 5668 to 5957, the prefix is 69-; from 5958 to 6029, the prefix is 70-; 71-274 to 71-281 is an inclusive set. The corresponding BMR number is also the

sample field number: early numbers (e.g. B55/10/2) refer to the sample number (2) and the 1:250 000 map sheet (B55/10); subsequent field numbers (e.g. 20-2071) refer to the sample (2071) from the New Guinea 1:250 000 map sheet (20NG). A few miscellaneous samples collected by private companies retain their original field numbers.

ANU no.	Field no.	Rock type	Text-figure
981	B55/5/2	Granodiorite	41
5426	B55/10/1	Granodiorite	26
5427	B55/14/1	Granodiorite	26
5428	B55/14/2	Granodiorite	26
5453	B55/14/11	Granodiorite	26
5454	B55/14/13	Granodiorite	26
5455	B55/5/17	Granodiorite	32
5456	B55/5/3	Diorite	32
5457	B55/5/6	Granodiorite	32
5458	B55/5/12	Granodiorite	12
5459	B55/14/12	Granodiorite	26
5460	B55/14/14	Granodiorite	26
5461	B55/10/6	Granodiorite	22
5462	B55/5/16	Granodiorite	32
5463	B55/5/4	Granodiorite	32
5464	B55/5/5	Granodiorite	32
5465	B55/5/7	Diorite	32
5466	B55/5/13	Granodiorite	12
5467	B55/10/3	Granodiorite	12
5468	B55/10/4	Diorite	12
5469	B55/10/5	Dolerite	12
5470	B55/10/7	Microdiorite	22
5472	Ra 114	Granodiorite	42
5473	Ab 539	Granodiorite	42
5474	Ab 581A	Granodiorite	42
5475	Ab 581B	Granodiorite	42
5476	Ab 581C	Gabbro	42
5482	20-2071	Aplite	41
5483	20-2079	Aplite	41
5484	20-2090	Aplite	32
5485	20-2091	Aplite	32
5486	20-2092	Aplite	32
5487	20-2096	Aplite	32
5491	20-2069	Granodiorite	41
5492	20-2044	Granodiorite	41
5493	20-2066	Granodiorite	41
5497	20-2089	Granodiorite	32
5498	20-2097	Gabbro	32
5499	20-2100	Granodiorite	32
5500	20-2101	Granodiorite	32
5630	12-2004	Basalt	8
5631	12-2005	Basalt	8
5633	12-2007	Basalt	8
5634	12-2008	Basalt	8
5635	12-2009	Basalt	8
5636	12-2011	Basalt	8
5637	12-2019	Dolerite	8
5639	21-2033	Brecciated basalt	10
5640	21-2034	Basanite	10
5641	21-2035	Basalt	10
5642	21-2036	Basalt	10
5643	21-2037	Basalt	10
5645	21-2044	Trachyte	10
5648	11-2159	Andesite	8
5649	03-2097	Diorite	42

ANU no.	Field no.	Rock type	Text-figure
5654	11-2168	Andesite	8
5655	28-2050	Microdiorite	22
5656	28-2051	Microdiorite	22
5657	28-2052	Microdiorite	22
5658	28-2053	Microdiorite	22
5659	28-2054	Microdiorite	22
5660	28-2067	Dolerite	22
5668	28-2057	Dolerite	22
5669	28-2058	Dolerite	22
5670	20-2102	Granodiorite	32
5671	20-2109	Diorite	32
5672	20-2047	Granodiorite	41
5673	20-2065	Granodiorite	41
5674	20-2086	Granodiorite	32
5675	20-2093	Granodiorite	32
5676	20-2027	Granodiorite	32
5677	20-2028	Granodiorite	32
5678	20-2009	Granodiorite	32
5679	20-2016	Microdiorite	32
5680	20-2033	Granodiorite	32
5681	20-2034	Granodiorite	32
5682	20-2039	Granodiorite	32
5683	20-2119	Aplite	12
5684	20-2137	Aplite	12
5685	20-2141	Aplite	12
5686	20-2194	Aplite	12
5687	20-2212	Aplite	12
5688	20-2104	Aplite	32
5689	28-2030	Gneissic granite	22
5690	28-2031	Biotite schlieren	22
5692	28-2033	Gneissic granite	22
5693	28-2034	Gneissic granite	22
5694	28-2035	Gneissic granite	22
5695	28-2036	Gneissic granite	22
5696	28-2037	Gneissic granite	22
5697	28-2038	Gneissic granite	22
5801	20-2117	Granodiorite	12
5802	20-2118	Granodiorite	12
5805	20-2129	Granodiorite	12
5807	20-2132	Granodiorite	12
5808	20-2186	Granodiorite	12
5809	20-2204	Granodiorite	12
5811	20-2122	Granodiorite	12
5813	20-2136	Granodiorite	12
5814	20-2130	Granodiorite	12
5815	20-2006	Gabbro	32
5817	20-2210	Granodiorite	12
5818	20-2244	Granodiorite	41
5819	20-2246	Pegmatite	32
5820	20-2247	Pegmatite	32
5821	20-2248	Pegmatite	32
5822	20-2249	Pegmatite	32
5823	20-2250	Pegmatite	32
5824	20-2251	Pegmatite	32
5826	20-2062	Dolerite	41
5827	20-2023	Granodiorite	42
5828	20-2024	Granodiorite	42
5829	12-2136	Granodiorite	42
5830	12-2142A	Granodiorite	42
5831	11-2181	Diorite	42
5832	11-2182	Diorite	42
5833	11-2185	Granodiorite	42
5834	11-2188	Foliated diorite	42
5836	28-2099	Gneissic granite	22
5837	28-2107	Microdiorite	22
5838	12-2123	Diorite	42
5839	12-2135	Diorite	42
5840	12-2144	Diorite	42
5841	11-2174	Diorite-pegmatite	42

ANU no.	Field no.	Rock type	Text-figure
5842	11-2192	Gabbro	42
5843	21-2112	Pegmatite	12
5844	21-2114	Pegmatite	12
5845	21-2140	Pegmatite	12
5846	21-2141	Pegmatite	12
5847	21-2143	Pegmatite	12
5848	21-2144	Pegmatite	12
5849	21-2145	Pegmatite	12
5850	21-2146	Pegmatite	12
5851	28-2062	Dolerite	22
5852	28-2076	Dolerite	22
5853	28-2078	Dolerite	22
5854	28-2086	Dolerite	22
5855	28-2091	Dolerite	22
5856	28-2092	Diorite	22
5858	28-2090	Microdiorite	22
5859	20-2001	Gabbro	32
5860	28-2094	Granodiorite	22
5861	28-2095	Granodiorite	22
5862	28-2025	Granodiorite	22
5863	28-2026	Granodiorite	22
5864	28-2070	Granodiorite	22
5865	28-2071	Granodiorite	22
5866	28-2072	Dolerite	22
5867	11-2203	Diorite	42
5870	21-0630	Andesite	10
5872	21-2533A	Andesite	10
5873	28-2060	Microdiorite	22
5874	28-2061	Microdiorite	22
5875	21-2136	Hornfels	12
5876	21-2138	Hornfels	12
5877	20-2004	Diorite	32
5879	21-2057	Microdiorite	10
5880	21-2645	Microdiorite	10
5881	11-2178	Hornblendite	42
5882A	20-2038A	Leucogranodiorite	32
5882B	20-2038B	Granodiorite	32
5883A	20-2041A	Mineralized granodiorite	42
5883B	20-2041B	Mineralized granodiorite	42
5883C	20-2041C	Mineralized granodiorite	42
5884	20-2045	Aplite	41
5885	20-2072	Aplite	41
5886	20-2095	Aplite	32
5887	20-2219	Leucogranite	32
5888	20-2220	Leucogranite	32
5893	03-2133	Microdiorite	42
5897	20-2216	Diorite	32
5898	20-2040	Aplite	32
5899	20-2217	Dolerite	32
5900	20-2229	Aplite	32
5957	20-2237	Aplite	32
5960	03-2081	Schist	42
5962A	03-2125A	Schist	42
5967	03-2130	Schist	42
5968	03-2131	Amphibolite	42
5970	03-2093	Diorite	42
5971	20-2003	Microdiorite	32
5972	20-2005	Microgranodiorite	32
5973	20-2214	Leucogranodiorite	32
5974	20-2215	Leucogranodiorite	32
5975	20-2216	Microdiorite	32
5976	20-2218	Aplite	32
5977	20-2221	Aplite	32
5998	MND-31	Granodiorite	—
6026	21-1600	Granodiorite	12
6029	20-1358	Diorite	—
2100	28-2100	Gneissic granite	22
2101	28-2101	Gneissic granite	22
2104	28-2104	Gneissic granite	22

ANU no.	Field no.	Rock type	Text-figure
2108	28-2108	Gneissic granite	22
2109	28-2109	Gneissic granite	22
2130	20-2130	Aplite	12
2135	20-2135	Granodiorite	12
2168	20-2168	Aplite	12
2191	20-2191	Diorite	12
B55/5/15	B55/5/15	Aplite	12
71-274	29-2020		26
71-275	29-2021		26
71-276	29-2022		26
71-277	29-2023	Quartz-sericite-	26
71-278	29-2024	graphite schist	26
71-279	29-2025		26
71-280	29-2026		26
71-281	29-2027		26
71-898	7152.0178	Amphibolite	—

APPENDIX 3: Ar^{40}/Ar^{36} AND K^{40}/Ar^{36} RATIOS DETERMINED FOR SAMPLES IN THE ARGON ISOCHRON PLOTS

Sample no.	Ar^{40}/Ar^{36} $x10^2$	K^{40}/Ar^{36} $x10^4$
Kubor Granodiorite biotites—Figure 16		
5458	95.53	68.68
5466	82.09	56.59
5801	87.97	60.99
5805	82.46	57.79
5807	138.60	98.77
5808	78.14	51.38
5809	102.31	65.83
5811	64.40	45.08
5813	167.97	121.25
5814	138.57	97.38
6026	126.61	83.34
Kubor Granodiorite hornblendes—Figure 18		
5458	28.61	18.61
5466	24.91	15.87
5801	22.27	13.96
5802	16.64	10.02
5805	36.22	23.66
5807	44.56	30.20
5808	11.82	5.91
5809	17.77	10.02
5811	13.90	8.05
5813	49.22	32.26
5817	5.03	1.54
Kubor muscovite pegmatites—Figure 19		
5843	97.77	69.50
5844	31.34	20.50
5845	130.68	93.69
5846	51.78	34.87
5847	132.88	95.16
5848	35.62	22.17
5849	28.67	18.67
5850	31.71	20.63

Sample no.	Ar^{40}/Ar^{36}	K^{40}/Ar^{36} $x10^4$
Morobe Granodiorite biotites—Figure 27		
5426	1481.4	156.37
5427-1	785.4	62.41
5427-2	986.7	90.56
5453	638.7	43.62
5454	944.3	82.99
5459	1490.3	150.48
Morobe Granodiorite hornblendes—Figure 29		
5426	402.3	12.48
5427	716.3	48.12
5454	469.2	21.98
5459	565.7	31.46

Sample no.	Ar^{40}/Ar^{36}	K^{40}/Ar^{36} $x10^4$
Akuna Intrusive Complex whole rocks—Figure 31		
5660	401.1	12.13
5668	572.9	28.23
5669	595.3	35.85
5851-1	459.5	16.70
5851-2	394.1	10.09
5852	583.1	31.56
5853	606.2	39.94
5854	761.1	54.33
5855	599.2	34.67
Bismarck Intrusive Complex biotites (Wilhelm-Marum area)—Figure 34		
5456	738.6	74.43
5457	1684.5	199.41
5463	1106.4	107.95
5464	1725.7	207.39
5497	1408.0	159.84
5499	873.4	85.78
5500	1249.2	135.83
5670	1285.6	140.13
5671	714.3	59.26
5676-1	875.7	79.63
5676-2	813.4	71.60
5681	2356.3	295.99
5682	1129.4	127.92
Bismarck Intrusive Complex hornblendes (Wilhelm-Marum area)—Figure 36		
5456	461.7	21.63
5457	583.5	39.25
5463	479.0	23.77
5464	401.9	14.58
5465-1	425.8	20.29
5465-2	395.3	17.38
5465-3	410.2	21.65
5498	410.9	13.91
5670	350.7	7.35
5671	669.8	51.53
5676	432.0	15.43
5680	423.7	17.70
5681-1	618.3	49.03
5681-2	582.1	41.96
5682	368.6	9.26
Bismarck Intrusive Complex pegmatites—Figure 39		
5819-1	887.1	117.72
5819-2	379.1	17.34
5820	722.8	83.43
5821	496.4	38.73
5822	705.1	81.83
5823	893.2	102.70
5824	698.5	79.92

APPENDIX 4: TIME SCALE FOR LATE PALAEOZOIC TO QUATERNARY BOUNDARIES

Phanerozoic boundary	Age	Reference
Pliocene-Pleistocene	1.8	Berggren, 1969b
Miocene-Pliocene	5.5	Berggren, 1969b
Oligocene-Miocene	22.5	Berggren, 1969b
Eocene-Oligocene	36	Berggren, 1969b
Palaeocene-Eocene	53	Funnell, 1964
Cretaceous-Palaeocene	65	Funnell, 1964
Jurassic-Cretaceous	135	Casey, 1964
Triassic-Jurassic	190	Howarth, 1964
Permian-Triassic	235	Webb & McDougall, 1967
Carboniferous-Permian	280	Francis & Woodland, 1964

CENTRAL HIGHLANDS, PLUTONIC INTRUSIVE ROCKS

PLATE 1

0   50   100   150 km

BISMARCK SEA

SEPIK RIVER

RAMU RIVER

MARKHAM RIVER

LAE

MT HAGEN

GOROKA

STRICKLAND RIVER

FLY RIVER

GULF OF PAPUA

PORT MORESBY
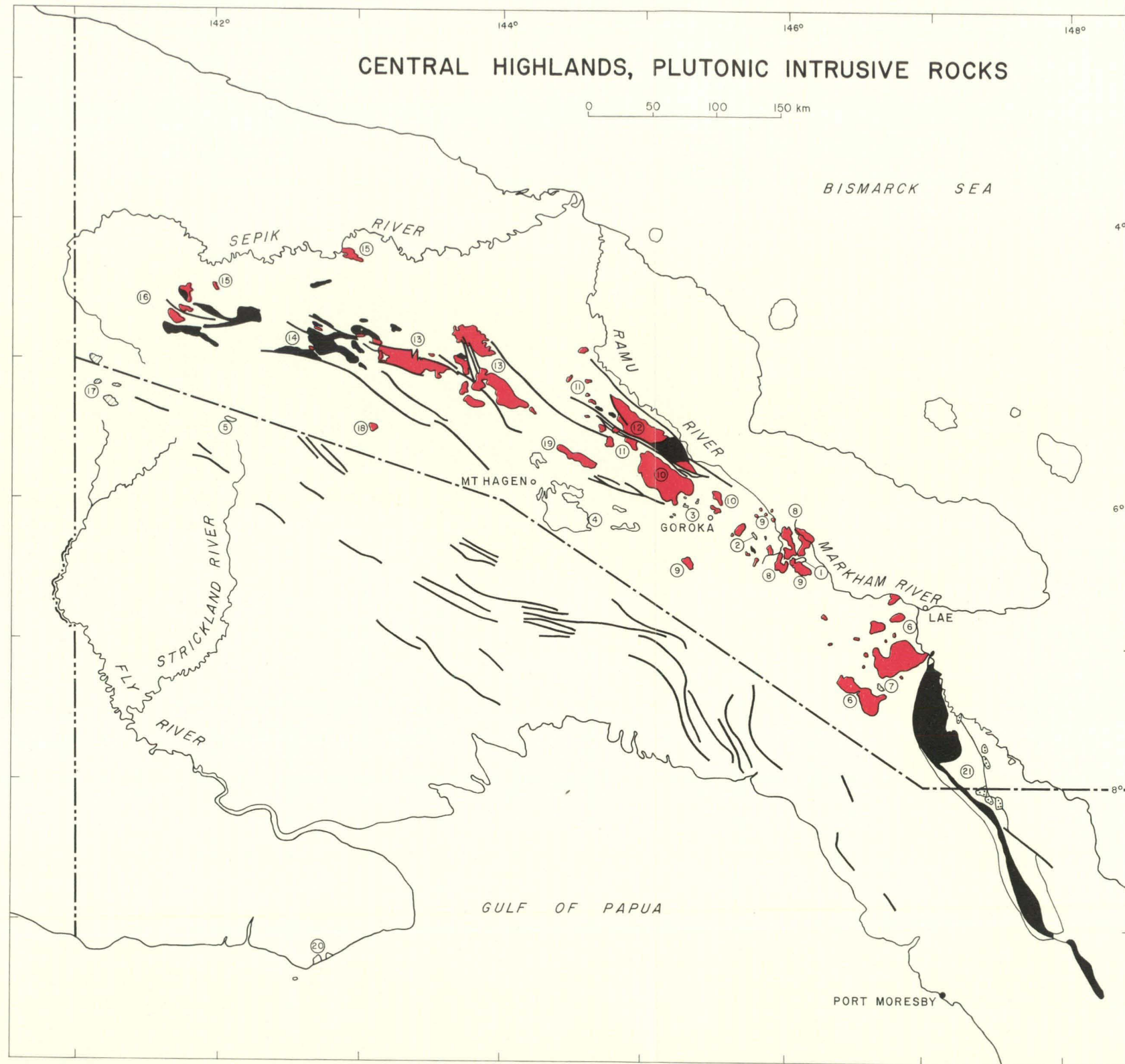
	UNIT	DETAILED TEXT-FIGURE No	TEXT-REFERENCE
1	Mount Victor Granodiorite	25	4·6
2	Gneissic intrusives into Bena Bena Formation	25	4·5
3	Urabagga intrusives	35	4·4
4	Kubor Granodiorite	15	4·2-B,C
5	Strickland Granite	—	4·3
6	Morobe Granodiorite	29	5·3-A
7	Lower Edie Porphyry	29	—
8	Akuna Intrusive Complex	25	5·3-B
9	Kainantu area — Michael Diorite	25,13	5·3-B
10	Bismarck Intrusive Complex	35	5·3-C
11	Oipo Intrusives	35	5·3-D
12	Marum Basic Belt	35	5·3-D
13	Maramuni Diorite	45	5·3-E
14	April Ultramafics	45	5·4
15	Chambri Diorite	45	5·2-A
16	Frieda Porphyry	45	—
17	Ok Tedi intrusives	—	—
18	Porgera intrusives	—	—
19	Kimil Diorite	—	5·3-D
20	Mabaduan Granite	—	2·3-A
21	Papuan Ultramafic Belt	—	2·3-C

Pliocene - Pleistocene intrusive

Miocene intrusive

Eocene intrusive

Pre-Tertiary intrusive

Ultramafic mass

Fault zone, structural trend

P/A/506